Universitat Autònoma de Barcelona

Bioprocess efficiency as a roadmap to establish Pichia pastoris as a reliable cell factory

Xavier Ponte Font

Universitat Autònoma de Barcelona

ESCOLA D'ENGINYERIA

Departament d'Enginyeria Química, Biològica i Ambiental

Bioprocess efficiency as a roadmap to establish *Pichia pastoris* as a reliable cell factory

Memòria per obtenir el grau de Doctor
per la Universitat Autònoma de Barcelona.
Programa de Doctorat en Biotecnologia

Directors: Francisco Valero i José Luis Montesinos

Xavier Ponte Font

Bellaterra, 2017

ABSTRACT

The present work is focused, with a bioprocess engineering point of view, in the production of the heterologous *Rhizopus oryzae* lipase expressed in the methylotrophic yeast *Pichia pastoris* under the control of the methanol-induced alcohol oxidase 1 promoter; and, specially, the improvement of the bioprocess efficiency by the use of proper operational strategies in fed-batch mode for bioreactors of different scale. With that, *P. pastoris* is stablished as a versatile, robust and competent platform for the production of recombinant proteins.

In a first part of the dissertation, the emphasis is put on reaching optimal levels of the main performance indexes of industrial interest at lab scale in methanol feeding strategies as the only carbon source and inducer. Prior to this final goal, though, preliminary studies and operational improvements were carried out to outcome system limitations and to give more versatility and robustness to the system. They included upgrades in system control and supervising in LabVIEW, installation of new hardware for instrumentation and a new feeding strategy for the nitrogen source added to the cultures. Later, a systematic study on the effect of the oxygen tension was conducted. It was found that, in normoxic conditions, dissolved oxygen can limit the process in both excess and lack. An optimal value of 25 % air saturation was found for all specific rates and results were validated by a consistency check and further data reconciling.

From that point, the optimization of the bioprocess in bench-top bioreactor by the mathematical design of methanol feeding profiles was fulfilled. From modelling data, and by the use of a simple, versatile optimization tool, the simulation of the optimal methanol concentration profiles were carried out to maximize product titer and volumetric productivity, and then compared to previous strategies and then successfully applied experimentally.

On the other hand, the next part of this document focuses on studies of scale down and up from the bench-top scale. The first change is downwards to a microbioreactor system of a 1000 µL scale. Cultures from that scale were successfully reproduced succesfully at lab scale to verify the system as suitable for clone screening and design of simple fed-batch strategies. Finally, the bioprocess was brought up to a 50 L scale. Unfortunately, the attempts did not succeed on reproduce the bioprocess efficiency, but it was possible to discard some of the hypothesis that were brought up, and to settle some other ones that can be further investigated in the future, like oxygen mass transfer limitations.

RESUM

El present document està centrat en un punt de vista d'enginyeria de bioprocés, de cara a la producció heteròloga de la lipasa de *Rhizopus oryzae*, expressada en el llevat metilotròfic *Pichia pastoris* sota el control del promotor de l'alcohol oxidasa 1, induïble amb metanol. Especialment, l'objectiu es focalitza a la millora de l'eficiència del bioprocés mitjançant l'ús d'estratègies d'operació en discontinu alimentat en bioreactors de diferent escala. Amb això, es pretén establir *P. pastoris* com una plataforma versàtil, robusta i competent per a la producció de proteïnes recombinants.

A la primera part de la tesi, l'èmfasi es troba en l'assoliment de nivells òptims dels principals índexs de rendiment d'interès industrial a escala de laboratori, utilitzant estratègies d'operació amb metanol com a font única de carboni i inductor del promotor. Prèviament a aquest objectiu, però, es van realitzar estudis preliminars i millores operacionals per tal de superar certes limitacions del sistema i per aportar-hi versatilitat i robustesa. Entre ells, es va actualitzar i incorporar millores al programa de supervisió i control del procés en LabVIEW, s'hi instal·là nou hardware d'instrumentació i es va implementar una nova estratègia d'alimentació de la font de nitrogen. Posteriorment, un estudi sistem àtic de l'efecte de la disponibilitat d'oxigen es va dur a terme. Es va obtenir que, en condicions de normòxia, l'oxigen dissolt pot limitar el procés tant per un excés com per nivells escassos. El 25 % de saturació d'aire es va establir com a valor òptim de cara a les velocitats específiques, i els resultats van ser validats per un test de consistència i reconciliació de dades.

A partir d'aquest punt, s'assolí l'optimització del bioprocés a escala de laboratori mitjançant el disseny de perfils d'alimentació de metanol amb eines matemàtiques d'optimització. A partir de dades de modelització i amb una eina d'optimització simple i versàtil, es van dur a terme les simulacions de perfils òptims de concentració de metanol per maximitzar la concentració de producte i la productivitat volumètrica, es van comparar amb estratègies anteriors i es van aplicar experimentalment amb èxit.

Per altra banda, la següent part del document se centra en estudis de canvi d'escala. El primer que es realitza és a escala de microbioreactor. Es van reproduir uns cultius realitzats a aquella escala al laboratori per verificar aquest sistema com a vàlid per realitzar-hi assajos d'expressió i selecció de soques i per dissenyar-hi estratègies simples d'operació en discontinu alimentat. Finalment, el bioprocés va ser portat a escala pilot de 50 L. Malauradament, els intents realitzats no van assolir reproduir l'eficiència del bioprocés, tot i que va ser possible descartar-ne algunes hipòtesis plantejades i proposar-ne d'altres que hauran de ser investigades en un futur, com ara limitacions en la transferència d'oxigen.

TABLE OF CONTENTS

1. Introduction: heterologous protein production by *Pichia pastoris*. A bioprocess engineering comprehensive design 1

2. Objectives 43

3. Preliminar results: *Pichia pastoris* producing *Rhizopus oryzae* lipase under P_{AOX1} control. first steps to the optimization of bioprocess efficiency..... 45

4. Bioprocess efficiency of *Rhizopus oryzae* production under the control of P_{AOX1} is oxygen tension dependent. 61

5. Towards optimal substrate feeding for heterologous protein production in *Pichia pastoris* fed batch process under P_{AOX1} control: a modelling aided approach. 91

6. The microbioreactor as a tool to evaluate fed-batch strategies and high-throughput clone screening.....123

7. Upgrading to the first step up to industry. pilot plant scale production of ROL by *Pichia pastoris* under P_{AOX1} control.....153

8. General conclusions..... 185

1 INTRODUCTION: HETEROLOGOUS PROTEIN PRODUCTION BY *Pichia pastoris.* A BIOPROCESS ENGINEERING COMPREHENSIVE DESIGN

1.1 Bioprocess engineering

"Bioprocess engineering is the discipline that puts biotechnology to work".

This forceful statement was published by the National Research Council in 1995 [1]. Since the quite recent inception of Biotechnology as an industrial applied science during this last century, bioprocess engineering has been stablished and promoted itself as an alternative to classic industrial processes and for the synthesis of new products.

Biotechnology can be divided into several color-classes, white biotechnology (industrial processes, fine chemical products, enzymes, biofuels), red biotechnology (pharma research), green biotechnology (agriculture), blue biotechnology (sea resources) and grey biotechnology (environmental bioengineering). Biotechnology and bioprocesses are, then, present in a wide heterogeneous range of fields. Some notorious examples are the production of biopharmaceuticals like recombinant second generation insulin or growth factors [2]; wastewater treatment plants or countless applications in the food industry, from brewery [3] to enzyme production for hydrolysis in milk manufacturing [4].

Another perfect example is the development of biorefineries. In that way, Herrera (2004) [5], appointed the importance of biotechnology in the energy industry, and its potential to, at the same time, reduce the economic and environmental impact of selects a few projects funded by the US Department of Energy, in which the production of biofuel was specially praised. He also reviewed the decreasing of the both footprints of some bioprocesses, in comparison to their classic production like the manufacturing of Vitamin B2 (by BASF).

Bioprocess engineering was more thoroughly defined by Doran (1995) [6], as an essential discipline for many food, chemical and pharmaceutical industries, which makes use if microbial, animal and plant cells, and components of cells such as enzymes to manufacture new products and destroy harmful wastes. Some other quotes can be found

around, which state that bioprocess engineers are those professionals who "bring engineering to life". However, it actually goes both ways. The bioprocess engineer is a multidisciplinary professional who analyzes the properties of biological material and works with them to discover beneficial uses. In addition, they develop the biological systems used in the manufacture of products. Bioprocess engineers troubleshoot and monitor production equipment related to the production process and also product quality, overseeing inspection procedures.

This chapter is conceived as a simple roadmap about some issues that are critical for the development of a bioprocess, directing the attention exclusively to its core, the bioreactor. The focus will be put on the excellence in production of heterologous proteins in *Pichia pastoris*, due to the approach of the experimental work of this thesis. In that way, Figure 1.1 summarizes all concepts that will be highlighted as a network, which shows the relationship and dependency between them. The different steps of the development of a bioprocess, here represented as scales, from the microbioreactor and shake flask, stepping into the heart of a bioprocess development, which is the bench-top bioreactor, followed by the intermediate pilot scales up to the final industrial production volume bioreactor.

1.2 The methylotrophic *Pichia pastoris* as a host for RPP

The methylotrophic yeast *Pichia pastoris* has become, during last three decades, one of the most effective, used and versatile cell factories to produce all sorts of recombinant proteins [7]. It was first described as a host during the second half of the 80s by James M. Cregg and his coworkers [8], as an alternative to classic *Saccharomyces cerevisiae*, still a fundamental cell host for many industrial bioprocesses nowadays. Among its advantages, the main reasons that made it emerge as a promising alternative are summed up:

First, its ability to grow in define media up to very high cell densities. In that matter, Heyland *et al.* (2010) [9] reported a 200 g L^{-1} biomass concentration, expressed in dry cell weight (DCW), after a culture using glucose as carbon source.

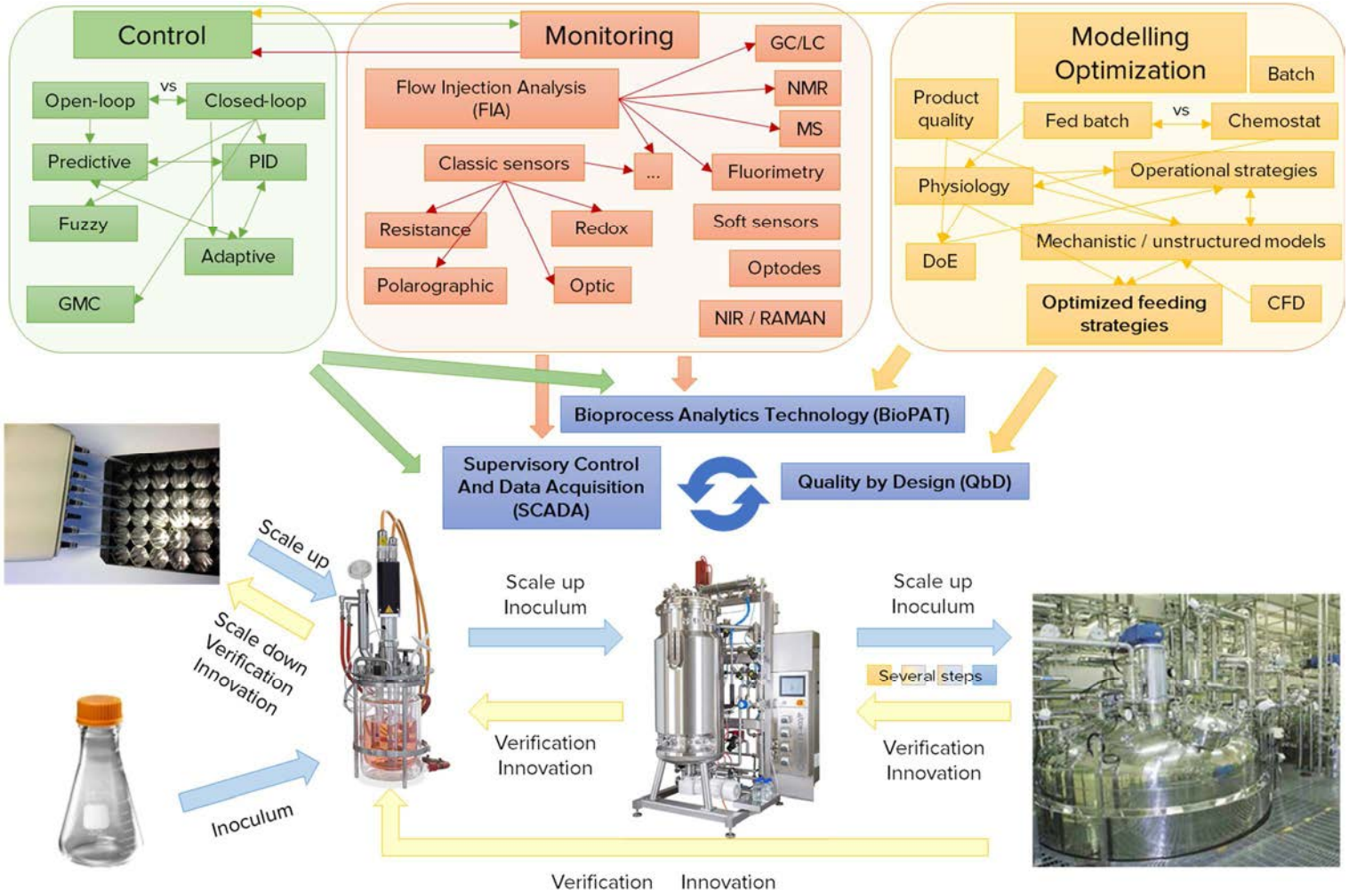

Figure 1.1 Bioprocess engineering design roadmap based on bioprocess efficiency.

Apart from that, it presents a set of strong, tightly regulated promoters, which will be announced and discussed further in this text, both inducible and constitutive, that allow very high protein titers. One of the highest values reported corresponds to the production of hydroxynitrile lyase from *Hevea brasiliensis*, at 22 g L^{-1} [10], under the alcohol oxidase 1 promoter (P_{AOX1}), corresponding to the one which will be thoroughly studied in this dissertation. This process was also one of the first successfully established industrial-scale bioprocess using *P. pastoris* as the biocatalyst [11].

When compared to other extended expression system, the major advantage of *P. pastoris* over *Escherichia coli* is that the first one is capable of performing post-translational modifications, such as conforming disulfide bonds and glycosylation of proteins. This means that in cases where disulfides bonds are necessary, *E. coli* might produce a misfolded protein, which is usually inactive or insoluble, or an inclusion body, needing a refolding procedure.

Besides, as stated, *S. cerevisiae* has been hegemonic among yeasts in industrial applications, some of them as important as insulin, hepatitis B surface antigen or hirudin, among others [12]. Three main reasons explain that: the large amount of information to modify it genetically, it presents a set of secretory pathways and it also performs post-translation modifications. However, some glycosylations led by this host system are not acceptable for many mammalian proteins. Moreover, *P. pastoris* overcomes *S. cerevisiae* in protein yield, e.g. the anticoagulant hirudin titer has been reported as three times higher in *P. pastoris* than its production in *Saccharomyces* [13]. Glycosylation is less extensive in *P. pastoris* in comparison, as well [14].

On the other hand, if *P. pastoris* is contrasted to expression systems like Chinese Hamster Ovary (CHO) cells, *Pichia* usually gives much better yields [12], apart from the low complexity of media it requires to grow, in comparison, which can consist on a single C-N-source broth.

Furthermore, it is very important to remark that Food and Drug Administration conceded *P. pastoris* the status of GRAS (generally recognized as safe). Some example of profited processes from this status are the production of phospholipase C intended for animal feed purposes in 2006 [15] and a biopharmaceutical product, a recombinant kallikrein inhibitor to treat hereditary angioedema in 2010 [16].

Since then, *P. pastoris* has been used to express a largely numerous amount of recombinant proteins. Cereghino *et al*. (2000) [7] listed more than 200 proteins, both for industry, research and model ones, that have been produced with *Pichia* as its host. Today the *P. pastoris* system is licensed to more than 160 companies in the biotechnology, pharmaceutical, vaccine, animal health, and food industries [17]. Among them, industrial consolidated processes can be found such as the production of an engineered thermophile DNase (Affymetrix USB, Santa Clara, CA) [18]. Potential biopharmaceutical proteins of interest are also developed in *P. pastoris* [17], such as vaccines (Tetanus toxin fragment C [19]), hormones (Human parathyroid hormone [20]) or antibody fragments (A33scFv [21]).

P. pastoris, specifically the wild type strain NRRL Y-11430 (originally from National Regional Research Center, ILL [8]), or CBS7435, has been classified as *Komagataella phaffii* [22]. This is the parental strain for the two most frequently used protein expression host strains GS115 (US Patent 4,879,231, Phillips Petroleum, 1989) and the prototrophic strain X-33. A set of most utilized and relevant strains of *P. pastoris* for the expression of RPP is further presented in this chapter. Among them, X-33, GS115 and KM71 are distributed commercially by Thermo Fisher Scientific (Waltham, MA), earlier Life Technologies and Invitrogen.

Despite what it has just been presented, *P. pastoris* main feature is precisely its ability to consume methanol as a sole carbon source (methylotroph). This is achievable thanks to the activity of the genes codifying for alcohol oxidase: *AOX1* and *AOX2*. They precisely constitute two of the main promoters, as it will be discussed followingly.

1.2.1 Expression promoters

As previously commented, one the main attractive features of *P. pastoris* Is the large number of available strong promoters which have allowed *Pichia* to overcome other cell factories in RPP yield. In Table 1.1**¡Error! No se encuentra el origen de la referencia.**, the most used promoters, both in research and industry, are listed.

Table 1.1 Main classic and recent expression promoters in *Pichia pastoris* [23]

Promoter (P)	Gene / Encodes for	Regulation	Repression	Expression	References
AOX1	Alcohol oxidase 1	Inducible. Methanol	Glucose glycerol, ethanol	Very strong ≃5% of poly(A)$^+$ RNA	[7]
AOX2	Alcohol oxidase 2	Inducible. Methanol	Glucose, glycerol, ethanol	Weak ≃ 10 % of P_{AOX1}	[24]
GAP	Glyceraldehyde 3-phosphate dehydrogenase	Constitutive	-	Very strong ≃ P_{AOX1}	[7,25]
FLD1	Formaldehyde dehydrogenase 1	Inducible. Methanol, methylamine	Glucose (in absence of methylamine)	Very strong ≃ P_{AOX1}	[26]
PEX8	Peroxisomal matrix protein	Inducible Methanol	Glucose	Weak	[7,27]
YTP1	Secretion GTPase	Constitutive	-	Weak (less 1 % of P_{GAP})	[28]
DAS1	Dehydroxyacetone synthase	Inducible Methanol	Glucose	Very strong ≃ P_{AOX1}	[29]
PGK1	Phosphoglycerate kinase	Constitutive	-	Weak ≃10 % of P_{GAP}	[30]
ENO1	Enolase	Constitutive	-	20 – 70 % P_{GAP}	[31]
CAT1	Involved in ROS defense	Inducible. Methanol, oleic acid	Derepressed (29 % of P_{GAP} on glucose)	Very strong ≃ P_{AOX1}	[32]

Among the promoters just listed, P_{AOX1} and P_{GAP} have stood out among the rest of them, as the numerous reports and applications show [7,23,33–35]. P_{AOX1} allows a very strong and tightly regulated induction of the RPP, by the use of methanol, acting simultaneously as inducer and carbon source. The fact that methanol is cheap, easy to obtain and the possibility to use it pure as feeding solution makes P_{AOX1} even more attractive. Methanol is also obtained as a residue or byproduct in numerous industrial processes, and can be reused as substrate [36].

The constitutive P_{GAP} has parallelly stood out as an alternative to P_{AOX1}, avoiding the use of methanol by achieving also a strong regulation of the gene to express, as reported, a wide range of recombinant proteins.

1.2.1.1 Alcohol oxidase promoters and methanol utilization (Mut)

Methanol utilization pathway takes place in the peroxisome of *P. pastoris* and as told, its first enzyme, alcohol oxidase (AOX), is codified by the genes *AOX1* and *AOX2*, being the former one responsible for the 90% of its sequencing [37]. In

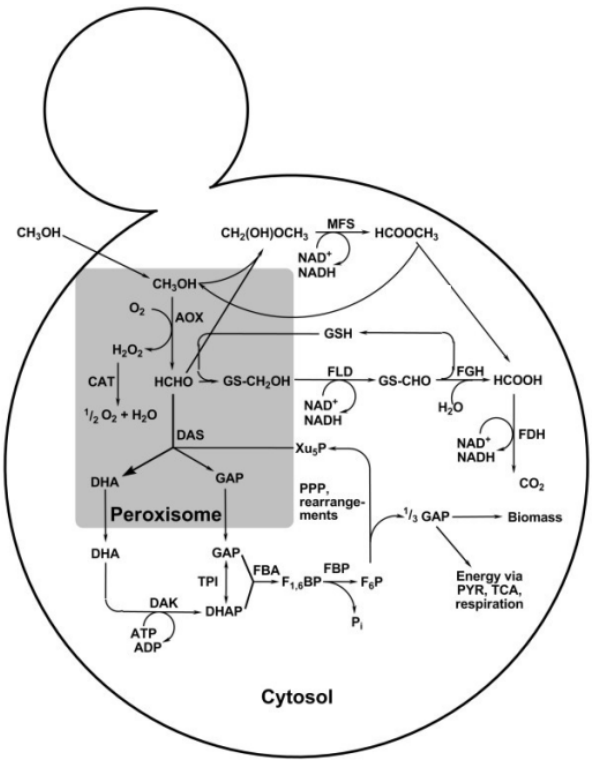

Figure ***1.2***, the methanol assimilation route is presented, along the main pathways it precedes or leads to in the cytosol.

Figure 1.2 Scheme of methanol utilization pathway of *P. pastoris* in the peroxisome and its linkage to other cytosolic routes [38].

As seen in Figure 1.2, first methanol is assimilated and oxidized to formaldehyde and hydrogen peroxide (AOX). Catalase enzyme then breaks into it and produces oxygen and water. Formaldehyde, then, is oxidized (deassimilation pathway) or assimilated in the cell metabolism by condensation with xylulose 5-phosphate. The latter peroxisomal condensation reaction is catalyzed by a special transketolase called dihydroxyacetone synthase, DAS, which converts xylulose 5-phosphate and formaldehyde into the C3-compounds dihydroxyacetone (DHA) and glyceraldehyde 3-phosphate (GAP), which are further metabolized in the cytosol. The energy production pathway, where NAD^+ is reduced to NADH, is driven mainly from formaldehyde, driven out of the peroxisome and then oxidized to formic acid by the formaldehyde dehydrogenase (FLD), which is further oxidized to CO_2 [38]. All genes in this pathway are, in different levels, induced by methanol. As commented, and as can be observed both in Table 1.1 and

Figure ***1.2***, some of the main promoters belong to the methanol assimilation route, i.e. P_{AOX1}, P_{AOX2} and P_{FLD1}. The latter took on importance due to the possibility of inducing the production of RPP by methylamine, avoiding methanol, with similar product yield in some examples in the literature if compared to P_{AOX1} [39].

The wild-type *Pichia* strains with fully functional *AOX1* and *AOX2* genes are commonly typified to have a methanol utilization plus phenotype (Mut^+). Genetic manipulation on these genes originated a set of strains that are widely used and reported in the literature for bioprocess engineering purposes. In Table 1.2, main commercial *Pichia* strains are gathered, along some examples of application of each one.

KM71 strain was originated by the truncation of the gene *AOX1* by removing a fragment of it and replacing it with the *ARG4* gene from *S. cerevisiae*. So, that generated an *AOX1*-defective strain, with an approximate 10 % of capacity of methanol uptake. This led to name this kind of strains as Methanol utilization slow (Mut^s). Despite this low methanol uptake, Mut^s recombinant strains have been used extensively, due to its mild operational conditions and low oxygen demands. Finally, methanol utilization minus (Mut^-) strains

(commercially MC-100-3) have, as well, inserted the gene *HIS4* to become *AOX2*-defective. Scarce studies have been found of the use of this kind of strain, though inducible by methanol, it requires a non-repressing alternative carbon source [43].

Table 1.2 Main *P. pastoris* strains used for transformation.

Strain	Genotype	Main feature	Application	Reference
NRRL* Y-11430 (CBS7435)	Wild type	Mut$^+$	Generation of the rest of strains	[8,40]
X-33 (ThermoFisher™)	Wild type	Mut$^+$ P_{AOX1} and P_{GAP} transformants	Selectable marker: zeocin resistance pPicZ and pGapZ plasmids	[41]
GS115	*his4*	Deficient in histidinol dehydrogenase Mut$^+$	Selectable markers: Zeocin resistance and *HIS4* gene P_{AOX1} and P_{GAP} transformants.	[8]
KM71	*Δaox1::ScARG4 his4 arg4***	Non-functional P_{AOX1}. Mut^s	Low methanol uptake rate processes	[42]
MC100-3	*his4 arg4 aox1Δ::ScARG4 aox2Δ::Pphis4*	Non-functional P_{AOX1} and P_{AOX2}. Mut$^-$	Methanol as inducer but not to be consumed	[37,43]
SMD1168	*his4 pepA*	Protease deficient strain Mut$^+$		[44]
PichiaPink™	*ade2*	Adenine deficient strain	Selection with adenine Protease reduced	[45,46]
GlycoSwitch™	*endoT****	Reduced N-glycan heterogeneity	Therapeutic application Human protein production	[47,48]

*National Regional Research Center, ILL.

***Sc* stands for a gene from *S. cerevisiae*; *Pp*, from *P. pastoris*.

***Expression of the fungal endoglycosidase endoT (non-published data [48]).

The present document has been build out from the work carried out using a modified X-33 strain expressing the *Rhizopus oryzae* lipase (ROL), transforming a single copy of the gene using a pPICZA-ROL, as described by Minning *et al.* (1998) [49].

1.2.2 State of the art. Current applications and development

1.2.2.1 Synthetic biology and metabolic engineering

Figure 1.3 summarizes the state of the art of three main trends which research in *P. pastoris*, in a synthetic biology point of view, is now being focused. The objectives are clear, mainly overcome the drawbacks *Pichia* present in front of other expression system in order to definitely give it a boost and establish as a hegemonic host for therapeutic proteins.

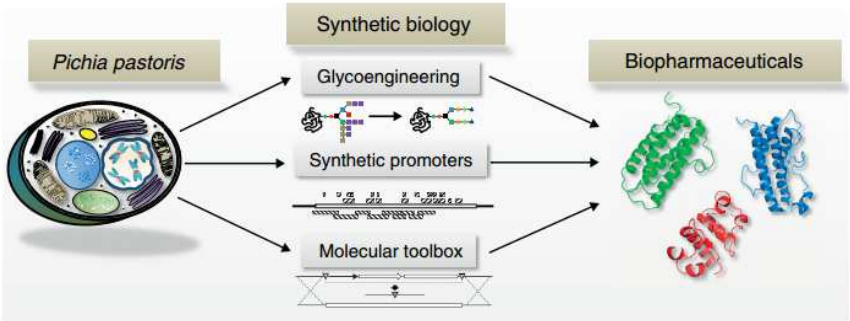

Figure 1.3 Current trends in synthetic biology research to promote biopharmaceutical heterologous production in *Pichia pastoris* [50].

Firstly, as commented, recent advances in glycoengineering of *P. pastoris* have allowed the development of new strains that successfully and productively fold RPP with a human glycosylation, avoiding hyperglycosylation and other phenomena that would lead to unsuitable products. The GlycoDelete™ technology has built the grounds of this path, presenting promising strains that are now available in the market (GlycoSwitch™) [48], mentioned in Table 1.2. From now on, the challenge goes through new innovative approaches to improve glycol-engineering of yeast, for example, regarding O-glycosylation [51].

Furthermore, the development of recent synthetic promoters is trying to push *Pichia* through a strong expression of RPP while avoiding the use of methanol. In that way, an example of a modification of P_{AOX1} successfully achieved derepression in glucose growth

through small deletion and point mutations [52]. This so-called derepressed promoters have been applied in several recent works for RPP, like phospholipase C from *Bacillus cereus*, using a mutated P_{AOX1} that gets de-repressed at limiting concentrations of glycerol [53].

Finally, bioinformatics tools have also boosted research in systems biology and metabolic engineering of *P. pastoris.* A wide understanding of this expression host has been pursued, and this has resulted in recent development of genome-scale models [54–56], and have been useful, for example, to predict overexpression and deletion mutants to enhance recombinant protein production, as well as to deepen into knowledge of, not only the central carbon metabolism, but also of sphingolipid biosynthesis and glycosylation pathways, as well as the oxidative phosphorylation electron transport chain [56].

Finally, recent brand-new technology in genetic engineering *CRISPR/Cas9* has been applied in *Pichia* and deserves to be mentioned. This technique is one of the most promising tools for targeted genome engineering because of its flexibility to achieve multiplexing, the ease of retargeting and the ability to introduce site specific modifications [57]. *CRISPR/Cas9* has been recently and successfully used for gene disruption studies, to introduce multiplexed gene deletions and to test the targeted integration of homologous DNA cassettes [58].

1.3 Monitoring, modelling and control of bioprocesses

1.3.1 Excellence in industrial bioprocesses: Process Analytics Technology (PAT), Quality by Design (QbD) and Supervisory Control and Data Acquisition (SCADA)

Any industrial process must achieve efficiency, reproducibility, quality, safety and traceability. To ensure that, it has been considered, in this dissertation, that two bioprocess quality procedures for good practices must be followed, i.e. PAT and QbD, along with SCADA procedures, which are essential to fulfill these objectives and codependent between them.

First, Process analytical technologies (PAT) are systems for analysis and control of manufacturing processes based on timely measurements of critical quality parameters and performance attributes of raw materials and in-process products, to assure acceptable bioprocess efficiency and final product quality. It is important to note that the term analytical in PAT is viewed broadly to include chemical, physical, microbiological, mathematical, and risk analysis at the same time. The application of the PAT to Bioprocesses is designed by BioPAT, a concept that was defined by Känsäkoski *et al.* (2006) [59], and was mainly intended to be applied to the industry of biopharmaceuticals. The goal of PAT is to enhance understanding and control the manufacturing process, and is achieved by following these steps:

1. **Identify** the critical or limiting quality that needs to be monitored and controlled. This is the key step to select the suitable strategy to work with.
2. Ensure **monitoring** quality ensuring by selecting the suitable technology, in case of need, through soft sensors which can monitor certain limiting parameters and not accessible directly by conventional sensors.
3. **Analyze** statistically the relationship between the critical quality attribute and the bioprocess efficiency.
4. **Control** the critical quality attributes within the levels stablished in the previous step.
5. Finally, **report** the performance of step 4, ensuring the objectives that were formulated have been accomplished and no unexpected perturbations have taken part during the process.

Secondly, Quality by Design (QbD) is a concept that is trying, recently, to make itself through, mostly, the biopharmaceutical industry. Despite being much related to PAT, it emphasizes its objectives in two main pillars: achieving the desired product quality and the need for it to be guaranteed from the design of the process. QbD approach, then, is expected to ‘‘build quality into the process’’ rather than ‘‘testing quality into the product’’ [60]. Process development based on QbD normally employs design of experiments (DoE) tools to comprehensively define the interaction between parameters of the process and quality of the product. This procedure has been widely applied in reported works, as said, mostly to obtain suitable heterologous biopharmaceutical products [60,61].

Finally, despite being conceptually more distant from the two previous quality guidelines, Supervisory Control and Data Acquisition (SCADA) is paramount to accomplish the objectives they present. SCADA is that software involved in the supervision of the full control architecture and, also, the responsible for the acquisition of every single data that is being monitored live and in real-time from the whole process and to ensure the communication between the system and all its peripherals. It is a purely software package that is positioned on top of hardware to which it is interfaced, usually by Programmable Logic Controllers (PLCs), or other commercial hardware modules [62]. Its reliability and robustness have made it predominant in industry of any field. Some examples of implementation to the biotech industry can be found in the literature [63,64], and Figure 1.4 shows a scheme of an hypothetical case of this application.

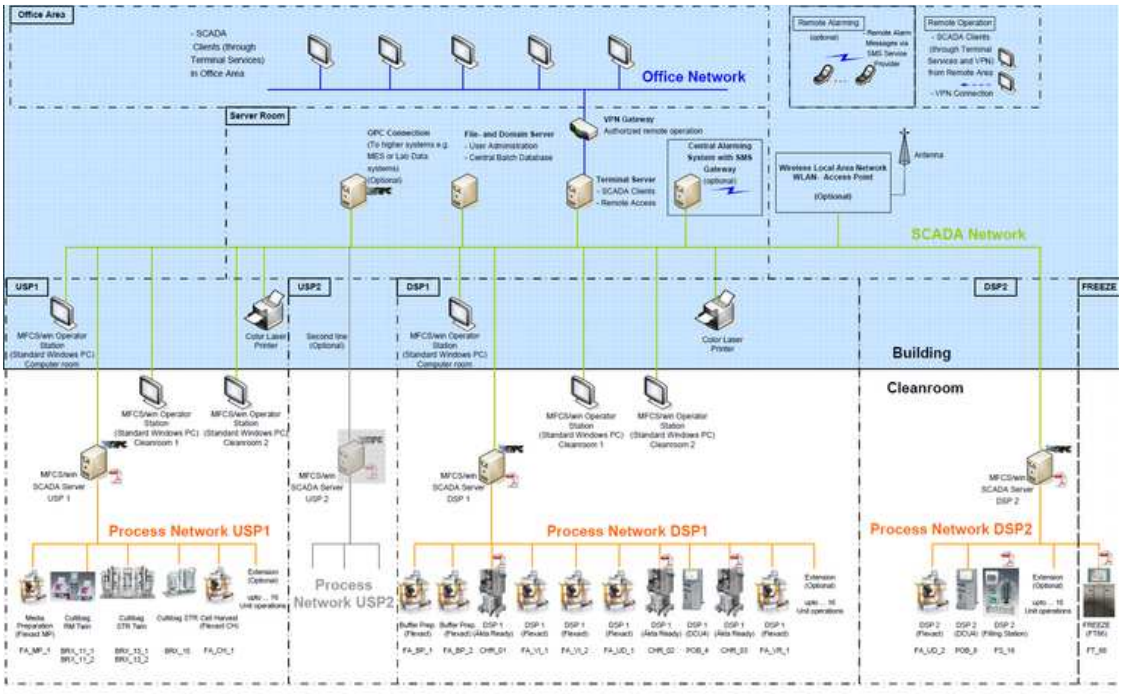

Figure 1.4 Diagram of a SCADA supervisory system of an hypothetic set of bioprocesses [65].

1.3.2 Operational strategies in bioreactors

A bioreactor is defined as any space, where a biochemical reaction or a set of them are carried out by the action of a biocatalyst, assuming an enzyme or a microorganism. The challenge of the bioprocess engineer in the first step is finding the suitable operational

strategy to obtain a product of interest in a profitable and most productive way as possible.

The objective, at the time of designing operational strategies, is always to pursue the maximization of one or various performance indexes (PI) of the bioprocess. That goes, therefore, in favor of bioprocess efficiency. One of the most common ones is productivity, which indicates the amount of interest product (in total amount or in concentration) per unit of time. Moreover, product yield is often considered, since it connotes the level of substrate exploitation. Product concentration is, as well, a key performance index in processes with a high-added value product. Finally, product quality is a criterion that may be critical for some processes, e.g. the glycosylation pattern of a recombinant protein (RP) intended for pharma applications.

1.3.2.1 Operational modes in bioreactors

A fed batch operational mode is that one in which one or more substrates are added throughout a determined amount of time of the process (in contrast to batch mode, where no inlets are present). This substrate is usually the limiting one, normally being the carbon source (but often nitrogen or even oxygen) to bring process, so processes where the inlets are specifically acid/base adjusting solution or antifoam are simply considered as batch or discontinuous mode. Strictly, there are no outlets, except for those intended for samples and, in case of aeration, the gas itself and possible stripped components from the broth.

Fed batch mode is the most extended one among bioprocesses involving growth of microorganisms, since their kinetics tend to show inhibitions to high concentrations of any substrate required for the metabolic performance, the production of secondary metabolites, or to any product that may eventually accumulate [66,67]. With that, fed batch allows to reach significantly higher levels of biomass and product concentration in comparison with a simple batch mode. Fed batch operation was first introduced in *S. cerevisiae* production in early 1900's and has gained relevance in the rest of applications of white biotechnology.

The opposed operations to batch and fed-batch are the continuous modes. The most extended one among ideally considered as "perfect mix regime" is the *chemostat*. Its main

feature in cell is that the specific growth rate (μ, h^{-1}) is physically adjustable by the dilution factor (D), as they are equal, just as it is deduced from the biomass individual mass balance. As it eventually reaches a steady state, also physiologic, *chemostat* is the most suitable method to characterize the physiology of the cells.

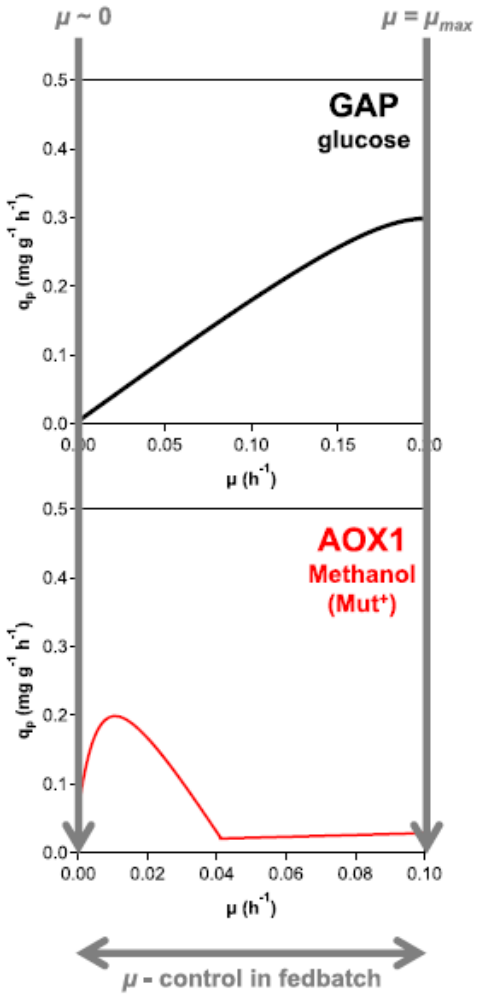

Figure 1.5 Example of relationship q_P - μ for two different *P. pastoris* expression systems [69].

Regarding the selection of the most suitable strategy in each process and for each operational mode, the possibilities are countless, not to say infinite. The design of operational strategies sometimes becomes an art where trial and error is the main rule of thumb. Kinetics of the cell physiology, though, has a main role in their conception. First of all, the characterization of the physiology of the cells is paramount to achieve success in the design of the best operational strategy. A very appropriate review on that matter, Egli (2015) [68] appointed the importance a rational kinetic study, always based on μ, and promoted all efforts on monitoring and control of the process, and therefore, the performance of the operational strategy itself, towards the control of this physiologic parameter, directly or indirectly, regardless of the microorganism that is acting as biocatalyst. That work also highlighted the importance of media components out of the limiting carbon source that can hamper the study or show limitation if the necessary ratios in respect to the C-source are not kept. Cos *et al.* (2006) [34] and Looser *et al.* (2014) [69] summarize the tendency of the last decades in the design of operational strategies for the particular case of heterologous proteins produced in *Pichia pastoris* (*Komagataella phaffii*). All of them rationally appoint the need to determine the relationship of the product specific rate (q_P, mg g^{-1} h^{-1}) and μ. In Figure 1.5, two different

examples of this kinetic relation are presented, for different promoters and RP. It can be perceived how two processes in the same organism present completely opposite tendencies of those profiles. Moreover, this relationship must be empirically determined in each case, and its shape will directly determine the most suitable strategies.

Some of these operational strategies have been gathered together in this section and classified followingly.

1.3.2.2 Limiting carbon source-based strategies

These strategies consist on conceiving a feeding profile of the limiting C-source to drive the culture into a certain region of the cell growth kinetics that favor, in a certain way, the bioprocess efficiency, which can be directed towards either obtaining a product of interest (endogenous or heterologous), or rather the cells themselves, or the elimination of a certain compound as a substrate.

The possibilities and complexity on the design of strategies are in a widespread range depending on the information of the kinetics and, at the same time, the availability of monitoring and control techniques at the disposal of the engineer. The general trend as the first step forward to an efficient bioprocess is an exponential feeding that can keep a constant μ. The objective here goes two ways: apart from stepping to bioprocess efficiency, reproducibility between different batches is fundamental. This method is widely applied in aerobic microbial processes (bacteria and yeasts) for its simplicity and low monitoring and control requirements. The most classic example is the recombinant protein production in *E. coli* under the control of promoters inducible by IPTG, which is not metabolized, where an exponential feeding rate is set to maintain a constant μ [70]. Little information of the cell physiology is needed, too, and a simple open-loop control of μ can be applied, following Equation 1.1, an expression deduced from the substrate mass balance, where a constant substrate concentration, and therefore, μ, is assumed:

$$F_t \approx \frac{(XV)_0 \cdot \mu_{SP} \cdot \exp(\mu_{SP}(t - t_0))}{Y^*_{X/S} \cdot S_{feed}}$$

Equation 1.1

Where F stands for the volumetric feeding rate (L h^{-1}), X is the biomass concentration (g L^{-1}), t is the process time (h), $Y^*_{X/S}$ is the global biomass-substrate yield (g g^{-1}) and S_{feed}, the

substrate concentration of the feeding solution (g L^{-1}). The subscript SP denotes the set-point of the variable and 0, the initial value.

The operational strategy just presented usually is put to practice by maintaining a substrate concentration that is near to zero, situation commonly named as substrate limited conditions or fed-batch (SLFB). It is important not to be confused with the concept of limiting substrate, meaning the one that will mainly govern the process kinetics.

Cell culture processes also employ this kind of feeding strategies, or even more simplistic ones, like stepwise increasing feeding profiles, willing to achieve more scalability, due to their higher complexity in respect to microbial cultures, and therefore, the larger amount of perturbations that could hamper that scalability, for instance, factors that can affect the glycosylation pattern of a monoclonal antibody [71] and therefore hampering product quality.

Besides, strategies based on substrate non-limited conditions (SNLFB) have been widely described and employed [72–74]. They require a substrate control which can be conducted directly or through measurement of indirect variables. Closed-loop control is more common in this case, since predictability is much more complex, even more when the growth rates are high, which corresponds to the normal situation at non-limited substrate conditions (saving some inhibition patterns).

This strategy goes in favor of achieving a tight regulation of promoters that are strongly induced or derepressed in conditions of growth at moderate or high C-source concentration, for those processes of recombinant protein production (RPP). Non-limited substrate conditions are widely applied mostly in microbial cultures, both bacteria and yeasts [74–76], and have also outstood among *P. pastoris* expressing heterologous proteins under the control of the alcohol oxidase promoter 1 (P_{AOX1}), very strongly induced by methanol, in strategies that received the name of methanol non-limited fed-batch (MNLFB) [34,69,74,77]. In those cases, the simplicity that methanol limited fed-batch (MLFB) alternatives would have offered was sacrificed in favor of boosting the performance indexes of the process.

1.3.2.3 Alternative fed-batch operational strategies

As stated previously, the design of operational strategies opens a whole world of possibilities. Apart from the alternatives already commented, other limiting parameters can be selected in order to design novel strategies based on them. They are usually considered for the need to deepen into the knowledge of the cell physiology, overcome tricky perturbations of the system and ensure reproducibility against them.

Though kinetic studies are usually carried out in chemostat, this system is very time consuming, especially at low μ, and requires high expenses in substrates, as the common criteria is to wait 4 or 5 residence times to ensure reaching the steady state. So, as a first example of alternative operational strategy, the dynamic pulsed feeding fed-batch was proposed by Dietzsch *et al.* (2011) [78]. In there, a single experiment was enough to determine the main maximum specific rates at different temperatures of a *Pichia pastoris* culture producing the horseradish peroxidase. In Figure 1.6, the performance of this strategy is shown, as the evolution of carbon dioxide evolution rate (CER) and the off-line values of specific methanol uptake rate (q_S) and the specific production rate (q_P). This method, though, present some drawbacks and it is not applicable to any expression system: it leads the process to be exposed to perturbations like cell aging or death or product accumulation. This information, though could be used by the authors afterwards for carrying out a process in the best conditions of temperature, and to perform another alternative operational strategy, a dynamic, using a SLFB-kind of procedure, and which is also suitable for working with mixed substrates [79,80].

Apart from this example, some other reported cases have been brought together in Table 1.3. There, strategies governed by the oxygen availability or temperature can be found, and as well C-source based ones with some more level of complexity, like the use of mixed substrates or the consecution of starving periods to enhance greater production.

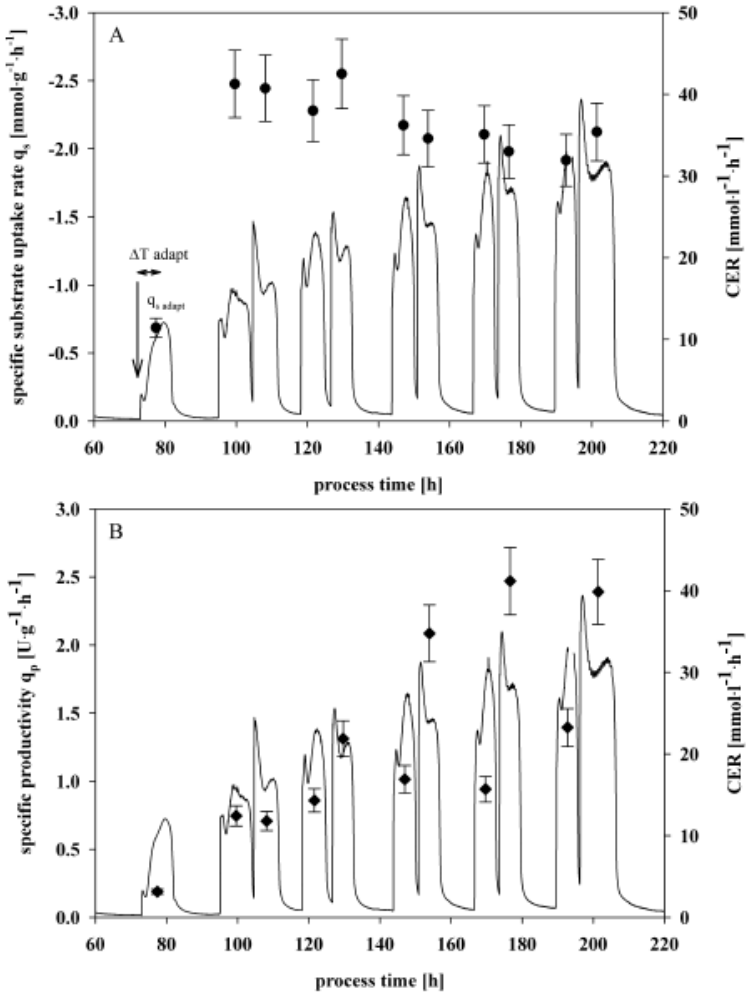

Figure 1.6 Example of a dynamic batch with pulses. Particular case of *P. pastoris*- based process where pulses of methanol were added at different temperatures to evaluate the effect on q_S and q_P [78]. Lines represent carbon dioxide evolution rate (CER) while points indicate either q_S or q_P

As seen in Table 1.3, particular aims of each process lead to choose which component or state variable will be the limiting (or limited) condition. For instance, in OLFB case the authors demonstrated the mAb they produced had a much better ratio of intact N-glycans at hypoxic conditions. Also, limiting the process by its temperature enabled, in TLFB strategy culture, to avoid the production of proteases.

Table 1.3 Examples of operational strategies employed in *P. pastoris* based on criteria out of limiting C-source or in combination with it.

Strategy	Feature	Goal or PI	Product	Op. mode	Reference
Oxygen limited fed batch (OLFB)	Growth at DO = 0% Pulsed feeding	Productivity Product quality	Glycosylated mAb	Fed-batch (growth) + Batch with pulses (induction)	[81]
Oxygen-limiting **+** **MNLFB**	Limitation of methanol and oxygen (in normoxia)	Physiology vs DO Productivity	*Rhizopus oryzae* lipase (ROL)	Fed-batch	[77]
Dynamic pulsed fed batch	Pulsed feeding Normoxia	Physiology vs temperature	Horseradish peroxidase	Fed-batch (batch with pulses)	[78]
MNLFB **+** **(SLFB)**	Dual C-source Growth (SLFB) and induction (MNLFB)	Productivity Repressing effect of C-source	ROL	Fed-batch	[82]
Temperature (T) limited fed-batch (TLFB)	Regulated T by a control of DO	Reduction of proteolysis	Fusion protein CALB + CBM	Fed-batch	[83]
Substrate limited fed-batch **+** **Carbon starving stages**	Periods of glucose starving enhance q_P	Productivity	Antibody fragment	Fed-batch	[84]

1.3.3 Monitoring and control of bioprocesses

The consecution and achievement of a robust, efficient, and reproducible operational strategy in a bioreactor is based on a solid ground in monitoring and control of the main process variables that govern and limit the process that is being performed in it. This section is not intended as an extensive review of the different options of monitoring and control of the state variables taking part in a bioprocess, which have been extensively reviewed, but to highlight the main trends and advances in automatic monitoring and advanced control.

1.3.3.1 Advances in monitoring of bioprocesses

In this section, some non-conventional and also recent advances in monitoring techniques will be reviewed.

This field, on one hand, is evolving towards non-invasive sensors, due to the increasing prominence of the single use bioreactor technology. Another application are microsensors, intended for cultures at scale smaller than the milliliter. An example is the use of optodes for monitoring the main state variables as pH or dissolved oxygen. Their versatility even allows to implement fluorometric detectors, able to monitor, for example, the level of metabolites as riboflavin, which can be indirectly correlated to the biomass concentration [85]. In Figure 1.7 a commercial image from m2p-labs (Baesweiler, Germany), who develop this technology, is shown.

Furthermore, focused beam reflectance measurement (FBRM) and in situ microscopy are also technologies developed for the in-line monitoring of cell count and cell size distribution, and are capable to provide information of changes of morphology of cells that can be indirectly linked to physiologic phenomena.

Moreover, flow injection analysis (FIA) has had, during last decades, a relevant role in monitoring of bioprocesses. It was introduced by Ruzicka and Hansen (1980) [87] and has quickly become accepted for chemical analysis and applied to life sciences because of its flexibility and short response time [88]. It consists on an automatic sampling and analysis that is accomplished by injecting a plug of sample into a flowing carrier stream.

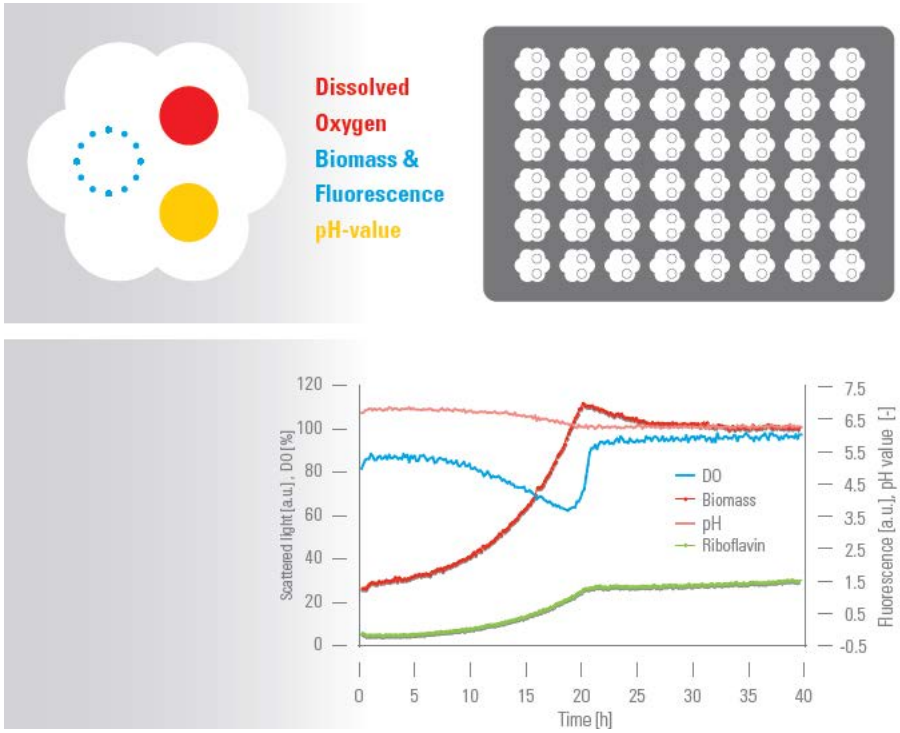

Figure 1.7 Online monitoring of dissolved oxygen and pH by optode technology in microbioreactors (m2p labs GmbH, Baesweiler, Germany) [86].

The versatility of FIA system allows a huge variety of sensors and analysis. Thousands of articles have been published about the application of this technology, but recently Trojanowicz and Kołacińska (2016) [89] carried out a comprehensive review highlighting some hundreds of classic and recent applications. Among those intended to the biotech field, detection of metabolites (both for bioprocess and metabolic flux analysis) and online activity assays, among many others, and can be coupled to powerful and like mass spectrometry (MS) and nuclear magnetic resonance (NMR) spectroscopy. In this document, different variations of the basic FIA are commented. One of them, the sequential injection analysis (SIA) is based on the mixing of the sample with a reagent in order to produce a measurable response [90]. An application for online monitoring methanol, as a substrate of a *P.pastoris* culture, was conducted by Surribas *et al.* (2003) [91], with the objective of designing and conducting bioprocess-efficient operational strategies. A scheme of this methodology is represented in Figure 1.8.

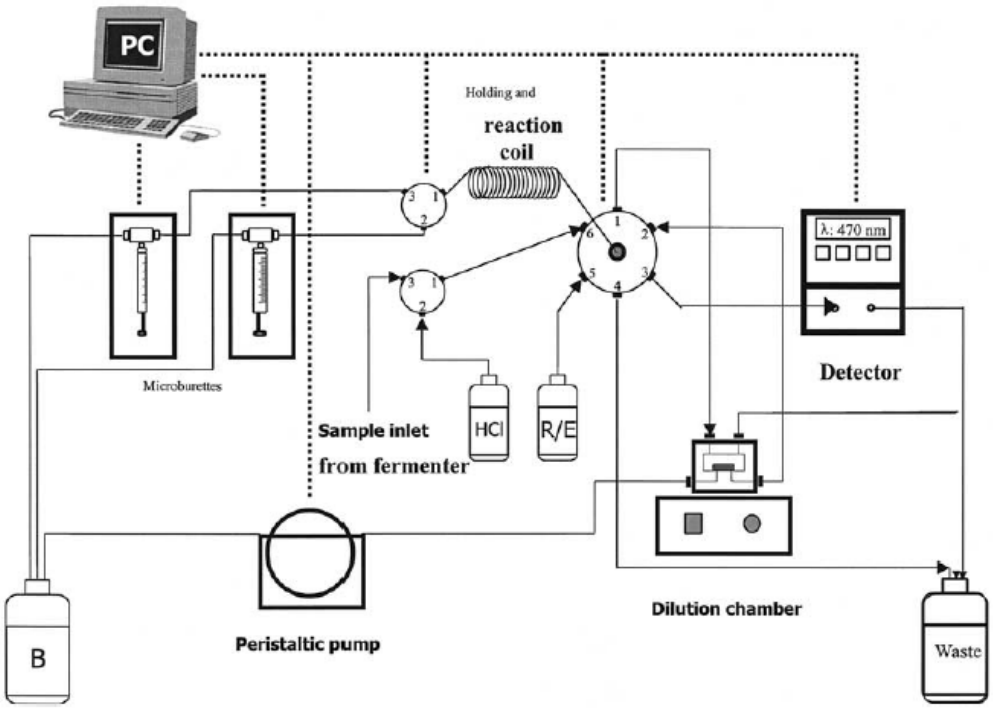

Figure 1.8 Scheme of a SIA built up for the online monitoring of methanol concentration of a *P. pastoris* culture in bioreactor [91].

Finally, it is very remarkable to highlight the recent development and implementation of the concept of software sensors (soft sensors). They are based on indirect measurements of non-accessible parameters, so they require modelling data apart from real time measurement from a hardware sensor [92]. The principle of soft sensors is schemed in Figure 1.9.

The hardware sensor is usually an in-line sensor, which does not require an extraction of the sample, like in SIA/FIA system. A notorious application is the NIR/MIR/RAMAN spectroscopy, allowing the monitoring of multiple metabolites. In the work published by Sivakesava *et al.* (2001) [93] glucose, lactic acid and optical density of a *Lactobacillus casei* could be monitored thanks to this technology. These technologies have been implemented, as well, in *Pichia pastoris* processes, and are widely reported in the literature. Among them, Fourier transform mid infrared (FT-MIR) and NIR spectroscopy for metabolite monitoring (methanol, glucose, lactate) [94–96], or even to perform real-time metabolic flux analysis [97], are some of the most notorious ones.

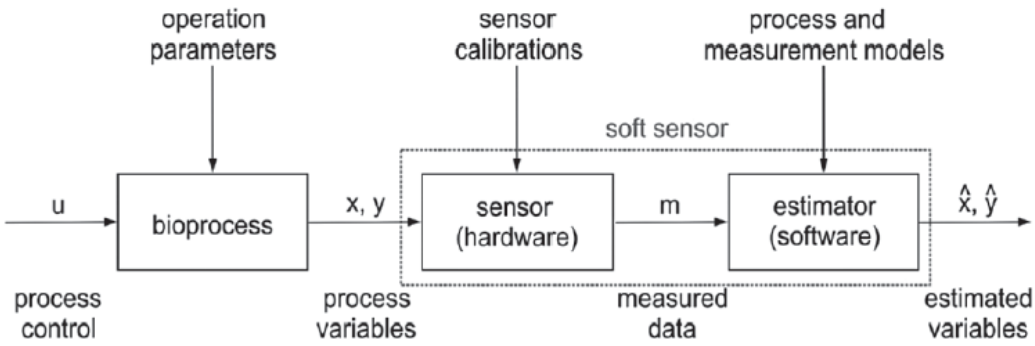

Figure 1.9 Soft sensor principle [92].

Some outstanding examples are, first, estimation of state variables and specific rates (growth, consumption and production) from NIR measurements in *E.coli* [98] or the on-line measurement of oxygen uptake rate (OUR) and carbon dioxide evolution rate (CER) from off-gas analysis in CHO cell cultures [99]. These sensors have also been applied to *Pichia pastoris* processes to successfully estimate specific growth rate, substrates and biomass concentration [100].

1.3.3.2 Main closed-loop control algorithms applied to bioprocesses

The consecution of a robust control is essential to successfully apply the operational strategies that could have been designed to enhance the desired levels of bioprocess efficiency and avoid, perturbations that could hamper the quality of the product.

Though open-loop control of μ (Equation 1.1) has been proved to be effective in some publications, other state variables of most processes must be kept at desired values by closed-loop control, to avoid perturbations, from the most straightforward, like temperature or pH, to other physiological parameters like specific rates or yields, as respiratory quotient (RQ) [101]. A few of closed-loop common types are commented followingly:

- Proportional-Integral-Derivative (PID)

PID represents one of the simplest and most used algorithms for control of all kinds of processes as it is simple to implement and easy to tune. The procedures to do so are quite straightforward (e.g. Ziegler–Nichols) and require no modelling of the system.

$$y(t) = k_c\left(\varepsilon(t) + \frac{1}{\tau_i}\int_0^t \varepsilon(t)\,dt + \tau_D\frac{\mathrm{d}\varepsilon(t)}{\mathrm{d}t}\right)$$

Equation 1.2

Where k_c is the proportional gain, τ_I is the integral time, τ_D derivative time constant, ε is the error (controller input), and y is the controller command (controller output).

- Generic model control (GMC)

GMC was proposed by Lee and Sullivan [102] as a need to overcome control discordances in processes presenting non-linear models. GMC, defines the performance objective in terms of time derivatives of the process output, minimizing the difference between the desired derivative of the process output and the actual derivative, by using information from modelling of the variable of interest. Equation 1.3 illustrates its algorithm:

$$\frac{dy}{dt} = K_1(y_{SP} - y) - K_2\int(y_{SP} - y)dt$$

Equation 1.3

Where y is the measured variable and y_{SP} is the desired value of the control variable. K_1 and K_2 are parameters of the control.

As examples, GMC was employed to control μ in a *E. coli* culture, outcoming PID performance [103].

- Fuzzy

This kind of control is based on the principles of fuzzy logic, i.e overcoming uncertainties without the need of complex models or knowledge of the dynamics of the system. Instead off that, the evaluation of the system dynamics is based uniquely on the experience of the user and an evaluation of the current state of the process, by converting quantitative data into qualitative parameters. Scarce studies, though, have used fuzzy control on biotech applications, since this kind of procedure lead to more process uncertainties due to non-linear process dynamics [104].

- Adaptive control

It consists on non-linear controller algorithms that contains parameters that can change and adapted along an on-going operation, in order to anticipate to system perturbations.

It can be based on previous experimental data or modeling of the system, or the observation of process dynamics behavior.

1.3.4 Optimization of bioprocesses. From modelling to application of customized feeding strategies.

Further knowledge of the system and the physiology is intended, in this section, as a step forward in the accomplishment of the optimal operational strategies. Before bringing any bioprocess up to production scale, it must be assured that the bioprocess engineer has taken the most out of the biocatalyst it is using. The thorough rational design of operational strategies, as explained in section 1.2.1, is the first step on accomplishing that goal. Nevertheless, the combination of mathematical modelling, advanced techniques in monitoring and control and optimization algorithms allows the consecution of next-level strategies, in the form of optimal feeding profiles, boosting the bioprocess efficiency.

The search of customized feeding profiles has been carried out last decades for several processes of RPP and other metabolites in different hosts. Modak *et al.* (1985) [105] reviewed and showed theoretical optimal feeding profiles for different cases of relationships q_P-μ (combinations of monotonical and non-monotonical behaviors) and for different performance indexes. Park (1988) *et al.* [106] built optimal policies for producing polypeptides from a baker's yeast strain out of previous modelled kinetics using a simple Monod-Haldane structure.

1.3.4.1 Modeling cell kinetics. Genome-scale, mechanistic and unstructured modelling

As just stated, kinetic modelling of the physiology of the cell must precede the conceiving of optimal feeding policies. However, possibilities among the complexity of models are very high.

In one hand, on top of the range, genome-scale models (GSM), that have been stablished as key in systems biology for lots of species of microorganisms since about 15 years ago, provide a very accurate approximation of the metabolic behavior of the cell, being able to detect bottlenecks at a very detailed level, either metabolic, transcription or secretion. They are very useful to detect, for instance, target genes for being overexpressed or knocked out to enhance the synthesis of a product of interest or rather to avoid

undesirable pathways, thus to build up efficient bioprocesses that can be driven to industrial scale [107]. Because of their complexity, however, they are often left apart or simplified to design concrete or definitive operational strategies.

In that way, mechanistic models are placed in the middle ground between GSM and the simplest unstructured models. They combine empirical data such as most of kinetics along with mass, heat and momentum balances [108]. Within this category, though, complexity grade is also heterogeneous, since models can be segregated, when distinguishing a cell within a population of different strains or species, and structured, if the cells are considered as a multiple chemical component. Despite this, the rule of thumb in modelling should always be to consider the simplest alternative as possible to describe the system and predict its behavior in future approximations. Simple unsegregated and unstructured models have demonstrated to be rather suitable and have been applied for optimization of bioprocess efficiency [109–112].

1.3.4.2 Optimization of operational feeding strategies

Though it will be thoroughly detailed in chapter 5, the main principles will also be described in this section. As a final step, optimization is fulfilled by following this procedure: built an objective function in which a desired performance index will be optimized; set up the suitable model to describe the bioprocess, as told in the previous section; fix constraints, both for indicating operational limits and avoid numerical discordances and divergences and, finally, select the numerical procedure to solve the whole problem. In this way, options are to be found from the simplest to the most intricate. Generally, numerical methods applied to RPP production are divided into stochastic [110,113] and deterministic ones [114]. Though the former class usually does not fully guarantee global optimality, the main drawback of deterministic ones is the high computing effort it requires.

1.4 Changes of scale in bioprocesses

The change of scale is the last step to culminate the design of a bioprocess, once the bioprocess efficiency has been already achieved by following the steps of previous sections.

Scaling, though, is not a straightforward path. It Is very common to come across the situation of significantly lower efficiencies when changing scale. Among other causes, mainly the unexpected changes of the system hydrodynamics are the main reason of finding these discordances, mostly in processes where three phases coexist, implying mostly problems of mass transfer limitation.

To sum up, the main objective in the change of scale procedure consists on selecting the conditions to reproduce the behavior of the whole set of state variables in the next scale. When this procedure involves the design of a new bioreactor, it is then called a scale-up (or down).

1.4.1 Scaling up to pilot and industrial scale

As it will be thoroughly detailed in chapter 7, bioprocesses are generally scaled up by a factor of 10. Some of the scaling-up methods are based on qualitative criteria (rule of thumb) or trial and error.

Rules of similarity are also applied by reproducing the operational parameter that is found the most limiting for the process. Among them, the most common ones are the oxygen mass transfer coefficient (k_La), mixing time, stirring power per volume unit (P/V) or maximum shear stress, among others. While the first one is more used in high-oxygen demanding processes, shear stress is the criterion for those cells that can be easily damaged.

Apart from that, limitations and discordances between scales are also solved by flow analysis, by techniques like real time distribution (RTD), empirical, or even computational fluid dynamics (CFD), based on modelling. There are some published works in the literature on CFD applied in pilot scale, for temperature distribution simulation [115], or to predict, for example, from a 10 L reactor, the flow dynamics of a wastewater bioreactor of 3200 L [116].

1.4.2 Scaling down. The rise of microbioreactors

The recent rise of the microbioreactor technology has given scale down a relevance in bioprocess design, as well as in genetic engineering. That is because of its great potential

as a high-throughput screening tool with a high level of monitoring and control of the process. As it will be more detailed in chapter 6, the technology of Robolector© (m2p-labs, Baesweiler, Germany) is sampling-automatic, and makes possible to have working volumes of less than 1mL, avoiding thus a great amount of resources in a microtiter plate of 48 wells. Apart from that, the most promising feature of this technology is the possibility of performing simple fed-batch operational strategies. Scale down procedure, then, takes all sense, since the establishment of this system, apart from clone screening, for testing host cells directly to the conditions of the bench-top scale bioreactor (or at least at similar ones), will definitely overcome shake flasks as the standard method to do so, since they are more time and resource consuming, less reproducible and do not allow fed-batch-continuous feeding strategies and complex monitoring.

Robolector, appearing in Figure 1.10, has been successfully applied for different expressions systems, like *Corynebacterium glutamicum* [117] and *P. pastoris* [85].

Figure 1.10 Sample image of RoboLector microbioreactor technology [86].

1.5 References

[1] M. Ladisch, The Role of Bioprocess Engineering in Biotechnology, Bridg. 34 (2004) 25–32.

[2] G. Walsh, Second-generation biopharmaceuticals, Eur. J. Pharm. Biopharm. 58 (2004) 185–196.

[3] C.P. Hollenberg, A.W.M. Strasser, Improvement of Baker's and Brewer's Yeast by Gene Technology, Food Biotechnol. 4 (1990) 527–534.

[4] T. Vasiljevic, P. Jelen, Production of β-galactosidase for lactose hydrolysis in milk and dairy products using thermophilic lactic acid bacteria, Innov. Food Sci. Emerg. Technol. 2 (2001) 75–85.

[5] S. Herrera, Industrial biotechnology-a chance at redemption, Nat. Biotechnol. 22 (2004) 671–675.

[6] P.M. Doran, Bioprocess Engineering Principles, 1st ed., Academic Press Inc., San Diego, 1995.

[7] J.L. Cereghino, J.M. Cregg, Heterologous protein expression in the methylotrophic yeast *Pichia pastoris*, FEMS Microbiol. Rev. 24 (2000) 45–66.

[8] J.M. Cregg, K.J. Barringer, A.Y. Hessler, K.R. Madden, Pichia pastoris as a host system for transformations, Mol. Cell. Biol. 5 (1985) 3376–3385.

[9] J. Heyland, J. Fu, L.M. Blank, A. Schmid, Quantitative physiology of Pichia pastoris during glucose-limited high-cell density fed-batch cultivation for recombinant protein production., Biotechnol. Bioeng. 107 (2010) 357–68.

[10] M. Hasslacher, M. Schall, M. Hayn, R. Bona, K. Rumbold, J. Lückl, H. Griengl, S.D. Kohlwein, H. Schwab, High-Level Intracellular Expression of Hydroxynitrile Lyase from the Tropical Rubber Tree *Hevea brasiliensisin* Microbial Hosts, Protein Expr. Purif. 11 (1997) 61–71.

[11] M. Ahmad, M. Hirz, H. Pichler, H. Schwab, Protein expression in *Pichia pastoris*: Recent achievements and perspectives for heterologous protein production, Appl.

Microbiol. Biotechnol. 98 (2014) 5301–5317.

[12] A.L. Demain, P. Vaishnav, Production of recombinant proteins by microbes and higher organisms, Biotechnol. Adv. 27 (2009) 297–306.

[13] J.H. Sohn, H.A. Kang, K.J. Rao, C.H. Kim, E.S. Choi, B.H. Chung, S.K. Rhee, Current status of the anticoagulant hirudin: Its biotechnological production and clinical practice, Appl. Microbiol. Biotechnol. 57 (2001) 606–613.

[14] C. Dale, A. Allen, S. Fogarty, *Pichia pastoris*: a eukaryotic system for the large-scale production of biopharmaceuticals, Biopharm. 12 (1999) 36–42.

[15] V. Ciofalo, N. Barton, J. Kreps, I. Coats, D. Shanahan, Safety evaluation of a lipase enzyme preparation, expressed in *Pichia pastoris*, intended for use in the degumming of edible vegetable oil, Regul. Toxicol. Pharmacol. 45 (2006) 1–8.

[16] C.A. Thompson, FDA approves kallikrein inhibitor to treat hereditary angioedema, Am. J. Heal. Pharm. 67 (2010) 93.

[17] C. Julien, Production of Humanlike Recombinant Proteins in *Pichia pastoris*, BioProcess Tech. 4 (2006) 22–31.

[18] F. Sarmiento, R. Peralta, J.M. Blamey, Cold and Hot Extremozymes: Industrial Relevance and Current Trends, Front. Bioeng. Biotechnol. 3:148 (2015).

[19] J. Clare, K. Sreekrishna, M. Romanos, Expression of tetanus toxin fragment C, Methods Mol. Biol. 103 (1998) 193–208.

[20] R. Vad, E. Nafstad, L.A. Dahl, O.S. Gabrielsen, Engineering of a Pichia pastoris expression system for secretion of high amounts of intact human parathyroid hormone, J. Biotechnol. 116 (2005) 251–260.

[21] L.M. Damasceno, I. Pla, H.J. Chang, L. Cohen, G. Ritter, L.J. Old, C.A. Batt, An optimized fermentation process for high-level production of a single-chain Fv antibody fragment in *Pichia pastoris*, Protein Expr. Purif. 37 (2004) 18–26.

[22] C.P. Kurtzman, Biotechnological strains of *Komagataella (Pichia) pastoris* are *Komagataella phaffii* as determined from multigene sequence analysis, J. Ind. Microbiol. Biotechnol. 36 (2009) 1435–1438.

[23] T. Vogl, A. Glieder, Regulation of Pichia pastoris promoters and its consequences for protein production., N. Biotechnol. 30 (2013) 385–404.

[24] K. Kobayashi, S. Kuwae, T. Ohya, T. Ohda, M. Ohyama, K. Tomomitsu, Addition of oleic acid increases expression of recombinant human serum albumin by the *AOX2*promoter in *Pichia pastoris*, J. Biosci. Bioeng. 89 (2000) 479–84.

[25] H.R. Waterham, M.E. Digan, P.J. Koutz, S. V. Lair, J.M. Cregg, Isolation of the *Pichia pastoris* glyceraldehyde-3-phosphate dehydrogenase gene and regulation and use of its promoter, Gene. 186 (1997) 37–44.

[26] S. Shen, G. Sulter, T.W. Jeffries, J.M. Cregg, A strong nitrogen source-regulated promoter for controlled expression of foreign genes in the yeast *Pichia pastoris*, Gene. 216 (1998) 93–102.

[27] H. Liu, X. Tan, K.A. Russell, M. Veenhuis, J.M. Cregg, *PER3*, a Gene Required for Peroisome Biogenesis in *Pichia pastoris*, Encodes a Peroxisomal Membrane Protein Involved in Protein Import, J. Biol. Chem. 270 (1995) 10940–10951.

[28] I.B. Sears, J. O'Connor, O.W. Rossanese, B.S. Glick, A versatile set of vectors for constitutive and regulated gene expression in *Pichia pastoris*, Yeast. 14 (1998) 783–790.

[29] J.F. Tschopp, P.F. Brust, J.M. Cregg, C.A. Stillman, T.R. Gingeras, Expression of the lacZ gene from two methanol-regulated promoters in *Pichia pastoris*, Nucleic Acids Res. 15 (1987) 3859–3876.

[30] J.R.M. de Almeida, L.M.P. de Moraes, F.A.G. Torres, Molecular characterization of the 3-phosphoglycerate kinase gene (*PGK1*) from the methylotrophic yeast *Pichia pastoris*, Yeast. 22 (2005) 725–737.

[31] G. Stadlmayr, A. Mecklenbräuker, M. Rothmüller, M. Maurer, M. Sauer, D. Mattanovich, B. Gasser, Identification and characterisation of novel *Pichia pastoris* promoters for heterologous protein production, J. Biotechnol. 150 (2010) 519–29.

[32] T. Vogl, L. Sturmberger, T. Kickenweiz, R. Wasmayer, C. Schmid, A.M. Hatzl, M.A. Gerstmann, J. Pitzer, M. Wagner, G.G. Thallinger, M. Geier, A. Glieder, A Toolbox of Diverse Promoters Related to Methanol Utilization: Functionally Verified Parts for

Heterologous Pathway Expression in *Pichia pastoris*, ACS Synth. Biol. 5 (2016) 172–186.

[33] B. Gasser, M.G. Steiger, D. Mattanovich, Methanol regulated yeast promoters: production vehicles and toolbox for synthetic biology, Microb. Cell Fact. 14 (2015) 196.

[34] O. Cos, R. Ramón, J.L. Montesinos, F. Valero, Operational strategies, monitoring and control of heterologous protein production in the methylotrophic yeast *Pichia pastoris* under different promoters: A review, Microb. Cell Fact. 5 (2006) 17.

[35] A.L. Zhang, J.X. Luo, T.Y. Zhang, Y.W. Pan, Y.H. Tan, C.Y. Fu, F.-Z. Tu, Recent advances on the *GAP* promoter derived expression system of *Pichia pastoris*, Mol. Biol. Rep. 36 (2009) 1611–1619.

[36] H.L. Chum, R.P. Overend, Biomass and renewable fuels, Fuel Process. Technol. 71 (2001) 187–195.

[37] J.M. Cregg, K.R. Madden, K.J. Barringer, G.P. Thill, C.A. Stillman, Functional characterization of the two alcohol oxidase genes from the yeast *Pichia pastoris*, Mol. Cell. Biol. 9 (1989) 1316–23.

[38] F.S. Hartner, A. Glieder, Regulation of methanol utilisation pathway genes in yeasts, Microb. Cell Fact. 5 (2006) 39.

[39] O. Cos, D. Resina, P. Ferrer, J.L. Montesinos, F. Valero, Heterologous production of *Rhizopus oryzae* lipase in *Pichia pastoris* using the alcohol oxidase and formaldehyde dehydrogenase promoters in batch and fed-batch cultures, Biochem. Eng. J. 26 (2005) 86–94.

[40] P. Koutz, G.R. Davis, C. Stillman, K. Barringer, J. Cregg, G. Thill, Structural comparison of the *Pichia pastoris* alcohol oxidase genes, Yeast. 5 (1989) 167–177.

[41] Stuart A. Rosenfield, Use of *Pichia pastoris* for Expression of Recombinant Proteins, Methods Enzymol. Vol 306. 306 (1999) 154–169.

[42] J.M. Cregg, K.R. Madden, Development of yeast transformation systems and construction of methanol-utilization-defective mutants of *Pichia pastoris* by gene

disruption, in: G.G. Stewart, I. Russell, R.. Klein, R.R. Hiebsch (Eds.), Biol. Res. Ind. Yeasts, Vol. II, CRC Press, Inc., Boca Raton, FL, 1987: pp. 1–18.

[43] V. Chiruvolu, J.M. Cregg, M.M. Meagher, Recombinant protein production in an alcohol oxidase-defective strain of *Pichia pastoris* in fedbatch fermentations, Enzyme Microb. Technol. 21 (1997) 277–283.

[44] Y. Yu, X. Zhou, S. Wu, T. Wei, L. Yu, High-yield production of the human lysozyme by *Pichia pastoris* SMD1168 using response surface methodology and high-cell-density fermentation, Electron. J. Biotechnol. 17 (2014) 311–316.

[45] B. Li, Y. Cao, L. Zhou, C. Liang, F. Sun, A novel protein expression system-PichiaPink™- and a protocol for fast and efficient recombinant protein expression, African J. Biotechnol. 10 (2011) 19464–19472.

[46] A. Várnai, C. Tang, O. Bengtsson, A. Atterton, G. Mathiesen, V.G. Eijsink, Expression of endoglucanases in *Pichia pastoris* under control of the *GAP* promoter, Microb. Cell Fact. 13 (2014) 57.

[47] L. Meuris, F. Santens, G. Elson, N. Festjens, M. Boone, A. Dos Santos, S. Devos, F. Rousseau, E. Plets, E. Houthuys, P. Malinge, G. Magistrelli, L. Cons, L. Chatel, B. Devreese, N. Callewaert, GlycoDelete engineering of mammalian cells simplifies N-glycosylation of recombinant proteins., Nat. Biotechnol. 32 (2014) 485–9.

[48] K. Claes, K. Vandewalle, B. Laukens, T. Laeremans, O. Vosters, I. Langer, M. Parmentier, J. Steyaert, N. Callewaert, Modular Integrated Secretory System Engineering in *Pichia pastoris* to Enhance G-Protein Coupled Receptor Expression, ACS Synth. Biol. 5 (2016) 1070–1075.

[49] S. Minning, C. Schmidt-Dannert, R.D. Schmid, Functional expression of *Rhizopus oryzae* lipase in *Pichia pastoris*: high-level production and some properties, J Biotechnol. 66 (1998) 147–156.

[50] T. Vogl, F.S. Hartner, A. Glieder, New opportunities by synthetic biology for biopharmaceutical production in *Pichia pastoris*, Curr. Opin. Biotechnol. 24 (2013) 1094–1101.

[51] B. Laukens, C. De Visscher, N. Callewaert, Engineering yeast for producing human

glycoproteins: where are we now?, Future Microbiol. 10 (2015) 21–34.

[52] F.S. Hartner, C. Ruth, D. Langenegger, S.N. Johnson, P. Hyka, G.P. Lin-Cereghino, J. Lin-Cereghino, K. Kovar, J.M. Cregg, A. Glieder, Promoter library designed for fine-tuned gene expression in *Pichia pastoris*, Nucleic Acids Res. 36 (2008) 1–15.

[53] S. Capone, J. Horvat, C. Herwig, O. Spadiut, Development of a mixed feed strategy for a recombinant *Pichia pastoris* strain producing with a de-repression promoter, Microb. Cell Fact. 14 (2015) 101.

[54] B.K. Chung, S. Selvarasu, C. Andrea, J. Ryu, H. Lee, J. Ahn, H. Lee, D.-Y. Lee, Genome-scale metabolic reconstruction and in silico analysis of methylotrophic yeast *Pichia pastoris* for strain improvement, Microb. Cell Fact. 9 (2010) 50.

[55] S.B. Sohn, A.B. Graf, T.Y. Kim, B. Gasser, M. Maurer, P. Ferrer, D. Mattanovich, S.Y. Lee, Genome-scale metabolic model of methylotrophic yeast *Pichia pastoris* and its use for in silico analysis of heterologous protein production, Biotechnol. J. 5 (2010) 705–715.

[56] M. Tomàs-Gamisans, P. Ferrer, J. Albiol, Integration and validation of the genome-scale metabolic models of *Pichia pastoris*: A comprehensive update of protein glycosylation pathways, lipid and energy metabolism, PLoS One. 11 (2016) 1–24.

[57] T. Gaj, C.A. Gersbach, C.F. Barbas, ZFN, TALEN, and CRISPR/Cas-based methods for genome engineering, Trends Biotechnol. 31 (2013) 397–405.

[58] A. Weninger, A.M. Hatzl, C. Schmid, T. Vogl, A. Glieder, Combinatorial optimization of CRISPR/Cas9 expression enables precision genome engineering in the methylotrophic yeast Pichia pastoris, J. Biotechnol. 235 (2016) 139–149.

[59] M. Känsäkoski, M. Kurkinen, N. von Weymarn, N. Pentti, P. Neubauer, E. Juuso, T. Eerikäinen, S. Turunen, S. Aho, P. Suhonen, Process analytical technology (PAT) needs and applications in the bioprocess industry, VTT Work. Pap. 60 (2006) 5–100.

[60] P.D. Bade, S.P. Kotu, A.S. Rathore, Optimization of a refolding step for a therapeutic fusion protein in the quality by design (QbD) paradigm, J. Sep. Sci. 35 (2012) 3160–3169.

[61] D. Zalai, A. Golabgir, P. Wechselberger, A. Putics, C. Herwig, Advanced Development Strategies for Biopharmaceutical Cell Culture Processes, Curr. Pharm. Biotechnol. 16 (2015) 983–1001.

[62] D. Bailey, E. Wright, Practical SCADA for industry, 1st ed., Elsevier, Burlington, 2003.

[63] M. Metzger, Logix-based system for distributed process control of semi industrial pilot plants, IFAC Proc. Vol. 37 (2004) 130–135.

[64] K. Joeris, A. Johnson, M. Brosnan, C. Cruz, C. Zhang, M. Burnett, K. Konstantinov, Integrating disparate analytical instrumentation into an automated process control system used in cell culture process development, in: 10th Int. IFAC Symp. Comput. Appl. Biotechnol., Cancún, 2007: pp. 407–410.

[65] Sartorius Stedim Biotech, Bioprocess Design Engineering, (2017). https://www.sartorius.es/sartoriusES/es/EUR/integrated-solutions/bioprocess-design-engineering (accessed June 23, 2017).

[66] S. Aiba, M. Shoda, M. Nagatani, Kinetics of product inhibition in alcohol fermentation, Biotechnol. Bioeng. 10 (1968) 845–864.

[67] J.H. Luong, Generalization of monod kinetics for analysis of growth data with substrate inhibition., Biotechnol. Bioeng. 29 (1987) 242–248.

[68] T. Egli, Microbial growth and physiology: A call for better craftsmanship, Front. Microbiol. 6 (2015) 1–12.

[69] V. Looser, B. Bruhlmann, F. Bumbak, C. Stenger, M. Costa, A. Camattari, D. Fotiadis, K. Kovar, Cultivation strategies to enhance productivity of *Pichia pastoris*: A review, Biotechnol. Adv. 33 (2014) 1177–1193.

[70] D. Calleja, A. Fernández-Castañé, M. Pasini, C. de Mas, J. López-Santín, Quantitative modeling of inducer transport in fed-batch cultures of *Escherichia coli*, Biochem. Eng. J. 91 (2014) 210–219.

[71] F. Li, N. Vijayasankaran, A. Shen, R. Kiss, A. Amanullah, Cell culture processes for monoclonal antibody production, MAbs. 2 (2010) 466–479.

[72] W. Zhang, M.A. Bevins, B.A. Plantz, L.A. Smith, M.M. Meagher, Modeling *Pichia*

pastoris growth on methanol and optimizing the production of a recombinant protein, the heavy-chain fragment C of botulinum neurotoxin, serotype A, Biotechnol. Bioeng. 70 (2000) 1–8.

[73] M. Jahic, A. Veide, T. Charoenrat, T. Teeri, S.-O. Enfors, Process technology for production and recovery of heterologous proteins with *Pichia pastoris*, Biotechnol. Prog. 22 (2006) 1465–73.

[74] J.M. Barrigón, J.L. Montesinos, F. Valero, Searching the best operational strategies for *Rhizopus oryzae* lipase production in *Pichia pastoris* Mut+ phenotype: Methanol limited or methanol non-limited fed-batch cultures?, Biochem. Eng. J. 75 (2013) 47–54.

[75] S. Alfenore, X. Cameleyre, L. Benbadis, C. Bideaux, J.L. Uribelarrea, G. Goma, C. Molina-Jouve, S.E. Guillouet, Aeration strategy: A need for very high ethanol performance in *Saccharomyces cerevisiae* fed-batch process, Appl. Microbiol. Biotechnol. 63 (2004) 537–542.

[76] M. Arndt, S. Kleist, G. Miksch, K. Friehs, E. Flaschel, J. Trierweiler, B. Hitzmann, A feedforward-feedback substrate controller based on a Kalman filter for a fed-batch cultivation of *Escherichia coli* producing phytase, Comput. Chem. Eng. 29 (2005) 1113–1120.

[77] X. Ponte, J.L. Montesinos-Seguí, F. Valero, Bioprocess efficiency in *Rhizopus oryzae* lipase production by *Pichia pastoris* under the control of P*AOX1* is oxygen tension dependent, Process Biochem. 51 (2016) 1954–1963.

[78] C. Dietzsch, O. Spadiut, C. Herwig, A dynamic method based on the specific substrate uptake rate to set up a feeding strategy for *Pichia pastoris*, Microb. Cell Fact. 10 (2011) 14.

[79] D. Zalai, C. Dietzsch, C. Herwig, O. Spadiut, A dynamic fed batch strategy for a Pichia pastoris mixed feed system to increase process understanding, Biotechnol. Prog. 28 (2012) 878–86.

[80] O. Spadiut, D. Zalai, C. Dietzsch, C. Herwig, Quantitative comparison of dynamic physiological feeding profiles for recombinant protein production with Pichia

pastoris, Bioprocess Biosyst. Eng. 37 (2014) 1163–1172.

[81] M. Berdichevsky, M. D'Anjou, M.R. Mallem, S.S. Shaikh, T.I. Potgieter, Improved production of monoclonal antibodies through oxygen-limited cultivation of glycoengineered yeast, J. Biotechnol. 155 (2011) 217–224.

[82] C. Arnau, C. Casas, F. Valero, The effect of glycerol mixed substrate on the heterologous production of a *Rhizopus oryzae* lipase in *Pichia pastoris* system, Biochem. Eng. J. 57 (2011) 30–37.

[83] M. Jahic, F. Wallberg, M. Bollok, P. Garcia, S. Enfors, Temperature limited fed-batch technique for control of proteolysis in *Pichia pastoris* bioreactor cultures, Microb. Cell Fact. 2:6 (2003).

[84] X. Garcia-Ortega, N. Adelantado, P. Ferrer, J.L. Montesinos, F. Valero, A step forward to improve recombinant protein production in *Pichia pastoris*: From specific growth rate effect on protein secretion to carbon-starving conditions as advanced strategy, Process Biochem. 51 (2016) 681–691.

[85] J. Hemmerich, N. Adelantado, J. Barrigón, X. Ponte, A. Hörmann, P. Ferrer, F. Kensy, F. Valero, Comprehensive clone screening and evaluation of fed-batch strategies in a microbioreactor and lab scale stirred tank bioreactor system: application on *Pichia pastoris* producing *Rhizopus oryzae* lipase, Microb. Cell Fact. 13 (2014) 36.

[86] m2p-labs | Microbioreactors, (2017). http://www.m2p-labs.com (accessed June 22, 2017).

[87] J. Růžička, E.H. Hansen, Flow injection analysis. principles, applications and trends, Anal. Chim. Acta. 114 (1989) 19–44.

[88] K. Schügerl, Progress in monitoring, modeling and control of bioprocesses during the last 20 years., J. Biotechnol. 85 (2001) 149–173.

[89] M. Trojanowicz, K. Kołacińska, Recent advances in flow injection analysis, Analyst. 141 (2016) 2085–2139.

[90] J. Ruzicka, G.D. Marshall, Sequential injection: a new concept for chemical sensors, process analysis and laboratory assays, Anal. Chim. Acta. 237 (1990) 329–343.

[91] A. Surribas, O. Cos, J.L. Montesinos, F. Valero, On-line monitoring of the methanol concentration in *Pichia pastoris*, Biotechnol. Lett. 25 (2003) 1795–1800.

[92] R. Luttmann, D.G. Bracewell, G. Cornelissen, K. V. Gernaey, J. Glassey, V.C. Hass, C. Kaiser, C. Preusse, G. Striedner, C.F. Mandenius, Soft sensors in bioprocessing: A status report and recommendations, Biotechnol. J. 7 (2012) 1040–1048.

[93] S. Sivakesava, J. Irudayaraj, D. Ali, Simultaneous determination of multiple components in lactic acid fermentation using FT-MIR, NIR, and FT-Raman spectroscopic techniques, Process Biochem. 37 (2001) 371–378.

[94] J. Crowley, B. Mccarthy, N.S. Nunn, L.M. Harvey, B. McNeil, Monitoring a recombinant *Pichia pastoris* fed batch process using Fourier transform mid-infrared spectroscopy (FT-MIRS), Biotechnol. Lett. 22 (2000) 1907–1912.

[95] J. Crowley, S.A. Arnold, N. Wood, L.M. Harvey, B. McNeil, Monitoring a high cell density recombinant *Pichia pastoris* fed-batch bioprocess using transmission and reflectance near infrared spectroscopy, Enzyme Microb. Technol. 36 (2005) 621–628.

[96] M. Goldfeld, J. Christensen, D. Pollard, E.R. Gibson, J.T. Olesberg, E.J. Koerperick, K. Lanz, G.W. Small, M.A. Arnold, C.E. Evans, Advanced near-infrared monitor for stable real-time measurement and control of *Pichia pastoris* bioprocesses, Biotechnol. Prog. 30 (2014) 749–759. doi:10.1002/btpr.1890.

[97] M.L. Fazenda, J.M.L. Dias, L.M. Harvey, A. Nordon, R. Edrada-Ebel, D. Littlejohn, B. McNeil, Towards better understanding of an industrial cell factory: investigating the feasibility of real-time metabolic flux analysis in *Pichia pastoris*, Microb. Cell Fact. 12 (2013) 51.

[98] B. Warth, G. Rajkai, C.F. Mandenius, Evaluation of software sensors for on-line estimation of culture conditions in an *Escherichia coli* cultivation expressing a recombinant protein, J. Biotechnol. 147 (2010) 37–45.

[99] M. Aehle, A. Kuprijanov, S. Schaepe, R. Simutis, A. Lübbert, Simplified off-gas analyses in animal cell cultures for process monitoring and control purposes, Biotechnol. Lett. 33 (2011) 2103–2110.

[100] J.M. Barrigon, R. Ramon, I. Rocha, F. Valero, E.C. Ferreira, J.L. Montesinos, State and Specific Growth Estimation in Heterologous Protein Production by *Pichia pastoris*, AIChe J. 58 (2012) 2966–2979.

[101] C.J. Franzén, Metabolic flux analysis of RQ-controlled microaerobic ethanol production by *Saccharomyces cerevisiae*, Yeast. 20 (2003) 117–132.

[102] P.L. Lee, G.R. Sullivan, Generic model control (GMC), Comput. Chem. Eng. 12 (1988) 573–580.

[103] M. Jenzsch, R. Simutis, A. Luebbert, Generic model control of the specific growth rate in recombinant Escherichia coli cultivations, J. Biotechnol. 122 (2006) 483–493.

[104] M. a. Hisbullah, K.B. Ramachandran, Design of a Fuzzy Logic Controller for Regulating Substrate Feed to Fed-Batch Fermentation, Food Bioprod. Process. 81 (2003) 138–146.

[105] J.M. Modak, H.C. Lim, Y.J. Tayeb, General characteristics of optimal feed rate profiles for various fed-batch fermentation processes, Biotechnol. Bioeng. 28 (1986) 1396–1407.

[106] S. Park, W.F. Ramirez, Optimal Production of Secreted Protein in Fed-Batch Reactors, AIChe J. 34 (1988) 1550–1558.

[107] M.A. Oberhardt, B.Ø. Palsson, J.A. Papin, Applications of genome-scale metabolic reconstructions, Mol. Syst. Biol. 5 (2009) 1–15.

[108] K. V. Gernaey, A.E. Lantz, P. Tufvesson, J.M. Woodley, G. Sin, Application of mechanistic models to fermentation and biocatalysis for next-generation processes, Trends Biotechnol. 28 (2010) 346–354.

[109] J.M. Barrigon, F. Valero, J.L. Montesinos, A macrokinetic model-based comparative meta-analysis of recombinant protein production by *Pichia pastoris* under *AOX1* promoter, Biotechnol. Bioeng. 112 (2015) 1132–1145.

[110] M. Maurer, M. Kühleitner, B. Gasser, D. Mattanovich, Versatile modeling and optimization of fed batch processes for the production of secreted heterologous

proteins with *Pichia pastoris*, Microb. Cell Fact. 5:37 (2006).

[111] W. Zhang, C.P. Liu, M. Inan, M.M. Meagher, Optimization of cell density and dilution rate in *Pichia pastoris* continuous fermentations for production of recombinant proteins, J. Ind. Microbiol. Biotechnol. 31 (2004) 330–334.

[112] H. Ren, J. Yuan, Model-based specific growth rate control for *Pichia pastoris* to improve recombinant protein production, J. Chem. Technol. Biotechnol. 80 (2005) 1268–1272.

[113] K. Kobayashi, S. Kuwae, T. Ohya, T. Ohda, M. Ohyama, K. Tomomitsu, High level secretion of recombinant human serum albumin by fed-batch fermentation of the methylotrophic yeast, *Pichia pastoris*, based on optimal methanol feeding strategy, J. Biosci. Bioeng. 90 (2000) 280–288.

[114] P.M. Bapat, N.U. Padiyar, N.N. Dave, S. Bhartiya, P.P. Wangikar, S. Dash, Model-Based Optimization of Feeding Recipe for Rifamycin Fermentation, AIChe J. 52 (2006) 4249–4257.

[115] X. Gao, D.P. Shi, X.Z. Chen, Z.H. Luo, Three-dimensional CFD model of the temperature field for a pilot-plant tubular loop polymerization reactor, Powder Technol. 203 (2010) 574–590.

[116] P. Dama, J. Bell, K.M. Foxon, C.J. Brouckaert, T. Huang, C.A. Buckley, V. Naidoo, D. Stuckey, Pilot-scale study of an anaerobic baffled reactor for the treatment of domestic wastewater, Water Sci. Technol. 46 (2002) 263–270.

[117] P. Rohe, D. Venkanna, B. Kleine, R. Freudl, M. Oldiges, An automated workflow for enhancing microbial bioprocess optimization on a novel microbioreactor platform, Microb. Cell Fact. 11 (2012) 144.

2. OBJECTIVES

The main aims that have been pursued by the consecution of this thesis are summarized here. In a general point of view, enhancing the bioprocess efficiency in the production of a lipase from *Rhizopus oryzae* (ROL) expressed in *Pichia pastoris* under the control of P_{AOX1}, using proper operational strategies with methanol as a sole carbon source and inducer. This objective can be divided into the following points: and in

- Enhancing the supervision, monitoring and control of this bioprocess carried out in a 5 L bench-top bioreactor, by the communication of new monitoring hardware and building easy-to-use, versatile and automatic applications for feeding strategies.
- To evaluate and characterize the influence of the oxygen tension on the bioprocess efficiency, so that to be able to deal with limitations it offers in a wide range within normoxic conditions.
- By the implementation of off-gas analyzers in fed-batch mode, experimental validation is sought by the elemental balances calculations and the
- The optimization of feeding strategies in bench-top scale, as one of the main pillars of this dissertation. With that, top levels of ROL bioprocess efficiency are sought in terms of the performance indexes of industrial interest.
- Finally, the change of scale of this process is sought in both ways, up to a pilot scale and to microbioreactor system. The consecution of this objective is not straightforward, due to the need to deal with a bioprocess based on methanol feeding strategies, a very volatile substrate, as well as very high oxygen-demanding.

3 PRELIMINAR RESULTS: *Pichia pastoris* PRODUCING *Rhizopus oryzae* LIPASE UNDER P_{AOX1} CONTROL. FIRST STEPS TO THE OPTIMIZATION OF BIOPROCESS EFFICIENCY

3.1 Introduction. First step process improvements in bench-top bioreactor fermentation

Previously to (and during) the following systematic studies to accomplish the main objective of this dissertation, some considerations were taken into account in a way to implement some improvements regarding, in one hand, monitoring and supervising of the system, but also about the feeding strategy used for the supplying of nitrogen source. With that, reproducibility and system robustness are expected to be improved.

3.1.1 Stirred-tank bioreactors

First of all, the aim of this section is to present the main equipment that has been exploited to cultivate *P. pastoris* for the experiments proposed for this PhD dissertation.

A total of three commercial stirred-tank bioreactors have been used: two bench-top and a pilot scale one. This last one belongs to the service *Planta Pilot de Fermentació* (Department of Chemical, Biological and Environmental Engineering, UAB, Barcelona, Spain). Their main geometric features, as well as general operation and instrumentation characteristics, are listed in Table 3.1.

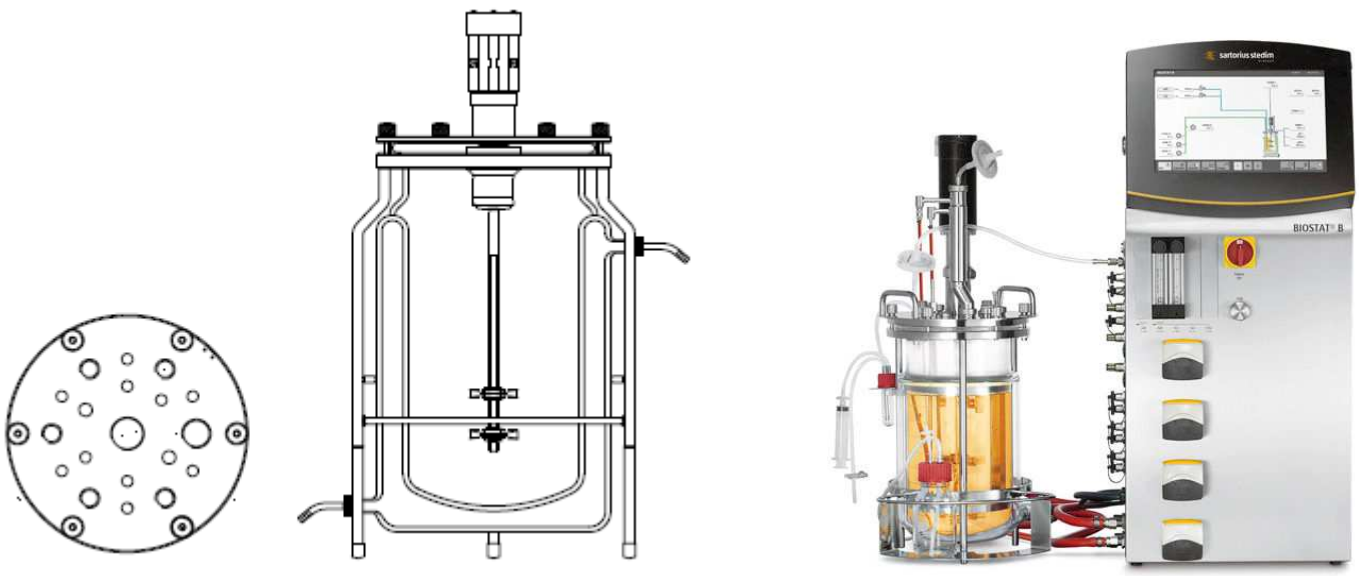

Figure 3.1 General lay-out of bench-top bioreactors supplied by the manufacturing companies. On the left, a scheme of ez-Control BioBundle 7L (Applikon). On the right, Biostat B 5L bioreactor for microbial cultures (Sartorius).

Table 3.1 Main geometric and general operation features of the bioreactors that have been used in this PhD thesis at the Department of Chemical, Biological and Environmental Engineering (UAB)

Specification	Units	Applikon *ez*-Control BioBundle[1]	Sartorius Biostat B[2]	Braun Biostat UD[2]
Scale	-	Lab	Lab	Pilot
Nominal volume	L	7	5	74
Max. working volume	L	4.7	4.3	53
Min. working volume	L	2	2	20
Inner diameter (D_I)	m	0.160	0.160	0.315
Inner height (H)	m	0.276	0.341	0.964
Liquid height (H_L) (without aeration)	m	0.235	0.215	0.685
Ratio H_L/D_I	-	1.5	1.3	2.2
Impellers	-	3 Rushton*	3 Rushton*	3 Rushton*
Heat exchange system	-	Jacketed	Jacketed	Jacketed
Heat exchange fluid	-	Water (external 5ºC cold water)	Water (external 5ºC cold water)	Water (external 5ºC cold water)
Dissolved oxygen detection	-	Polarographic	Optic	Polarographic
Off-gas composition analysis	-	BlueSens BCPreFerm O_2 and CO_2	No	No
Stirring rate range	rpm	0-1500	0-2000	0-800
Aeration rate range	L min^{-1}	0-10 (air) 0-3 (O_2)	0-10 (air) 0-5 (O_2)	0-200 (air) 0-50 (O_2)
Aeration rate instrumentation	-	Mass flow controllers (MFC)	MFC	Rotameters
Automatic gas mix	-	No	No	Yes (Air-O_2-N_2)

*2 impellers are submerged at initial broth volume

[1] Applikon Biotechnology B.V, Delft, Netherlands.

[2] Sartorius Stedim Biotech, Göttingen, Germany.

3.1.2 Monitoring, control and supervision of the bioprocess. National Instruments LabVIEW

LabVIEW (National Instruments, Austin, TX), which stands for Laboratory Virtual Instrumentation Engineering Workbench is a graphical programming language first released in 1986. It implements a language that differs from other ones based on written code, allowing easy conception of new applications and modification of the ones already existing. Each function or program is stored as a virtual instrument (VI), and it is structured and hierarchically organized in different subvirtual instruments (subVI) [1].

LabVIEW stands out as a very suitable and versatile platform for bench-top instrumentation and automation, as a tool that integrates peripheral communications, manages process flow, executes all kinds of control algorithms and allows the continuous data acquisition of any variable of the system being monitored. With that, every node in the flow diagram is then present in a front panel, where the user can build and distribute, functionally and aesthetically, an organized control panel to rationally supervise the process at real time. In Figure 3.2, it is shown a sample window of a small part of the VI that was used for the run of the cultures carried out.

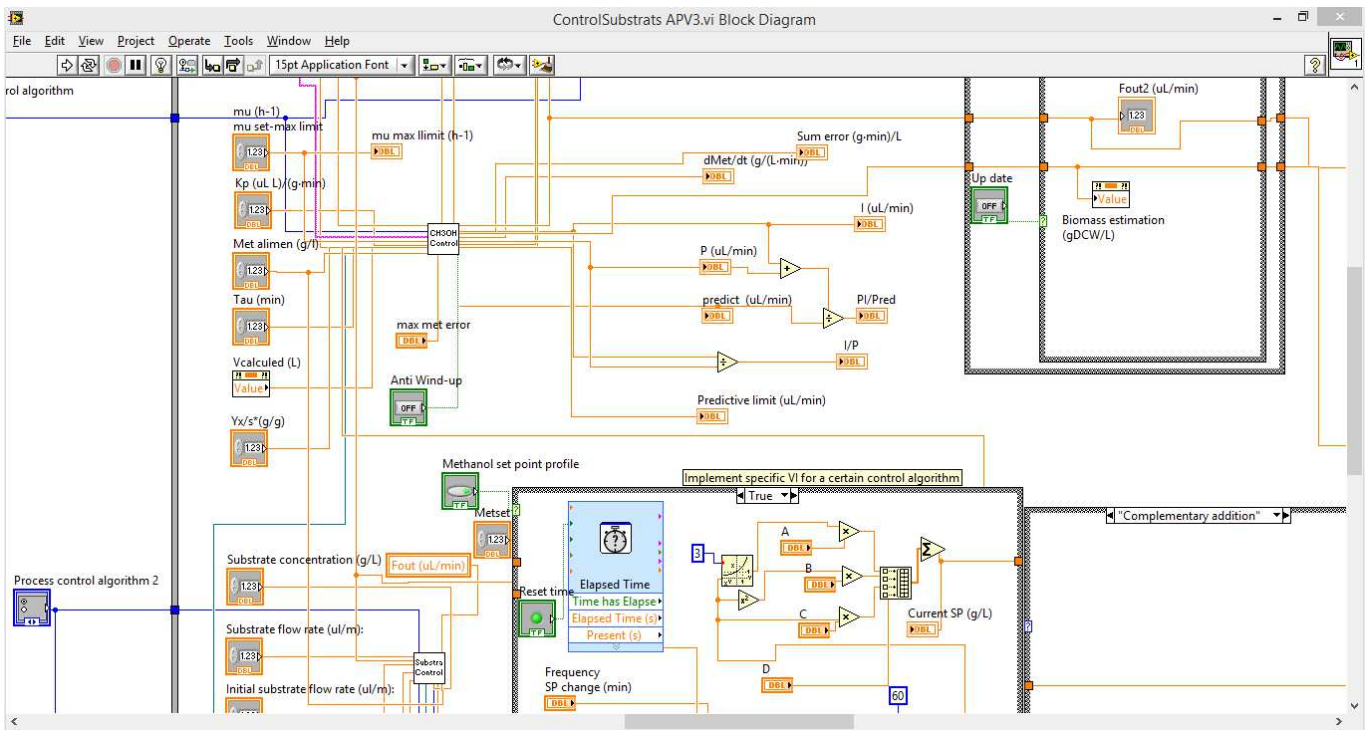

Figure 3.2 Sample fragment of the flow-chart code of the program used for monitoring and control of fed-batch processes with *P. pastoris*. Data flows from left to right through the strings. Circled boxes are subprograms (subVI).

In this part of the VI, and concretely at the up-left zone, a subVI is present (white box), and contains the programming for the automatic feeding of methanol according to different feeding modes depending on the strategy that will be applied. These modes are one of the set of options that this VI lets the user select. In Figure 3.4, this part of the front panel is depicted.

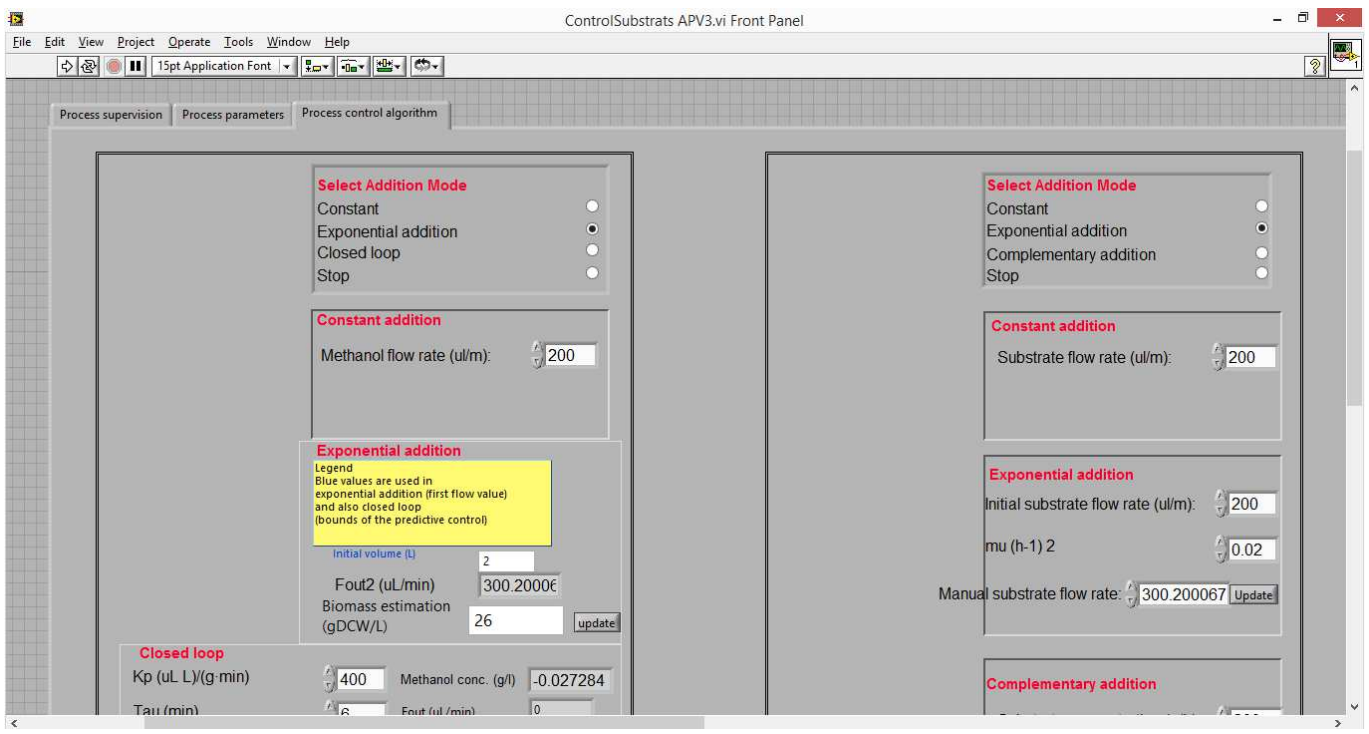

Figure 3.3 Fragment of the front panel corresponding to the flow-chart VI present in Figure 3.2. Here, part of the substrates feeding control is shown.

3.1.2.1 A LabVIEW VI for monitoring and controlling P. pastoris *cultures under different feeding strategies*

LabVIEW has been the pillar of the communications, supervision, control and monitoring of *P. pastoris* fermentations carried out by the Bioprocess Engineering and Applied Biocatalysis Group, where the PhD candidate belongs to. Labview VI (VI) that was developed and subsequently updated by the previous PhD students O. Cos, R. Ramon and J.M. Barrigón [2,3] has been used in the fermentation experiments of all the present dissertation. During the present work, several updates have been carried out to this VI and will be listed and detailed in section 3.2.

The structure of the program is detailed as follows:

- Peripheral communications

This VI is programmed to receive and send data from/to Digital Control Units (DCU) from bench-top reactors, in two different versions, one for a Biostat B (Sartorius Stedim Biotech, Göttingen, Germany) and a Biobundle (Applikon Biotechnology B.V, Delft, Netherlands). The PC and the DCU are connected physically by Ethernet, and they communicate by an OPC standard protocol, enabling the data flow back and forth through the interaction between the OPC server and the client (supplied by the bioreactor company). Within the set of data, it can be found temperature, pH, dissolved oxygen (DO), stirring rate, gas flow (air and O_2), which are both monitored and controlled. In Figure 3.4, the communication part of the VI for the DCU is represented, where inlet and outlet data are observed going through the subVI built for this communication just mentioned.

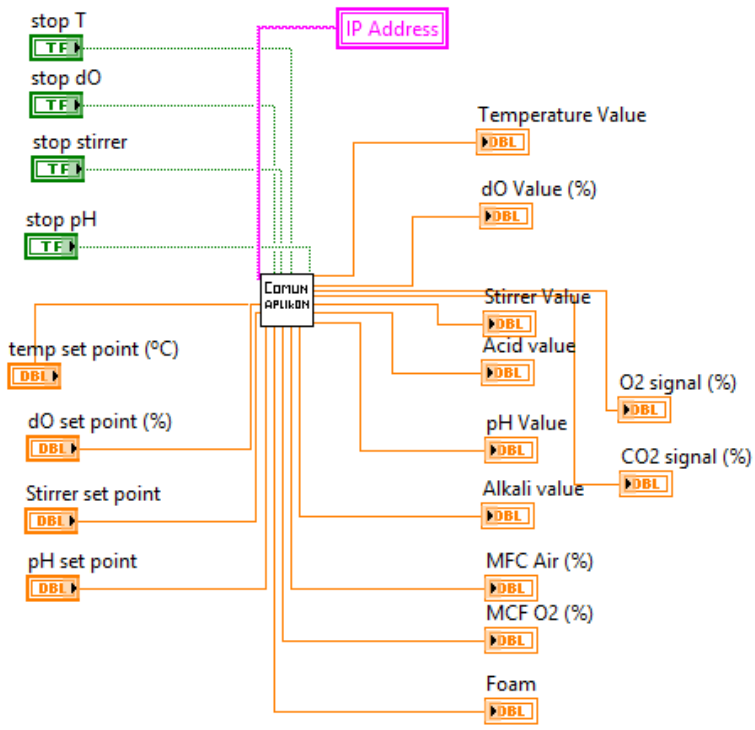

Figure 3.4 Portion of the VI where data regarding some of the set-point values (left) are sent to subVI that manages all DCU communications (COMUN APPLIKON). On the right, current values of state variables are monitored and further acquired.

A set of external devices are also connected through RS-232C connections and send data to the PC via a COM communication protocol. Among them, there is the Methanol Sensor System (Raven Biotech, Vancouver, Canada), which can monitor methanol concentration along the process, and 2 microburettes (Hach Lange Spain, Barcelona, Spain) that can work, parallelly, as the driving element of the feeding solutions intended to be introduced in the vessel.

- Inlet data. Control, supervision of the process and constraints

Within this section, set points of all controls of state variables (and their tuned and physiologic parameters) are included, as well as specifications of communication protocols:

a. COM port for methanol sensor and each microburette.
b. IP address for DCU interaction.

Calibration values of the methanol sensor are also required and can be changed in situ for recalibration, just like the frequency that data acquisition is settled, stablished as 60 s by default.

More specifically, controls regarding feeding strategies, or what is the same, those ones using feeding rate as the manipulated variable, are listed followingly, and coincide with the different feeding modes that are available in the VI:

a. Constant feeding rate (F)
b. Closed-loop control of methanol concentration (*S*)

This option is exclusive for a methanol feeding strategy, applied then only for strains expressing RPP under P_{AOX} promoters (all Mut phenotypes). It is based on a predictive-PI control law to maintain the desired levels of methanol concentration, following what Equation 3.1 describes. This coupled control strategy enables to minimize problems from tuning (PI) and, at the same time, overcome uncertainties or mismatches from the kinetic model (predictive, Equation 3.2) [2,3].

$$F_{t+1} \approx F_t - \frac{V_t}{(S_{feed} - S_t)} \frac{dS_t}{dt} + K_P \left(\varepsilon_{t+1} + \frac{1}{\tau_I} \int_{t_0}^{t+1} \varepsilon_t \, dt \right)$$

Equation 3.1

The first-time derivative of *S* from Equation 3.1 Is obtained through spline-smoothed online time intervals and is constrained according to Equation 3.2:

$$0 \geq \frac{dS}{dt} \geq -\frac{1}{Y^*_{X/S}} \mu_{max} X_0 \exp(\mu_{max} t)$$

Equation 3.2

Where μ_{max} stands for the maximum specific growth rate (h^{-1}) and X_0 (g L^{-1}) is the concentration at the moment when the control is turned on.

c. Open-loop control of specific growth rate (μ)

As mentioned in chapter 1 (Equation 1.1), this control allows the consecution of a constant specific growth rate at substrate-limited conditions using a pre-programmed exponential feeding strategy, without requiring any measured variable. This control is applicable to any substrate, in addition to methanol, and can be also paired to the closed-loop control by the use of two microburettes at the same time. This is a common practice in Mut^s phenotype cultures, which usually grow from the assimilation of mixed C-substrates [4].

- Data acquisition

All inlet and outlet variables are automatically stored (every 60 seconds by default) in two files, in order not to lose data in case of a sudden shut down of the system. Selected variables are also plotted for the user to supervise the process at any time.

Figure 3.5 Bench-top bioreactor (Biostat B) full equipment to produce RPP by *Pichia pastoris*. From left to right, a microburette, the vessel of the bioreactor, the DCU and the PC for supervision, control and data acquisition.

3.2 LabVIEW VI upgrades

In order to fulfill particular process needs, both for this dissertation and other ones, several new implementations have been proposed and put to practice

3.2.1 New device communications

- O_2 / CO_2 sensors for CER/OUR and elemental balances estimation in fed-batch cultures

Two BCPreFerm optic detectors (BlueSens gas sensor GmbH, Herten, Germany; Figure 3.6) were installed for the detection of O_2 and CO_2 fractions in the off-gas of the fermenter. With that, carbon dioxide evolution rate (CER) and oxygen uptake rate (OUR) can be obtained for physiologic characterization and also for the calculation of elemental balances. In this case, and specifically in chapter 4, carbon (CB) and degree of reduction (or electron, EB) balances were applied for validating experimental results through a consistency check and reconcile the physiologic parameters obtained.

The connection was stablished as an additional outlet variable coming from the DCU through OPC. As the signal from both sensors comes as a raw % of maximum intensity, a linear relationship between the signal and the value of each gas fraction was chosen, by including two input values (slope and offset) for calibration in the VI, which could be even changed at any time during the process.

Figure 3.6 BCPreFerm O_2 or CO_2 analyzer

Additionally, an O_2 Maihak S710 analyzer (Sick AG, Waldkirch, Germany) was available in the facilities and was communicated to the VI by a RS-232C connection and intended to use as a backup. Apart, no inner calibration inputs were needed to be included for this device, as it is calibrated externally.

3.2.2 New feeding strategies. Complementary addition and closed-loop control of methanol concentration profiles

The upgrades in this section were necessary for the operation of the cultures of the following chapters of the dissertation, or at least part of them.

In the first place, complementary addition mode was implemented for the second microburette (right panel from Equation 3.3), for specific bioprocess needs of nitrogen source (N-source), which will be further detailed in section 3.3. Despite the specificity of the application, this mode was conceived as versatile, and consisted as a continuous inlet feeding rate that is automatically calculated from the first microburette feeding rate at any time of the bioprocess. This is especially useful for substrates that need to be supplied by their stoichiometrically dependence to the limiting

substrate. For that purpose, two inlet parameters are required: the relationship between the two substrates, represented as a yield in mass units ($Y_{A/B}$), being A the supplementary substrate, and B the limiting one), and the concentration of the substrate in the feeding solution.

Furthermore, and for different reasons, which will be thoroughly explained in chapter 5, a significant modification was performed to the closed-loop control mode. A versatile application was built to implement methanol concentration profiles, in the way that the user has the option of introducing a preset *S* profile that would last a determined amount of time, and so the controller is capable of periodically updating the set point of *S* to accomplish the requirements. For performing this, a set of inlet parameters have been included:

- Scalars A, B, C and D, which characterize the profile of *S* in function of time (t, hours), following a polynomial function, as Equation 3.3 shows:

$$S_{SP}(t) = At^3 + Bt^2 + Ct + D$$

Equation 3.3

- Time interval of the S_{SP} change, in minutes. By default, it is set to 30 min, and it is recommended to be higher than the methanol sensor time response (5 min to reach the 90 % of the maximal signal).

Apart from these features, for further needs of hypothetical processes and enhancing higher versatility of this mode, it would be convenient to implement a function that can stop the feeding control or when the set final time of the S profile is finished, or to be able to input alternative functions for the building of profiles, e.g. exponential.

At Figure 3.7, the part of this new feeding mode within the VI is represented.

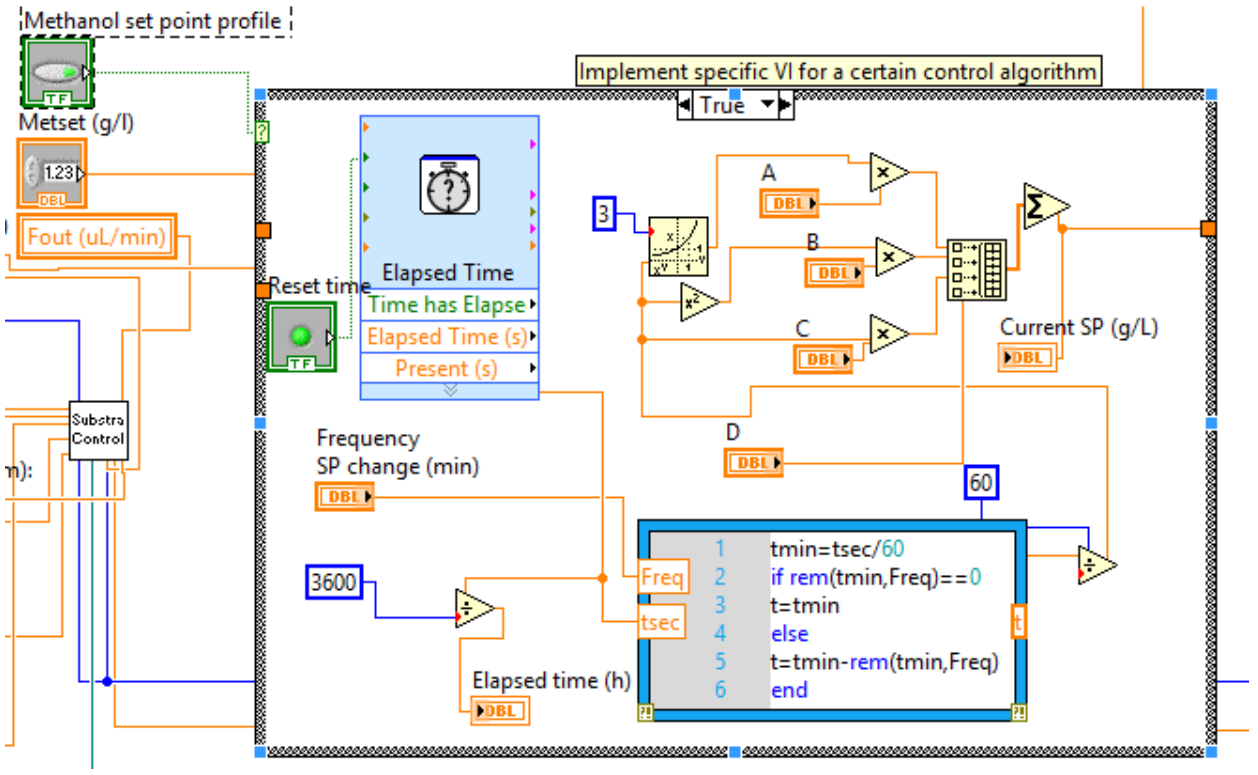

Figure 3.7 Loop for the update of methanol set point ("Metset" in the image). Inside the True/False box (or *if* loop), the S_{SP} for a given time is calculated and then sent to the subVI of the closed-loop S control.

3.2.3 Predictive–PI adaptive gain control of methanol concentration

An improved version of the methanol closed-loop was incorporated to the system, by adding a component of adaptive control to the PI element. By doing so, the parameters K_P and τ_I can be updated online so that the control is able to

adapt to the system dynamics, that is, estimated volume changes and current substrate concentration. Thus, the Predictive-PI adaptive gain control strategy was adapted from what is described elsewhere [3], that can be also derived from the general model control (GMC) theory, as the following equation escribes:

$$F_{t+1} \approx F_t - \frac{V_t}{(S_{feed} - S_t)}\frac{dS_t}{dt} + \frac{K_P \cdot V_{t+1}}{(S_{feed} - S_{t+1})}\left(\varepsilon_{t+1} + \frac{1}{\tau_I}\int_{t_0}^{t+1} \varepsilon_t \, dt\right)$$

Equation 3.4

This upgrade was implemented to prevent the system from instabilities of the controlled variable and major discordances from its set point, mostly in those processes where S_{SP} is not constant and, so, a quick response is required from the system. Therefore, this control strategy was used for experiments carried out in chapter 5 and its effectiveness is accomplished.

3.3 Stablishing a N-source systematic feeding strategy to seek reproducibility

3.3.1 Antecedents and objectives

Bioprocess operational strategies are governed by the limiting substrate, which corresponds, most commonly, to the carbon source. However, the lack or the excess of other substrates and accumulation of some products (inside or outside the cell), can trigger metabolic responses that may bring the system to unexpected perturbances and undesired behavior, lower the product quality and/or bioprocess efficiency. The effect of those situations has been thoroughly studied during last decades, and will not be reviewed here.

Nitrogen, as the commonly third macroelement (in dry cell), plays a main role in any culture, as a prime element for the synthesis of main biomolecules as amino acids, proteins, and nucleic acids.

The aim of this process modification is to outcome process limitations that could be due to the particular way of the nitrogen source to be introduced, as well as to improve the reproducibility of experiments.

Specifically, in operation of a *P. pastoris* cultivations using a MNLFB strategy, during the three phases of the process, i.e. the glycerol batch (GBP), the transition phase (TP), and the methanol induction phase (MIP), nitrogen is supplied to the cells by feeding solutions of NH_4OH (GBP, also for pH control) and NH_4Cl (TP and MIP, where pH is adjusted with KOH). This change of nitrogen source during operation is motivated by the interaction that the NH_3 evaporating from the fed aqueous NH_4OH with the methanol sensor, which compromises the good performance of its control. The alternative proposed by Arnau *et al.* (2011) [4] for a mixed substrate Mut^s culture is NH_4Cl to be introduced alongside glycerol in the same solution. However, for those cultures where the only substrate fed is methanol, NH_4Cl was not possible to be dissolved at the desired concentrations, and diluting the methanol feeding solution would have compromised the bioprocess efficiency. Barrigon *et al.* (2013) [3], who worked with Mut^+ strains, introduced manual pulses of NH_4Cl (40 g of ammonium chloride in a 200 g L^{-1} solution, implying an approximately final concentration of 15-20 g NH_4Cl per liter of broth) when the cultures reached values of biomass concentration (X) of approximately 30-35 g L^{-1} and 50-60 g L^{-1} of dry cell weight. This boosts ammoniacal nitrogen (N-NH4) concentrations up to high levels, and this sudden shock of ionic force could cause stress to the cells, as it will be appreciated followingly.

3.3.2 Materials and methods

3.3.2.1 Strain

The wild type *P. pastoris* X-33 strain containing the vector pPICZαROL was used for the heterologous expression of *Rhizopus oryzae* lipase under the control of the P_{AOX1} (Mut^+ phenotype) [5].

3.3.2.2 Inoculum preparation

Inocula for bioreactor were cultured in 1 L baffled shake flasks at 30 °C, 150 rpm (HT Multitron incubator, Infors AG, Bottmingen, Switzerland), for 24 hours, in YPD medium (10 g of yeast extract, 20 g of peptone, 20 g of D-glucose and 500 µg of zeocin per liter of distilled water, initial pH 7.4). The already grown culture was centrifuged at 4500 x g and the cells were re-suspended in bioreactor culture medium and used to inoculate the 5 L Applikon Biobundle bioreactor. Initial fermentation volume was 2 L and OD_{600} close to 2.5.

3.3.2.3 Fed-batch bioreactor cultivation

The basal salts medium contained, per liter of distilled water: H_3PO_4 (85%) 26.7 mL, $CaSO_4$ 0.93 g, K_2SO_4 18.2 g, $MgSO_4 \cdot 7H_2O$ 14.9 g, KOH 4.13 g, glycerol 40 g, 2 mL of biotin solution (20 mg L^{-1}), 5 mL of trace salts solution and 0.5 mL of antifoam agent (A6426, Sigma-Aldrich Co., St. Louis, MO, USA). Trace salts solution was composed, per liter of distilled water, of $CuSO_4 \cdot 5H_2O$ 6.0 g, NaI 0.08 g, $MnSO_4 \cdot H_2O$ 3.0 g, $Na_2MoO_4 \cdot 2H_2O$ 0.2 g, H_3BO_3 0.02 g, $CoCl_2$ 0.5 g, $ZnCl_2$ 20.0 g, $FeSO_4 \cdot 7H_2O$ 65.0 g, biotin 0.3 g, H_2SO_4 98% 5 mL.

The whole fermentation process consisted of three stages:

- Glycerol batch phase (GBP)

During this stage, pH was controlled by adding NH_4OH 30% (v/v) and dissolved oxygen (DO) was kept higher than 25% air saturation, by regulating the stirring rate between 600-1000 rpm, and introducing 1 vvm of air.

- Transition phase (TP)

A pre-programmed glycerol feeding rate under carbon limited conditions and methanol feeding rate stepwise increased were applied to assure a methanol concentration lower than inhibitory concentration to favor the derepression of P_{AOX1}. This consisted on a 5 h fed batch stage as previously described [6]. Glycerol (50 % w/w with 5 mL of trace salts solution and 2 mL of biotin solution per liter) and pure methanol (with 5 mL of trace salts solution and 2 mL of biotin solution per liter) solutions were used as feeding. pH was controlled by the addition of KOH 5 M during both this phase and the next one. DO_{SP} was, as well, kept at 25 %.

- Methanol induction phase (MIP)

The cells grew under methanol non-limited conditions; where methanol concentration was controlled throughout this stage at 3 g L^{-1}, previously described as optimal substrate concentration [3]. Methanol feed solution contained 5 mL of trace salts solution and 2 mL of biotin solution per liter of pure methanol. DO was kept at 25 % air saturation, controlled by a cascade-based control scheme, which involved regulating both stirring rate between 800 and 1000 rpm and total inlet gas flow rate of air and additional pure oxygen in a range of 0-1 vvm. Nitrogen needs were fulfilled, for FBN1, by a pulse of 200 mL of a 200 g L^{-1} solution of NH_4Cl. For the rest of the options (FBN2 and FBO259), a continuous feed was introduced, according to the yield from methanol, which calculation is explained further in this section.

Temperature was kept at a value of 30 ºC and pH at 5.5 throughout the three phases of the process.

3.3.2.4 Methanol determination and control

Methanol concentration was monitored by the Methanol Sensor System (Raven Biotech Inc., Vancouver, Canada) and controlled by performing a predictive-PI control strategy, as described elsewhere [3]

3.3.2.5 N-NH_4^+ analysis by colorimetry

Free ammonia was analyzed through a colorimetric assay performed with an Ammonium cuvette test 2.0 - 47 mg/L NH_4-N (Hach, Loveland, CO). It is based on an Indophenol Blue method and it is incubated 15 minutes at room temperature, to be then analyzed in a DR3900 spectrophotometer (Hach) with a preset protocol. The samples that contained more than 47 mg L^{-1} of N-NH_4^+ were diluted to fit in the linear range of the method.

3.3.2.6 Dry cell weight analysis

Biomass concentration was measured as the dry cell weight (DCW) per liter of culture. Culture from each sample was centrifuged at 4500 x g for 5 minutes. The pellet was subjected to two cycles of washing with NaCl 0.9 % and centrifugation at 4500 g for 5 minutes. Afterwards, the pellet was dried at 105 ºC until constant weight. Determinations were performed by triplicate and the relative standard deviation was about 5 %.

3.3.2.7 Extracellular ROL activity assay

Culture broth was centrifuged at 10000 x g for 1 min to remove cells. A colorimetric assay was performed in a Cary Varian 300 spectrophotometer (Varian Inc., Palo Alto, USA) at 30 ºC and pH 7.25 (400 mM Tris-HCl + 10 mM $CaCl_2$ buffer) using the Roche lipase colorimetric kit (Roche, Mannheim, Germany) at 580 nm for 4 minutes, as previously described [7]. RSD was estimated as 5 %.

3.3.2.8 Calculation of kinetic parameters from macroscopic balances

Considering the culture to grow under fully aerobic conditions, all macroscopic biochemical reactions can be summed up into a black box model described by Equation 3.5***Equation 3.1***, which represents an oxidative and oxidoreductive growth, on a C-molar basis:

$$S + Y^*_{O_2/S}\, O_2 + Y^*_{NH_3/S}\, NH_3 \rightarrow Y^*_{X/S}\, X + Y^*_{CO_2/S}\, CO_2 + Y^*_{P/S}\, P$$

Equation 3.5

Where *S* is set as the limiting substrate that serves both as carbon and energy source; *X* represents biomass; *P*, the possible products and $Y_{i/S}$ are global stoichiometric yield respect to substrate.

Specific rates of each component from Equation 3.5- μ and q_i (g_i g_X^{-1} h^{-1} or mol_i g_X^{-1} h^{-1}) - and overall yields are defined positive as what the following expressions describe:

$$q_i = \frac{r_i}{X}$$

Equation 3.6

$$Y^*_{i/j} = \frac{r_i}{r_j} = \frac{q_i}{q_j}$$

Equation 3.7

Where r_i denotes the volumetric conversion rate of element *i* from Equation 3.5.

For an ideal stirred tank-reactor, considering conversion rates of biomass formation, substrate uptake and product formation, the following mass balance equations for the fed-batch operation can be formulated:

$$\frac{d}{dt}\begin{bmatrix} XV \\ SV \\ PV \end{bmatrix} = \begin{bmatrix} \mu \\ q_S \\ q_P \end{bmatrix} XV + \begin{bmatrix} -F_o\, X \\ F\, S_i - F_o\, S \\ -F_o\, P \end{bmatrix}$$

Equation 3.8

Where symbols of each state variable from general biochemical reaction equation represent their concentration in g L^{-1} or mol L^{-1} (of culture broth); V (L) is the culture volume, μ (h^{-1}), the specific growth rate; S_i (g L^{-1}), concentration of methanol in the feeding solution; F (L h^{-1}), feeding flow rate; F_o (L h^{-1}), outlet flow rate.

- Calculation of the nitrogen-carbon source yield ($Y'_{N/S}$)

Equation 3.9 is a simplified expression to calculate the value of this yield.

$$Y^*_{N/S} = \frac{C_{N,i}V_i - C_{N,f}V_f}{S_{consumed}} \approx \frac{C_{N,i}V_i - C_{N,f}V_f}{\rho_S \cdot \int_{t_i}^{t_f} F_S dt}$$

Equation 3.9

Where $Y'_{N/S}$ is the NH_4Cl yield from methanol (g g^{-1}); C stands for concentration (g L^{-1}); and the subscript N refers to NH_4Cl; S, to methanol; I initial and f, final.

This expression assumes that methanol concentration is kept perfectly constant, since the only consumption term comes from the feeding rate. The value that was calculated and used for FBN2 strategy was 0.11 g g^{-1}. Once the feasibility of this strategy was demonstrated, it was decided to be applied to the rest of fed-batch cultures of this thesis.

3.3.3 Proposal and implementation

Following the procedure of Barrigón *et al.* (2013) [3] regarding the in preliminary studies of this thesis, some MNLFB cultures in *Pichia pastoris* using the same Mut^+ strain (see section 3.3.2) were carried out to produce *Rhizopus oryzae* lipase (ROL). One of these (FBN1), is represented in Figure 3.8 as the evolution of its specific rates of ROL activity production (q_P), and methanol uptake (q_S) along time of MIP phase. Alongside with FBN1, the evolution of the same variables, but for a strategy where NH_4Cl is introduced continuously and stoichiometrically proportionally to the carbon source throughout the MIP (FBN2), is also represented. This was achieved by the use of the new "complementary addition" mode implemented in LabVIEW, which has been described in section 3.2.2. The details of the requirements of this mode for this strategy are present in section 3.3.2.

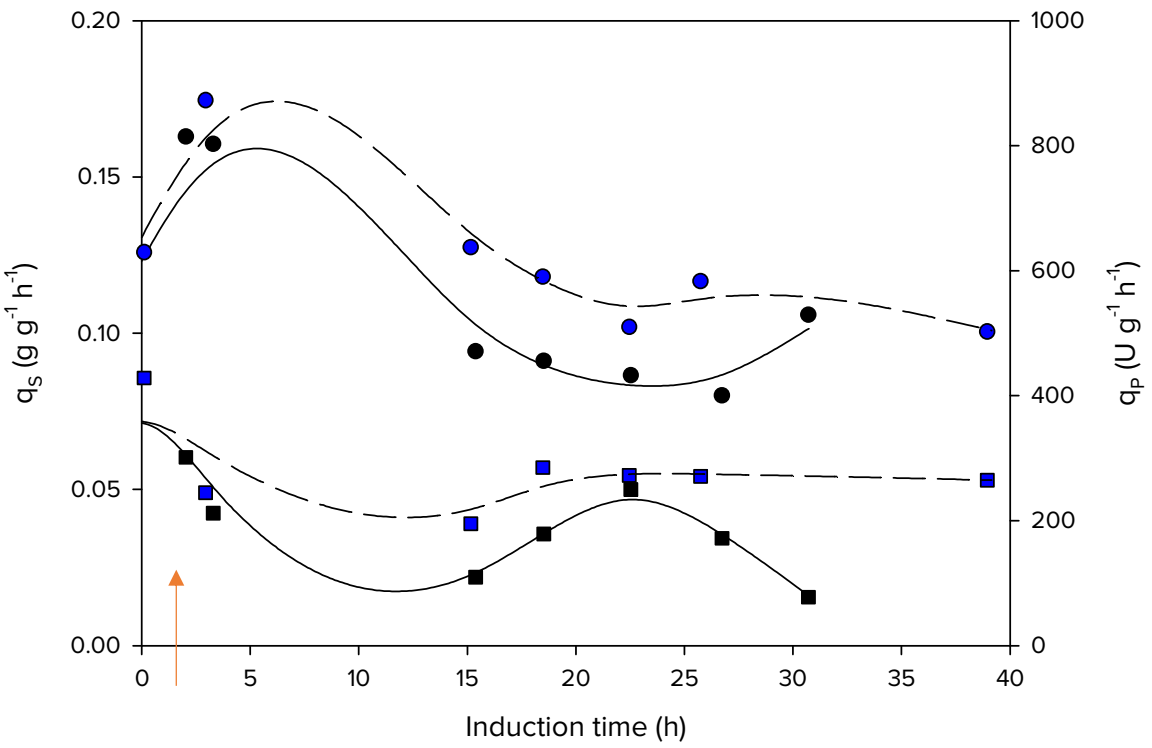

Figure 3.8 Induction time evolution of q_S (●) and q_P (■) for FBN1 (solid lines) and FBN2 (dashed lines). The arrow points out the time where the NH_4Cl pulse was introduced in FBN1 strategy.

As observed, FBN1 specific rates experiment a decay in a point that is very close to the start of this phase, and to the point of introduction of the pulse of NH_4Cl. FBN2 culture, also experiment this fall in production and methanol uptake rates, but less dramatically, and they maintain themselves more stable at middle-end point of the process. The feasibility is also observed in Table 3.2 where the productivity and mean specific rates of both strategies are shown. Comparison is also carried out with another strategy that was proposed for the study of chapter 4, but that is identical to FBN2.

Table 3.2 Process and physiologic parameters ± indicates standard error (SE).

Parameter	Units	FBN1	FBN2	FBO25[8]
Nitrogen feeding	-	Pulse	Continuous	Continuous
Volumetric productivity	U mL^{-1} h^{-1}	3.42	5.35	5.49
μ_{mean}	h^{-1}	0.029 ± 0.001	0.031 ± 0.001	0.034 ± 0.001
$q_{P,mean}$	U g^{-1} h^{-1}	152 ± 12	239 ± 19	256 ± 22

It can be stated that the strategies that had continuous feeding of NH_4Cl were quite reproducible in terms of production, achieving very similar productivities and excreting active ROL at very similar rate, so that brings to think that a NH_4Cl effect can have an influence on production, given the excess on the first hours of the MIP. In Figure 3.9 the profiles of N-NH4 alongside the fermentation have been included, to point out the differences in operation between them.

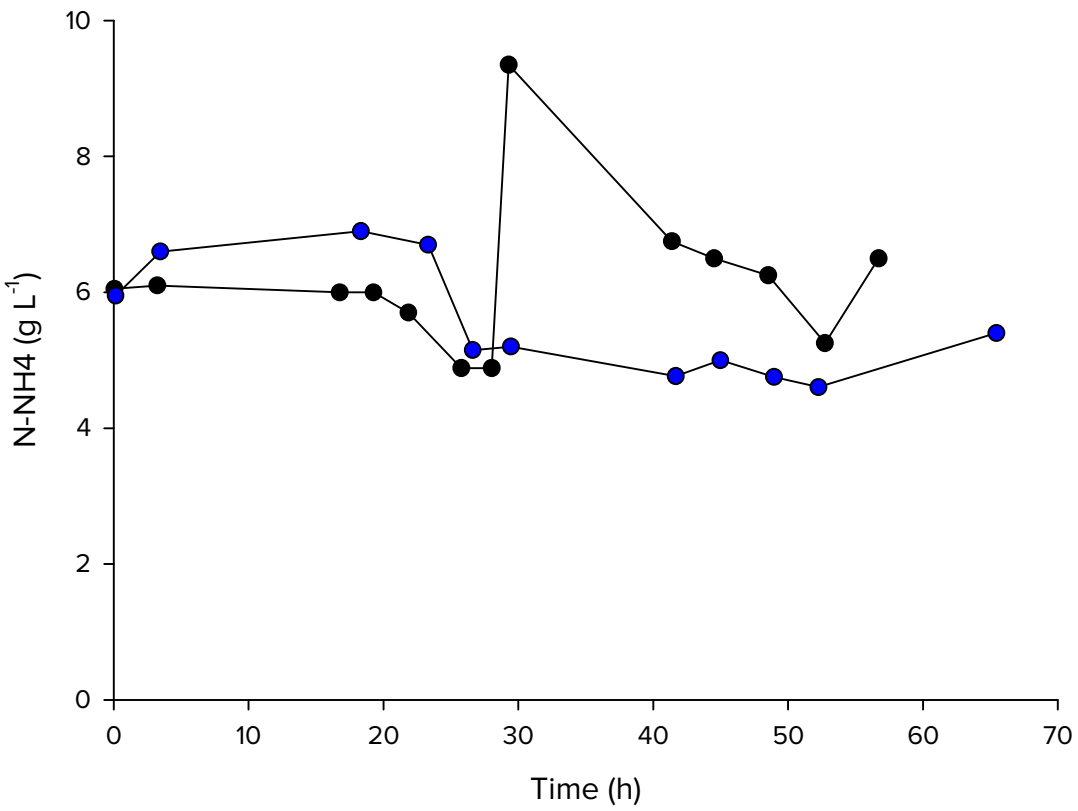

Figure 3.9 Time evolution of free ammonia nitrogen for FBN1 and FBN2.

The first drop in both strategies corresponds to the TP of each case, where NH_4OH has already been shifted to KOH. Then, a smooth profile of this compound is achieved for FBN2, while the signal in FBN1 is much more unstable, as expected.

3.4 Conclusions

The consecution of the upgrades that have been detailed in this section set the grounds of the research of this dissertation. They contribute to the development of new operational strategies and to the robustness of the system, facts that build the firsts steps to bioprocess optimization and, as well, to bring complex operational strategies up to a larger scale.

Concretely, successful control algorithm modifications help to prevent fluctuations on the controlled variable in complex operational strategies, which are not empirically easy to predict by biosystems kinetics or modelling,

Moreover, a bioprocess where nitrogen-source levels are rather constant has been achieved, prevents physiologic perturbations, as its smooth conditions avoid fluctuations, being themselves easily reproducible to other scales.

3.5 References

[1] C. Elliott, V. Vijayakumar, W. Zink, R. Hansen, National Instruments LabVIEW: A Programming Environment for Laboratory Automation and Measurement, J. Assoc. Lab. Autom. 12 (2007) 17–24.

[2] O. Cos, R. Ramon, J.L. Montesinos, F. Valero, A Simple Model-Based Control for *Pichia pastoris* Allows a More Efficient Heterologous Protein Production Bioprocess, Biotechnol. Bioeng. 95 (2006) 145–154.

[3] J.M. Barrigón, J.L. Montesinos, F. Valero, Searching the best operational strategies for *Rhizopus oryzae* lipase production in *Pichia pastoris* Mut^+ phenotype: Methanol limited or methanol non-limited fed-batch cultures?, Biochem. Eng. J. 75 (2013) 47–54.

[4] C. Arnau, C. Casas, F. Valero, The effect of glycerol mixed substrate on the heterologous production of a *Rhizopus oryzae* lipase in *Pichia pastoris* system, Biochem. Eng. J. 57 (2011) 30–37.

[5] O. Cos, A. Serrano, J.L. Montesinos, P. Ferrer, J.M. Cregg, F. Valero, Combined effect of the methanol utilization (Mut) phenotype and gene dosage on recombinant protein production in *Pichia pastoris* fed-batch cultures., J. Biotechnol. 116 (2005) 321–335.

[6] S. Minning, A. Serrano, P. Ferrer, C. Solà, R.D. Schmid, F. Valero, Optimization of the high-level production of *Rhizopus oryzae* lipase in *Pichia pastoris*, J. Biotechnol. 86 (2001) 59–70.

[7] D. Resina, A. Serrano, F. Valero, P. Ferrer, Expression of a Rhizopus oryzae lipase in Pichia pastoris under control of the nitrogen source-regulated formaldehyde dehydrogenase promoter, J. Biotechnol. 109 (2004) 103–113.

[8] X. Ponte, J.L. Montesinos-Seguí, F. Valero, Bioprocess efficiency in *Rhizopus oryzae* lipase production by *Pichia pastoris* under the control of P_{AOX1} is oxygen tension dependent, Process Biochem. 51 (2016) 1954–1963.

4 BIOPROCESS EFFICIENCY IN *Rhizopus oryzae* LIPASE PRODUCTION BY *Pichia pastoris* UNDER THE CONTROL OF P_{AOX1} IS OXYGEN TENSION DEPENDENT

This chapter has been published as a research paper in the journal *Process Biochemistry*:

X. Ponte, J.L. Montesinos-Seguí, F. Valero, Bioprocess efficiency in *Rhizopus oryzae* lipase production by *Pichia pastoris* under the control of P*AOX1* is oxygen tension dependent, Process Biochem. 51 (2016) 1954–1963.

4.1 Introduction

Fed batch is the most common operating mode to achieve high productivities of heterologous protein. Recently, a large number of operational strategies have been tried and developed in *P. pastoris* recombinant protein production under different promoters, based on the limitation of substrates or other state variables as temperature [1-3]. One of the most used options with P_{AOX1}, due to its simplicity, as stated in chapter 1, consists on growing the cells in methanol limited cultures (MLFB), where a constant specific growth rate (μ) is maintained by the action of an open loop control [4]; therefore, no online methanol measuring is required. However, recent studies proved this strategy to be in clear disadvantage in respect to a methanol non-limited induction (MNLFB) for the case of *Rhizopus oryzae* lipase production (ROL) [3], in which an excess of methanol is kept along the process. This methodology, however, implies high demands of substrates, even more when the cultured strain shows a Mut^+ phenotype, since its maximum specific methanol consumption rate ($q_{S,max}$) is much higher than Mut^s strains; concretely appointed around 4-fold increment when comparing both kinds of phenotypes [5].

On the other hand, oxygen stands out as a key substrate to design suitable operational strategies, as the growth of *P. pastoris* under methanol is considerably high oxygen-demanding, due to the need to fulfill oxidation of methanol to formaldehyde [6]. The impact of oxygen supply on the heterologous production has been studied for different recombinant production hosts, because the oxygen transfer rate (OTR) is usually one of the most limiting bottlenecks for high cell density cultivations of microorganisms [7]. In

Escherichia coli cultivations, oxygen limitation leads to a stress response and by-product formation such as acetate, which inhibits both growth and recombinant protein production [8,9]. The impact of the oxygen limitation was, as well, studied in *Saccharomyces cerevisiae*, observing the production of ethanol and glycerol as by-products of the cultivation [10].

Publications about the effect of oxygen transfer limitation on recombinant protein production in *P. pastoris*, for both P_{AOX1} and P_{GAP}-based systems, have become more and more popular over last years, with studies that evidenced improvements on protein final titer and quality or even on specific production rate [11-16]. For instance, in reference to DO effects, the highest recombinant glucose isomerase (rGI) titer and specific activity was obtained at DO of 15 % under P_{GAP} control [16].

The non-limitation by oxygen is evidenced by the positive values of dissolved oxygen tension (DO), normally above 30 % air saturation [17-19]. In P_{AOX1}-based systems, the non-accumulation of methanol, as well as the non-generation of by-products, indicates that cells are growing in fully aerobic methanol metabolism (normoxic conditions).

As a counterpart, some studies have explored the impact of an excess of oxygen supply. Concretely, Lee *et al.* (2002) drastically improved final titer of heterologous protein when working at higher DO (30-50 % air saturation) [20], while Jazini *et* al. (2014) conducted a continuous operation with a 70 % set point of DO [21]. Under this condition, final productivity was found slightly lower than the one obtained at DO of 25 %.

Even so, scarce systematic studies have been published about P_{AOX1}-based systems in order to identify the optimal DO culture conditions that lead to maximal productivities and yields for the protein of interest [18,21].

In the present work, a thorough study of a wide range of dissolved oxygen conditions for recombinant *P. pastoris* producing ROL under P_{AOX1} in fed batch cultivations has been performed, searching the best conditions to improve bioprocess efficiency, including yields and productivities. Thus, the work is not related to oxygen transfer limitation in either hypoxic or normoxic conditions when growth is limited by oxygen transfer rate (OTR), and so that, when this value is kept constant. In this particular case, OTR changed

(increased) along the process to keep DO set point values. Systematic and reliable studies concerning specific rates comprising cell growth, substrate consumption and product formation have been carried out, where consistency test and data reconciliation were fulfilled to trustworthily establish the dependency of those parameters to oxygen tension.

4.2 Materials and methods

4.2.1 Strain

The wild type *P. pastoris X-33* strain containing the vector pPICZαROL was used for the heterologous expression of *Rhizopus oryzae* lipase under the control of the P_{AOX1} (Mut^+ phenotype) [5].

4.2.2 Inoculum preparation

Inocula for bioreactor were cultured in 1 L baffled shake flasks at 30 °C, 150 rpm (HT Multitron incubator, Infors AG, Bottmingen, Switzerland), for 24 hours, in YPD medium (10 g of yeast extract, 20 g of peptone, 20 g of D-glucose and 500 µg of zeocin per liter of distilled water, initial pH 7.4). The already grown culture was centrifuged at 4500 x g and the cells were re-suspended in bioreactor culture medium and used to inoculate a 5 L Applikon Biobundle bioreactor (Applikon Biotechnology B.V., Delft, The Netherlands). Initial fermentation volume was 2 L and OD_{600} close to 2.5.

4.2.3 Fed-batch bioreactor cultivation

The basal salts medium contained, per liter of distilled water: H_3PO_4 (85%) 26.7 mL, $CaSO_4$ 0.93 g, K_2SO_4 18.2 g, $MgSO_4 \cdot 7H_2O$ 14.9 g, KOH 4.13 g, glycerol 40 g, 2 mL of biotin solution (20 mg L^{-1}), 5 mL of trace salts solution and 0.5 mL of antifoam agent (A6426, Sigma-Aldrich Co., St. Louis, MO, USA). Trace salts solution was composed, per liter of distilled water, of $CuSO_4 \cdot 5H_2O$ 6.0 g, NaI 0.08 g, $MnSO_4 \cdot H_2O$ 3.0 g, $Na_2MoO_4 \cdot 2H_2O$ 0.2 g, H_3BO_3 0.02 g, $CoCl_2$ 0.5 g, $ZnCl_2$ 20.0 g, $FeSO_4 \cdot 7H_2O$ 65.0 g, biotin 0.3 g, H_2SO_4 98% 5 mL.

The whole fermentation process consisted of three stages, glycerol batch phase (GBP), transition phase (TB) and methanol induction phase (MI), as described in chapter 3. Particularities of this case of study are detailed followingly:

- *Methanol induction phase (MIP)*

The cells grew under methanol non-limited conditions; where methanol concentration was controlled throughout this stage at 3 g L^{-1}, previously described as optimal substrate concentration [3]. Nitrogen needs were fulfilled by the addition of NH_4Cl solution (200 g of NH_4Cl, 5 mL of trace salts solution and 2 mL of biotin solution per liter). Its flow rate was directly linked to the methanol one and was calculated online, by the previously stoichometrically estimated ammonium chloride/methanol yield ($Y^*_{N/S}$), which was established as 0.11 g g^{-1}.

DO was controlled by a cascade-based control scheme, which involved regulating both stirring rate between 800 and 1000 rpm and total inlet gas flow rate of air and additional pure oxygen in a range of 0-1 vvm. Four types of experiments were carried out using different DO set points (DO_{SP}) during this phase: 5, 10, 25 and 50 % in respect to air saturation (~ $2.3 \cdot 10^{-4}$ mol O_2 L^{-1}). Actual DO conditions differed slightly from those, due to the difficulty to maintain DO conditions at the extremes of the experimental DO range. So, mean DO values for the cultures were: 7%, 10%, 25% and 45 % differing from the nominal DO_{SP}.

Temperature was kept at a value of 30 °C and pH at 5.5 throughout the three phases of the process.

4.2.4 Analytical methods and monitoring

4.2.4.1 Off-gas analysis

CO_2 and O_2 molar fractions from the off-gas were measured online by BCpreFerm sensors (BlueSens gas sensor GmbH, Herten, Germany). The total humid off-gas flow rate was not measured directly and it was calculated by inert balance around the reactor. To properly estimate this flow rate, determination of its water composition was necessary. It can be calculated from the quotient between the off-gas O_2 composition without bioreaction, due

to water stripping, and the corresponding inlet O_2 molar fraction. Inlet air composition was obtained from a 12 h measurement average before inoculating. Thus, through O_2 and CO_2 balances, estimation of oxygen uptake rate (OUR), carbon dioxide evolution rate (CER), and respiratory quotient (RQ) were carried out [22], as well as their corresponding specific rates for O_2 (q_{O2}) and CO_2 (q_{CO2}). A lower residual standard deviation (RSD) than 5 % was considered for both online CO_2 and O_2 molar fractions.

4.2.4.2 Methanol determination and control

Methanol concentration was monitored by the Methanol Sensor System (Raven Biotech Inc., Vancouver, Canada) and controlled by performing a predictive-PI control strategy, as described elsewhere [3].

Apart from that, it was also quantified offline by HPLC as previously reported [19]. RSD was estimated about 2 %.

4.2.4.3 *Dry cell weight analysis*

Biomass concentration was measured as the dry cell weight (DCW) per liter of culture, as described in chapter 3. Determinations were performed by triplicate and the relative standard deviation was about 5 %.

4.2.4.4 Extracellular ROL activity assay

Culture broth was centrifuged at 10000 x g for 1 min to remove cells, and the supernatant was subjected to a colorimetric assay at 30 ºC and pH 7.25 (400 mM Tris-HCl + 10 mM $CaCl_2$ buffer) using the Roche lipase colorimetric kit (Roche, Mannheim, Germany) at 580 nm for 4 minutes, as previously described [23]. RSD was estimated as 5 %.

4.2.4.5 Protein quantification

Extracellular protein concentration was determined with the Pierce™ Coomassie (Bradford) Protein Assay Kit (Prod. No. 23200, Rockford, IL, USA), according to the manufacturer's instructions. Bovine serum albumin (BSA) was used as the protein standard for the calibration curve. Assays were taken in triplicate and the RSD was about 5%.

4.2.5 Calculations

4.2.5.1 Mass balances and kinetic parameters

Considering the culture to grow under fully aerobic conditions, all macroscopic biochemical reactions can be summed up into a black box model described by Equation 4.1, which represents an oxidative and oxidoreductive growth, on a C-molar basis:

$$S + Y^*_{O_2/S}\, O_2 + Y^*_{NH_3/S}\, NH_3 \rightarrow Y^*_{X/S}\, X + Y^*_{CO_2/S}\, CO_2 + Y^*_{P/S}\, P$$

Equation 4.1

Where S is set as the limiting substrate that serves both as carbon and energy source; X represents biomass; P, the possible products and $Y^*_{i/S}$ are global stoichiometric yield respect to substrate.

Specific rates of each component from Equation 4.1- μ and q_i($g_i\ g_X^{-1}\ h^{-1}$ or $mol_i\ g_X^{-1}\ h^{-1}$) - and overall yields are defined positive as what the following expressions describe:

$$q_i = \frac{r_i}{X}$$

Equation 4.2

$$Y^*_{i/j} = \frac{r_i}{r_j} = \frac{q_i}{q_j}$$

Equation 4.3

Where r_i denotes the volumetric conversion rate of element i from Equation 4.1.

For an ideal stirred tank-reactor, considering conversion rates of biomass formation, substrate uptake and product formation, the following mass balance equations for the fed-batch operation can be formulated:

$$\frac{d}{dt}\begin{bmatrix} XV \\ SV \\ PV \\ O_2V \\ CO_2V \end{bmatrix} = \begin{bmatrix} \mu \\ q_S \\ q_P \\ q_{O_2} \\ q_{CO_2} \end{bmatrix} XV + \begin{bmatrix} -F_o\, X \\ F\, S_i - F_o\, S \\ -F_o\, P \\ OTR\, V - F_o\, O_2 \\ -CTR\, V - F_o\, CO_2 \end{bmatrix}$$

Equation 4.4

Where symbols of each state variable from general biochemical reaction equation represent their concentration in g L^{-1} or mol L^{-1} (of culture broth); V (L) is the culture volume, μ (h^{-1}), the specific growth rate; S_i (g L^{-1}), concentration of methanol in the feeding solution; F (L h^{-1}), feeding flow rate; F_o (L h^{-1}), outlet flow rate, which includes sampling and stripping losses in case of methanol; OTR (mol L^{-1} h^{-1}), the oxygen transfer rate; and CTR (mol L^{-1} h^{-1}), the carbon dioxide transfer rate.

V was calculated afterwards taking into account all terms from total material balance:

$$\frac{dV}{dt} = \frac{\rho_F \ F - \rho_{ev} \ F_{ev} + \rho_{base} \ F_{base} + \rho_{AF} F_{AF} - \rho \ F_o + M_{GAS}}{\rho}$$

Equation 4.5

Where ρ_i (g L^{-1}) denotes the density of component i and F_i (L h^{-1}) the volumetric flow rate, where subscript F refers to feeding; *ev*, to water that is stripped out of the reactor; *base*, to either NH_4OH or KOH solution for pH control; *AF*, to antifoam feed solution; *o*, to outlet and, no subscript means feeding for volumetric flow rate and culture broth for density. M_{GAS} (g h^{-1}) is the net gas flow rate, defined as the following equation does:

$$M_{GAS} = W_{O_2} \ OUR \ V - W_{CO_2} \ CER \ V$$

Equation 4.6

Where W_{O2} (g mol^{-1}) is O_2 molar mass; W_{CO2} (g mol^{-1}), CO_2 molar mass; OUR or r_{O2} (mol L^{-1} h^{-1}), oxygen uptake rate; and CER or r_{CO2} (mol L^{-1} h^{-1}), carbon dioxide evolution rate, being OUR and CER considered equal to OTR and CTR respectively.

Numerical methods used to calculate discrete and mean specific rates for each experiment were as it is specified elsewhere [3], and carried out by the use of *Matlab* (The MathWorks Inc., Natick, MA USA).

When working at different μ and no significant changes of metabolism are observed between conditions, yields associated to growth (intrinsic) and maintenance coefficients of each component can be found by the following expression:

$$q_i = Y^*_{i/X}\,\mu = Y_{i/X}\,\mu + m_{i/X} \quad (7)$$

Equation 4.7

Where $Y_{i/X}$ ($g_i\ g_X^{-1}$ or $mol_i\ g_X^{-1}$) is the intrinsic yield between the *i* component and biomass and $m_{i/X}$ ($g_i\ g_X^{-1}\ h^{-1}$ or $mol_i\ g_X^{-1}\ h^{-1}$), the maintenance coefficient for the *i* component.

4.2.5.2 Macroscopic balances, consistency check and data reconciliation

Macroscopic balances are essential tools to validate experimental data and do not require much knowledge about the biochemistry of the system [24]. $Y^*_{i/j}$ and q_i are usually affected by random errors, propagated from inaccuracies of measurements of state variables, which may lead to gross errors.

Concretely, carbon (C-balance) and reduction degree (e-balance) balances were the ones used as constraints to perform consistency check of the experimental data. μ, q_S, q_{O2} and q_{CO2} were included in the set of measured conversion rates. q_P was not considered in this procedure instead and no hint of any considerable byproduct was spotted by HPLC analysis. Therefore, system was overdetermined when gases specific rates were measured and a consistency check could be carried out, summed up in Equation 4.8:

$$h = \varepsilon\, P^{-1} \varepsilon$$

Equation 4.8

Where *h* is the statistical parameter that will serve as criteria to stablish whether each of measured specific rates contains significant errors from the measurement. ε corresponds to the error attributed to each specific rate.

If *h* exceeds to the threshold value of χ^2-test with a confidence level of 95 %, it is then stablished that the specific rate contained too much significant errors for being considered within balances calculations. In the case of the present work, mostly every data satisfied the conditions imposed in this consistency check.

Furthermore, a reconciliation data procedure was carried out to all data subjected to the check taking into account *h* values of each specific rate and the accomplishment of both macroscopic balances. As it is explained in more detail elsewhere [25], new optimal

specific rates satisfying the black box model were calculated by minimizing the variance between measured rates and their corresponding reconciled values, obtaining then a δ vector of new estimated errors for each reconciled rate.

4.3 Results and discussion

4.3.1 Process performance and general behavior

The aim of this section is to discuss the performance of the process by showing the results achieved with a DO set point of 5 % during the methanol induction, as a case example, due to its particularities and more prolonged time of operation when it is compared to the rest of the experiments from the set. More concretely, this experiment comes out to be a rather representative case to witness how the culture behaved when subjected to significant changes of oxygen tension availability.

In figure 4.1, main state variables are represented versus operation time.

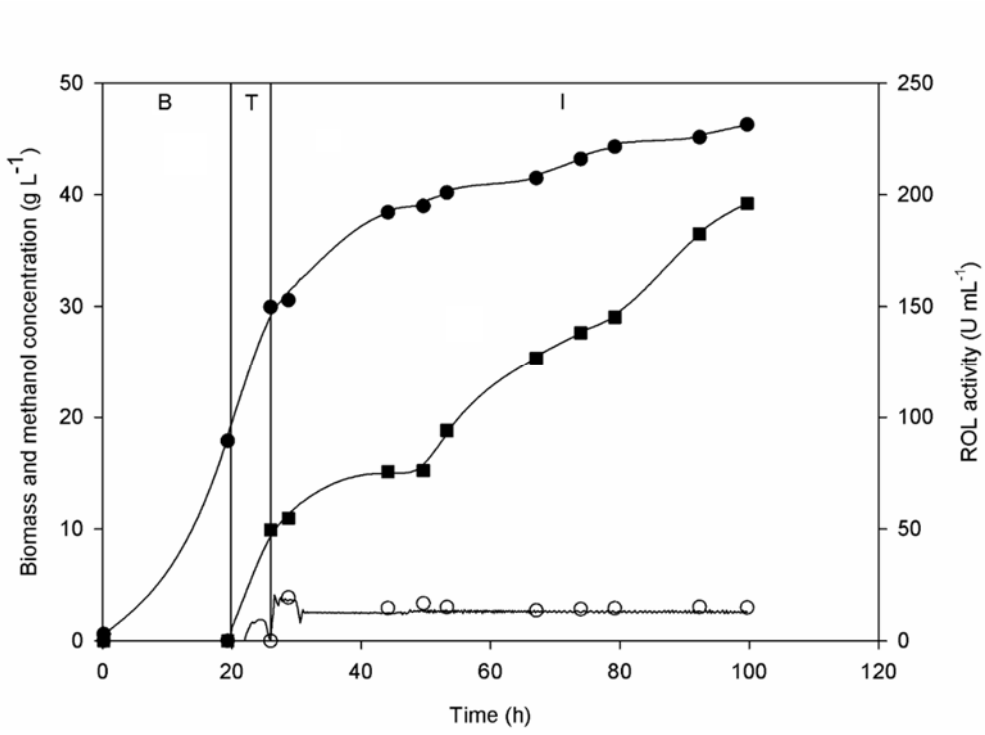

Figure 4.1 Offline experimental time profiles of biomass concentration (●), methanol concentration (○) and ROL activity (■) for DO_{SP} of 5 %. Online methanol concentration data is also shown by a solid line. Biomass and ROL lines are smoothed from the offline data set. (B) batch phase; (T), transition phase and (I), induction phase.

Biomass profile clearly distinguishes the three different phases of the bioprocess, where a fast growth was achieved during glycerol batch phase, a slight decrease of its variation was observed at transition phase since methanol was introduced as a carbon source and cells still consume glycerol, and finally a progressive decrease that began at the first hours of methanol induction phase. This last fact is attributed to both the usage of methanol as a sole carbon source and the level of DO, which was the lowest of all the experimental set. Methanol concentration was controlled at 3 g L^{-1}, and so the continuous line denotes a good performance of the control system set out for the process, which was also validated by offline HPLC measured data.

Apart from that, as it has been previously mentioned, carbon (C-balance) and degree of reduction (e-balance) balances were performed both globally and locally, results being gathered in Figure 4.2.

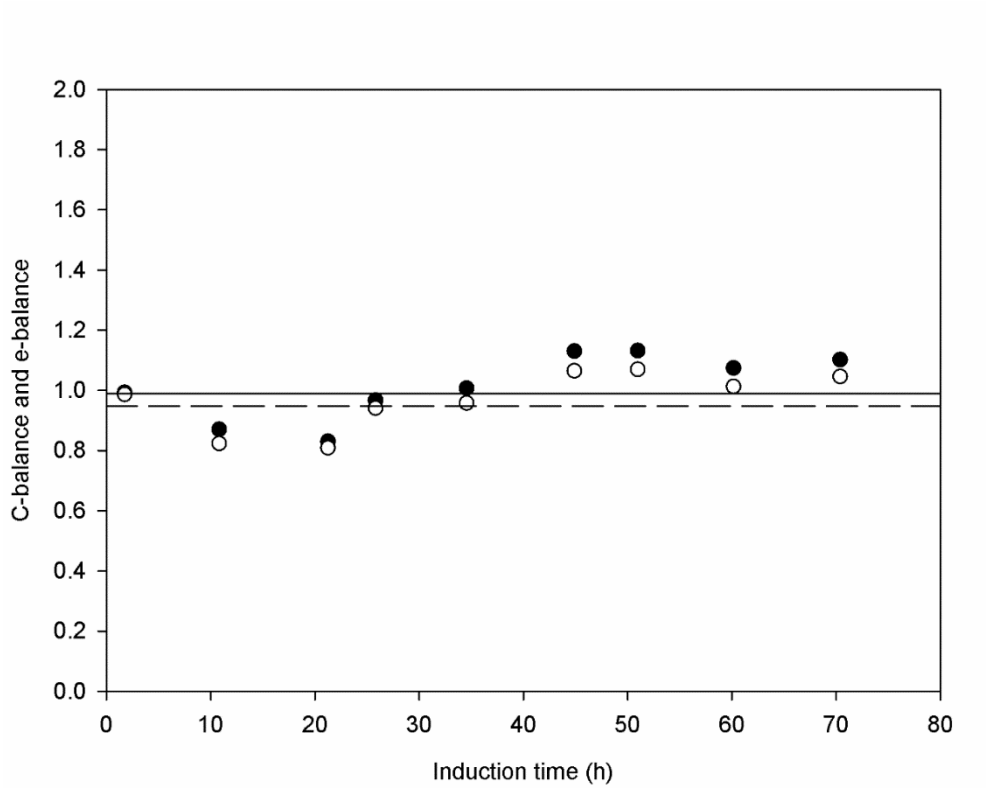

Figure 4.2 Discrete balances (carbon (●), degree of reduction (○)) and overall balances (carbon (-), degree of reduction (--)) from the induction phase of the culture conducted at DO_{SP} of 5 %.

They are quite trustworthy results, as global C-balance only deviated 1 % and e-balance 3 % from unit. On the other hand, discrete calculations of both balances produced two series of points around total accomplishment of balances, which generally deviated within ± 10 %. Those divergences can be attributed to error propagation, as balances gathered up most measured variables together (except for oxygen in the case of C-balance and carbon dioxide in e-balance). Another published work presented similar errors when performing both C and e-balances from *P. pastoris* culture data [22]. Thus, results obtained validated measured data carried out throughout the bioprocess and also pointed out no hint of any considerable byproduct, fact that was further corroborated by HPLC analysis.

Data presented from this point and so on has been subjected to a reconciliation procedure, as detailed in materials and methods section.

4.3.2 Yields and specific rates determination and analysis

Reconciled specific rates of growth (μ), methanol (q_S) and oxygen (q_{O2}) uptake, carbon dioxide (q_{CO2}) production and RQ, as well as their corresponding yields from substrate ($Y^*_{i/S}$) are presented in Figure 4.3 and Figure 4.4.

It must be remarked that data concerning specific production rate (q_P) has not been included in this reconciliation procedure, due to its non-consideration within the contribution to both C and e-balances. Even so, q_P is also represented in Figure 4.3A and its yield from biomass ($Y^*_{P/X}$), in Figure 4.4.

Firstly, what concerns about specific rates, it can be observed from Figure 4.3 that those ones considered to contribute to balances suffered a drop from the beginning of the induction phase to approximately 20 h later that comprised, more or less, the 50 % of their initial value. This should be associated to the adaptation period that cells underwent when changing conditions of dissolved oxygen from transition phase (DO_{SP} of 25 %) to the specific ones at the induction stage. Besides, it may also be related to the influence of high level expression on cell physiology since ROL secretion appears to impose a metabolic burden on *P. pastoris* affecting negatively at the beginning of the induction phase [3]. From that point, saving some smooth fluctuations, those mentioned specific rates remained constant until the end of the process.

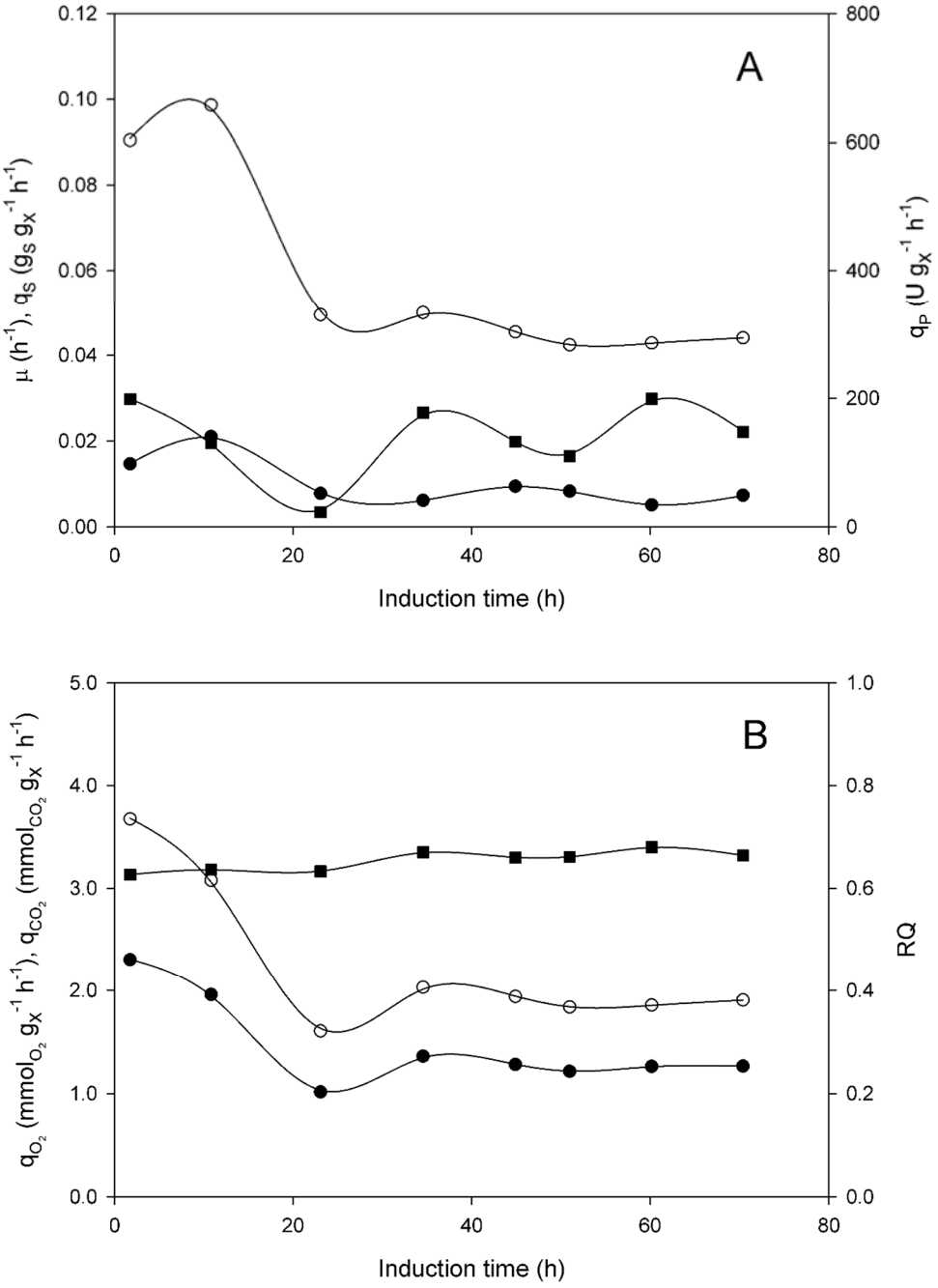

Figure 4.3 (A) Specific growth rate (μ, ●), specific substrate uptake rate (q_s, ○) and specific production rate (q_P, ■) during time of induction, with a DO_{SP} of 5 %. **(B)** Specific oxygen uptake rate (q_{O2}, ●), carbon dioxide production rate (q_{CO2}, ○) and respiratory quotient (RQ, ■) during time of induction, with a DO_{SP} of 5 %.

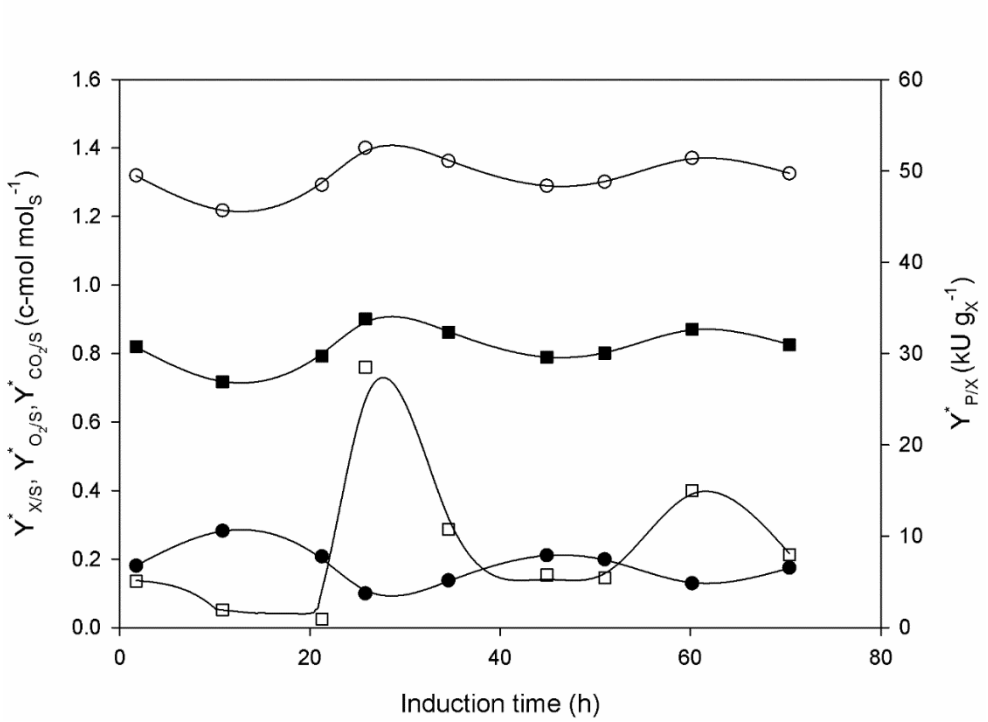

Figure 4.4 Yields of biomass ($Y^*_{X/S}$, ●), oxygen ($Y^*_{O2/S}$, ○) and carbon dioxide ($Y^*_{CO2/S}$, ■) in respect to the substrate and product to biomass yield ($Y^*_{P/X}$, □) during induction time of the culture carried out under conditions of DO_{SP} of 5 %.

Moreover, respiratory quotient (RQ) profile, represented in Figure 4.3B, can be considered constant during the stage of the process when it was evaluated, including a range of values from 0.61 to 0.65, with good agreement to those found from other *P. pastoris* cultures when growing in methanol as a sole carbon source [26,27].

Besides, the time evolution of yields along induction phase, shown in Figure 4.4 denoted no significant changes on metabolism when the already mentioned adaptation step took place, at least when referred to biomass, methanol and gases. This statement is backed up by both the facts that no byproducts were detected at significant amounts when samples were analyzed by HPLC and the fulfillment of balances all along the induction phase that has been previously discussed and represented in Figure 4.2.

At the same time, and as a counterpart, heterologous production of ROL along the induction phase behaved totally different when compared to the rest of state variables, in terms of both q_P and $Y^*_{P/X}$. A sudden drop of those two variables was observed during the

adaptation period and was followed by a progressive recovery. However, this last variable described a pronounced spike shortly after the first 20 h of induction.

The slowdown of the q_P suggests that ROL production might be more sensitive to sudden changes of oxygen supply. Besides, the calculation of discrete specific rates is made from mass balances where first derivatives need to be estimated. Although original data is smoothed, the resulting propagated error is significantly higher than for the mean specific rates, which are based on linear regression analysis, and in some way possible errors on state variables are filtered. This fact may provoke, in addition, some oscillations on discrete specific rates and yields, concretely on q_P and specially on $Y'_{P/X}$.

4.3.3 Comparative study on the effect of oxygen tension during induction

Considering the previous hypothesis that DO level could have a significant role on leading *P. pastoris* to changes on its bioprocess efficiency throughout the range of the study, specific growth, consumption and production rates and the relationships that exist between them (yields) are set as key physiological parameters to describe this behavior [28].

4.3.3.1 Influence on specific rates

In Figure 4.5A, mean specific growth (μ_{mean}), methanol uptake ($q_{S,mean}$) and ROL production ($q_{P,mean}$) rates are presented versus the mean level of DO during the induction phase from each culture. On the other hand, specific rates regarding the as phase ($q_{O2,mean}$ and $q_{CO2,mean}$) are shown along with the mean respiratory quotient (RQ) in figure 5B.

Global yields are depicted in Figure 4.6. In Table 4.1, mean specific rates are also specified for further discussion and comparison.

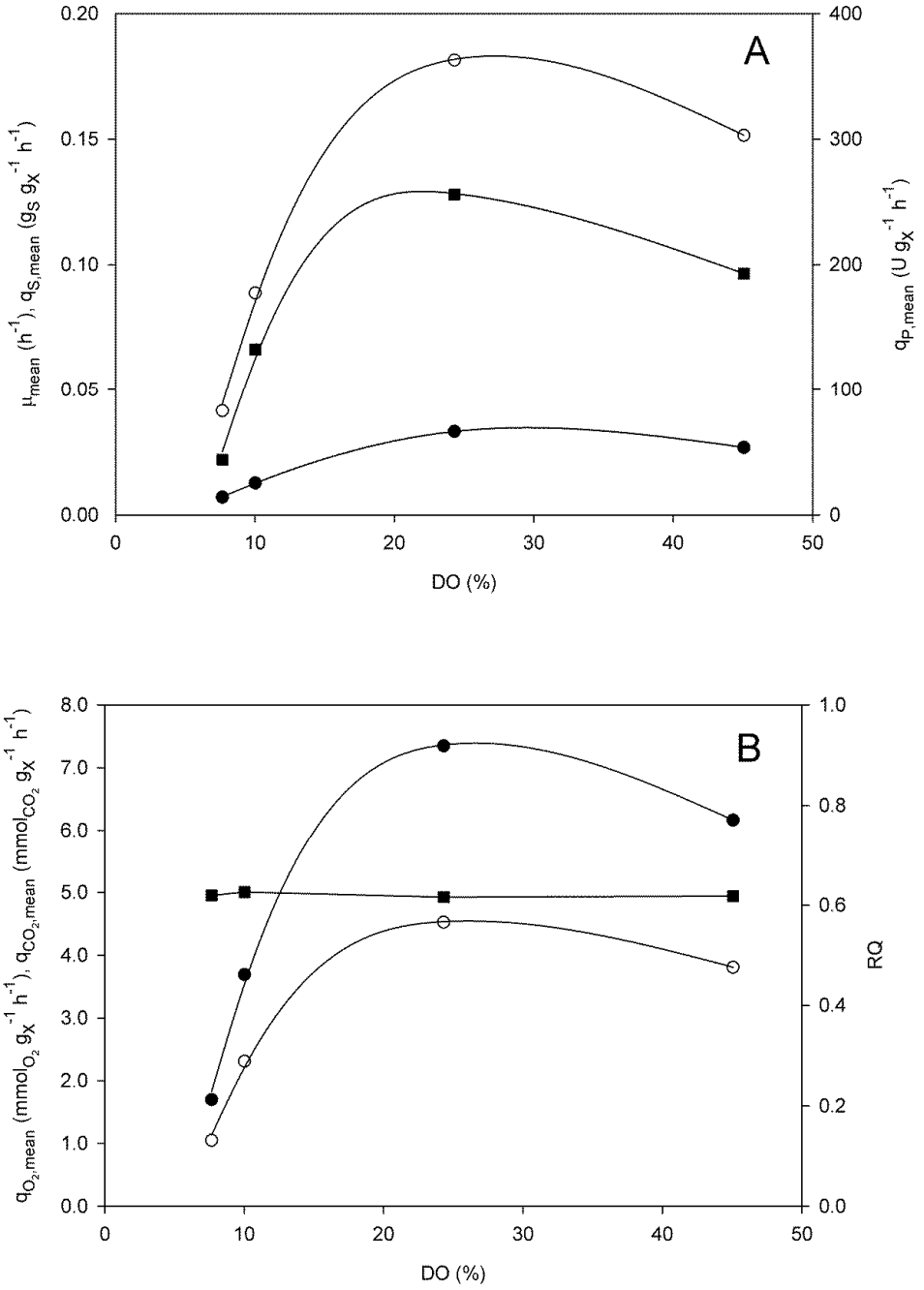

Figure 4.5 (A) Mean specific rates for growth (μ_{mean}, ●), methanol uptake ($q_{s,mean}$, ○) and ROL activity production ($q_{P,mean}$, ■) depending on DO level maintained throughout induction phases at the different cultures. **(B)** Mean specific rates for oxygen uptake ($q_{O2,mean}$,●) and carbon dioxide production ($q_{CO2,mean}$, ○), with respiratory quotient (RQ, ■) at different DO during the induction phase.

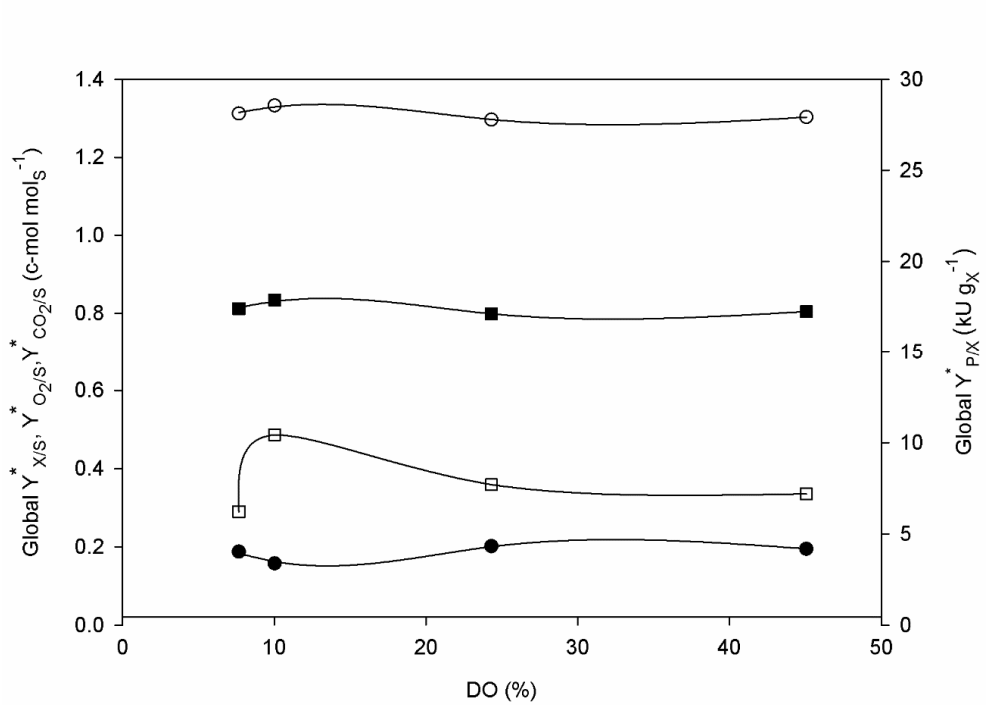

Figure 4.6 Global yields in respect to substrate and biomass ($Y^*_{X/S}$(●), $Y^*_{O2/S}$(○), $Y^*_{CO2/S}$(■), $Y^*_{P/X}$(□)) at different conditions of DO.

Table 4.1 . Comparison chart gathering the main process data regarding productivity, growth, consumption and production specific rates, as well as $Y^{*}_{P/X}$, maximal applied OTR and extracellular protein, obtained at different nominal DO values during the induction phase. ± indicates standard error (SE) from regression analysis

DO_{SP}	%	5	10	25	50
Final ROL activity	U mL^{-1}	195	315	368	303
$Y^{*}_{P/X}$	U g_X^{-1}	6220	10430	7700	7190
Total Productivity	kU h^{-1}	5.19	9.93	20.3	14.9
Vol. Productivity	U mL^{-1} h^{-1}	1.97	2.99	5.49	4.60
μ_{mean}	h^{-1}	0.007 ± 0.001	0.013 ± 0.001	0.034 ± 0.001	0.028 ± 0.001
$q_{s,mean}$	g_S g_X^{-1} h^{-1}	0.041 ± 0.004	0.089 ± 0.008	0.181 ± 0.016	0.151 ± 0.013
$q_{P,mean}$	U g_X^{-1} h^{-1}	43.9 ± 3.8	132 ± 11	256 ± 22	193 ± 17
$q_{O2,mean}$	$mmol_{O2}$ g_X^{-1} h^{-1}	1.70 ± 0.15	3.69 ± 0.32	7.35 ± 0.63	6.16 ± 0.53
$q_{CO2,mean}$	$mmol_{CO2}$ g_X^{-1} h^{-1}	1.05 ± 0.09	2.31 ± 0.20	4.53 ± 0.39	3.81 ± 0.33
OTR ≈ OUR	$mmol_{O2}$ $L^{-1}h^{-1}$	49.0	111	265	209
Extracellular protein	mg_{prot} L^{-1}	127	166	174	158

The recombinant protein produced by *P. pastoris* has a strong influence on the specific methanol uptake rate (q_S) as reported by some authors [11,29]. Thus, q_S is found between 0.05 and 0.57 $g_S\ g_X^{-1}\ h^{-1}$, and normally it is linearly dependent on the specific growth rate, as shown in Figure 4.7 for this work.

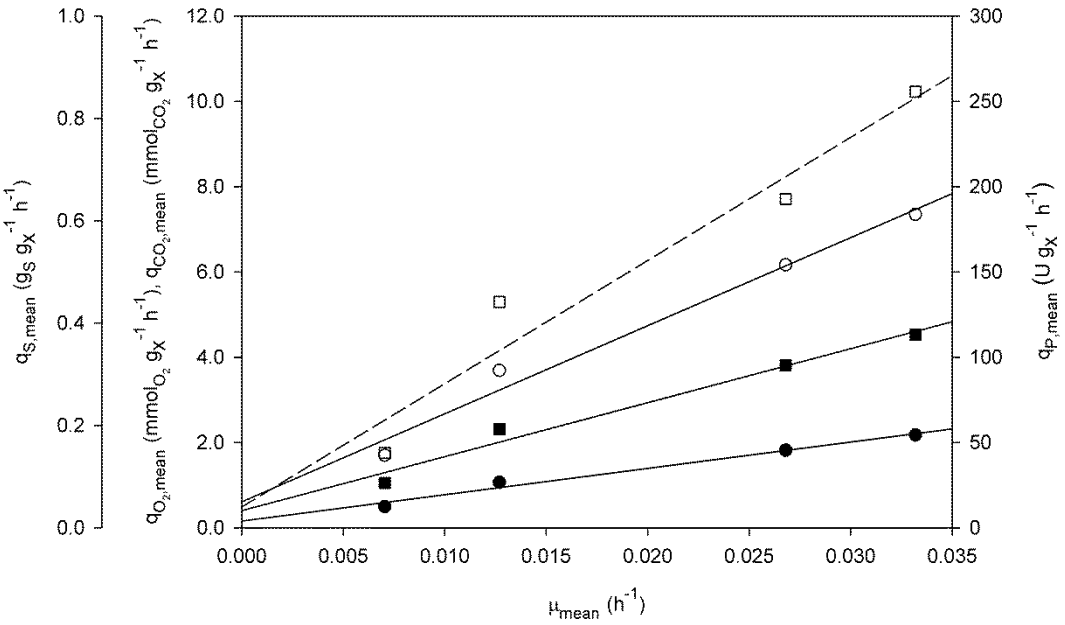

Figure 4.7 Correlation of specific rates ($q_{s,mean}$ (●), $q_{O2,mean}$ (○), $q_{CO2,mean}$ (■) and $q_{P,mean}$ (□)) with specific growth rate, μ_{mean}. Straight lines represent the corresponding correlation in which slope is the intrinsic yield and offset, the maintenance coefficient.

It is quite clear that oxygen tension has an important effect on the behavior of the culture in a way that slowed down the specific growth rate when it was brought under a lack of this substrate, as expected. Sufficient DO should be maintained because of methanol utilization metabolism [30,31]. To assure this, OTR values imposed for *P. pastoris* P_{AOX}-based cultures at normoxic conditions (fully aerobic) range typically from 50 to 300 mmol $L^{-1}\ h^{-1}$ [15,32]. Actual maximal values for this work are presented in table 1 and fit within the normal range applied for Mut^+ strains. By contrast, in cases where the operational strategy consisted on limiting the culture growth by OTR (DO near 0), this rate presented values placed below 50 mmol $L^{-1}\ h^{-1}$ [13]. Apart from that, commonly OTR applied to *P. pastoris* P_{GAP}-based strains are significantly lower than those for P_{AOX1} strains [16].

The decrease on the specific growth rate was seemingly observed when an excess of oxygen was supplied to the culture (DO_{SP} of 50 %), showing also a decrease on specific

rates of CO_2 production, methanol and oxygen uptake, though less pronounced when compared to the opposite end of the DO spectrum.

4.3.3.2 Analysis on global yields

Regarding the different global yields, while biomass, oxygen and CO_2 ones remained constant throughout the DO range tested, $Y'_{P/X}$ showed a spike-like maximum at DO 10 % (Figure 4.6). Besides, despite oxygen limitation including fully aerobic conditions is generally regarded as unfavorable [20,27] and supposed to negatively affect the expression of foreign genes [33], a maximum of product yield ($Y'_{P/X}$) was found at DO_{SP} of 10 %. This seems consistent with other published works where an increase of product yield occurred in conditions of oxygen transfer limitation, facts that are attributed to the reduction of either post-translational modifications at low oxygen availability [32] or cell lysis [34]. However, this fact does not concur with maximum $q_{P,mean}$ (found at DO around 25 %, Figure 4.5A), unlike what with a P_{GAP}-driven strain Baumann *et al.* (2007) [12] and Khatri and Hoffmann (2005) [11] with a Mut^+ strain respectively found. They achieved higher product titers and specific rate in chemostat when working at hypoxic and normoxic conditions respectively, both of them under oxygen transfer limiting conditions.

Furthermore, μ_{mean} increase was considerably higher than the $Y'_{P/X}$ decrease when DO_{SP} of 10 % and 25 % are compared (2.5-fold versus 1.4-fold), so that $q_{P,mean}$ increased. Extracellular protein shown in table 1 followed the same trend, within the experimental error, as titer achieved expressed as final ROL activity.

Similar results were found when examining total productivities and titer achieved (Table 4.1), where the best result was the one obtained at DO_{SP} of 25 %, as well as reported for a Mut^S strain by Jazini et al. (2014) [21], and the one that corresponds to 10 % was found more than 2-fold lower than the optimal one.

It is also quite remarkable to point out the response of the culture against DO availability in terms of mean specific oxygen uptake rate ($q_{O2,mean}$), represented in Figure 4.5B, which, as expected, was lower when approaching conditions of DO limitation (DO of 7-10 %). Nevertheless, when bringing the cells under certain excess of oxygen (DO_{SP} of 50 %), $q_{O2,mean}$ decreased as well, and thus a maximal value of this rate was found around a DO

of 25 %. All of these facts showed $q_{O2,mean}$ profile versus DO to behave the same way $q_{S,mean}$ and μ_{mean} did, and it is contrasted by a nearly invariable $Y'_{O2/S}$ values in all DO range tested (figure 4.6).

$q_{CO2,mean}$ described an analogue behavior so that a constant profile of RQ was obtained (Figure 4.5B). Hence, this indicates that no substantial metabolic changes occurred between different conditions of oxygen tension within the spectrum of DO tested.

This last statement is supported by what is shown in Figure 4.7, where the different mean specific rates are represented versus μ_{mean}. As the relation between $q_{O2,mean}$ and μ_{mean} can be correlated to a straight line, an intrinsic yield between oxygen and biomass ($Y_{O2/X}$) is maintained in all DO range, and the relatively low maintenance coefficient obtained ($m_{O2,X}$) (table 2) led to a weak dependence of $Y'_{O2/X}$ to μ_{mean}, and, therefore, to DO level (25 % of deviation between the maximum and minimum obtained). A similar trend is shown by those profiles that refer to methanol uptake and CO_2 production. Each intrinsic yield ($Y_{i/X}$) and maintenance coefficient ($m_{i/X}$) calculated is presented in Table 4.2.

Table 4.2 Intrinsic yields ($Y_{i/X}$) and maintenance coefficients ($m_{i/X}$) from biomass. ± indicates standard error (SE) from regression analysis

$Y_{S/X}$	$g_S\ g_X^{-1}$	5.14 ± 0.44
$m_{S/X}$	$g_S\ g_X^{-1}\ h^{-1}$	0.013 ± 0.010
$Y_{CO2/X}$	$mol_{CO2}\ g_X^{-1}$	0.127 ± 0.003
$m_{CO2/X}$	$mol_{CO2}\ g_X^{-1}\ h^{-1}$	$(4.0 \pm 3.0) \cdot 10^{-4}$
$Y_{O2/X}$	$mol_{O2}\ g_X^{-1}$	0.206 ± 0.020
$m_{O2/X}$	$mol_{O2}\ g_X^{-1}\ h^{-1}$	$(6.1 \pm 4.6) \cdot 10^{-4}$
$Y_{P/X}$	$U\ g_X^{-1}$	7220 ± 1240
$m_{P/X}$	$U\ g_X^{-1}\ h^{-1}$	12 ± 28

If they are compared to values from previous works [3,35], the results from this work are generally 15 % - 25 % lower both regarding $Y_{i/X}$ and $m_{i/X}$. The reason for $Y_{S/X}$ and $m_{S/X}$ variations from references are attributed to operational improvements carried out to

minimize methanol stripping. They mainly consisted on the position of the feed inlet and the optimization of the off-gas condensation system.

The deviation from references turned out to be higher in the case of product, both for $Y_{P/X}$ and $m_{P/X}$. Nevertheless, it would be bold to state that $q_{P,mean}$ and μ_{mean} are not so well correlated as a straight line, mainly because of the maximal value of $Y^{*}_{P/X}$ at DO_{SP} of 10 %, which hinted changes on metabolism associated to heterologous protein production.

In Table 4.3, global yields corresponding to $Y^{*}_{X/S}$, $Y^{*}_{O2/S}$, $Y^{*}_{O2/X}$ and $Y^{*}_{CO2/S}$ are listed together with some representative values from literature for their comparison. Values for both Mut^{+} and Mut^{s} strains with methanol as single substrate are included to highlight whether phenotype associated differences appeared. It can be observed that global yields reached similar values normally attained for other authors.

However, some results about $Y^{*}_{X/S}$ could be unrealistic or even inconsistent with the C-balance owing to potential loss of methanol through the off-gas stream, generation of by-products and the presence of large errors in biomass determination [29]. $Y^{*}_{X/S}$ values about 0.5 g g^{-1} are common to glycerol or glucose uptake. On the other hand, carbon from methanol can be dissimilated in CO_2 to a ratio of 80% [36], so $Y^{*}_{X/S}$ can be as low as ~ 0.2 g g^{-1} as a result.

Accordingly, $Y^{*}_{O2/X}$ values above ~ 0.09 mol O_2 $g_{biomass}^{-1}$ and $Y^{*}_{O2/S}$ close to the value of 0.047 mol O_2 g_S^{-1}, stoichiometric conversion coefficient for the methanol flux to energy metabolism (1.5 mol O_2 C-mol_S^{-1}), confirm the oxygen conditions applied are comparable between other published works when normoxic environment is kept by maintaining DO > 5% [26,35,37-39].

Complete oxidation of methanol to carbon dioxide would give a $Y^{*}_{CO2/S}$ of 0.031 mol CO_2 g_S^{-1}. Most of the global yields in Table 4.3 are close to this value, thus indicating that similar normoxic conditions are attained. Moreover, the lower value of $Y^{*}_{X/S}$, the higher the $Y^{*}_{CO2/S}$ is, in order to accomplish the C-balance. In a similar way, higher values of $Y^{*}_{X/S}$ should be accompanied with lower $Y^{*}_{O2/S}$ if e-balance is conserved.

Table 4.3 Comparison of yields from methanol for recombinant protein production processes in *P. pastoris* under the control of P_{AOX}.

Phenotype	Product	Operational strategy	μ (h^{-1})	T (°C)	pH	$Y^{*}_{X/S}$ (g g^{-1})	$Y^{*}_{O2/S}$ (mol g^{-1})	$Y^{*}_{O2/X}$ (mol g^{-1})	$Y^{*}_{CO2/S}$ (mol g^{-1})	Reference
X33 (Mut^{+})	ROL	S = 3 g L^{-1}	0.034$^{\#}$	30	5.5	0.19$^{\#}$	0.041$^{\#}$	0.22$^{\#}$	0.025$^{\#}$	This work
X33 (Mut^{+})	ROL	MLFB	0.020	30	5.5	0.21	0.040	0.19	0.025	[35]
GS115 (Mut^{+})	scFv	S = 3-30 g L^{-1}	0.060-0.080	30	6.0	0.26	-	-	-	[11]
YGLY4140 (Mut^{+})	IgG1	MLFB	0.008	24	6.5	0.30*	0.028	0.09	-	[38]
GS115 (Mut^{+})	Chymotrypsinogen B	S = 4 g L^{-1}	0.040-0.075	25-30	3.0-5.5	0.32	0.034	0.11	-	[39]
KM71H (Mut^{s})	Horseradish peroxidase	Continuous	0.009	28	5.0	0.18-0.27^{+}	-	-	0.022-0.025	[21]
GS115 (his4) (Mut^{s})	Angiostatin	MLFB	0.006	30	5.0	0.11	0.042	0.38	0.027	[26]
CBS7435 (Mut^{s})	Horseradish peroxidase	Pulses MetOH 1%	0.022	28	5.0	0.38^{+}	0.033	0.09	0.018	[37]

$^{\#}$ Values at optimal productivity

*Transformed from WCW to DCW by a factor of 4.2 WCW/DCW [38].

$^{+}$ Biomass elemental composition and ash content [5].

4.3.3.3 Bioprocess optimization

In Figure 4.8, evolution of total production of ROL activity (kU) expressed as increments from the start of each induction phase (Δ(PV)) is displayed.

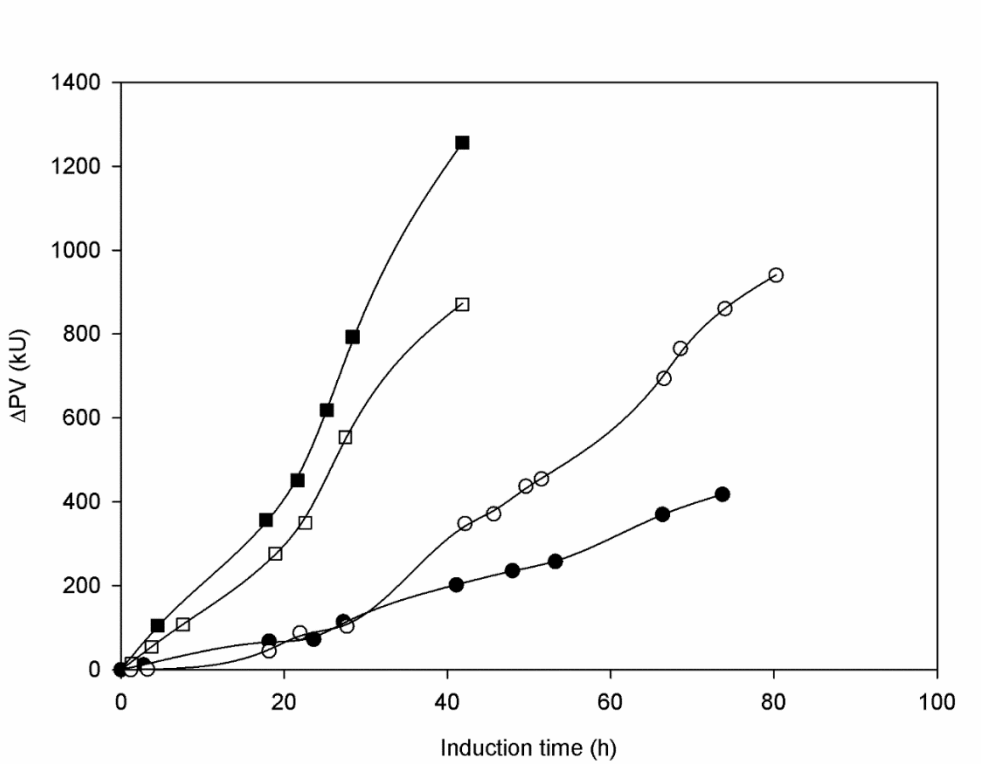

Figure 4.8 Evolution of incremental total production (Δ(PV)) during induction time at each condition of DO_{SP} (5 % (●), 10 % (○), 25 % (■) and 50 % (□)).

As previously stated, the best productivity, estimated from the slope, was achieved when working at DO_{SP} of 25 %. Apart from that, oxygen excess (DO_{SP} of 50 %) turned out to be more favorable than limitation, i.e. DO_{SP} of 5 % and 10 %, which behaved more similar to each other and their profiles were even superposed during the first hours of induction phase.

Bioprocess efficiency, quantified in terms of yield and productivities at the different DO_{SP} studied, is depicted in Figure 4.9.

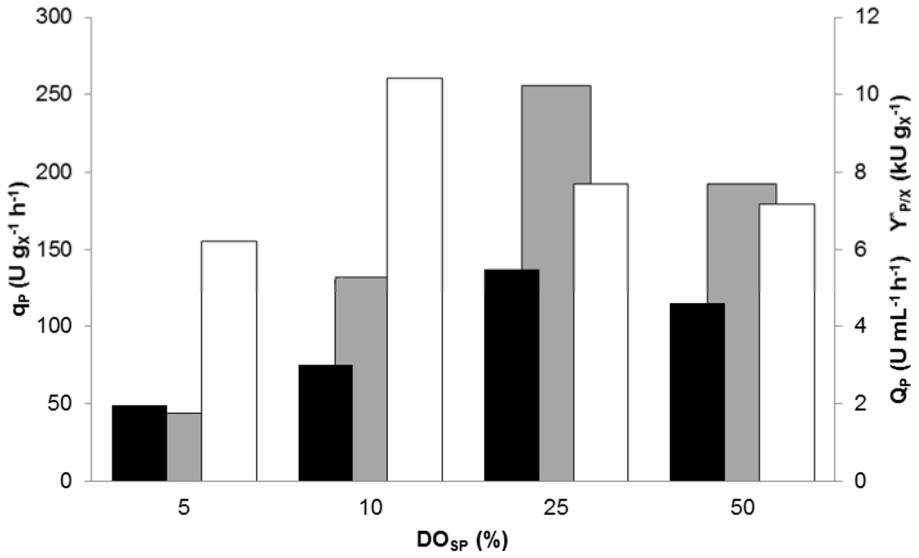

Figure 4.9 Bioprocess performance criteria: volumetric productivity (Q_P, black), specific production rate (q_P, grey) and yield ($Y'_{P/X}$, white) at different DO_{SP}

DO around 25 % was found to be the best operating condition for ROL productivity (Q_P), with 4-fold increase in respect to DO_{SP} of 5% and also corresponded with the highest specific rate for ROL activity production (q_P). However, the highest overall product yield ($Y'_{P/X}$) was obtained around DO of 10 % with an increase of 45 % when compared with maximal DO_{SP} of 50 % studied. Specific production rates and $Y'_{P/X}$ were lower at the extremes of the DO range tested.

In the case of *P. pastoris* growth on glycerol or glucose, oxygen limitation has been reported to lead to a shift to respiro-fermentative metabolism and the generation of a set of by-products such as ethanol, arabitol or succinate [40,41]. However, regarding the present case, with methanol as the only carbon source, no by-products were detected above the lower limit of detection, fact that was verified by the accomplishment of C-balances, suggesting that the main effect of the oxygen tension limitation was the decrease of all the specific rates. Since all of them are rather linearly correlated with μ (Figure 4.7), the lower consumption rate of methanol, the lower production rate of ROL is.

Finally, maximal ROL volumetric productivity attained was similar to the previously obtained for MNLFB cultures at 3 g L^{-1} but with DO about 30 % [7]. On the other hand, product to biomass yield and titer were significantly higher (46 % and 31 %, respectively). These facts, though, become consistent with the μ_{mean} values obtained for both cases.

4.4 Conclusions

The results validate that oxygen availability related to DO under normoxic conditions is a key parameter to reach higher yields and productivities. Taking into account the results obtained, it can be asserted that oxygen tension is a key variable that will allow improving the reliability of the system by keeping DO at optimal conditions when *P. pastoris* recombinant cultures are induced by methanol. This statement is reinforced when realizing that every specific rate slowed down at the right end of DO range, pointing out the need to optimize the DO conditions. Therefore, the optimization of this variable is required in the case of *P. pastoris* cultures expressing heterologous proteins under the control of P_{AOX1} to maximize production. That statement implies that the general trend of simply restricting the DO above 30 %, without control leads to wide variability regarding this environmental condition.

On the other hand, conditions of moderate DO limitation did not favor the bioprocess efficiency in terms of substrate uptake, growth and productivity of ROL, establishing the optimum around a DO of 25 %. This optimal DO condition represents an improvement on ROL productivity about 4-fold higher in respect to the lower DO set point investigated of 5 %. Similarly, at DO of 10 % the product to biomass yield ($Y_{P/X}$) is the highest and an enhancement of 45% is reached when compared with maximal DO_{SP} of 50 % studied, a condition frequently considered as positive to improve *P. pastoris* process efficiency.

In summary, some advantages arise from a practical point of view when moderate DO limitation is applied: first, productivity, yield and titer can be optimized controlling oxygen tension in the cultures. Second, the specific production rate depends on the specific uptake rate, and therefore, also on specific growth rate. Third, processes carried out under lower DO conditions require less oxygen transfer capacity, which becomes critical in large scale and/or high-density cultures during protein production with methanol, and so, reducing the oxygen supply and energy requirements.

The whole approach followed in this work, since it is systematic and rational based, can be applied for the production of different target proteins although their DO optimal values may result different from the obtained for the case of ROL.

4.5 References

[1] M. Jahic, F. Wallberg, M. Bollok, P. Garcia, S.O. Enfors, Temperature limited fed-batch technique for control of protelysis in *Pichia pastoris* bioreactor cultures, Microb. Cell Fact. 2:6 (2003).

[2] O. Cos, R. Ramón, J.L. Montesinos, F. Valero, Operational strategies, monitoring and control of heterologous protein production in the methylotrophic yeast *Pichia pastoris* under different promoters: A review, Microb. Cell. Fact. 5:17 (2003).

[3] J.M. Barrigón, J.L. Montesinos, F. Valero, Searching the best operational strategies for *Rhizopus oryzae* lipase production in *Pichia pastoris* Mut^+ phenotype: Methanol limited or methanol non-limited fed-batch cultures? Biochem. Eng. J. 75 (2013) 47-54.

[4] W. Zhang, M.A. Bevins, B.A. Plantz, L.A. Smith, M.M. Meagher, Modelling *Pichia pastoris* growth on methanol and optimizing the production of a recombinant protein, the heavy-chain fragment C of botulinum neurotoxin, serotype A, Biotechnol. Bioeng. 70 (2000) 1-8.

[5] O. Cos, A. Serrano, J.L. Montesinos, P. Ferrer, J.M. Cregg, F. Valero, Combined effect of the methanol utilization (Mut) phenotype and gene dosage on recombinant protein production in *Pichia pastoris* fed-batch cultures, J. Biotechnol. 116 (2005) 321-335.

[6] J. Jordà, S.S. de Jesús, S. Peltier, P. Ferrer, J. Albiol, Metabolic flux analysis of recombinant *Pichia pastoris* growing on different glycerol/methanol mixtures by iterative fitting of NMR-deried ^{13}C-labelling data from proteinogenic amino acids, New Biotechnol. 31 (2014) 120-132.

[7] D. Porro, M. Sauer, P. Branduardi, D. Mattanovich, Recombinant protein production in yeasts, Mol. Biotechnol. 31 (2005) 245-257.

[8] M.A. Eiteman, E. Altman. Overcoming acetate in *Escherichia coli* recombinant protein fermentations. Trends Biotechnol. 24 (2006) 11.

[9] S.Y. Lee, High cell-density culture of *Escherichia coli*, Trends Biotechnol. 14:3 (1996) 98-105.

[10] M.G. Wiebe, E. Rintala, A. Tamminen, H. Simolin, L. Salusjärvi, M. Toivari, J. T. Kokkonen, J. Kiuru, R. Ketola, P. Jouhten, A. Huuskonen, H. Maaheimo, L. Ruohonen, M. Penttilä. Central carbon metabolism of *Saccharomyces cerevisiae* in anaerobic, oxygen-limited and fully aerobic steady-state conditions and following a shift to anaerobic conditions, FEMS 8 (2008) 140-154.

[11] N.K. Khatri, F. Hoffmann, Impact of methanol concentration on secreted protein production in oxygen-limited cultures of recombinant *Pichia pastoris*, Biotechnol. Bioeng. 93:5 (2006) 871-879.

[12] K. Baumann, M. Maurer, M. Dragosits, O. Cos, P. Ferrer, D. Mattanovich, Hypoxic fed-batch cultivation of *Pichia pastoris* increases specific and volumetric productivity of recombinant proteins, Biotechnol. Bioeng. 100:1 (2007) 177-183.

[13] M. Berdichevsky, M. d'Anjou, M.R. Mallem, S.S. Shaikh, T.I. Potgieter, Improved production of monoclonal antibodies through oxygen-limited cultivation of glycoengineered yeast, J. Biotechnol. 155 (2011) 217-224.

[14] W.C. Liu, T. Gong, Q.H. Wang, X. Liang, J.J. Cheng, P. Zhu, Scaling-up fermentation of *Pichia pastoris* to demonstration-scale using new methanol-feeding strategy and increased air pressure instead of pure oxygen supplement, Sci. Rep. 6 (2016) 18439.

[15] F. Carly, H. Niu, F. Delvigne, P. Fickers, Influence of methanol/sorbitol co-feeding rate on p*AOX1* induction in a *Pichia pastoris* Mut^+ strain in bioreactor with limited oxygen transfer rate, J. Ind. Microbiol. Biotechnol. 43 (2016) 517-523.

[16] H. Günes H, P. Çalik. Oxygen transfer as a tool for fine-tuning recombinant protein production by *Pichia pastoris* under glyceraldehyde-3-phospate dehydrogenase promoter, Bioprocess Biosyst. Eng. 39:7 (2016) 1061-1072.

[17] A. Surribas, R. Stahn, J.L. Montesinos, S.O. Enfors, F. Valero, M. Jahic. Production of a *Rhizopus oryzae* lipase from *Pichia pastoris* using alternative operational strategies, J. Biotechnol. 130 (2007) 291-299.

[18] S. Tang, L. Boehme, H. Lam, Z. Zhang Z, *Pichia pastoris* fermentation for phytase production using crude glycerol from biodiesel production as the sole carbon source, Biochem. Eng. J. 43 (2009) 157-162.

[19] C. Arnau, C. Casas, F. Valero, The effect of glycerol mixed substrate on the heterologous production of a *Rhizopus oryzae* lipase in *Pichia pastoris* system, Biochem. Eng. J. 57 (2011O 30.37.

[20] C.Y. Lee, S.L. Lee, K.H. Jung K H, Katoh S, Lee E K. High dissolved oxygen tension enhances heterologous protein expression by recombinant *Pichia pastoris*. Process Biochem. 2003;38:1147-1154.

[21] M. Jazini, G. Cekici, C. Herwig, Quantifying the effects of frequency and amplitude of periodic oxygen-related stress on recombinant protein production in *Pichia pastoris*, Bioengineering 1 (2014) 47-61.

[22] P. Wechselberger, P. Sagmeister, C. Herwig, Model-based analysis on the extractability of information from data in dynamic fed-batch experiments, Biotechnol. Prog. 29 (2013) 285-296.

[23] D. Resina, A. Serrano, F. Valero, P. Ferrer, Expression of a *Rhizopus oryzae* lipase in *Pichia pastoris* under control of the nitrogen source-regulated formaldehyde dehydrogenase promoter, J. Biotechnol. 109 (2004) 103-113.

[24] N.S. Wang, G. Stephanopoulos, Application of macroscopic balances to the identification of gross measurement errors, Biotechnol. Bioeng. 25:9 (1983) 2177-2208.

[25] R.T.J.M. Van der Heijden, J.J. Heijnen, C. Hellinga, B. Romein, K.C.A.M. Luyben, Linear constraint relations in biochemical reaction systems: I. Classification of the

calculability and the balanceability of conversion rates, Biotechnol. Bioeng. 43 (1993) 3-10.

[26] J. Xie, R. Yang, Q. Zhou, P. Du, R. Gan, Q. Ye, Efficiencies of growth and angiostatin expression in cultures of *Pichia pastoris* fed with mixed carbon sources, Chem. Biochem. Eng. Q. 27:2 (2013) 235-244.

[27] M.E. Bushell, M. Rowe, C.A. Avignone-Rossa, J.N. Wardell, Cyclic fed-batch culture for production of human serum albumin in *Pichia pastoris*, Biotechnol. Bioeng. 82 (2003) 678-693.

[28] T. Egli, Microbial growth and physiology: a call for better craftsmanship, Front. Microbiol. 6:287 (2015).

[29] J.M. Barrigón, F. Valero, J.L. Montesinos, A macrokinetic model-based comparative meta-analysis of recombinant protein production by *Pichia pastoris* under *AOX1* promoter, Biotechnol. Bioeng. 112:6 (2015) 1132-1145.

[30] R. Couderc, J. Baratti, Oxidation of methanol by the yeast *Pichia pastoris*. purification and properties of the alcohol oxidase, Agric. Biol. Chem. 44:10 (1980) 2279-2289.

[31] A.A. Sibirny, V.I. Titorenko, M.V. Gonchar, V.M. Ubiyvovk, G.P. Ksheminskaya, O.P. Vitvitskaya, Genetic control of methanol utilization in yeasts, J. Basic Microbiol. 28:5 (1988) 293-319.

[32] O. Trentmann, K.N. Khatri, F. Hoffmann, Reduced oxygen supply increases process stability and product yield with recombinant *Pichia pastoris*, Biotechnol. Prog. 20 (2004) 1766-1775.

[33] J.L. Cereghino, J.M. Cregg, Heterologous protein expression in the methylotrophic yeast *Pichia pastoris*, FEMS 24 (1999) 45-66.

[34] T. Charoenrat, M. Ketudat-Cairns, H. Stendahl-Andersen, M. Jahic, S.O. Enfors. Oxygen-limited fed-batch process: an alternative control for *Pichia pastoris* recombinant protein processes, Bioprocess Biosyst Eng 27 (2005) 399–406.

[35] J.M. Barrigón, R. Ramón, I. Rocha, F. Valero, E.C. Ferreira, J.L. Montesinos. State and specific growth estimation in heterologous protein production by *Pichia pastoris*, AIChE J. 58:10 (2012) 2966-2979.

[36] J. Jordà, P. Jouhten, E. Cámara, H. Maaheimo, J. Albiol, P. Ferrer, Metabolic flux profiling of recombinant protein secreting *Pichia pastoris* growing on glucose:methanol mixtures, Microb. Cell Fact. 11:57 (2012).

[37] F.W. Krainer, C. Dietzsch, T. Hajek, C. Herwig, O. Spadiut, A. Glieder, Recombinant protein expression in *Pichia pastoris* strains with an engineered methanol utilization pathway, Microb. Cell Fact. 11:22 (2012).

[38] T.I. Potgetier, S.D. Kersey, M.R. Mallem, A.C. Nylen, M. d'Anjou M, Antibody expression kinetics in glycoengineered *Pichia pastoris*. Biotechnol. Bioeng. 6 (2010) 918-927.

[39] S. Curvers, P. Brixius, T. Klauser, J. Thömmes, D. Weuster-Botz, R. Takors, C. Wandrey C. Human chymotrypsinogen B production with *Pichia pastoris* by integrated development of fermentation and downstream processing. Part 1. Fermentation, Biotechnol. Prog. 17 (2001) 495-502.

[40] M. Carnicer, K. Baumann, I. Töplitz, F. Sánchez-Ferrando, D. Mattanovich, P. Ferrer, J. Albiol J. Macromolecular and elemental composition analysis and extracellular metabolite balances of *Pichia pastoris* growing at different oxygen levels, Microb. Cell Fact. 8:65 (2009).

[41] X. Liu, B. Jia, X. Sun, J. Ai, L. Wang, C. Wang, F. Zhao, J. Zhan, W. Huang, Effect of initial pH on growth characteristics and fermentation properties of *Saccharomyces cerevisiae*, J. Food Sci. 80 (2015) 800–808.

5 TOWARDS OPTIMAL SUBSTRATE FEEDING FOR HETEROLOGOUS PROTEIN PRODUCTION IN *Pichia pastoris* FED-BATCH PROCESS UNDER P_{AOX1} CONTROL: A MODELLING AIDED APPROACH

This chapter has been submitted as a research paper to the journal *Processs Biochemistry*, with the same title.

5.1 Introduction

The most common design criteria for bioprocess efficiency are product yield ($Y_{P/S}$, g product g^{-1} substrate), productivity (Q_P, g product L^{-1} h^{-1}) and final titer (P_F, g product L^{-1}). Whereas the first one is interesting to be boosted in processes of low cost products (high volumes), productivity and titer are typically more sought in high-added value ones. Heterologous protein expression systems can usually be optimized by using improved strains in combination with an optimal engineering strategy avoiding highly complex media in order to reduce costs and facilitate downstream processes [1,2].

The advances in monitoring and control have contributed to the development of operational strategies in fed-batch mode to enhance bioprocess efficiency, involving limitation of process variables like methanol and oxygen availability [3–5], which may control kinetic parameters such as specific rates of growth, substrate uptake or production.

The knowledge and characterization of the kinetics of the culture is key to optimize and design the proper operational strategy to achieve high product yield and a robust and reproducible process. In that way, as stated in section 1, Egli (2015) [6] appointed the control of μ to be essential for that purpose, by achieving a physiological stability in dynamic cultures as batch and fed-batch, which leads to the reproducibility of the process, a fundamental goal in an industrial point of view. Methanol limited fed-batch (MLFB) is a clear example of physiological control where constant μ is maintained throughout the fed-batch culture [7]. This parameter is also critical, in some cases, to achieve high titers and good product quality [8], for instance, requiring moderate or even low μ to ensure the correct protein folding or to avoid cell stress. In that way, specific rate of the secreted protein (q_P) vs specific growth rate (μ) is a kinetic

pontrelationship that is essential to be known. It depends on several genetic and physiological factors such as the codon usage of the expressed gene, the gene copy number, efficient transcription, translation, processing, folding and degradation in the endoplasmic reticulum and secretion out of the cell [2,9]. This relationship needs to be determined empirically in the production of recombinant proteins with *Pichia pastoris* because is not predictable a priori [10].

Hensing *et al.* (1995) [11] discussed about bioprocess optimization depending on several shapes of q_P in respect to μ for yeasts *Hansenula polymorpha* and *Kluyveromyces marxianus*. Looser *et al.* (2015) [8] presented examples of production kinetics, comparing some of them from both P_{AOX1} and P_{GAP}-based cultures, where q_P generally increased with μ in P_{GAP} cases, while P_{AOX1} strategies mostly described profiles with highest q_P at moderate μ [12]. Accordingly, P_{GAP}-based systems commonly present a linear dependence between q_P and μ [13], and are carried out by using pre-programmed feeding profiles to maintain constant values of μ close to the maximum to achieve high productions. Besides, Maurer *et al.* (2006) [14] described a Monod-type model for the q_P-μ kinetics for the production of an antibody fragment (Fab) under P_{GAP} control.

However, for systems under P_{AOX1} control it is even much more challenging to achieve high productivity, as high q_P at low μ implies high product yield ($Y'_{P/X}$) and lets the culture reach top levels of protein titer before coming across operational limitations caused by high biomass concentration, e.g. heat exchange and oxygen transfer as the most common ones. The compromise between the desired highest q_P as possible at moderate μ gives ground to the development of new operational strategies in fed-batch mode, where optimal profiles of μ are built to maximize design parameters of the process, regarding the production of the desired protein.

Optimization of recombinant protein production processes has been usually carried out by finding a solution through the *Pontryagin's maximum principle* (PMP) [15–17], the *Green's theorem* [18] or dynamic programming methods [19,20]. Numerical methods can be applied and are divided into deterministic and stochastic ones. Commonly, techniques applied to the first approach are gradient-based local methods like *Sequential Quadratic Programming* [21]. The main disadvantages of these methods are the computing effort and local optima, especially when the number of state and control variables increases. Stochastic metaheuristic algorithms,

belonging to the class of *Evolutionary Computation*, are used because of their interesting performance/computing time ratio, although global optimality cannot be guaranteed. *Evolutionary algorithms* (EA), *Differential Evolution* and *Particle Swarm Optimization* have been applied to obtain optimal feeding profiles in different fed-batch fermentation processes [22].

Maximization of production for a secreted coffee bean α-galactosidase in *P. pastoris* Mut^+ phenotype was carried out considering a nonlinear function for $q_P=f(\mu)$, where the dynamic optimization problem was solved analytically to provide some type of optimal μ time-trajectories from PMP by minimizing the *Hamiltonian* of the system [23]. Kobayashi *et al.* [19] implemented an optimized μ-profile from dynamic programming in *P. pastoris* P_{AOX1}-based system to maximize the production of Human Serum Albumin resulting in a continuously exponential decrease of μ throughout the induction phase. An analogue profile was developed and implemented for a P_{GAP} strain producing an antibody fragment (Fab) despite presenting completely opposite q_P vs μ relationships, as mentioned [22]. An optimization tool based on calculus of variations was developed, as special case of PMP, which was evaluated with the use of the generalized reduced gradient (GRG) method. The platform built on *Microsoft Excel*® used *Solver* software to simply find a solution for optimal time profiles of μ in fed-batch cultures of *P. pastoris* making use of modelling data from product generation and substrate uptake kinetics.

The objective of this work is in the way to satisfy the need of strategies for systematic bioprocess development in the cell factory *P. pastoris* under P_{AOX1} for the heterologous protein production. Thus, after the definition and analysis of optimized profiles (OP) by numerical methods from the use of a process model for systems with substrate inhibition patterns on both q_P and μ, the experimental comparison with the most suitable alternatives previously reported has been carried out. As model protein, 1-3 positional selective recombinant *Rhizopus oryzae* lipase (ROL) [24] has been selected, because of its multiple applications in pharma [25], food [26,27] and energy industries [28,29].

By accomplishing the stated, a simple optimization platform would be established, and transferable to other expression systems and/or to produce other target products.

5.2 Materials and methods

5.2.1 Strain

The wild type *P. pastoris X-33* strain containing the vector pPICZαROL was used for the heterologous expression of ROL under the control of the P_{AOX1} (Mut^+ phenotype) [30].

5.2.2 Inoculum preparation

Inoculum for bioreactor was cultured in 1 L baffled shake flasks at 30 °C, 150 rpm (HT Multitron incubator, Infors AG, Bottmingen, Switzerland), for 24 hours, in YPD medium (10 g of yeast extract, 20 g of peptone, 20 g of D-glucose and 500 µg of zeocin per liter of distilled water), initial pH 7.4. The already grown culture was centrifuged at 4500 x g and the cells were re-suspended in bioreactor culture medium and used to inoculate a 5 L Sartorius Biostat B bioreactor (Sartorius, Göttingen, Germany). Initial fermentation volume was 2 L and OD_{600} close to 2.5.

5.2.3 Fed-batch bioreactor cultivation

Cells were inoculated in basal salts medium, which contained, per liter of distilled water: H_3PO_4 (85%) 26.7 mL, $CaSO_4$ 0.93 g, K_2SO_4 18.2 g, $MgSO_4{\cdot}7H_2O$ 14.9 g, KOH 4.13 g, glycerol 40 g, 2 mL of biotin solution (20 mg L^{-1}), 5 mL of trace salts solution and 0.5 mL of antifoam agent (A6426, Sigma-Aldrich Co., St. Louis, MO, USA). Trace salts solution was composed, per liter of distilled water, of $CuSO_4{\cdot}5H_2O$ 6.0 g, NaI 0.08 g, $MnSO_4{\cdot}H_2O$ 3.0 g, $Na_2MoO_4{\cdot}2H_2O$ 0.2 g, H_3BO_3 0.02 g, $CoCl_2$ 0.5 g, $ZnCl_2$ 20.0 g, $FeSO_4{\cdot}7H_2O$ 65.0 g, biotin 0.3 g, H_2SO_4 98 % 5 ml.

The fermentation was performed as described elsewhere [31], being divided into the phases of glycerol batch (GBP), transition (TP) and methanol induction (MIP). This last stage was optimized as stated before, carrying out a methanol non-limited fed-batch strategy (MNLFB), by finding the best methanol concentration time profile.

During GBP, pH was controlled by adding NH_4OH 30 % (v/v) and DO was kept higher than 25% air saturation, by regulating the stirring rate between 600-1000 rpm, and introducing 1 vvm of air. TP consisted in a 5 h pre-programmed glycerol feeding rate under carbon limited conditions and methanol feeding rate stepwise increased, where cells adapt to methanol as a carbon

source [32]. Glycerol (50 % w/w with 5 mL of trace salts solution and 2 mL of biotin solution per liter) and pure methanol (with 5 mL of trace salts solution and 2 mL of biotin solution per liter) solutions were used as feeding. pH was controlled by the addition of KOH 5 M during both this phase and the next one. DO was, as well, kept at 25 % air saturation.

Finally, during MIP, methanol was added as inducer and sole carbon source, and controlled according to each operational strategy. Methanol feed solution contained 5 mL of trace salts solution and 2 mL of biotin solution per liter of pure methanol. Nitrogen needs were fulfilled by the addition of NH_4Cl solution (200 g of NH_4Cl, 5 mL of trace salts solution and 2 mL of biotin solution per liter). Its flow rate was directly linked to the methanol one and was automatically calculated online, by the previously estimated ammonium chloride/methanol requirements: 0.12 g g^{-1} to maintain the suitable NH_4^+ concentration [33,34].

DO was controlled at 25% in respect to air saturation (~ $2.3 \cdot 10^{-4}$ mol O_2 L^{-1}) by a cascade-based control, which involved regulating the stirring rate between 800 and 1000 rpm and total inlet gas flow rate of air and additional pure oxygen, being within the range 1-2 vvm. Temperature was kept at a value of 30 °C and pH at 5.5, throughout the three phases of the process.

5.2.4 Analytical methods and monitoring

5.2.4.1 Methanol determination and control

Methanol concentration was monitored by the Methanol Sensor System (Raven Biotech Inc., Vancouver, Canada) and controlled by performing a predictive-adaptive PI control strategy adapted from what is described elsewhere [7], that can be also derived from the general model control (GMC) theory, as the following equation describes:

$$F_{t+1} \approx F_t - \frac{V_t}{(S_{feed} - S_t)} \frac{dS_t}{dt} + \frac{K_P \cdot V_{t+1}}{(S_{feed} - S_{t+1})} \left(\varepsilon_{t+1} + \frac{1}{\tau_I} \int_{t_0}^{t+1} \varepsilon_t \, dt \right)$$

Equation 5.1

where F is the substrate feeding rate [L h^{-1}], V_t volume of culture broth [L], S_{feed} methanol feeding concentration [g L^{-1}], S_t residual methanol concentration [g L^{-1}], K_P gain of the controller [min^{-1}], τ_I integral time constant of the controller [min], ε_t error or deviation from substrate set point [g L^{-1}].

Apart from that, methanol concentration was also quantified offline by HPLC as previously reported [35]. Residual standard deviation (RSD) was estimated to be about 2 %.

5.2.4.2 Dry cell weight analysis

Biomass concentration was measured as the dry cell weight (DCW) per liter of culture, as described in chapter 2 and 3. Determinations were performed by triplicate and the relative standard deviation was about 5 %.

5.2.4.3 Extracellular ROL activity assay

ROL activity was measured by colorimetry, as it is described in previous sections.

5.3 Theory/calculation

5.3.1 The process model

The fermentation process for ROL production by *P. pastoris* Mut^+ phenotype is considered here. Yields, productivities and specific production rate in each methanol limited fed-batch (MLFB) condition were very low, obtaining the best results at the lowest specific growth rates. Similar results were obtained for methanol non-limited fed-batch (MNLFB) strategy at methanol set-point concentrations up to 2 g L^{-1}. However, for methanol set-points higher than 2 g L^{-1}, a significant increase in the production was observed. At a methanol set-point of 3 g L^{-1}, the highest product yield ($Y^{*}_{P/X}$), volumetric and specific productivity and mean specific production rate ($q_{P,mean}$) were obtained, though in terms of ROL production high values were found in the whole range of 3-10 g L^{-1} [7]. Accordingly, a first-principles-based (mechanistic) model of the bioprocess was firstly developed to properly describe behavior of substrate, biomass and ROL production [12].

5.3.1.1 Mass balances and stoichiometric equations

The calculations on this section were carried out as it is explained in chapter 4.

5.3.1.2 Kinetic model for ROL production

The model selected includes non-monotonic substrate functions (also called *bell-shaped*) for cell growth and ROL production, as shown below:

$$q_i = \frac{q_{max,i}\, S}{K_{s,i} + S + \frac{S^2}{K_{I,i}}}$$

Equation 5.2

where q_i is the i-specific rate, $q_{max,i}$ the nominal maximum value of the i-specific rate, $K_{S,i}$ [g L^{-1}] the substrate non-monotonic increasing model constant, $K_{I,i}$ [g L^{-1}] the substrate inhibition non-monotonic increasing model constant [12]. When working at different μ and no significant changes of metabolism are observed between conditions, yields associated to growth (intrinsic) and maintenance coefficients of each component can be found by the following expression:

$$q_i = Y_{i/X}\, \mu + m_{i/X}$$

Equation 5.3

where $Y_{i/X}$ is the intrinsic yield between the *i* component (substrate, O_2, CO_2) and biomass, $m_{i/X}$ the maintenance coefficient for the *i* component. Hence, the bioprocess model was updated to include specific rates for oxygen consumption and carbon dioxide production, as well as their contribution to variation of volume during the process.

The dynamic model defined by mass balances can be used to test a set of possible operating strategies, e.g. by comparing different control strategies in a series of simulations solving the bioprocess model consisting of this set of ordinary differential equations (*ODEs*) and algebraic equations. To solve dynamic equations, the *Matlab*'s ordinary differential equation solver function *ode45* was used.

Besides, to give simplicity to the whole optimization approach, and once confirmed that an error below 0.1% for the main state variables and performance indexes was obtained, *Microsoft Excel*® (2010) was used for the exploitation step of the model for bioprocess optimization. It allows the approximation of a model by numerically solving system equations and the optimization of an objective function by modifying the decision variables, while different constraints can be imposed [14]. In the current platform, to improve numerical solutions, new features were included, such as phase plots, non-monotonic functions and critical substrate concentrations for specific rates, net gas flow rate to estimate volume variation, determination of optimal *S*-

profiles, optional restrictions on oxygen transfer rate and, finally, maximization of the number of decision variables, as well as the use of central differences to compute derivatives.

5.3.2 Global optimization approach

From an industrial point of view, the usual purpose of model development is to improve process efficiency and to provide a quantitative basis for control. In this way, the mathematical model can be used to understand and evaluate the necessary trade-off among the different operating alternatives [36]. That is necessary to define target functions to be optimized, which can be used as design criteria and are discussed below.

5.3.2.1 Design criteria and performance indexes

As it has been mentioned before, $Y_{P/S}$, Q_P and P_F are the most common performance indexes selected to assess bioprocess efficiency. Moreover, among others, specific productivities and yields on both biomass and substrate can also be considered. High values for these indexes result in the reduction of capital and operating costs. Q_P is defined as follows:

$$Q_P = \frac{\Delta(PV)}{V \cdot \Delta t}$$

Equation 5.4

These criteria are firstly based on the calculation, estimation and/or quantification of the total amount of key product obtained (*PV*) as follows:

$$\Delta(PV) = \int_{t_{ind}}^{t_f} q_P\,(XV)dt$$

Equation 5.5

This quantification is normally carried out within the MIP, where methanol is used as the carbon and inducer substrate. The selected methanol feeding strategy used during the MIP is one of the most important factors to maximize heterologous protein production.

5.3.2.2 Process optimization methodology

Generally, to enhance bioprocess efficiency considering only upstream, a fermentation is expected to produce the maximum amount of product in the minimum process time (Q_P or space

time yield, STY), which requires to reach the maximum concentration of biomass (X) with a high specific production rate (q_P) in the minimum process time as possible to harvest a product with the desired quality specifications [8]. The dynamic model can be used for systematic simulation-based analysis of feasible feeding alternatives such constant flow rate, stepwise increased flow rate, exponential/open-loop μ control (MLFB), closed-loop S control (MNLFB) and customized feeding polices.

Usually, the feeding profile is directly optimized as decision variable, whereas in other applications the goal of the optimization is to find the best values for μ such the volumetric productivity or STY is then maximized. This later kind of operation belongs to the class of physiological state control, which has important advantages that accounts for cell growth and physiology, substrate uptake, productivity and product quality. The relationship between product formation and biomass growth mainly governs the production process. This μ-profile can be implemented through different control procedures, involving from the simplest, consisting in an open-loop control structure based on mass balances by a μ-dependent exponential feeding [14,23], to a more complex closed-loop control, including the use of software sensors, predictive and adaptive control [37–39]. However, when μ and q_P are a non-monotonic function and their dependence on S does not coincide, the implementation of such optimized μ-profiles is hampered by the multiplicity of S-μ-q_P states. Hence, another control variable different from μ and based on a rational approach is required. That is the case of ROL production under the control of P_{AOX1}, where inhibition patterns by methanol are observed for specific rates of growth (μ) and ROL secretion (q_P) [12]. These profiles are represented in Figure 5.1.

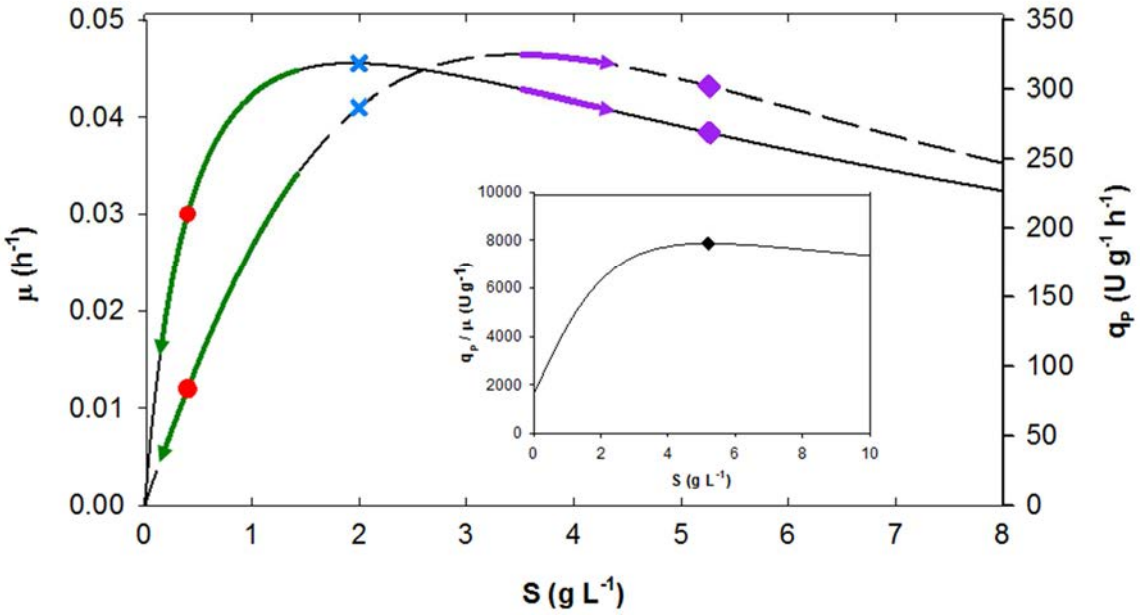

Figure 5.1 Kinetic model plots. *S* profiles of μ (—) and q_P (---), including operational conditions for the simulated feeding strategies. The following profiles are depicted: CF (green line), CM (●), CS (x), OP1 (♦) and OP2 (purple line). The subplot (down right) represents the quotient q_P-μ along *S*. The (♦) point indicates its maximum.

Since ROL production is clearly favored in conditions of methanol excess (MNLFB strategy), methanol concentration (*S*) is presented as the ideal and easy-to-implement state variable to be defined along the induction phase, which also prevents multiplicity of *S*-μ-q_P states. Consequently, once *S*-profile was determined, *F*-profiles and μ-profiles were straightforwardly obtained from the combination of mass balances and growth kinetics.

Numerical methods were considered to obtain a simple and versatile tool capable to be applied in a wide range of systems with different model structure and particular characteristics. Techniques regarding both deterministic and stochastic numerical methods were tested using *Excel Solver®* (2010). Concretely, they consisted on the *Generalized reduced gradient* (GRG) nonlinear solving method because of the actual non-complexity of the system under study, and the Evolutionary solving method that uses an *Evolutionary algorithm* (EA) as a subclass of *Evolutionary Computation* (EC), due to proven suitable performance/computing time ratio.

The interdependence of product formation and biomass growth is of key importance regardless of the selected criterion for the optimization, maximizing either yield or productivity [12]. Nevertheless, it must also be considered that the biomass growth in a bioprocess is limited, which may be due to biological and different physical restrictions, mainly heat and mass transfer. Although a maximum of biomass concentration needs to be set, mainly to reduce costs and facilitate downstream processes, often oxygen availability is the most important limitation for aerobic processes. For this reason, the volumetric mass transfer coefficient of oxygen (k_La) is often used as scaling-up criterion.

Accordingly, a maximum biomass concentration of X_{max} = 55 g L^{-1} was imposed as restriction, due to operational limitations of mass and energy transfer. A maximum working volume (V_{max}) of 5 L and methanol concentration (S_{max}) of 10 g L^{-1} were considered to be within the actual operational range. Final time was a free variable to allow optimizing the selected performance indexes. Total substrate added was not imposed as constraint, since for this kind of process and with methanol as substrate, its contribution on total cost is not significant, if it is compared to other capital and operating costs.

5.3.2.3 Implementation features of the optimized profiles

The accomplishment of the optimal *S*-profiles obtained by the optimization algorithms for the different performance criteria applied were reached by the implementation of a reliable dynamic control into the system. The methanol closed-loop control employed is based on a previously developed predictive-PI feedback controller which has been intensively applied with success in MNLFB cultures [7] as well as in strategies involving mixed substrates [35]. In the present work, the feedback controller has incorporated adaptation of the controller parameters over the fermentation process, to take into account the dynamics of the system. The controller ensures that the residual methanol concentration (*S*) in the culture broth is tracked with the minimum of error (MRE ≈ 2 %).

This alternative, then, allows a simple implementation of an optimized μ profile with *S* as the controlled variable, thanks to the conjunction with the S-μ-q_P model. That would minimize costs in an industrial application, and at the same time, avoid an open-loop control that would cause the process to be hampered by system perturbations [40].

5.4 Results and discussion

The challenging task of improving efficiency in the recombinant protein production (RPP) processes decomposes into several aspects necessary to fulfil. The basic features and characteristics outlined in the previous sections comprise system knowledge, data gathering, modelling of the system, exploitation of the model to explore promising alternatives, system optimization and finally verification and analysis of the feasible operating strategies.

The first three aspects were successfully developed in previous works [7,12] and the subsequent ones corresponding to model exploitation for simulation and process optimization, as well as the concluding rational analysis of the different alternatives have been developed extensively in the present work.

5.4.1 Process simulation for model exploitation

Model exploitation was carried out to reduce experimental effort and quickly identify the most promising alternatives, which could then be verified and analyzed later by new experimental data. Initial conditions of fed-batch for the state variables were X(0) = 27 g L^{-1}; P(0) = 50 U mL^{-1}; V(0) = 2 L. S(0) was set to 1 g L^{-1} in process simulations where F profile was predefined, because it is the common residual concentration attained at the end of the TP, before the MIP started.

Model parameters used for the performed simulations concerning the MIP are listed in Table 1. The ones corresponding to μ, q_P and q_S were adapted from firstly obtained [7,12] considering new experimental data [31]. The intrinsic yields and maintenance coefficients of q_{O2} and q_{CO2}, now included in the extended model, are also indicated [39].

Table 5.1 Summary of model parameters and errors. Relationship between specific rates (μ, q_P) and the substrate (methanol) concentration, intrinsic yields and maintenance coefficients for q_S, q_{O2} and q_{CO2}. CV % coefficient of variation. RMSE %, Normalized root mean squared error.

	Model parameters				Model error
	Parameter	Units	Value	CV %	RMSE %
μ [h^{-1}]	μ_{max}	h^{-1}	0.069	17.2	9.0
	$K_{S,X}$	g L^{-1}	0.50	29.0	7.6*
	$K_{I,X}$	g L^{-1}	7.5	44.3	
	$S_{crit,X}$	g L^{-1}	1.9	-	
q_P [U g^{-1} h^{-1}]	$q_{max,P}$	U g^{-1} h^{-1}	2200	>100	11
	$K_{S,P}$	g L^{-1}	10.0	>100	8.0*
	$K_{I,P}$	g L^{-1}	1.2	>100	
	$S_{crit,P}$	g L^{-1}	3.5	-	
q_S [g g^{-1} h^{-1}]	$Y_{S/X}$	g g^{-1}	5.14	8.6	5.7
	$m_{S/X}$	g g^{-1} h^{-1}	0.013	76.9	
q_{O2} [mol_{O2} g^{-1} h^{-1}]	$Y_{O2/X}$	mol_{O2} g^{-1}	0.206	9.7	6.3
	$m_{O2/X}$	mol_{O2} g^{-1} h^{-1}	$6.1 \cdot 10^{-4}$	75.4	
q_{CO2} [mol_{CO2} g^{-1} h^{-1}]	$Y_{CO2/X}$	mol_{CO2} g^{-1}	0.127	2.4	6.8
	$m_{CO2/X}$	mol_{CO2} g^{-1} h^{-1}	$4.0 \cdot 10^{-4}$	75.0	

ROL fed-batch production in *P. pastoris* Mut$^+$ phenotype under different feeding strategies - constant methanol flow rate (CF), exponential addition (CM, μ open-loop control or MLFB), linear-increasing μ profile (LM), closed-loop methanol concentration control (CS, MNLFB) and optimized feeding profiles (OP1 and OP2) - were simulated and assessed for bioprocess efficiency. They are listed in Table 5.1.

Table 5.2 List of simulated operational strategies for the methanol induction phase (MIP) and their design criteria.

Nomenclature	Strategy	Description
CF	Constant F	F = 14 g h^{-1}
CM	Exponential addition Constant μ	μ = 0.03 h^{-1}. MLFB $F \approx \frac{(XV)_0 \cdot \mu \cdot \exp(\mu_{SP}(t-t_0))}{Y^*_{X/S} \cdot S_{feed}}$
LM	Linear increasing μ	From μ = 0.01 to 0.04 h^{-1}. MLFB
CS	Constant S	S = 2 g L^{-1}. MNLFB
OP1	Optimal S-profile 1	Maximum final titer (P). MNLFB
OP2	Optimal S-profile 2	Maximum final volumetric productivity (Q_P). MNLFB

5.4.1.1 Simulation of the standard feeding strategies

Simulations CF, CM, LM and CS, which emulate operational strategies commonly implemented in heterologous protein production processes in *P. pastoris* [7,8,41], are to be discussed in this section.

For that purpose, simulated time evolution of state variables (*S, X, PV),* manipulated variable *(F)* and specific rates (μ and q_P) are shown in Figure 5.2 (*F, S* and μ) and Figure 5.3 (*X, PV* and q_P) for the standard strategies and optimized feeding profiles (which will be discussed later on).

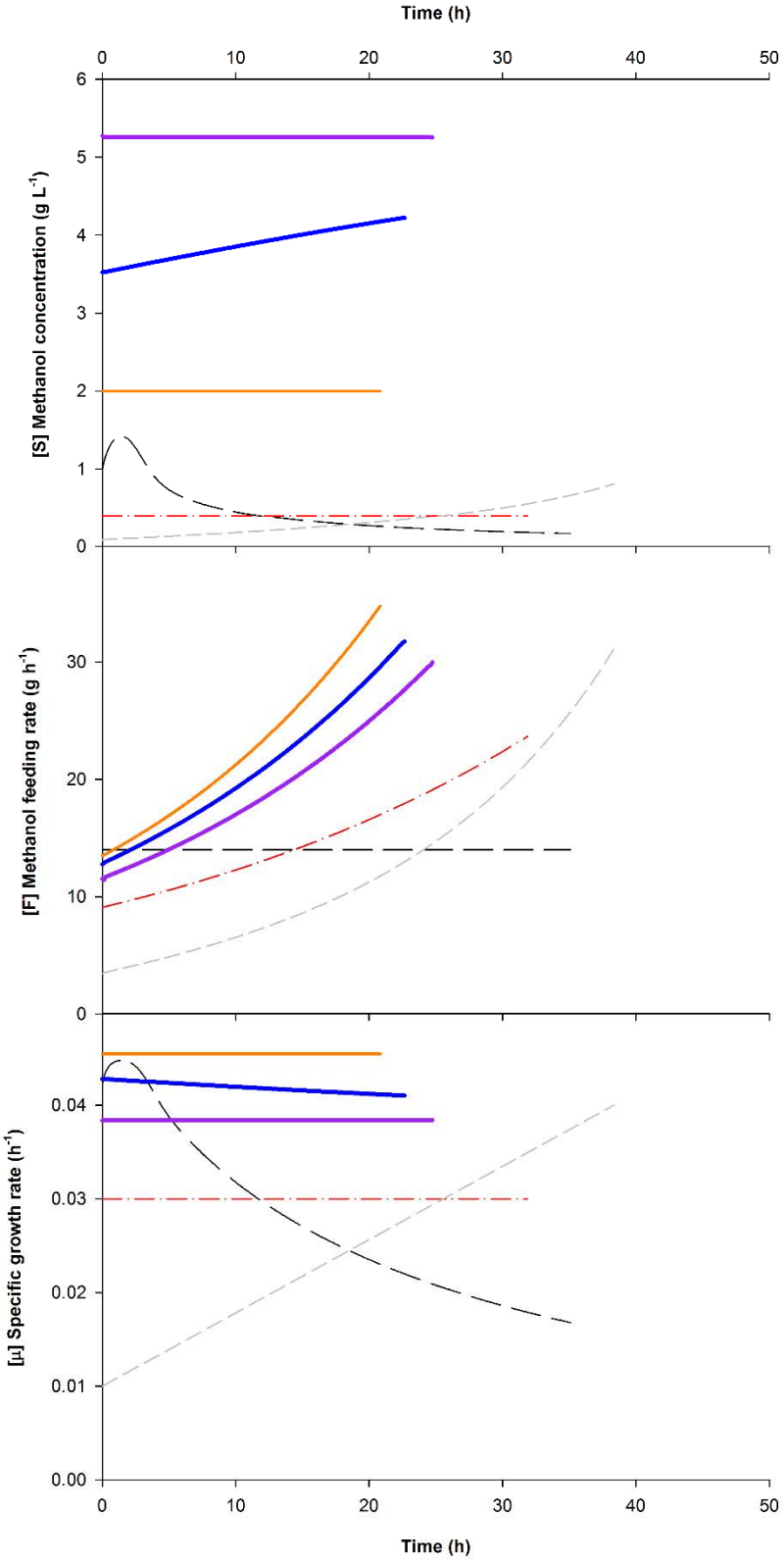

Figure 5.2 Simulation results. Substrate concentration (*S*), substrate feeding rate (F) and specific growth rate (μ) time profiles for different feeding strategies: CF (——), CM (— · —), LM (---), CS (orange —), OP1 (purple thick —), OP2 (blue thick —).

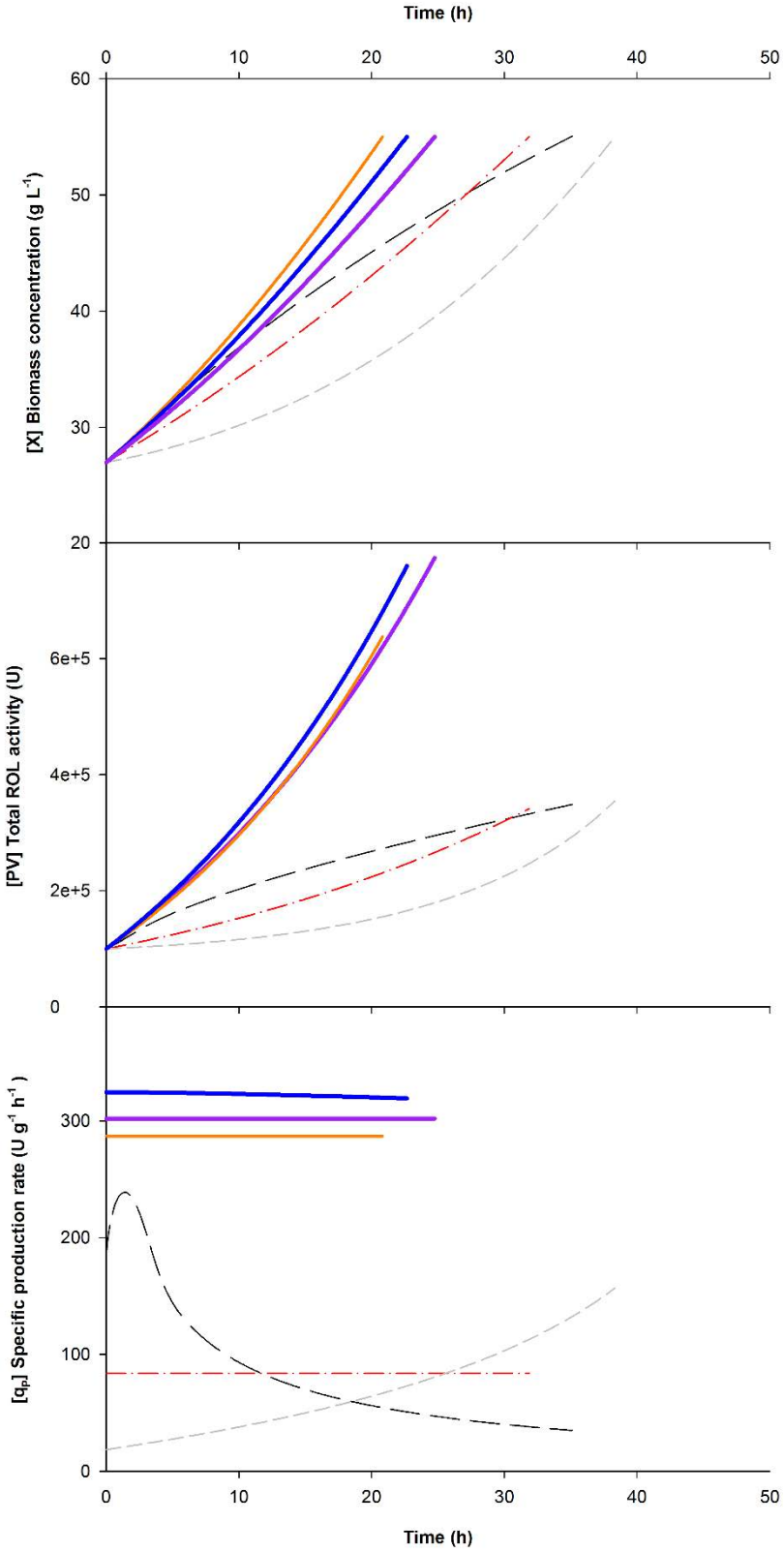

Figure 5.3 Simulated biomass (*X*), total amount of product (*PV*) and specific production rate (q_P) for different standard feeding strategies and the optimal profiles: CF (— —), CM (— · —), LM (---), CS (orange thick ——), OP1 (purple thick ——), OP2 (blue thick ——).

The restriction of a fixed final X is clearly reflected in Figure 5.3, and it is essential for a proper comparison between strategies. CM and CS strategies let stable time profiles of specific rates (μ, q_P) and substrate concentration (S). Both contribute to physiologic stability, process reliability and repeatability in front of the greatly decaying exponentially-like time evolution of specific rates and substrate concentration in CF. On the other hand, LM presents an additional drawback: methanol accumulates over the second half of the induction phase. This fact would make impossible to implement the open-loop control of μ (pre-programmed F profile) that is meant to be carried out as well in CM.

Moreover, as discussed by Barrigón *et al.* 2015 [12], and hinted in simulated profiles in Figure 5.3, MNLFB strategy (CS), located in the substrate inhibition areas which are above critical substrate concentration ($S_{crit,X}$), led to significantly higher values of both ROL titer and productivity. Hence, if a single substrate (methanol) for the induction phase is considered, optimization procedure like fine-tuning or improvement of the MNLFB strategy would lead to the best results in terms of bioprocess efficiency dictated by total titer and productivity. This strategy, though, is more complex and higher energy and substrate demanding [31].

5.4.1.2 Optimized feeding profiles by simulation

Simulation results corresponding to the optimized profiles obtained for different design criteria based on performance indexes P_F (OP1) and Q_P (OP2) are presented in Table 5.3.

Considering, first, variations of $Y^*_{X/S}$ not to be significant within the operation range for μ and q_S; second, the final volume among the runs to be similar and, finally, the same initial conditions for the induction phase, a similar total added substrate can also be expected. Thus, optimization results for the specific productivity (U g^{-1} h^{-1}), total productivity (U h^{-1}), total product (PV) and product yield ($Y^*_{P/S}$) as design criteria are expected to be very similar to the ones obtained with Q_P and P_F. Moreover, neither Q_P nor P_F optimization results show major improvement between each other's performance indexes.

Table 5.3 Optimization performance indexes. Simulation results for the different design criteria and optimization algorithms applied: GRG and EA. ± indicates 95 % confidence intervals. Productivities and yields were calculated over all fermentation time.

Performance index	Design criteria			
	Final titer (OP1) P_F [U mL^{-1}]		*Volumetric productivity* (OP2) Q_P [U L^{-1} h^{-1}]	
	GRG	*EA*	*GRG*	*EA*
Final titer P_F [U mL^{-1}]	305	303 ± 1	300	298 ± 1
Volumetric productivity Q_P [U L^{-1} h^{-1}]	6250	6225 ± 47	6421	6403 ± 4
Yield of product on biomass $Y'_{P/X}$ [U g^{-1}]	5539	5511 ± 14	5446	5425 ± 9
Specific productivity [U g^{-1} h^{-1}]	114	116 ± 1	117	118 ± 1
Incremental total product ΔPV [U]	$6.74 \cdot 10^5$	$(6.68 \pm 0.05) \cdot 10^5$	$6.60 \cdot 10^5$	$(6.56 \pm 0.01) \cdot 10^5$

GRG and EA were used as alternative optimization methods to state whether significant differences appear. GRG did not show differences between different simulations when distinct initial values and main parameters were applied. Besides, EA, as stochastic metaheuristic algorithm and belonging to the class of EC, was set to run for several times (N = 30) to check the stability and reproducibility of the solution it provided. The 95 % confidence intervals for the performance indexes are included, as well, in Table 5.3. It can be stated that mostly no significant differences were observed between the overall performances of the two algorithms when compared.

Furthermore, observing S profiles from Figure 5.2, OP1 and OP2 present remarkable differences from each other. To achieve the highest P_F, the optimizer found, as final solution, a constant S operation at maximum $Y^*_{P/X}$ (indicated in Figure 1), whereas maximizing Q_P required an increasing S-profile within maximum q_P and $Y^*_{P/X}$, (corresponding to a constant and decreasing μ profile, respectively). Both are located in the MNLFB spectrum ($S > S_{crit,X}$), as expected, though not exactly at the maximum point of q_P, but in higher S ranges (Figure 5.1). This fact can be attributed to, first, the non-coincidence, (and, at the same time, proximity) between the maxima of μ and q_P in respect to S. Second, and related to the previous reason, the substrate inhibition pattern that both μ and q_P describe makes the compromise of high q_P at moderate growth possible, so that higher levels of product can be obtained before reaching the top operational limit of X. This is especially relevant when optimizing P_F, since shorter process time can be given up in favor of higher product concentrations. This statement is reinforced by the fact that S values of OP2 are lower than OP1's, because there, both P_F and process time have to be balanced to obtain the highest Q_P.

Moreover, as expected, OP1 and OP2 are the foremost in terms of PV (Figure 5.3), when compared to the standard strategies, despite being much closer to CS. The time to achieve those levels of PV is also significantly shorter, boosting Q_P, in consequence.

Finally, to sum up, from these simulations, it can be stated that OP1, compared to the most used MLFB strategy of constant μ (CM) achieves a 2.2-fold higher titer, whilst OP2 outcomes it with a 2.4-fold higher volumetric productivity.

5.4.2 Experimental results with optimized profiles. Comparison among alternative feeding strategies

In the first place, Figure 5.4A and Figure 5.4B show time evolution of incremental total activity (ΔPV), logarithmic total biomass ratio ($ln(XV/(X_0V_0))$), and total substrate in the bioreactor (SV) for both OP1 and OP2 experimental results and simulations. Optimized simulation profiles have been extended to the actual final experimental time.

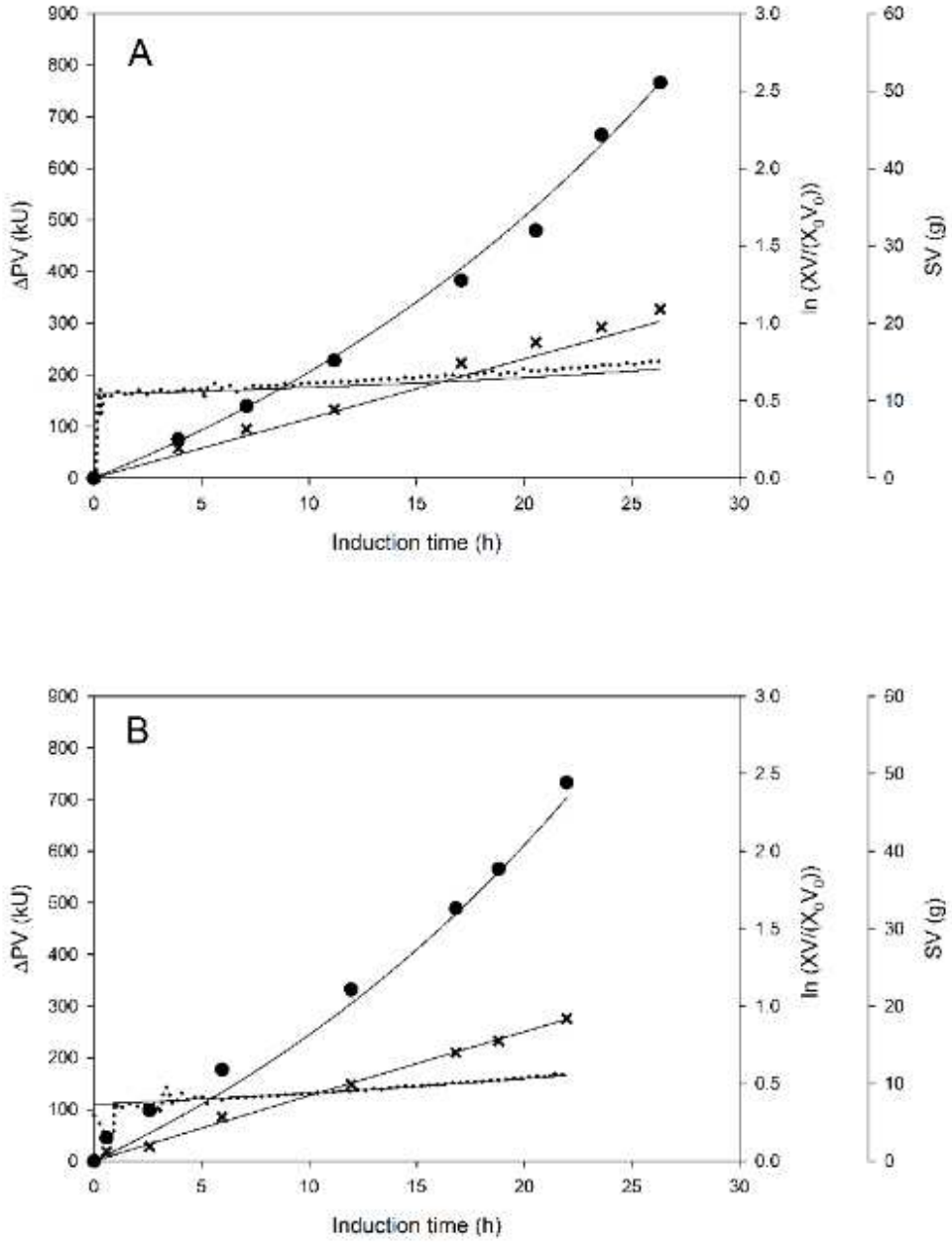

Figure 5.4 Experimental (symbols) and simulated (solid lines) optimal time profiles. (A) OP1. (B) OP2. Incremental total activity (ΔPV) (●), logarithmic total biomass ratio (ln(XV/(X_0V_0))) (x), total substrate (SV) (···).

It can be stated that, saving slight differences, experimental data showed a good agreement with simulated results for *ΔPV*, obtaining a final relative error lower than 5 % for both OP1 and OP2. Only minor differences are observed between simulated and experimental values for biomass and substrate, caused by slight inaccuracies in process modelling, monitoring and control.

Apart from that, a comparison with the most suitable alternatives previously reported with *P. pastoris* expressing ROL under the control of P_{AOX1} has been also carried out, and their data is presented in both Table 5.4 and Figure 5.5.

Table 5.4 gathers the final performance indexes and mean specific rates obtained for each case. As it is clearly reflected, a general positive progression is observed, from less to more complex strategies (left to right in Table 5.4), in terms of the key operating conditions.

More specifically, a trade-off between q_P and μ can be carried out to maximize a given performance index. Two different kinds of operational strategy, methanol limited (MLFB) and methanol non-limited fed-batch (MNLFB) cultures (this latter with different levels of control) have been intensively analyzed previously [7,42]. As mentioned, these most commonly applied control strategies allow maintaining rather constant the key specific rates for cell growth (μ) and substrate uptake (q_S) through the quasi-steady state hypothesis for the substrate while seeking to maximize target protein production. As can be seen in Table 5.4, yields, productivities and specific production rate in MLFB (constant μ of 0.015 h^{-1}) were the lowest ones in those terms. Following this last one, the great fluctuations the *S*-profile underwent in MNLFB non-automatic control strategy made those conditions to produce results that resembled much more to MLFB ones. Besides, in previous non-optimized MNLFB operations [7] the values of these parameters were significantly exceeded. The maximum product yield ($Y^*_{P/X}$) and P_F at a methanol set-point of 10 g L^{-1} was obtained, although volumetric and specific productivity and mean specific production rate ($q_{P,mean}$) were higher at 3 g L^{-1}.

Table 5.4 Bioprocess efficiency comparison. Substrate feeding strategies with *P. pastoris* expressing ROL under control of P_{AOX1}. ± indicates standard deviation (SD). Productivities and yields are calculated over all fermentation time.

		Non-automatic MNLFB [30]	MLFB [7]	MNLFB1 [7]	MNLFB2 [7]	MNLFB Max.Titer OP1	MNLFB Max.Vol. Productivity OP2
Key operating condition	**Units**	**Non-automatic control** $S < 5$ g L^{-1}	$\mu = 0.015$ h^{-1}	$S = 3.0$ g L^{-1}	$S = 10$ g L^{-1}	S and μ constant	S and μ time profile
ROL titer	[U mL^{-1}]	150	135	280	294	303	302
$Y'_{P/X}$	[U g^{-1}]	2470	2644	5282	5635	5509	5395
Volumetric Productivity	[U L^{-1} h^{-1}]	3000	1857	5406	4264	5777	6224
Specific Productivity	[U g^{-1} h^{-1}]	49	36	102	82	105	111
μ_{mean}	[h^{-1}]	0.036	0.014±0.001	0.046±0.002	0.025±0.001	0.037±0.001	0.040±0.006
$q_{S,mean}$	[g g^{-1} h^{-1}]	0.14	0.07±0.01	0.20±0.01	0.14±0.01	0.19±0.01	0.17±0.01
$q_{P,mean}$	[U g^{-1} h^{-1}]	130	46±4	322±13	175±6	276±12	307±7

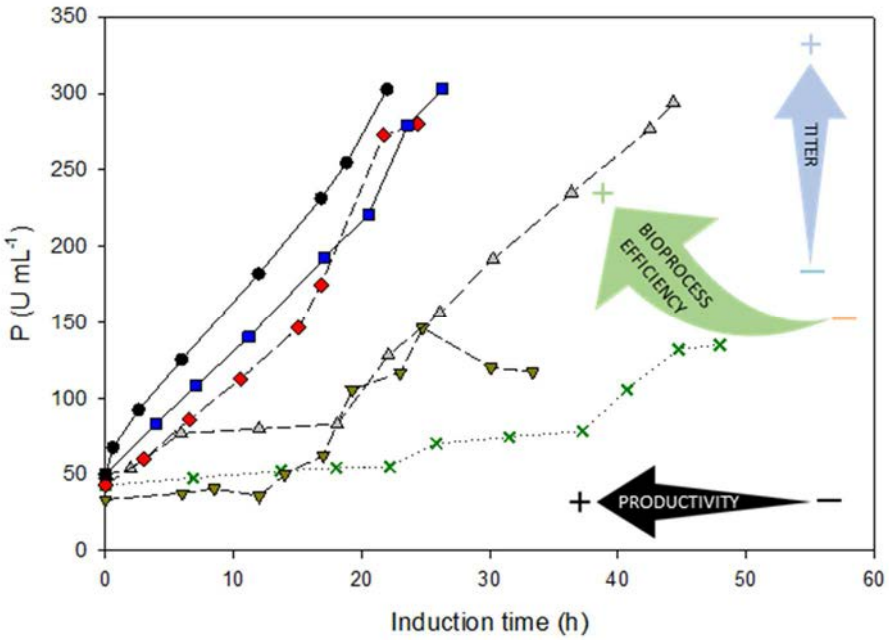

Figure 5.5 Experimental ROL activity (P) time profiles. OP1 (■), OP2 (●) and alternative strategies: non-automatic MNLFB (▼), MLFB (x), MNLFB1 (♦), MNLFB2 (▲).

Finally, fine-tuning of the MNLFB operation by the implementation of substrate optimal profiles make OP1 and OP2 stand out among the rest. On one hand, OP1 surpassed, as expected, 10 g L^{-1} MNLFB strategy in terms of ROL final activity, though the restriction of final biomass limits this parameter not to be considerably higher, even though $Y'_{P/X}$ has been boosted more than a 20 % (10 % for specific productivity) from the mentioned strategy. This top level of P_F is reached, but, with a 25 % higher volumetric productivity than from a substrate concentration of 10 g L^{-1} and slightly lower one than from the 3 g L^{-1} case. On the other hand, the performance of OP2 fulfilled the expectations achieving the highest Q_P, concretely surpassing the previous best strategy in those terms (3 g L^{-1} MNLFB) with more than a 15 %. As expected, and hinted in the kinetic model (Figure 1), $Y'_{P/X}$ was lower in the S spectrum where OP2 induction phase is located. Accordingly, specific productivity was also superior. μ also experimented higher changes during this operation (see SD in μ_{mean}), as expected in a case where the S-profile did not consist on a constant value. q_P is higher than OP1, but lower than 3 g L^{-1} MNLFB case, as well as the model predicted.

Additionally, Table 5.5 gathers the needs and complexity of monitoring and control of each operational strategy that has been just discussed. With it, the following observations can be appointed.

First, non-automatic MNLFB case required both little knowledge of the cell physiology and no online monitoring. However, it resulted too time consuming and results were clearly outcome by the following MNLFB alternatives.

Second, MLFB strategy let the variable μ to be indirectly controlled with no real-time information from the process and so, low labor needs. Still, as it is only implementable within the limited range of S, improvement of bioprocess efficiency is not achievable in the present system and in addition, $Y'_{X/S}$ needs to be previously determined for an appropriate μ control.

Moreover, by increasing online monitoring complexity, a fine S-control was achieved in MNLFB and boosted the values of the main performance indexes of industrial interest. This case also required little higher labor, but still negligible if it is compared to the non-automatic control case.

Finally, optimizations of Q_P and P_F were successfully fulfilled with no more operational complexity requirements in respect to the MNLFB strategies. Further knowledge of the physiology of the strain used, though, was needed. A simple macrokinetic model was employed for simulation, obtaining results, as seen, that fit adequately into the predictions. A simple predictive control plus an adaptive PI feedback control was applied in this case and no further advanced control structure had to be considered.

Furthermore, most of the facts previously stated are clearly reflected in Figure 5.5. Time evolution of P provides a plain idea of how the performance of the different strategies had run in terms of P_F and Q_P (from the slopes of the profiles). A whole range of improvement is perfectly appreciated, from the worst case scenario, which was working in the limited spectrum of S, below $S_{crit,x}$ (MLFB), to the MNLFB strategies, with a high heterogeneity of results between the least complex one (non-automatic control of S), constant S = 10 g L^{-1} and the rest. Finally, and most remarkably, OP1 and OP2 performances have overcome 3 g L^{-1} MNLFB strategy in P_F and in Q_P, respectively, which corresponds to one of the main objectives of the whole approach presented in this work.

Table 5.5 Summary of the main control and monitoring features. Operational strategies of ROL production in *P. pastoris* under methanol carbon source, published and from the present study.

Operational strategy	Non-automatic **MNLFB** [38]	**MLFB** [17]	**MNLFB1** [17]	**MNLFB2** [17]	**OP1**	**OP2**
Model-based	S	$S - X$	S	S	$S - X - P$ $q_S - \mu - q_P$	$S - X - P$ $q_S - \mu - q_P$
Goal	S<5 g L^{-1}	Constant μ	Constant S 3 g L^{-1}	Constant S 10 g L^{-1}	Max P_F	Max Q_P
Control structure	Non-automatic Predictive	Feed forward	Predictive + Feedback PI	Predictive + Feedback PI	Predictive + Feedback adaptive PI	Predictive + Feedback adaptive PI
Controlled variable (in bold)	$\boldsymbol{S} < S_{max}$ $\mu \neq ct$	$\boldsymbol{\mu} = \mu_{SP} < \mu_{crit}$ Limited S	$\boldsymbol{S} = S_{SP} > S_{crit}$ $\mu \approx ct$	$\boldsymbol{S} = S_{SP} > S_{crit}$ $\mu \approx ct$	$\boldsymbol{S}$ profile $S_{SP} = ct$	$\boldsymbol{S}$ profile Tracking S_{SP}
Feeding strategy (manipulated variable)	$F_{t+1} \approx F_t - \frac{V_t}{(S_{feed} - S_t)} \frac{dS_t}{dt}$	$F_t \approx \frac{(XV)_0 \cdot \mu_{SP} \cdot \exp(\mu_{SP}(t - t_0))}{Y^*_{X/S} \cdot S_{feed}}$	$F_{t+1} \approx F_t - \frac{V_t}{(S_{feed} - S_t)} \frac{dS_t}{dt}$ $+ K_P \left(\varepsilon_{t+1} + \frac{1}{\tau_I} \int_{t_0}^{t+1} \varepsilon_t \, dt \right)$	$F_{t+1} \approx F_t - \frac{V_t}{(S_{feed} - S_t)} \frac{dS_t}{dt}$ $+ K_P \left(\varepsilon_{t+1} + \frac{1}{\tau_I} \int_{t_0}^{t+1} \varepsilon_t \, dt \right)$	$F_{t+1} \approx F_t - \frac{V_t}{(S_{feed} - S_t)} \frac{dS_t}{dt}$ $+ \frac{K_P \cdot V_{t+1}}{(S_{feed} - S_{t+1})} \left(\varepsilon_{t+1} + \frac{1}{\tau_I} \int_{t_0}^{t} \varepsilon_t \, dt \right)$	$F_{t+1} \approx F_t - \frac{V_t}{(S_{feed} - S_t)} \frac{dS_t}{dt}$ $+ \frac{K_P \cdot V_{t+1}}{(S_{feed} - S_{t+1})} \left(\varepsilon_{t+1} + \frac{1}{\tau_I} \int_{t_0}^{t+1} \varepsilon_t \, dt \right)$
Requirements of monitoring	S offline Estimated volume	-	S online Estimated volume	S online Estimated volume	S online Estimated volume	S online Estimated volume
Needed inputs	S_{feed} V_0	μ_{SP} $Y^*_{X/S}$ $(XV)_0$ S_{feed} t_0	S_{SP} V_0 S_{feed} K_P τ_I	S_{SP} V_0 S_{feed} K_P τ_I	S_{SP} V_0 S_{feed} K_P τ_I	S_{SP} V_0 S_{feed} K_P τ_I

5.5 Conclusions

Bioprocess optimization of the *P. pastoris* system expressing ROL under P_{AOX1} control has been carried out, as a significant progress in the improvement of the main key performance indexes of interest has arisen. The study presents itself as the culmination of a process that began with the identification of a product with industrial interest and its expression in *P. pastoris*, the implementation of simple fed-batch operational strategies, which were followed by the design of new alternatives which required more instrumentation and control complexity that were able to boost the bioprocess efficiency, and that led to the complete characterization of the process kinetics and its modelling.

From that point, the optimization and simulation of optimal *S-μ-F* profiles and their further experimental implementation in the current system made it possible to reach the top levels of the main parameters for industrial interest. Concretely, a 2.2-fold higher P_F and 3.4-fold higher Q_P, compared to the best previously implemented MLFB strategy (open-loop μ control), and 1.15-fold higher and 1.08-fold higher than 3 g L^{-1} MNLFB strategy, respectively, was obtained; and so 1.45-fold higher Q_P and 1.03-*fold* higher P_F than 10 g L^{-1} MNLFB. All of that was possible, most importantly, without increasing significantly neither process complexity nor operational and labor costs.

The whole approach, aiming to cover the requirements of strategies for systematic bioprocess development from a bioprocess engineering point of view, has been shown as valid to improve efficiency in recombinant protein production processes. The basic features comprise system knowledge, data gathering, modelling of the system, exploitation of the model to investigate promising alternatives, system optimization and finally verification and analysis of the feasible operating strategies. The advantages of the procedure are its simplicity, flexibility and transferability, since user-friendly software is applied, allowing every scientist and engineer to impose further biological and technological constraints to different design criteria, for example, total or specific yields and productivities. This model-based *roadmap* can also be used as a *platform* to design new alternative operating modes, and even to produce other proteins of interest, for cell factories with substrate inhibition patterns on both q_P and μ, which, like the

present case, cause multiplicity states for S-μ-q_P that make the process optimization and operation more complex and challenging.

5.6 References

[1] K. Sreekrishna, *Pichia*, Optimization of Protein Expression, Encycl. Ind. Biotechnol. 190 (2010) 695–701.

[2] G. Potvin, A. Ahmad, Z. Zhang, Bioprocess engineering aspects of heterologous protein production in *Pichia pastoris*: A review, Biochem. Eng. J. 64 (2012) 91–105.

[3] M. Jahic, F. Wallberg, M. Bollok, P. Garcia, S. Enfors, Temperature limited fed-batch technique for control of proteolysis in *Pichia pastoris* bioreactor cultures, Microb. Cell Fact. 2:6 (2003).

[4] A. Surribas, R. Stahn, J.L. Montesinos, S.O. Enfors, F. Valero, M. Jahic, Production of a *Rhizopus oryzae* lipase from *Pichia pastoris* using alternative operational strategies, J. Biotechnol. 130 (2007) 291–299.

[5] M. Berdichevsky, M. D'Anjou, M.R. Mallem, S.S. Shaikh, T.I. Potgieter, Improved production of monoclonal antibodies through oxygen-limited cultivation of glycoengineered yeast, J. Biotechnol. 155 (2011) 217–224.

[6] T. Egli, Microbial growth and physiology: A call for better craftsmanship, Front. Microbiol. 6 (2015) 1–12.

[7] J.M. Barrigón, J.L. Montesinos, F. Valero, Searching the best operational strategies for *Rhizopus oryzae* lipase production in *Pichia pastoris* Mut+ phenotype: Methanol limited or methanol non-limited fed-batch cultures?, Biochem. Eng. J. 75 (2013) 47–54.

[8] V. Looser, B. Bruhlmann, F. Bumbak, C. Stenger, M. Costa, A. Camattari, D. Fotiadis, K. Kovar, Cultivation strategies to enhance productivity of *Pichia pastoris*: A review, Biotechnol. Adv. 33 (2015) 1177–1193.

[9] O. Cos, R. Ramón, J.L. Montesinos, F. Valero, Operational strategies, monitoring and control of heterologous protein production in the methylotrophic yeast *Pichia pastoris* under different promoters: a review, Microb. Cell Fact. 5:17 (2006).

[10] T.I. Potgieter, S.D. Kersey, M.R. Mallem, A.C. Nylen, M. D'Anjou, Antibody expression

kinetics in glycoengineered *Pichia pastoris*, Biotechnol. Bioeng. 106 (2010) 918–927.

[11] M.C.M. Hensing, R.J. Rouwenhorst, J.J. Heijnen, J.P. van Dijken, J.T. Pronk, Physiological and technological aspects of large-scale heterologous-protein production with yeasts, Antonie Van Leeuwenhoek. 67 (1995) 261–279.

[12] J.M. Barrigon, F. Valero, J.L. Montesinos, A macrokinetic model-based comparative meta-analysis of recombinant protein production by *Pichia pastoris* under AOX1 promoter, Biotechnol. Bioeng. 112 (2015) 1132–1145.

[13] X. Garcia-Ortega, P. Ferrer, J.L. Montesinos, F. Valero, Fed-batch operational strategies for recombinant Fab production with *Pichia pastoris* using the constitutive *GAP* promoter, Biochem. Eng. J. 79 (2013) 172–181.

[14] M. Maurer, M. Kühleitner, B. Gasser, D. Mattanovich, Versatile modeling and optimization of fed batch processes for the production of secreted heterologous proteins with *Pichia pastoris*, Microb. Cell Fact. 5:37 (2006).

[15] J.M. Modak, H.C. Lim, Y.J. Tayeb, General characteristics of optimal feed rate profiles for various fed-batch fermentation processes, Biotechnol. Bioeng. 28 (1986) 1396–1407.

[16] S. Park, W.F. Ramirez, Optimal Production of Secreted Protein in Fed-Batch Reactors, AIChe J. 34 (1988) 1550–1558.

[17] I.Y. Smets, J.E. Claes, E.J. November, G.P. Bastin, J.F. Van Impe, Optimal adaptive control of (bio)chemical reactors: Past, present and future, J. Process Control. 14 (2004) 795–805.

[18] H. Ohno, E. Nakanishi, T. Takamatsu, Optimal control of a semibatch fermentation, Biotechnol. Bioeng. 18 (1976) 847–864.

[19] K. Kobayashi, S. Kuwae, T. Ohya, T. Ohda, M. Ohyama, K. Tomomitsu, High level secretion of recombinant human serum albumin by fed-batch fermentation of the methylotrophic yeast, *Pichia pastoris*, based on optimal methanol feeding strategy, J. Biosci. Bioeng. 90 (2000) 280–288.

[20] S. Ochoa, A new approach for finding smooth optimal feeding profiles in fed-batch fermentations, Biochem. Eng. J. 105 (2016) 177–188.

[21] P.M. Bapat, N.U. Padiyar, N.N. Dave, S. Bhartiya, P.P. Wangikar, S. Dash, Model-Based Optimization of Feeding Recipe for Rifamycin Fermentation, AIChe J. 52 (2006) 4249–4257.

[22] M. Rocha, R. Mendes, O. Rocha, I. Rocha, E.C. Ferreira, Optimization of fed-batch fermentation processes with bio-inspired algorithms, Expert Syst. Appl. 41 (2014) 2186–2195.

[23] W. Zhang, J. Sinha, L. a Smith, M. Inan, M.M. Meagher, Maximization of production of secreted recombinant proteins in *Pichia pastoris* fed-batch fermentation, Biotechnol. Prog. 21 (2005) 386–393.

[24] M. Guillén, M.D. Benaiges, F. Valero, Immobilization and stability of a *Rhizopus oryzae* lipase expressed in *Pichia pastoris*: Comparison between native and recombinant variants, Biotechnol. Prog. 27 (2011) 1232–1241.

[25] P.G. Quintana, M. Guillén, M. Marciello, F. Valero, J.M. Palomo, A. Baldessari, Immobilized heterologous *Rhizopus oryzae* lipase as an efficient catalyst in the acetylation of cortexolone, European J. Org. Chem. (2012) 4306–4312.

[26] P.A. Nunes, P. Pires-Cabral, M. Guillén, F. Valero, D. Luna, S. Ferreira-Dias, Production of MLM-type structured lipids catalyzed by immobilized heterologous *Rhizopus oryzae* lipase, J. Am. Oil Chem. Soc. 88 (2011) 473–480.

[27] C. Tecelão, M. Guillén, F. Valero, S. Ferreira-Dias, Immobilized heterologous *Rhizopus oryzae* lipase: A feasible biocatalyst for the production of human milk fat substitutes, Biochem. Eng. J. 67 (2012) 104–110.

[28] A. Canet, M.D. Benaiges, F. Valero, Biodiesel synthesis in a solvent-free system by recombinant *Rhizopus oryzae* lipase. Study of the catalytic reaction progress, J. Am. Oil Chem. Soc. 91 (2014) 1499–1506.

[29] K. Bonet-Ragel, A. Canet, M.D. Benaiges, F. Valero, Synthesis of biodiesel from high FFA alperujo oil catalysed by immobilised lipase, Fuel. 161 (2015) 12–17.

[30] O. Cos, A. Serrano, J.L. Montesinos, P. Ferrer, J.M. Cregg, F. Valero, Combined effect of the methanol utilization (Mut) phenotype and gene dosage on recombinant protein production in *Pichia pastoris* fed-batch cultures., J. Biotechnol. 116 (2005) 321–335.

[31] X. Ponte, J.L. Montesinos-Seguí, F. Valero, Bioprocess efficiency in *Rhizopus oryzae* lipase production by *Pichia pastoris* under the control of P_{AOX1} is oxygen tension dependent, Process Biochem. 51 (2016) 1954–1963.

[32] S. Minning, A. Serrano, P. Ferrer, C. Solà, R.D. Schmid, F. Valero, Optimization of the high-level production of *Rhizopus oryzae* lipase in *Pichia pastoris*, J. Biotechnol. 86 (2001) 59–70.

[33] D.B. Choi, E.Y. Park, Enhanced production of mouse a-amylase by feeding combined nitrogen and carbon sources in fed-batch culture of recombinant *Pichia pastoris*, Process Biochem. 41 (2006) 390–397.

[34] X.W. Yu, X. Lu, L.S. Zhao, Y. Xu, Impact of $NH4^+$ nitrogen source on the production of *Rhizopus oryzae* lipase in *Pichia pastoris*, Process Biochem. 48 (2013) 1462–1468.

[35] C. Arnau, C. Casas, F. Valero, The effect of glycerol mixed substrate on the heterologous production of a *Rhizopus oryzae* lipase in *Pichia pastoris* system, Biochem. Eng. J. 57 (2011) 30–37.

[36] L.R. Formenti, A. Nørregaard, A. Bolic, D.Q. Hernandez, T. Hagemann, A.L. Heins, H. Larsson, L. Mears, M. Mauricio-Iglesias, U. Krühne, K. V. Gernaey, Challenges in industrial fermentation technology research, Biotechnol. J. 9 (2014) 727–738.

[37] Z.I.T.A. Soons, J.A. Voogt, G. van Straten, A.J.B. van Boxtel, Constant specific growth rate in fed-batch cultivation of Bordetella pertussis using adaptive control, J. Biotechnol. 125 (2006) 252–268.

[38] A.C.A. Veloso, I. Rocha, E.C. Ferreira, Monitoring of fed-batch *E. coli* fermentations with

software sensors, Bioprocess Biosyst. Eng. 32 (2009) 381–388.

[39] M. Dabros, M.M. Schuler, I.W. Marison, Simple control of specific growth rate in biotechnological fed-batch processes based on enhanced online measurements of biomass, Bioprocess Biosyst. Eng. 33 (2010) 1109–1118.

[40] L. Mears, S.M. Stocks, G. Sin, K. V. Gernaey, A review of control strategies for manipulating the feed rate in fed-batch fermentation processes, J. Biotechnol. 245 (2017) 34–46.

[41] O. Spadiut, D. Zalai, C. Dietzsch, C. Herwig, Quantitative comparison of dynamic physiological feeding profiles for recombinant protein production with *Pichia pastoris*., Bioprocess Biosyst. Eng. 37 (2014) 1163–1172.

[42] O. Cos, D. Resina, P. Ferrer, J.L. Montesinos, F. Valero, Heterologous production of *Rhizopus oryzae* lipase in *Pichia pastoris* using the alcohol oxidase and formaldehyde dehydrogenase promoters in batch and fed-batch cultures, Biochem. Eng. J. 26 (2005) 86–94.

6 THE MICROBIOREACTOR AS A TOOL TO EVALUATE FED-BATCH STRATEGIES AND HIGH-THROUGHPUT CLONE SCREENING

This chapter has been published as a research paper at the journal *Microbial Cell Factories*:

J. Hemmerich, N. Adelantado, J. Barrigón, X. Ponte, A. Hörmann, P. Ferrer, F. Kensy, F. Valero, Comprehensive clone screening and evaluation of fed-batch strategies in a microbioreactor and lab scale stirred tank bioreactor system: application on *Pichia pastoris* producing *Rhizopus oryzae* lipase, Microb. Cell Fact. 13 (2014) 36

6.1 Introduction

In the overall *P. pastoris* bioprocess based on P_{AOX1}, one of the most important bottlenecks is the clone selection, because the reproducibility of the cultures in shake flasks is rather low and time consuming when the number of potential clones to screen is high [1]. The use of microtiter plates can increase the throughput of clone screening procedures, but reproducibility and scalability when using methanol is limited. Low reproducibility is mainly caused by “edge effects” [2], which stands for uneven evaporation distribution throughout a microplate; especially that evaporation is higher in the outer wells of a microplate. This is observed when placing microplates on standard floor shakers without controlled atmosphere, e.g. for relative humidity. With the use of volatile substrates like methanol, this effect is even more pronounced. Furthermore, the optimization of operational fed-batch strategies at high cell densities can be expensive and time consuming. Although mathematical modelling can reduce the number of experiments, the application of new approaches to solve these drawbacks is necessary. In this context, the use of microbioreactors is an excellent alternative to minimize these pitfalls.

Microbioreactors (MBR) are, essentially, miniaturized versions of well-established bioreactor systems like stirred tank reactors (STR). Due to the micro-scale of these MBR, an exact scale-down of technical equipment needed for the operation of STR is not possible in all cases. For example, tubing and pumps are commonly used to feed nutrients or adjust pH into the STR during fed-batch cultivations. To translate a fed-batch process into a MBR is not a practical solution, because pumps for it are not commercially available or practical for handle the

necessarily small volumes of several micro- or nanoliters. Regarding MBR, other mechanisms have to be applied, like the integration of pipetting robots or microfluidic structures for liquid delivery to the broth [3–5].

Furthermore, mixing and aeration of fermentation broth is usually achieved using mechanically agitated stirrers in STR with well-known and described impact on fluid dynamics. In MBR, this is achieved by shaken microplates. Aeration in cultivation of oxygen-demanding cell types like *E. coli* or yeast (*S. cerevisiae*, *P. pastoris*) is a critical parameter. In STR, oxygen transfer rate (OTR) is improved by increasing stirring and aeration rate, diminishing air bubble size and using pure oxygen or air enriched with oxygen instead of air. Similar strategies can be used partly for MBR, where an increase of the OTR in shaken microtiter plates has been achieved by means of new geometric design of the wells [6], or submerged injection of air/oxygen [7].

Until now, only a few applications of MBR using *P. pastoris* in bioprocess development can be found in literature, although several laboratories have been using microtiter plates for clone screening purposes [8.9].

One MBR system was described for cultivation of *P. pastoris* [7]. For the feeding strategy used in that example, the cultivation cassette had to be removed from the machine and placed under a laminar flow cabinet to add several substrate shots manually. In contrast, the RoboLector platform is able to perform fed-batch operational strategies, which are closer to commonly applied conditions in STR. Because of the integration of an automated liquid handling system in the RoboLector MBR, there was no need to remove the cultivation cassette (i.e. FlowerPlate) from the incubation machine (i.e. BioLector). Therefore, it was possible to add nutrients much more frequently without interruption of shaking and thus, without interruption of oxygen transfer. This high frequency of nutrient addition was a key parameter in mimicking a typical STR fermentation with *P. pastoris*. Additionally, the MBR strategy of enzymatic glucose release with daily addition of methanol could be applied in the BioLector alone without the integrated liquid handling system, and also in other MBR.

Comparable to the approach of feeding nutrients at a high frequency, there is an example found in literature [10], where six parallel operated bubble columns with a working volume of several hundred milliliters were used. Due to the volume, this system should not be considered as a microbioreactor, but as a minibioreactor system. These bubble columns can be equipped with pO_2- and pH-electrodes, while a pump is giving shots of 1 mL of methanol to the fermentation broth. Similar to the MBR RoboLector approach described here, the authors report the usefulness of a scale-down approach to develop suitable process parameters, which are to be transferred into classical STR. It should be mentioned that this system required more resources for set up because of necessary cleaning and sterilization procedures, wiring and calibration of the electrodes and tubing set up for the pumping system.

Another kind of minibioreactor uses up to eight specialized shake flasks as culture vessels in parallel [11,12]. These flasks are equipped with caps having gas and pressure sensors, whereas the lower part is geometrically equal to standard shake flasks. The sensors determine respiration activities of the cultures, namely oxygen uptake rate (OUR), carbon dioxide evolution rate (CER) and respiratory quotient (RQ). The authors recommend to culture replicates in standard shake flasks under same conditions, which serve for sampling and subsequent analytics. Also, there is technical equipment for sampling and feeding of the individual measuring flasks available (HiTec Zang, Herzogenrath, Germany).

Data monitoring and manipulation of MBR cultivations are essential to generate results, which are of high process relevance, especially when it comes to translating results into pilot and production scale. This is a fundamental requirement for on-going studies in those scales. Finally, the ultimate aim of MBR studies in biotechnological developments is to shift as many steps as possible into the microliter scale. Therefore, suitable MBR systems have to operate in a reliable and robust way with user friendly handling to facilitate the high throughput needs.

With current techniques in molecular biology, huge clone pools are easily generated, resulting from the combinatory use of different genetic libraries for e.g. promoters [13,14], protein variants [15] or secretion signals [16]. In combination with different cultivation setups to be evaluated (e.g. feeding strategy, medium background, induction strength and optimal time point of induction), the resulting number of experiments grows very fast with each factor to be investigated [17]. In

this context, with the use of MBR it becomes possible to investigate comprehensive studies on clone screening and process optimization jointly due to the ability to perform several cultivations in parallel. Additionally, the use of software tools like Design-of-Experiments (DoE) and genetic algorithms will boost performance, as the number of experiments to be conducted can be reduced in a meaningful way.

The aim of this study is to demonstrate that the RoboLector automated microbioreactor platform is a suitable tool to minimize the clone selection step and to optimize fed-batch mixed substrates (methanol and other carbon source) operational strategies for the P_{AOX1}-based *P. pastoris* system, using a set of Mut^+ phenotype strains producing a heterologous *Rhizopus oryzae* lipase (ROL) as a case example. The RoboLector MBR system is the integration of the BioLector MBR system [18] into a liquid handling robot. RoboLector was used as it matches some important requirements for bioprocess development [3,19]

6.2 Results and discussion

6.2.1 Clone selection

The clones used for the present work had been previously obtained prior to it. Two different series of X-33-derived strains expressing a lipase from *R. oryzae* (ROL) under the P_{AOX1}promoter had been constructed. In the first series, a pre-existing X-33 strain expressing ROL [20] had been transformed with an expression vector containing the induced form of the *P. pastoris' HAC1* transcriptional factor under the control of P_{AOX1} (Clones 1–6). The second strain series was obtained by replica plating of X-33/pPICZαA_ROL transformants on agar plates containing increasing concentrations of zeocin, aiming at the selection of transformants with multiple copies of the *ROL* expression cassette (Clones 7–12). From each series of strains, six transformants were selected for further studies at MBR scale.

For reference and comparison purposes, expression experiments were initially performed in shake flasks, following a two-step procedure for Mut^+ strains similar to the standard protocol described in the Invitrogen guidelines, that is, growing cells in minimal glycerol medium and subsequently transferring growing cells to a shake flask with fresh minimal methanol medium [21]. As previously described [22], ROL expression levels in shake flasks were rather low, close

to the detection limit of the lipase activity assay, making it difficult to assess clonal variation and perform a reliable clone ranking.

6.2.2 Microbioreactor cultivation

As a collaboration, the experimental work of this section was carried out by m2p-labs team (Baesweiler, Germany) at their facilities.

6.2.2.1 Effects of cultivation media in clone screening

In order to check the effect of cultivation media in clone screening two different media were selected: YNB and Syn6. Clone screening was conducted similarly to the proposal in Invitrogen's guide [21] and as applied often in literature [16,23–27]: Clones were grown in the selected media, following induction of P_{AOX1}-driven expression by daily addition of methanol. In contrast to YNB medium, Syn6 medium and its variants are known to promote high cell densities and product titers [28].

Syn6 medium showed better performance in terms of lipolytic activity than YNB (Figure 6.1).

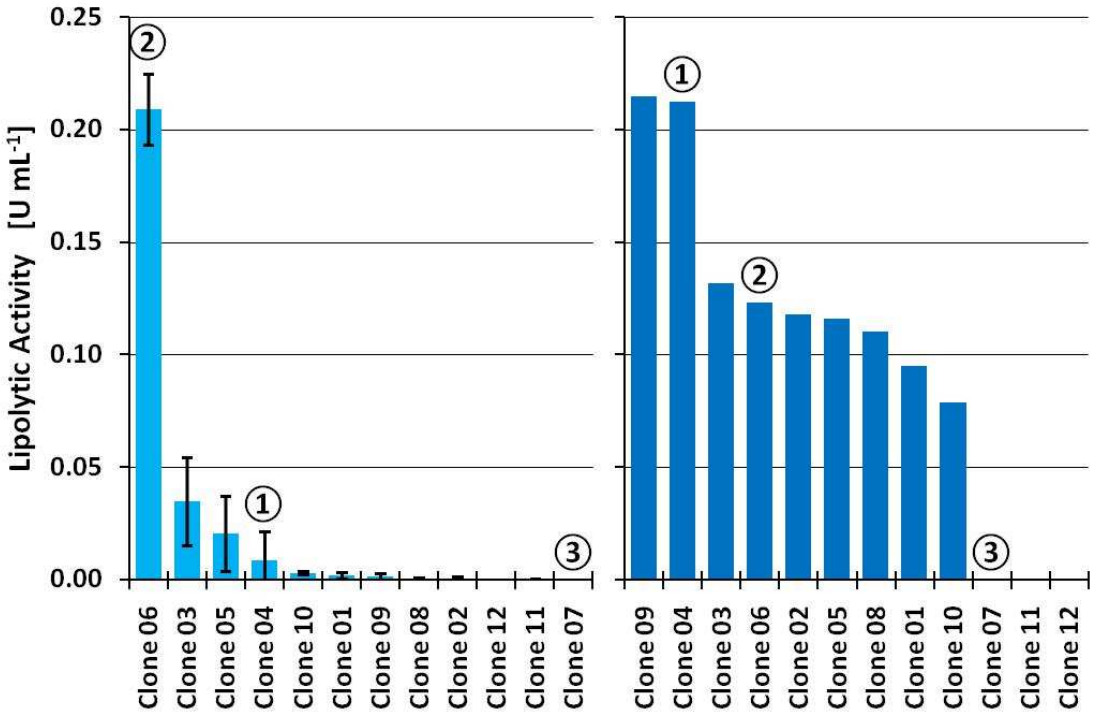

Figure 6.1 Clone rankings obtained in YNB (A) after 80 h and Syn6 medium (B) after 72 h during MBR cultivations. Ranking criteria was volumetric lipolytic activity.

Nine of twelve clones showed greater activity lipolytic than 0.05 U mL^{-1}, but in YNB medium only one clone did. On the other hand, the ranking of clones was different when comparing the two media, i.e. clone 2 was the best one in YNB, while in Syn6 medium the best clones were 9 and 4.

In terms of clonal variation, the series of clones possibly containing multiple copies of the *ROL* gene, showed greater variability than the *HAC1*-transformants series. Strikingly, some of the clones presumably harboring multiple *ROL* copies (clones 11 and 12) produced almost no detectable activity in any of the growth conditions tested. Previous studies [22,29] have shown that ROL triggers the unfolded protein stress response (UPR), resulting in reduced biomass yields [30]. Moreover, recent studies suggest that increased *ROL* copy number could result in increased stress levels and, consequently, to a stronger reduction in biomass and product yields [31]. Undetectable lipolytic activity in clones 7, 11 and 12 was consistent with the observation that these clones reached higher biomass levels than the producing clones, that is, no metabolic burden was observed as a result of ROL production. This suggests that these clones might present some genetic modification(s) because of the transformation and clone selection process [32] that resulted in reduced or no active product formation.

In order to check the performance of the different clones in this screening, further bioprocess development with clones 4, 6 and 7 (as indicated in Figure 6.1) was conducted to justify the selection of a high-producing clone and to validate the scalability of the microbioreactor.

6.2.2.2 Microbioreactor for evaluation of operational fed-batch strategies

With the possibility of in parallel, but independently operated cultivations in the microbioreactor system, two fed-batch strategies for the clones were evaluated at the same time. The first strategy was based on feeding glucose as main carbon source by the enzymatic release of single glucose molecules from a soluble glucose polymer which cannot be metabolized by *P. pastoris*. To induce recombinant gene expression, methanol was added automatically to a final concentration of 1% v/v in intervals of 24 h.

The second strategy was implemented by the pulsed addition of a mixture of glycerol (main carbon source), methanol (inducer) and NH_4OH (N-source) at two different feeding rates.

- Strategy 1: Enzymatic continuous glucose feeding with MeOH induction

The time course of microbioreactor cultures in terms of biomass, lipolytic activity, pO_2 and accumulated volume is shown in Figure 6.2.

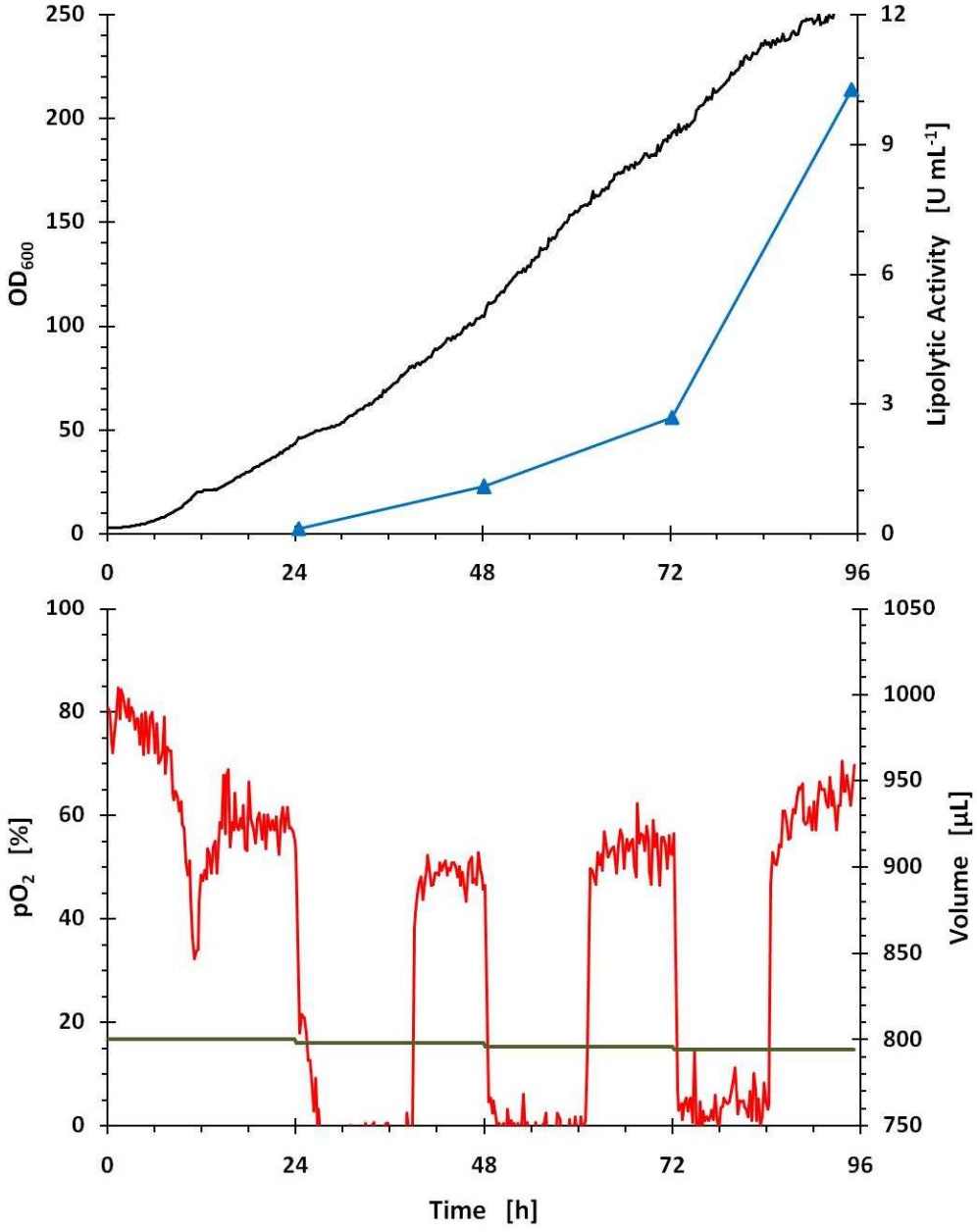

Figure 6.2 Growth kinetics from RoboLector microbioreactor system for clone 4. Operational fed-batch strategy was enzymatic feeding of glucose with MeOH addition in 24 h intervals. (—) OD_{600}; (▲) lipolytic activity; (—) pO_2 and (—) volume.

Glucose is released at a nearly constant rate by enzymatic action on the glucosepolymer. Up to around 12 h, released glucose accumulates due to glucose consumption rate is lower than glucose release rate. After 12 h, accumulated glucose is exhausted, and glucose-limited growth occurs. Therefore, glucose concentration in the medium is zero. Thus, growth is limited by the glucose release rate clearly shown by pO_2 levels resting at a constant level between methanol consumption phases.

The specific growth rate decreased along the fermentation from 0.035 to 0.012 h^{-1} as was expected due to the constant glucose release throughout the bioprocess. This low specific growth rate, far from the maximum value (0.2 h^{-1}) helps the de-repression of P_{AOX1} [30]. The specific growth rate can be controlled by modulating the quantity of glucose-liberating enzyme avoiding glucose accumulation. ROL is produced along the fermentation with the highest specific production rate during the last 24 hours.

- Strategy 2: Pulsed feeding of glycerol/MeOH

The performance of biomass, lipolytic activity, pO_2 and accumulated volume from pulse addition of a mixed substrate (glycerol/MeOH) at low rate of 2 µL h^{-1}, and high rate of 4 µL h^{-1}, is presented in figure 3 and figure 4, respectively.

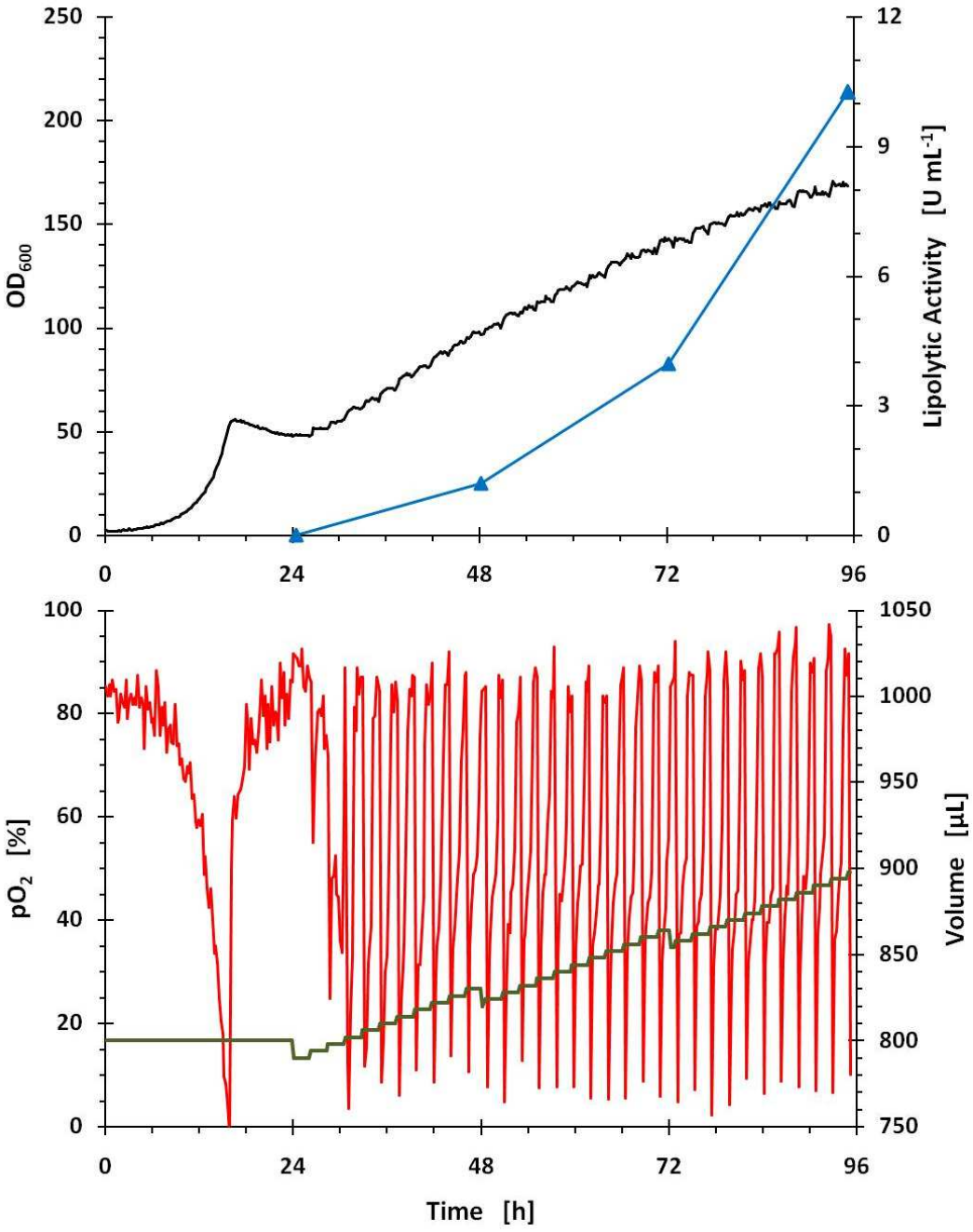

Figure 6.3 Growth kinetics from RoboLector microbioreactor system for clone 4. Operational fed-batch strategy was pulsed dosing of glycerol/MeOH at a rate of 2 µL h^{-1}. (——) OD_{600}; (▲) lipolytic activity; (——) pO_2 and (——) volume.

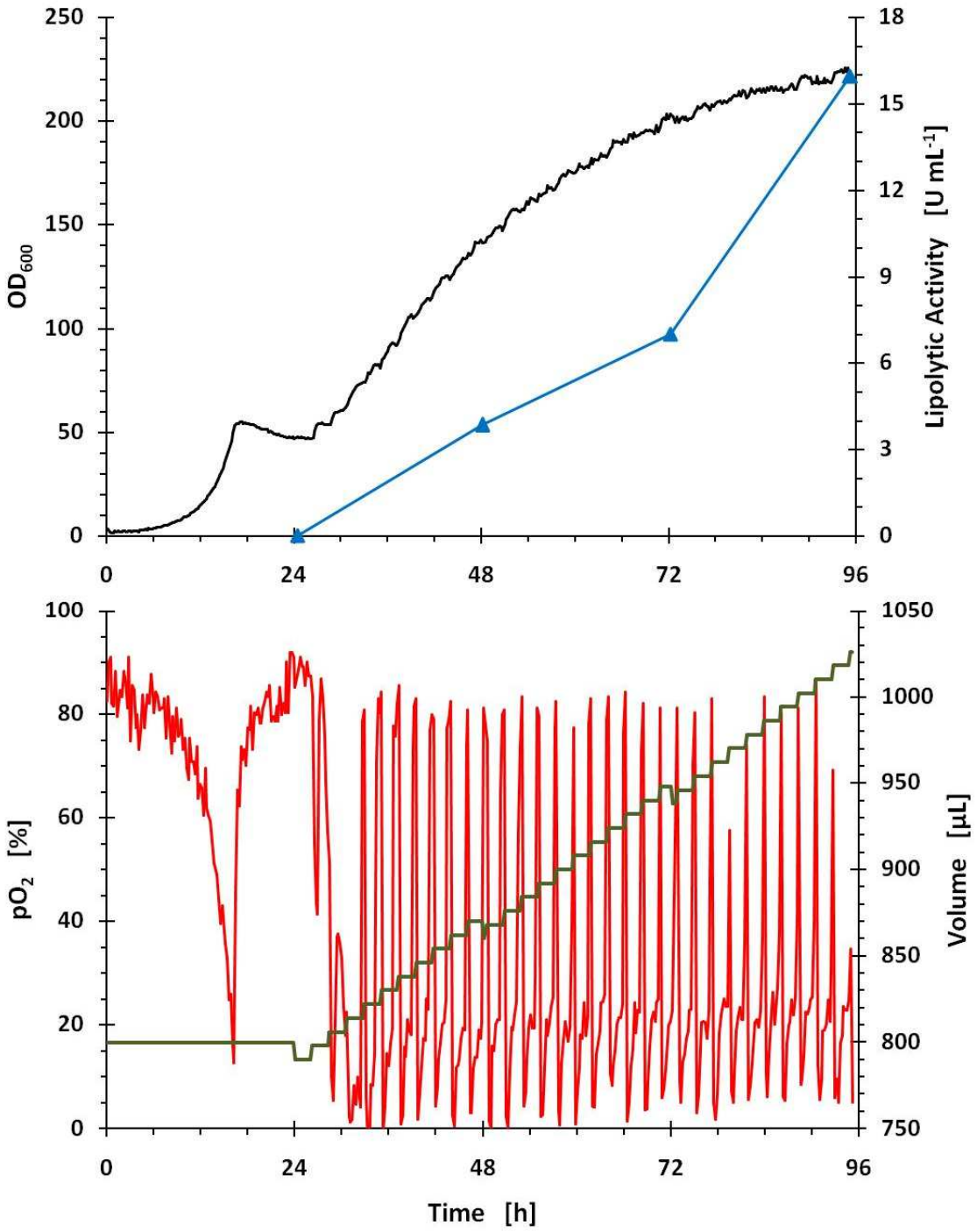

Figure 6.4 Growth kinetics from RoboLector microbioreactor system for clone 4. Operational fed-batch strategy was pulsed dosing of glycerol/MeOH at a rate of 4 µL h^{-1}. (——) OD_{600}; (—▲—) lipolytic activity; (——) pO_2 and (——) volume

The pO_2 time courses for both dosing rates demonstrate clearly, that the culture is able to metabolize previously added nutrients before the next substrate pulse bolus feed occurs. That means overfeeding does not occur.

As expected, the specific growth rate at low feeding rate is lower than at a high feeding rate which is also reflected in ROL activity over time. Again, as observed in cultivations with enzymatic feeding of glucose with MeOH induction, the highest increase in lipolytic activity occurs during the last 24 hours.

More interesting is the comparison between the specific activities with respect to biomass produced and methanol consumed (Table 6.1).

Table 6.1 Comparison of process variables and specific activities for clone 4 under different fed-batch strategies in microbioreactor after 96 h.

Fed-batch strategy	Biomass [OD_{600}]	ROL activity [U mL^{-1}]	Specific activity [U mL^{-1} OD_{600}^{-1}]	MeOH added [mg]	Final volume [mL]	Specific activity on methanol [U mg^{-1}_{MeOH}]
Glucose feeding	255	10.3	0.040	19	0.794	0.43
Low glycerol feeding	169	10.3	0.061	28.2	0.898	0.33
High glycerol feeding	222	16	0.072	56.4	1.026	0.29

In terms of specific activity with respect to biomass produced, high glycerol feeding rate is the best strategy: 1.2-fold higher than low glycerol feeding rate and 1.8-fold higher than glucose feeding. However, specific activity with respect to methanol consumed should be the key variable for the comparison between the three strategies, because methanol is the inducer of the production and total methanol added was different for the three operational strategies. Comparing this parameter, glucose feeding is the best strategy, 1.3-fold higher than low glycerol feeding and 1.5-fold higher than high glycerol feeding. Thus, the methanol added is the key

parameter in terms of maximizing ROL production. Studies using glycerol as co-substrate in Mut^S phenotype producing ROL demonstrated that there is an optimal relation μ_{Gly}/μ_{MeOH}. When this specific relation is overcome a decrease in specific activity is observed [34]. Under the glycerol feeding rates tested, this relation has not been surpassed.

6.2.2.3 Comparison of clone rankings for different fed-batch strategies in microbioreactor system

Finally, the performances of the three selected clones were compared for the three fed-batch operational strategies and batch bioprocess (Figure 6.5).

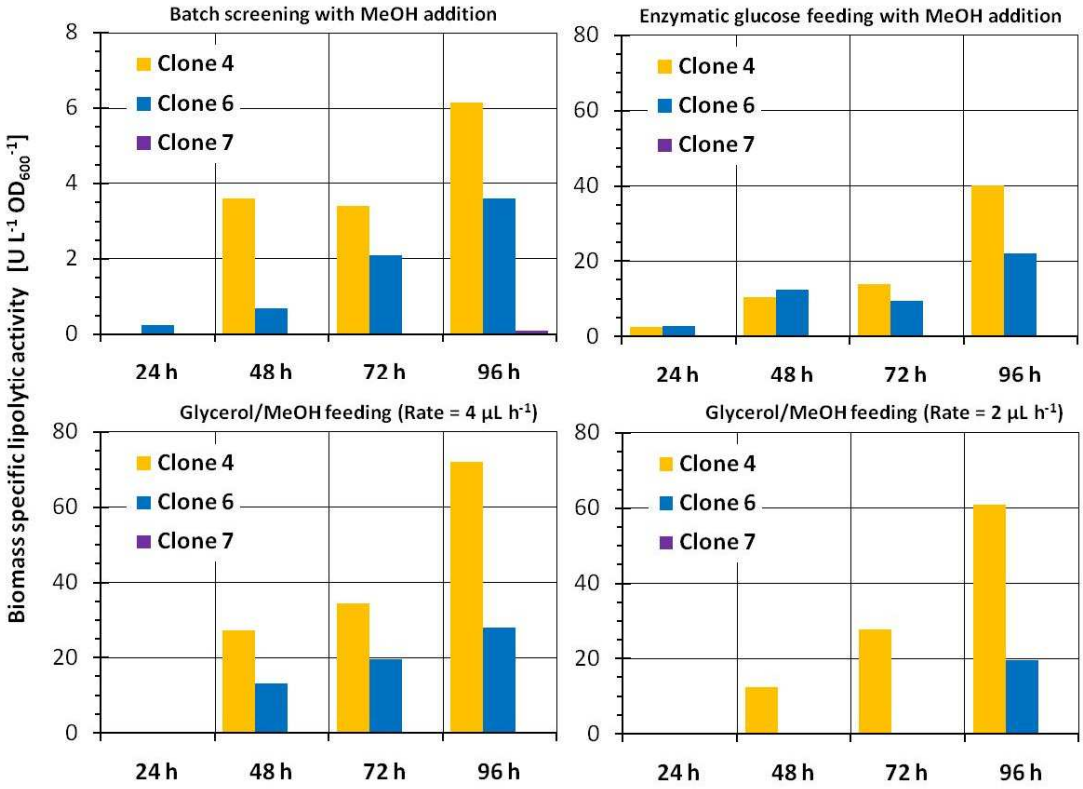

Figure 6.5 Comparison of clone ranking for clones 4 and 6 obtained in different cultivation modes in RoboLector microbioreactor system (single runs). Clone 7, which was also cultivated in STR next to clones 4 and 6, produced hardly any product and is therefore not shown in the figure. Medium background was Syn6 production medium. A: Batch screening with methanol induction. B: Enzymatic glucose feeding with methanol induction. C: Feeding of glycerol/methanol at 4 µL h^{-1}. D: Feeding of glycerol/methanol at 2 µL h^{-1}. Different scales are used in A (values between 0 to 8) and B to D (values between 0 to 80).

Interestingly, when the same background medium is used (Syn6 medium), the clone rankings are maintained between different cultivation modes, at least for the clones applied in this study. These results cannot be directly transferred to other hosts expressing other genes-of-interest, which highlights the need of tools like MBR when developing bioprocesses from scratch. This is supported by the observations in [35], where different clone rankings were obtained for two *H. polymorpha* clone libraries when cultivating in batch mode on glycerol, batch mode on glucose and fed-batch mode on glucose.

As expected, the lowest specific activities were observed in batch growth with subsequent MeOH addition every 24 hours, which were lower by one order of magnitude when compared with fed-batch strategies. The higher activities obtained in fed-batch cultivations facilitate the detection of the expressed product and at the same time ensures a more reliable clone selection.

6.2.3 Lab scale bioreactor cultivations

In the present study, it is of interest to demonstrate if clone ranking and fed-batch operational strategies could be transferred from a microbioreactor unit (800 µL) to a classical stirred tank bioreactor (3 L), with a scale-up factor covering three orders of magnitude (factor > 3000). Enzymatic glucose fed-batch mode and low feeding rate of glycerol/MeOH were the two selected strategies to compare scale up of the bioprocess with clone 4. The results obtained for both strategies are presented in Table 6.2, Figure 6.6 and Figure 6.7.

Table 6.2 Comparison of process variables and specific activities for clone 4 under different fed-batch strategies in lab-scale bioreactor after 96 h.

Fed-batch strategy	Biomass [OD_{600}]	ROL activity [U mL^{-1}]	Specific activity [U mL^{-1} OD_{600}^{-1}]	MeOH added [mg]	Final volume [mL]	Specific activity to methanol [U mg^{-1}_{MeOH}]
Glucose feeding	138 ±4.2	9.8±0.6	0.071	71010	3700	0.51
Low glycerol feeding	140±0.1	12±1.2	0.086	118350	3400	0.34

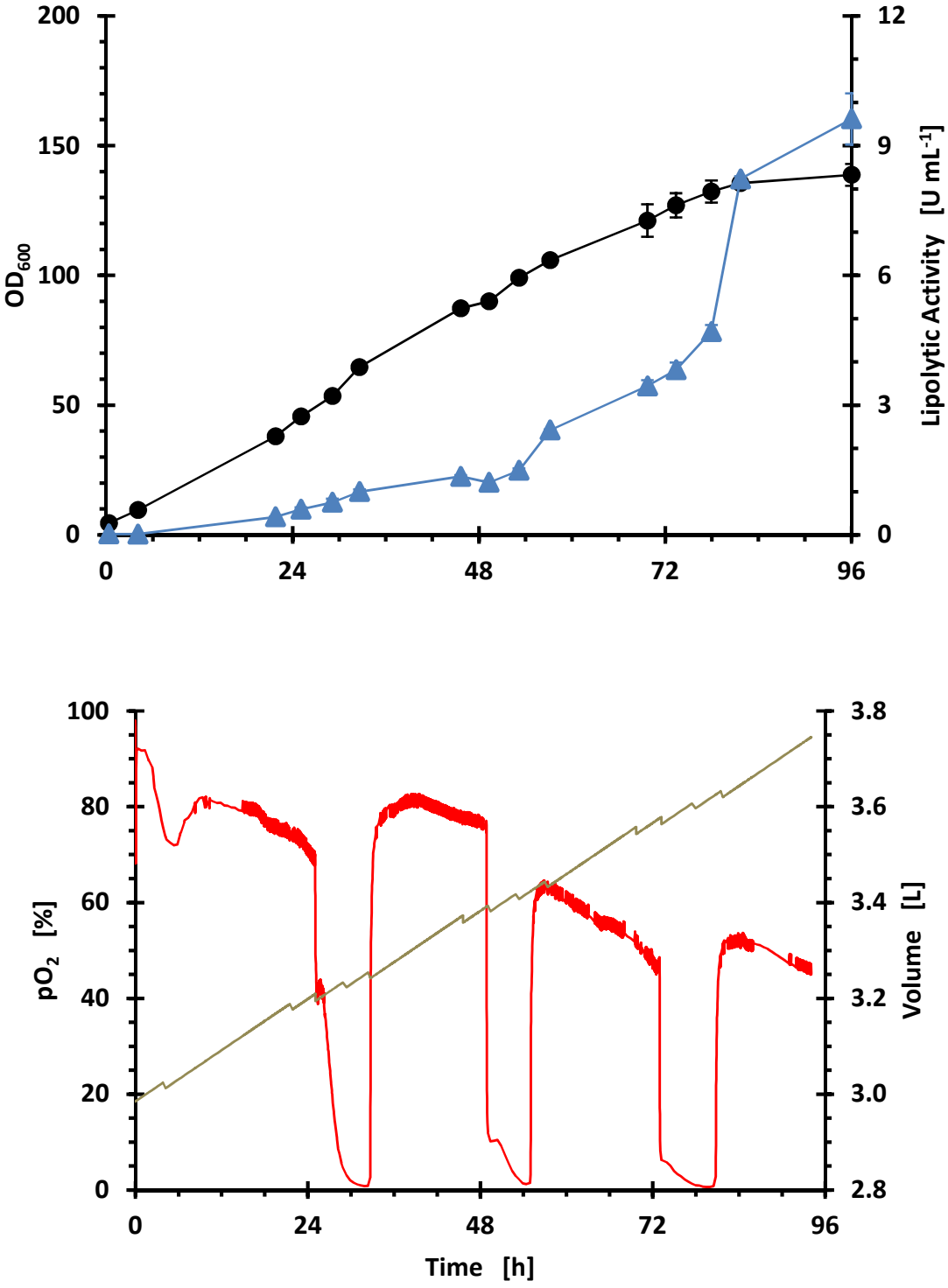

Figure 6.6 Operational fed-batch strategy of constant feeding of glucose with MeOH addition in 24 h intervals in lab scale bioreactor cultivating clone 4. (●) OD_{600}; (▲) lipolytic activity; (—) pO_2 and (—) volume.

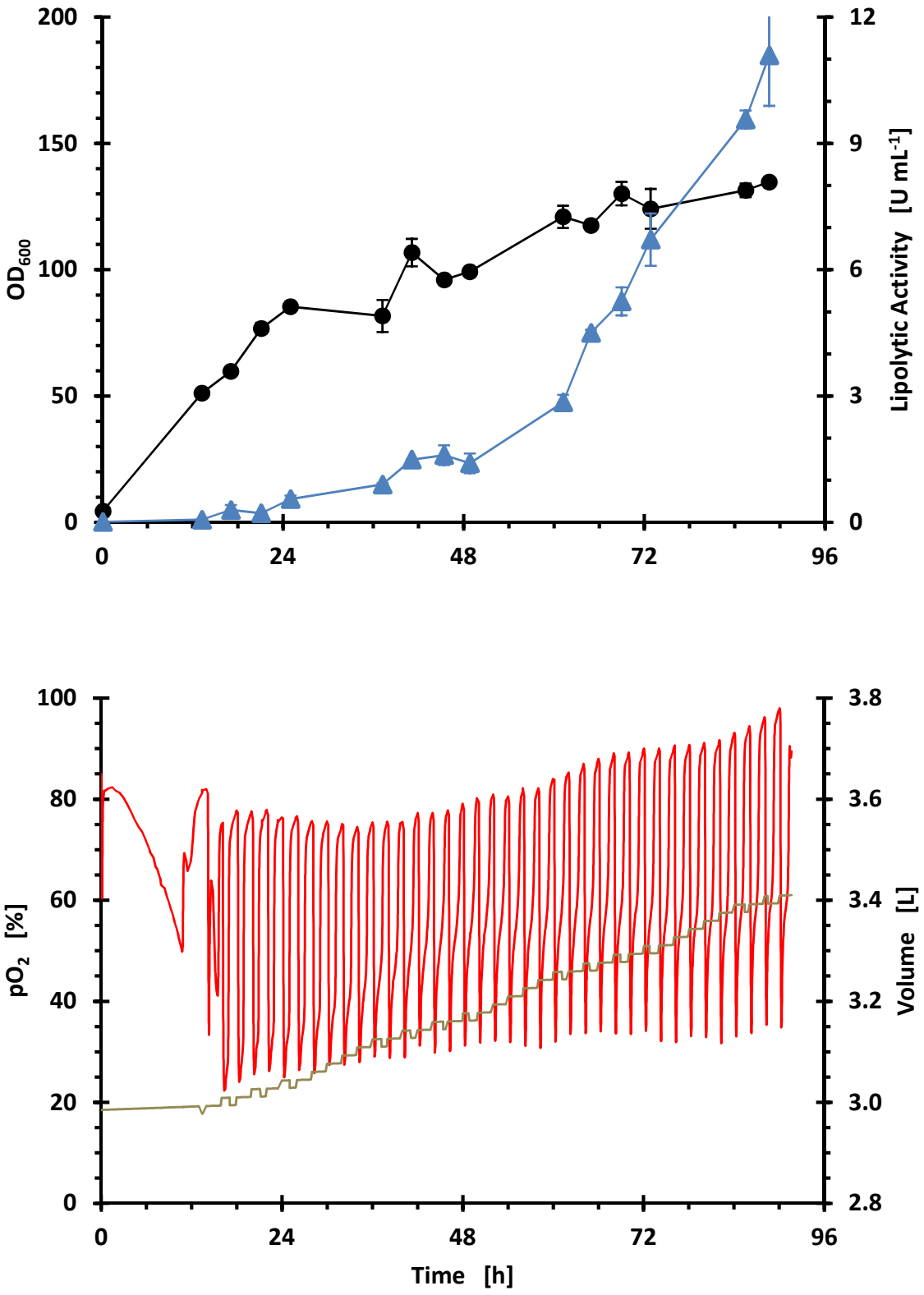

Figure 6.7 Operational fed-batch strategy of pulsed addition of glycerol and MeOH in lab scale bioreactor cultivating clone 4. (●) OD_{600}; (▲) lipolytic activity; (—) pO_2 and (—) volume.

6.2.3.1 Comparison of operational fed-batch strategies and scales

One of the targets of the bioprocess scale up was to obtain similar oxygen consumption profile to avoid that differences in the ROL production could be attributed to the different oxygen transfer conditions. Aeration conditions in lab bioreactor were chosen in order to get a similar OTR to that in the microbioreactor, in which OTR values of 50 – 65 mmol L^{-1} h^{-1} were determined with the method of sulphite oxidation [36] for the applied operating conditions, as specified in materials & methods section. Similar oxygen profiles were obtained for both strategies in both bioreactors as can be seen from the comparison between using glucose (Figure 6.2, Figure 6.6) and using glycerol (Figure 6.3, Figure 6.7).

The use of enzymatic release of glucose is an uncommon strategy for lab and industrial bioreactors, where feeding is realized by pumping concentrated nutrient solutions into the bioreactor. In MBR the enzymatic glucose release was estimated around 1 $g_{Glucose}$ L^{-1} h^{-1}. This feeding rate was applied to lab bioreactor with a constant 500 µL glucose solution addition (300 g L^{-1}) every 3 minutes. The final biomass concentration was lower in lab scale. According with this data, mean specific growth rate was 0.019 h^{-1} for STR *versus* 0.024 h^{-1} for MBR. Therefore, the glucose release rate of 1 $g_{Glucose}$ L^{-1} h^{-1} for the MBR was estimated lower than the real one.

Nevertheless, similar lipolytic activity values were reached at the end of the bioprocess for both bioreactors (Table 6.1 and

Table 6.2). Although the total methanol added per cultivation volume was slightly lower in STR, specific activity with respect to methanol was slightly higher, 1.2-fold. This fact could be related to the lower specific growth rate reached in lab bioreactor and subsequently a lower repression of P_{AOX1}.

Whereas glycerol and sorbitol are frequent co-substrates used in heterologous protein production under P_{AOX1} promoter, the use of glucose as co-substrate is rarely described in literature due to the strong repression of the promoter [37]. Nevertheless, recent chemostat studies have shown the potential of glucose as a co-substrate for the P_{AOX1}-based *P. pastoris* system under de-repressing conditions [30,38]. In contrast, the closely related methylotrophic

yeast *Hansenula polymorpha* shows high expression rates when grown on glucose as sole carbon source, even if expression of the *gene-of-interest* is driven by a promoter originating from its MeOH-assimilation pathway [28]. However, at this low constant glucose feeding rate the amount of glucose available to the culture is taken up immediately. As shown in recent chemostat studies performed under carbon-limiting conditions [30,38], this "carbon starvation" may expose P_{AOX1} to de-repressing conditions, leading to full induction upon the addition of methanol.

The scale-up of low glycerol feeding rate fed-batch strategy, from an operational point of view was more successful due to the better reproducibility of the feeding profile. The time courses of OD_{600}, lipolytic activity, pO_2 and volume are presented in Figure 6.7. pO_2 was maintained at values higher than 20%, that is slightly higher than the one observed in microbioreactor (Figure 6.3), where values lower than 20% were reached at the beginning of every mixed substrate addition pulse. However, in terms of lipolytic activity and specific activity with respect to methanol the values were quite similar (5 – 15% difference) in both bioreactors.

In terms of specific activity with respect to biomass, this value was 1.2-fold higher in lab bioreactor than in microbioreactor. A plausible explanation for such differences would be caused by the different dissolved oxygen profiles, since oxygen availability affects methanol assimilation rate and, in particular, *AOX1* transcriptional levels [39], even in glucose-only growth conditions [40]. Transient oxygen-limiting conditions observed in microbioreactor cultivations after each methanol pulse may result in a reduction of *AOX1* transcriptional levels, as previously shown in shake flask cultures equipped with pO_2 online monitoring [41].

The comparison of lipolytic activity values reached for both strategies and bioreactors is presented in Figure 6.8.

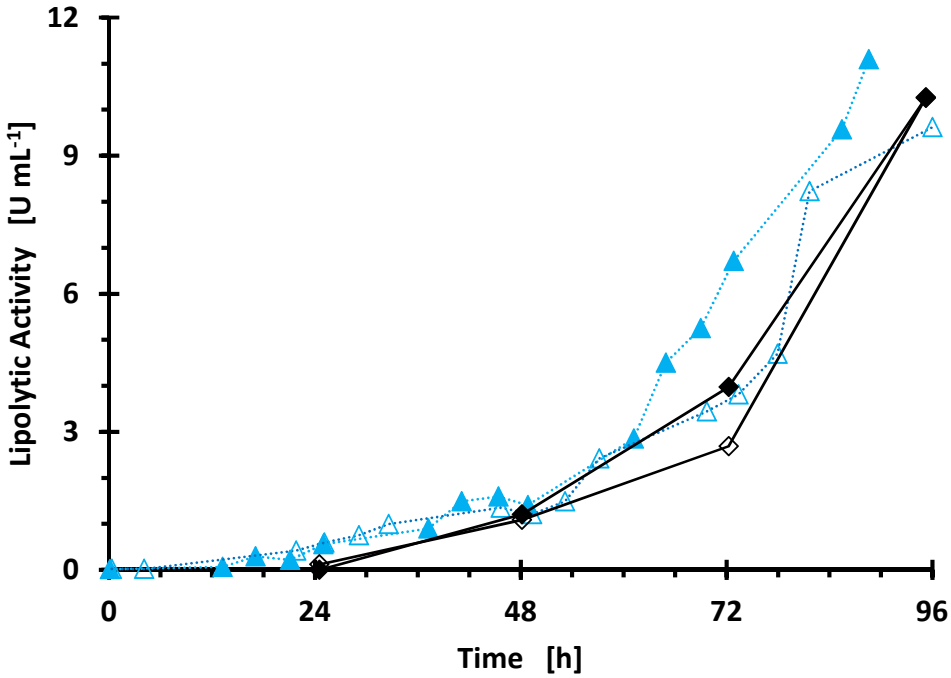

Figure 6.8 Comparison of fed-batch operational strategies and scales in respect to volumetric lipolytic activity for cultivations with clone 4 (X33-ROL-Hac1_sc5). refers to lab scale bioreactor with glycerol/MeOH feeding, to lab scale bioreactor with glucose and MeOH feeding, to microbioreactor with glycerol/MeOH feeding and to microbioreactor with glucose and MeOH feeding.

The patterns of lipolytic activity time courses are quite similar, with a difference of less than 10% for the final lipolytic activity.

For the verification of clone ranking in lab scale, clones 4, 6 and 7 were tested at low glycerol feeding rate fed-batch strategy. The lipolytic activity at 96 hours for both scales is shown in **Figure 6.9**.

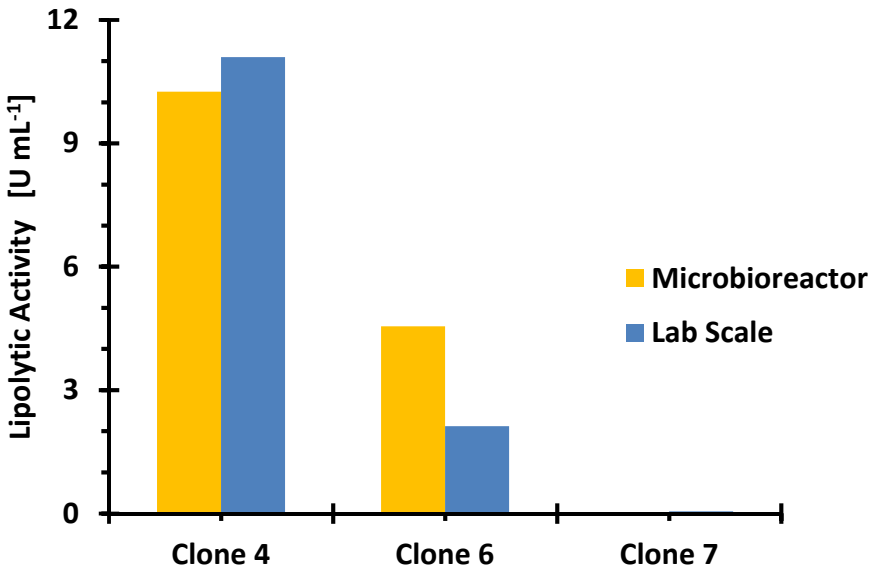

Figure 6.9 Comparison of clone ranking after 96 h for microbioreactor and lab scale. Operational strategy was feeding of glycerol/MeOH at low rate. Ranking was judged by final volumetric lipolytic activity.

Not only the ranking was maintained but also the activity levels reached were quite similar. These results are quite remarkable because in many cases clone selection made by conventional approaches like shake flask cultivations do not correspond with the production expectations when they are tested at lab or pilot plant scale.

6.3 Conclusions

The results presented in this study demonstrate the feasibility of the RoboLector MBR system in bioprocess development with *P. pastoris* as microbial cell factory. The RoboLector MBR system proved to be an ideal tool regarding this application. In particular, the implementation of fed-batch strategies in microbioreactors has demonstrated the excellent performance for clone selection with the P_{AOX1}-based *P. pastoris* system using methanol as inducing substrate. Also, the results prove that the RoboLector platform is compatible with the use of a volatile and high O_2-demanding substrate such as methanol. Furthermore, different operational fed-batch strategies at microscale for *P. pastoris* and clone screenings were performed and evaluated, which were scalable to conventional lab scale stirred tank bioreactor, covering three orders of magnitude (factor > 3000). In addition, the influence of media composition in clone selection was demonstrated. The capabilities of the RoboLector MBR system accounted for the success of the study: online monitoring of relevant fermentation parameters, integration of pipetting robot for manipulation of cultures at a high frequency based on online monitored data, utilization of FlowerPlates allowing up to 48-fold parallel cell culturing at elevated oxygen transfer rates and scalability of clone ranking and fed-batch operational strategies (particularly mixed feeds) into classical STR. With real-time insights into the metabolic behaviour of the individual cultures, it becomes possible to react also in real-time accordingly. Thus, the full potential of the automated liquid handling system integrated into the RoboLector MBR could be applied in our study. Moreover, the development of these strategies may be also suitable for clone screening and fermentation development with other industrially important expression hosts.

In conclusion, the exciting area of MBR systems is still in motion to further expand the possibilities of such systems. Currently, there are more and more analytical systems which are designed to perform tasks for bioprocess development in a high-throughput manner. In future, the integration of such machines into already existing sophisticated systems like the RoboLector makes MBR even more powerful and will contribute to next-level biotechnological developments until complete upstream and downstream processing can be executed by MBR systems.

6.4 Methods

6.4.1 Organisms

The *P. pastoris* X-33/pPICZ□ROL strain [20] was used as starting strain to generate a series of transformants co-overexpressing the spliced form of *HAC1* from *P. pastoris*. Isolation the spliced form of *HAC1* from *P. pastoris* was performed following a strategy based on [42].

Competent *P. pastoris* cells were prepared and transformed according to [43]. The pPIC3.5K-*HAC1spliced* was linearized in the *HIS4* gene with *Nco*I for integration targeting of the construct in this locus. Transformants were plated on YPD agar plates containing 250 mg L^{-1} geneticin. In order to verify the integration of the *HAC1spliced* cassette, a PCR was performed on purified genomic DNA of the transformants with the forward primer 5'-GACTGGTTCCAATTGACAAGC-3' (*AOX1* promoter region) and the reverse primer 5'-GCCGCCTATTCCTGGAAGAATAC-3', with the following cycling conditions: 2 min 95 °C, followed by 35 cycles of 45 s at 94 °C, 45 s at 55 °C, 1 min 72 °C.

The series of strains potentially having multiple copies of the *ROL* expression cassette was obtained by transforming X-33 (Invitrogen) competent cells with pPICZαA-ROL [29], as described in [39].

6.4.2 Cultivation media

Syn6 production medium contained per liter: 20 g glycerol; 7.66 g $(NH_4)_2SO_4$; 9 g K_2HPO_4; 3.3 g KCl; 3 g $MgSO_4 \cdot 7\ H_2O$; 0.33 g NaCl; 0.1 mol MES; 4.202 g citric acid·H_2O; 1 g $CaCl_2 \cdot H_2O$; 10 mL vitamin solution; 10 mL micro elements solution and 10 mL trace elements solution. Vitamin solution contained per 100 mL: 20 mg d-Biotin and 2 g Thiamine·HCl. Micro elements solution contained per 100 mL: 1 g $(NH_4)_2Fe(SO_4)_2 \cdot 6\ H_2O$; 0.08 g $CuSO_4 \cdot 5\ H_2O$; 0.3 g $ZnSO_4 \cdot 7\ H_2O$; 0.4 g $MnSO_4 \cdot H_2O$ and 1 g Titriplex III. Trace elements solution contained per 20 mL: 2 mg $NiSO_4 \cdot 6\ H_2O$; 2 mg $CoCl_2 \cdot 6\ H_2O$; 2 mg H_3BO_3; 2 mg KI and 2 mg $Na_2MoO_4 \cdot 2\ H_2O$. The pH-value of the medium was adjusted to 6.4 with KOH. Cultivations with enzymatic glucose release were conducted with a proprietary formulation based on a Syn6 medium.

YNB screening medium contained per liter: 10 g glycerol; 1.34 g Yeast Nitrogen Base without amino acids and ammonium (Difco); 5 g $(NH_4)_2SO_4$; 0.4 mg d-Biotin and 0.1 mol Na_2HPO_4/NaH_2PO_4 (pH 6.0).

YPD preculturing medium contained per liter: 10 g yeast extract, 20 g peptone, 20 g glucose.

6.4.3 Shake flasks cultivations

Triplicate shake flask cultures were performed as follows: 25 mL of BMG medium were inoculated with a fresh colony and incubated over night at 25 °C and 150 rpm (Infors Shaker, 25 mm shaking diameter). After 20 hours, cells were centrifuged (3000 x g, 5 min) and resuspended into 25 mL BMM medium to an initial OD_{600} of 1.0. After 24 hours of induced expression, OD_{600} and lipolytic activity of the cultures were measured.

6.4.4 Microbioreactor cultivations

The microbioreactor was a RoboLector system, which consists of a BioLector device (G-BL-100, m2p-labs, Baesweiler, Germany) integrated into a PerkinElmer Multiprobe II Ex liquid handling robot. The BioLector device monitored from a incubated microplate the following parameters for each well of the microplates within a measurement interval of 13 min: scattered light (proportional to biomass concentration), riboflavin fluorescence ($\lambda_{Ex.}$ = 488 nm, $\lambda_{Em.}$ = 520 nm), NAD(P)H fluorescence ($\lambda_{Ex.}$ = 365 nm, $\lambda_{Em.}$ = 450 nm) and dissolved oxygen tension (DO or pO_2) via integrated optodes in the bottom of the microplate's wells. Scattered light readings were translated into OD_{600} with values determined at end of the MBR cultivations. The incubation chamber of the BioLector device controlled relative humidity above 85% to minimize evaporation from the microplate's wells.

Cultivations were carried out exclusively in 48 well FlowerPlates (MTP-48-BO, m2p-labs, Baesweiler, Germany), shaking frequency of1100 rpm, shaking diameter of 3 mm, initial volume of 800 µL per well, maximum allowed volume of 1100 µL per well due to volume increase caused by feeding.Cultivation temperature was 28 °C. FlowerPlates were sealed with a gas permeable membrane with a pre-slitted silicone layer (F-GPRS48-10, m2p-labs, Baesweiler, Germany) for penetration by robotic tips. MeOH addition of 8 µL was programmed in 24 h intervals for cultivations conducted in batch mode and enzymatic glucose fed-batch mode. Feeding of the

nutrient mixture (200 g L^{-1} glycerol, 25% v/v MeOH and 1.5% w/w NH_4OH) was programmed to start after 24 h with a pulsing rate of 4 µL or 8 µL every 2 h (i.e. 2 µL h^{-1} or 4 µL h^{-1}). Automated sampling was programmed in 24 h intervals for all cultivation modes. Feeding and sampling was performed without interruption of shaking. Sampling volume was 10 µL. Assay of lipolytic activity performed immediately at-line to MBR cultivations after sampling. Cultivations were started with initial OD_{600} of 2.5, inoculated from precultures grown overnight in 20 mL YPD medium in 250 mL Erlenmeyer flasks, at a shaking frequency of 250 rpm, a shaking diameter of 25 mm and 28 °C.

6.4.5 Bioreactor cultivations

Pre-inoculum for bioreactor cultures were grown for 24 h in 1 L baffled shake flasks at 30 °C, 150 rpm, in YPD medium containing 1 mL of a zeocin solution (100 mg mL^{-1}, InvivoGen). Shake flasks contained 200 mL of YPD medium. The culture was centrifuged at 8000 rpm, 15 min and the harvested cells were re-suspended in bioreactor culture medium and used to inoculate a 5 L Biostat B bioreactor (Braun Biotech, Melsungen, Germany) at an initial optical density of 3. Cells were cultured under the following cultivation conditions: initial volume 3 L, stirring rate 600 rpm, temperature 28 °C, pH controlled at 5.0 by adding NH_4OH 30% (v/v), air flow rate 3 L min^{-1}. The cultivation started with a 20 g L^{-1} glycerol batch phase. When glycerol was exhausted, fed-batch phase was initiated, lasting for approximately 72 hours.

6.4.6 Biomass analysis

Biomass analysis was performed by measuring triplicates of the optical density at a wave length of 600 nm in cuvettes of 1 cm path length.

6.4.7 Lipolytic activity assay

Samples from MBR cultivations were diluted with phosphate buffered saline (PBS) and analyzed for lipolytic activity at 30 °C in 96 well microplates using a TECAN microplate reader pre-heated to 30 °C. Dilution factor of samples was 20 and resulted in a linear increase of absorption at 410 nm for at least five minutes. 10 µL of diluted sample were mixed with 190 µL of freshly prepared reaction mix (1 volume of 30 mg p-nitrophenylpalmitate (pNPP) in 10 mL isopropanol and 9 volumes of 90 mL potassium phosphate buffer (100 mM, pH 8) containing 111.1 mg gum arabic and 207 mg sodium deoxycholate). For calculation of released amount of p-nitrophenol

(pNP) from pNPP under assay conditions, a calibration was done by using 10 µL of a pNP solution with known concentrations instead of 10 µL diluted sample. Measurement interval of absorption readings at 410 nm was set to 45 s, with 10 s of shaking before each measurement. Increase in absorption due to autohydrolysisof pNPPcould not be detected during measurement time. Volumetric activity under assay conditions for the release of 1 µM of pNP per min per mL of sample volume was calculated as follows: Activity [U mL^{-1}] = $A_{410\ nm}$ [a.u. min^{-1}] * Slope of pNP-calibration [$\mu mol_{pNP} L^{-1} a.u.^{-1}$] * dilution factor * 0.001.

For bioreactor cultures, extracellular lipolytic activity was measured by using a p-nitrophenylbutyrate (pNPB) assay. Cells were removed by centrifugation (13,000 rpm, 3 min). Then, samples were diluted with PBS and lipolytic activity was followed spectophotometrically in a cary Varian 300 spectophotometer (Varian Inc., Palo Alto, USA) at 30 °C after mixing in a 1 mL cuvette 40 µl of sample and 960 µL of freshly prepared, pre-warmed reaction mix (1 volume of 19 mg pNPB in 10 mL isopropanol mixed with 9 volumes of 250 mMTris-HCl, pH 7.5). Linear increase of absorption at 410 nm was followed for five minutes. Volumetric activity under assay conditions for the release of 1 µM of pNP per min per mL of sample volume was calculated as follows: Activity [U mL^{-1}] = $A_{410\ nm}$ [a.u. min^{-1}] * Slope of pNP-calibration [$\mu mol_{pNP} L^{-1} a.u.^{-1}$] * dilution factor * 0.001. In order to compare data a correlation between both methods (pNPP and pNPB) was conducted, applying a ROL dilution series with known concentration in the two methods.

6.5 References

[1] C.L. Brooks, M. Morrison, M. Joanne Lemieux, Rapid expression screening of eukaryotic membrane proteins in *Pichia pastoris*, Protein Sci. 22 (2013) 425-433.

[2] B.K. Lundholt, K.M. Scudder, L. Pagliaro, A simple technique for reducing edge effect in cell-based assays, J. Biomol. Screen. 8 (2003) 566-570.

[3] P. Rohe, D. Venkanna, B. Kleine, R. Freudl, M. Oldiges, An automated workflow for enhancing microbial bioprocess optimization on a novel microbioreactor platform, Microb. Cell Fact. 11:144 (2012).

[4] R. Puskeiler, K. Kaufmann, D. Weuster-Botz, Development, parallelization, and automation of a gas-inducing milliliter-scale bioreactor for high-throughput bioprocess design (HTBD), Biotechnol. Bioeng. 89 (2005) 512-523.

[5] M. Funke, A. Buchenauer, W. Mokwa, S. Kluge, L. Hein, C. Müller, F. Kensy, J. Büchs, Bioprocess control in microscale: Scalable fermentations in disposable and user-friendly microfluidic systems, Microb. Cell Fact. 9:86 (2010).

[6] M. Funke, S. Diederichs, F. Kensy, C. Müller, J. Büchs, The baffled microtiter plate: Increased oxygen transfer and improved online monitoring in small scale fermentations, Biotechnol. Bioeng. 103 (2009) 1118-1128.

[7] K. Isett, H. George, W. Herber, A. Amanullah, Twenty-four-well plate miniature bioreactor high-throughput system: Assessment for microbial cultivations, Biotechnol. Bioeng. 98 (2007) 1017-1028.

[8] K. Baumann, N. Adelantado, C. Lang, D. Mattanovich, P. Ferrer, Protein trafficking, ergosterol biosynthesis and membrane physics impact recombinant protein secretion in *Pichia pastoris*, Microb. Cell Fact. 10:93 (2011).

[9] M. Boettner, C. Steffens, C. Mering von, P. Bork, U. Stahl, C. Lang, Sequence-based factors influencing the expression of heterologous genes in the yeast *Pichia pastoris* - A comparative view on 79 human genes, J. Biotechnol. 130 (2007) 1-10.

[10] S. Curvers, P. Brixius, T. Klauser, J. Thömmes, D. Weuster-Botz, R. Takors, C. Wandrey, Human Chymotrypsinogen B production with *Pichia pastoris* by integrated development of fermentation and downstream processing. Part 1. Fermentation, Biotechnol. Prog. 17 (2001) 495-502.

[11] T. Anderlei, W. Zang, M. Papaspyrou, J. Büchs, Online respiration activity measurement (OTR, CTR, RQ) in shake flasks, Biochem. Eng. J. 17 (2004) 187-194.

[12] T. Anderlei, J. Büchs, Device for sterile online measurement of the oxygen transfer rate in shaking flasks, Biochem. Eng. J. 3478 (2000) 1-6.

[13] X. Qin, J. Qian, G. Yao, Y. Zhuang, S. Zhang, J. Chu, GAP promoter library for fine-tuning of gene expression in *Pichia pastoris*, App. Env. Microbiol. 77 (2011) 3600-3608.

[14] F.S. Hartner, C. Ruth, D. Langenegger, S.N. Johnson, P. Hyka, G.P. Lin-Cereghino, J. Lin-Cereghino, K. Kovar, J.M. Cregg, A. Glieder: Promoter library designed for fine-tuned gene expression in *Pichia pastoris*, Nucleic Acids Res. 36(12):e76 (2008).

[15] A.G. Sandström, K. Engström, J. Nyhlen, A. Kasrayan, J. Bäckvall, Directed evolution of *Candida antarctica* lipase A using an episomaly replicating yeast plasmid, Protein Eng. Des. Sel. 22 (2009) 413-420.

[16] A. Murasugi, Y. Tohma-Aiba, Comparison of three signals for secretory expression of recombinant human midkine in *Pichia pastoris*, Biosci. Biotechnol. Biochem. 65 (2001) 2291-2293.

[17] R. Legmann, B. Benoit, R.W. Fedechko, C. L. Deppeler, S. Srinivasan, R.H. Robins, E.L. McCormick, D.A. Ferrick, S.T. Rodgers, A.P. Russo: A strategy for clone selection under different production conditions, Biotechnol. Prog. 27 (2011) 757-765.

[18] F. Kensy, E. Zang, C. Faulhammer, R. Tan, J. Büchs, Validation of a high-throughput fermentation system based on online monitoring of biomass and fluorescence in continuously shaken microtiter plates, Microb. Cell Fact. 8:31 (2009).

[19] R. Huber, D. Ritter, T. Hering, A. Hillmer, F. Kensy, C. Müller, L. Wang, J. Büchs, Robo-Lector - A novel platform for automated high-throughput cultivations in microtiter plates with high information content, Microb. Cell Fact. 8:42 (2009).

[20] S. Minning, A. Serrano, P. Ferrer, C. Solá, R.D. Schmid, F. Valero, Optimization of the high-level production of *Rhizopus oryzae* lipase in *Pichia pastoris*, J. Biotechnol. 86 (2001) 59-70.

[21] Thermofisher: *Pichia* fermentation process guidelines version Version B053002. Available online: https://tools.thermofisher.com/content/sfs/manuals/pichiaferm_prot.pdf, last accessed 10/07/2017.

[22] D. Resina, M. Maurer, O. Cos, C. Arnau, M. Carnicer, H. Marx, B. Gasser, F. Valero, D. Mattanovich, P. Ferrer, Engineering of bottlenecks in *Rhizopus oryzae* lipase production in *Pichia pastoris* using the nitrogen source-regulated FLD1 promoter, N. Biotechnol. 25 (2009) 396-403.

[23] S. Kim, Optimization of the functional expression of *Coprinuscinereus* peroxidase in *Pichia pastoris* by varying the host and promoter, J. Microbiol. Biotechnol. 19 (2009) 966-971.

[24] C.C. Lee, T.G. Williams, D.W. Wong, G.H. Robertso, An episomal expression vector for screening mutant gene libraries in *Pichia pastoris*, Plasmid 54 (2005) 80-85.

[25] M. Mack, M. Wannemacher, B. Hobl, P. Pietschmann, B. Hock, Comparison of two expression platforms in respect to protein yield and quality: *Pichia pastoris* versus *Pichia angusta*, Protein Express. Purif. 66 (2009) 165-171.

[26] S. Hellwig, F. Emde, N.P.G. Raven, M. Henke, P. van der Logt, R. Fischer, Analysis of single-chain antibody production in *Pichia pastoris* using on-line methanol control in fed-batch and mixed-feed fermentations, Biotechnol. Bioeng. 74 (2001) 344-352.

[27] S. Hellwig, F. Robin, J. Drossard, N.P.G. Raven, C. Vaquero-Martin, J.E. Shively, R. Fischer, Production of carcinoembryonic antigen (CEA) N-A3 domain in *Pichia pastoris* by fermentation, Biotechnol. Appl. Biochem. 30 (1999) (Pt 3) 267-275.

[28] A.F. Mayer, K. Hellmuth, H. Schlieker, R. Lopez-Ulibarri, S. Oertel, U. Dahlems, A.W. Strasser , A.P. van Loon, An expression system matures: a highly efficient and cost-effective process for phytase production by recombinant strains of *Hansenula polymorpha*, Biotechnol. Bioeng. 63 (1999) 373-381.

[29] D. Resina, M. Bollók, N.K. Khatri, F. Valero, P. Neubauer, P. Ferrer, Transcriptional response of *P. pastoris* in fed-batch cultivations to *Rhizopus oryzae* lipase production reveals UPR induction, Microb. Cell Fact. 6:21 (2007).

[30] J. Jordà, P. Jouhten, E. Cámara, H. Maaheimo, J. Albiol, P. Ferrer, Metabolic flux profiling of recombinant protein secreting *Pichia pastoris* growing on glucose:methanol mixtures. Microb. Cell Fact. 11:57 (2012).

[31] E. Cámara, J. Jordà, P. Jouhten, H. Maaheimo, J. Albiol, P. Ferrer, Impact of recombinant protein production on the energy metabolism of *Pichia pastoris* growing on glucose:methanol mixtures, [Abstract]. 2nd Conference on Microbial Stress: from molecules to systems, Belgirate, Italy. 2012.

[32] J.M. Viader-Salvadó, E.L. Cab-Barrera, L.J. Galán-Wong, M. Guerrero, M. Guerrero-Olazarán Genotyping of recombinant *Pichia pastoris* strains. Cell Mol Biol Lett 2006, 11:348-359.

[33] A. Surribas, D. Resina, P. Ferrer, F. Valero F, Riboflavin may interfere with on-line monitoring of secreted green fluorescence protein fusion proteins in *Pichia pastoris*, Microb. Cell Fact. 6:15 (2007).

[34] C. Arnau, C. Casas, F. Valero, The effect of glycerol mixed substrate on the heterologous production of a *Rhizopus oryzae* lipase in *Pichia pastoris* system, Biochem. Eng. J. 57 (2011) 30-37.

[35] M. Scheidle, M. Jeude, B. Dittrich, S. Denter, F. Kensy, M. Suckow, D. Klee, J. Büchs, High-throughput screening of *Hansenula polymorpha* clones in the batch compared with the controlled-release fed-batch mode on a small scale. FEMS Yeast Res. 10 (2010) 83-92.

[36] R. Hermann, N. Walther, U. Maier, J. Büchs, Optical method for the determination of the oxygen-transfer capacity of small bioreactors based on sulfite oxidation, Biotechnol. Bioeng. 74 (2001) 355-363.

[37] H. Hang, X. Ye, M. Guo, J. Chu, Y. Zhuang, M. Zhang, S. Zhang, A simple fermentation strategy for high-level production of recombinant phytase by *Pichia pastoris* using glucose as the growth substrate, Enzy. Microb. Technol. 44 (2009) 185-188.

[38] L. Paulová, P. Hyka, B. Branská, K. Melzoch, K. Kovar, Use of a mixture of glucose and methanol as substrates for the production of recombinant trypsinogen in continuous cultures with *Pichia pastoris* Mut$^+$. J. Biotechnol. 157 (2012) 180-188.

[39] S. Kim, S. Warburton, I. Boldogh, C. Svensson, L. Pon, M. d'Anjou, T.A. Stadheim, B. Choi, Regulation of alcohol oxidase 1 (AOX1) promoter and peroxisome biogenesis in different fermentation processes in *Pichia pastoris*, J Biotechnol 2013, 166:174-181.

[40] K. Baumann, M. Carnicer, M. Dragosits, A.B. Graf, J. Stadlmann, P. Jouhten, H. Maaheimo, B. Gasser, J. Albiol, D. Mattanovich, P. Ferrer, A multi-level study of recombinant *Pichia pastoris* in different oxygen conditions, BMC Syst. Biol. 4:141 (2010).

[41] M. Ruottinen, M. Bollok, M. Kogler, A. Neubauer, M. Krause, E. Hamalainen, J. Myllyharju, A. Vasala, P. Neubauer, Improved production of human type II procollagen in the yeast *Pichia pastoris* in shake flasks by a wireless-controlled fed-batch system, BMC Biotechnol. 8:33 (2008).

[42] M. Guerfal, S. Ryckaert, P.P. Jacobs, P. Ameloot, K. van Craenenbroeck, R. Derycke, N. Callewaert, The HAC1 gene from *Pichia pastoris*: characterization and effect of its overexpression on the production of secreted, surface displayed and membrane proteins, Microb. Cell Fact. 9:49 (2010).

[43] J. Lin-Cereghino, W.W. Wong, S. Xiong, W. Giang, L.T. Luong, J. Vu, S.D. Johnson, G.P. Lin-Cereghino, Condensed protocol for competent cell preparation and transformation of the methylotrophic yeast *Pichia pastoris*., BioTechniques 38:44 (2005) 46, 48.

7 UPGRADING TO THE FIRST STEP UP TO INDUSTRY. PILOT PLANT SCALE PRODUCTION OF ROL BY *Pichia pastoris* UNDER P_{AOX1} CONTROL

7.1 Introduction

As stated in the first chapter of this dissertation, the full development of a bioprocess culminates in its scaling up to the industrial scale. Generally, chemical processes are developed in the smallest scale possible for them to be generally transferred up to a factor of about 50000, or even 80000 for fixed bed reactors [1].

Figure 7.1. Facilities of a pilot plant fermentation process from Northeast Biomanufacturing Center and Collaborative (Blue Bell, PA) [2].

In fermentation processes, the old rule of thumb of using a 10 factor has still been applied during the last decades, due to the higher uncertainty they present in respect to chemical ones. For example, a scale up of the production of a monoclonal antibody in a mammalian cell culture from 3 L to 2500 L was carried out using 4 steps of increasing volume [3]. Also, Martinez and his coworkers [4] successfully accomplished a step of 10-increasing factor in lab scale of an immobilized *P. pastoris* culture. Recently, as well, Vaz de Arruda *et al.*

(2017) [5] reproduced the production of xylitol by *Candida guilliermondii* in three different scales of stirred tank bioreactors, from 2.4 to 125 L.

7.1.1 Scaling up of bioprocesses. General issues

The final step of bringing a bioprocess up to the production scale is particularly challenging, due to the large number of process variables that are seriously affected by the change of scale, from physical and chemical, to essential biological parameters [6].

In the first place, geometric particular features of the vessel and its elements can cause foam, mixing problems, shear stress and heat transfer limitation, among others. Concretely, mixing times of reactors around the scale of 10-50 L oscillate between 1-5 s, while in the 100-500 L scale fit in the 20-30 s and the 10000 L, on the other hand, can reach 2 min [6]. Villadsen *et al*. (2011) appointed mixing as the main issue to deal with at the time of scaling up a bioprocess, where three different phases are simultaneously present, and attributed, literally, the 60 % of problems associated with industrial processes to inadequate mixing. Uniformity then, is complex to achieve due to mass transfer limitations, especially when trying to supply any substrate in a gaseous phase. For instance, algae cultures are completely dependent on CO_2 as the main carbon source. Therefore, defective mixing may trigger direct process limitations that jeopardize reproducibility from little scale. Sedimentation of biomass may be, as well, a consequence of this lack of heterogeneity.

Apart from that, when operating large scale bioreactors, other features must be taken into consideration, such as sterility or cleaning, which, despite not being included in the bioprocess itself, seriously affect the productivity of the process.

Besides the commented gradients caused by inadequate mixing, some other factors, reasonably easy to handle with in small scales, are a serious concern at industrial and even pilot ones. For instance, multiple feed inlets, which can compromise homogeneity. On the other hand, dangerous or flammable are much more regulated and restricted industrial scale, because of its potential hazard is not comparable as when is used at little scales.

Secondly, limitations from a chemical nature, like gradients of pH, temperature, viscosity may be a problem in large scales. As well, cleaning, flexibility for alternate use and accessibility to all the internal area of the vessel are exponentially more complex as scale increases. They may seem simple or straightforwardly recognizable, but Reisman (1993) [6] exemplifies in his review, apart from other issues already appointed, some of the main problems which commonly arise at large scale fermenters:

Non-scalability of some time-based recipes. This fact can be due to many reasons: enlargement of filling/emptying times, of heating/cooling cycles, mixing limitations or even regulatory or safety issues.

The complexity of guaranteeing sterility in large vessels or restricted areas.

Finally, in a more biological aspect of the matter, concerns of the age of the culture are utterly important, especially at very large scales where intermediate steps of inoculation are needed. Solà and Gòdia (1994) [1] illustrate very reasonably the dependence of the number of generations (N_g) on the final volume (V) by the following equation, assuming exponential growth:

$$N_g = 1.44 \left(\ln V + \ln \frac{X}{x_0} \right)$$

Equation 7.1

Where X is the final biomass concentration and x_0 the initial number of cells in the original inoculum.

7.1.2 Scaling-up methods

It is highly probable that, at least once, every person belonging to the field of bioprocess engineering have heard the statement “scaling-up is an art”. It is true that most successful are based on experience, and there exist no ultimate rule to follow, or at least no rule that can be considered to stand up among the rest. Hereon are some of them briefly presented.

First, one of the most applied rules of thumb is the concept of similarity [1], which is easily explained by Equation 7.2:

$$m' = k\, m$$

Equation 7.2

Where m is an arbitrary process variable and k, the scale factor; m' is the scaled value of m. The basis of similarity takes ground by the following idea, if two systems can be described by the same differential equation system, then it can be assumed that with the same contour constraints, both systems will behave the same way.

Depending on the concrete bioprocess and its limitations, some of the following examples of similarities should be considered. They are classified according to a few classes of similarities, which, normally, in this order, one is a prerequisite of the following ones:

Geometric, dynamic, thermal, mass concentration and biochemical similarity [1].

Among this classes of similarities, the most common are constant gas power input per liquid volume (P_g/V), shear stress, oxygen transfer rate (OTR) or global volumetric gas transfer coefficient (k_La).

7.1.3 Oxygen transfer

As commented, there exist numerous factors that can trigger process limitations when processes are brought up to larger scale, such as substrate availability in the whole volume, light requirements by photosynthetic organisms or even foam formation, among many others. Oxygen transport to the cells, though, stands out among the rest, as most industrial bioprocesses are aerobic, and is a molecule with a very low solubility in water (between 2.0 and 2.8 · 10^{-4} mol O_2 L^{-1} at common bioprocess temperatures, 20-40ºC).

OTR depends proportionally on the volumetric gas transfer coefficient (k_La), as Equation 7.3 explains:

$$OTR = k_L a \cdot \left(C^*_{O_2} - C_{O_2}\right)$$

Equation 7.3

Where OTR (mol_{O2} L s^{-1}); k_La (s^{-1}); k_L, the individual coefficient of mass transfer (m s^{-1}); a, the interphase superficial area between the gas phase and the liquid (m^2m^{-3}). C^*_{O2} (mg L^{-1}) is the saturation oxygen concentration in the liquid phase.

k_La is dependent and can be correlated to stirrer speed (N), gas superficial velocity (v_s), power input per volume (P/V) and liquid effective viscosity (μ_e) [7], as the following expression asserts:

$$k_L a = K\, v_s^a \left(\frac{P}{V}\right)^b \mu_e^c$$

Equation 7.4

Being K, a, b and c parameters of the correlation.

At the same time, from oxygen individual mass balance (liquid phase), it can be deduced:

$$OUR = OTR + \frac{dC_{O_2}}{dt}$$

Equation 7.5

$$OUR = r_{O_2} = q_{O_2} X$$

Equation 7.6

Where OUR, or r_{O2}, is the oxygen uptake rate ($mol_{O2}\ L^{-1}\ h^{-1}$); q_{O2}, the specific oxygen uptake rate ($mol_{O2}\ g_X^{-1}\ h^{-1}$), and X ($g_X\ L^{-1}$), the biomass concentration.

7.1.4 Scaling up vs. change of scale

The case here presented is not strictly a scale up, but rather the adaptation of the conditions of the already productive process of production of ROL under the control of P_{AOX1} up to a scale of 50 L, carried out in an already built up commercial bioreactor. Geometric similarity is not, then a variable that can be manipulated or used as a design parameter. Shear stress, on the other hand, can be manipulated as well as both mass and energy transfer.

The challenge that came up consisted on mimicking the oxygen transfer conditions carried out at 5 L, in this case, DO was selected as the parameter to be similar in pilot scale, due to the lack of off-gas analysis in that situation that would have allowed to estimate OTR along the process. However, it has already been demonstrated that the physiology of the cell, regarding growth and substrate consumption kinetics, along with

the production and secretion of active ROL, is dependent on the availability of oxygen [8]. This is reflected on a limitation at normoxic conditions (DO>0), at the extremes the range of 0-50 %, and being optimum at mild concentrations. So that, it was of extreme importance to transfer those conditions to that larger scale, apart from the operational strategy specifications regarding methanol feeding.

7.2 Objectives

The main purposes conceived to fulfill with the work of the present section of the dissertation are diverse and listed followingly:

- To transfer the production of *Rhizopus oryzae* lipase (ROL) by *P. pastoris* from the lab scale to a to a 10-times larger scale. The process was regulated by the *AOX1* promoter, using a methanol non-limited fed-batch (MNLFB) strategy. This has been reported, both published and in other chapters of this thesis, to be the most productive (in terms of volumetric productivity, Q_P) among strategies that employ methanol as a sole carbon source.
- To outcome the main issues that are originated from a change of scale, and stablish their causes. In this matter, oxygen transfer stands among the rest, and will be thoroughly discussed all along.
- Finally, to kinetically study the behavior of the culture in function of the oxygen availability, in terms of production, but also growth and substrate uptake.

7.3 Materials and methods

7.3.1 Bioreactors and process development in different scales

The set of different bioreactors employed for the results of the present document, both bench-top and pilot scale ones, have already been listed in chapter 3.

Barrigón, in his PhD dissertation (2015) [9] gathered together, in a single figure, the k_La specifications of all bioreactors used in this chapter in either scale, among others, in function of the stirring rate and vvm of air:

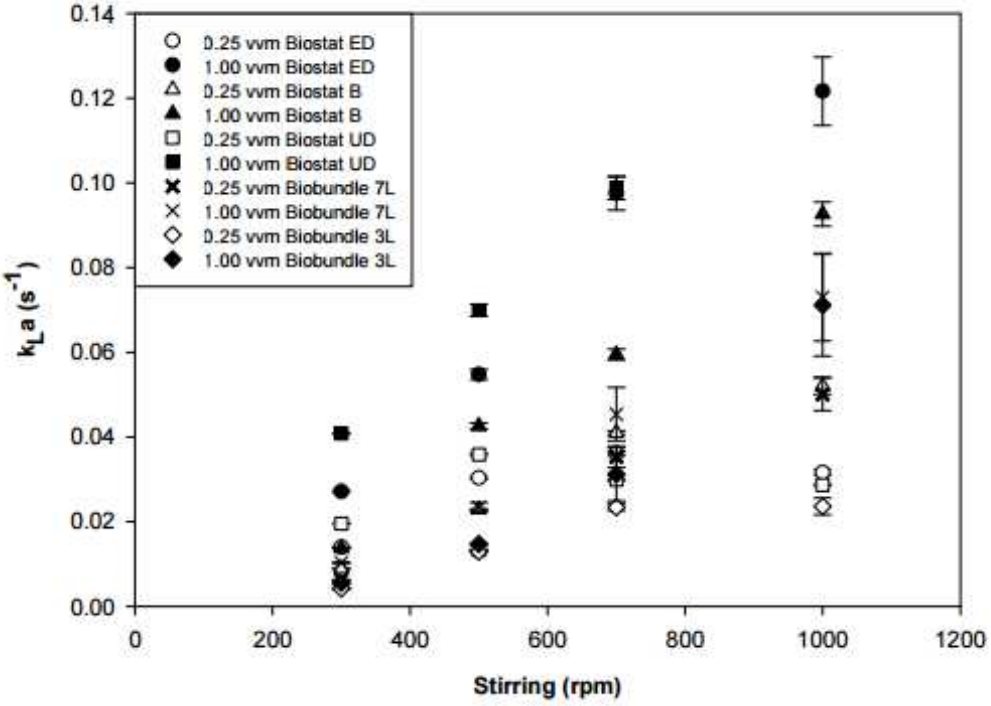

Figure 7.2 k_La specifications for different bioreactors in function of the stirring rate and vvm of air [9].

From what is shown in Figure 7.2, Biostat UD (pilot, 50 L) offers a higher profile of k_La for all stirring rate in comparison to Biostat B (5 L) and Biobundle (7 L).

So, a priori, if the criterion that is pursued is maintaining a similar k_La, so that OTR is also alike during the fermentation, then stirring rate at Biostat UD fermentations must necessarily be lower. Concretely, if methanol induction phases at bench-top scale are carried out at 1000 rpm and 1 vvm, then the stirring rate in the Biostat UD should be maintained around 500 rpm.

Pilot scale cultures were carried out in a 50 L Biostat UD (Sartorius) in fed-batch operation mode.

Initial volume was set at 20 L. Cells were inoculated in basal salts medium (BSM), which contained, per liter of distilled water: H_3PO_4 (85%) 26.7 mL, $CaSO_4$ 0.93 g, K_2SO_4 18.2 g, $MgSO_4{\cdot}7H_2O$ 14.9 g, KOH 4.13 g, glycerol 40 g, 2 mL of biotin solution (20 mg L^{-1}), 5 mL of trace salts solution and 0.5 mL of antifoam agent (A6426, Sigma-Aldrich Co., St. Louis, MO, USA). Trace salts solution was composed, per liter of distilled water, of $CuSO_4{\cdot}5H_2O$

6.0 g, NaI 0.08 g, $MnSO_4 \cdot H_2O$ 3.0 g, $Na_2MoO_4 \cdot 2H_2O$ 0.2 g, H_3BO_3 0.02 g, $CoCl_2$ 0.5 g, $ZnCl_2$ 20.0 g, $FeSO_4 \cdot 7H_2O$ 65.0 g, biotin 0.3 g, H_2SO_4 98 % 5 ml.

The fermentation was performed as described elsewhere [8], being divided into the phases of glycerol batch (GBP), transition (TP) and methanol induction (MIP).

This last stage was performed according to the conditions that wanted to be reproduced from the lab scale. The strategy used consisted on a methanol non-limited fed batch (MNLFB), controlling methanol concentration at a set point of 3 g L^{-1} during the MIP. DO, as stated, was mimicked from the bench-top process, and was kept throughout the MIP at a value around 25 % air saturation. Stirring rate levels are kept between 300 and 600 rpm (expected from Figure 7.2), regulated by the DO cascade control. Once reached its maximum, pure O_2 was introduced by a gas mixer, along with air, keeping a range of 1-2 vvm throughout the process.

Apart from that, another alternative was put into practice to evaluate the effect of the oxygen tension. For reasons of availability of this bioreactor, this was needed to be carried out in a single experiment, so that an adapted version of the methodology that Dietzsch et al. (2011) [10] carried out was conducted. It consisted on a methanol pulsed feeding strategy (MPF). Three different values of DO were tested: 70, 25 and 50 % (air saturation), for reasons that will be thoroughly discussed in section 7.4.3. For each set point of DO (DO_{SP}), 2 sets of 3 pulses of approximately 5 g L^{-1} (L of culture) were introduced. In an overnight period between the two sets of pulses at DO_{SP} 70 %, a methanol constant rate was settled not to leave the culture in starvation. A 90 % of the feeding rate for the in situ calculated $q_{S,max}$ was set as initial condition for this period in order not to cause methanol accumulation in the medium. Conditions of stirring and aeration were the same as the previous strategy.

7.3.1.1 Applikon Biobundle 7L

The lab scale fermentation meant to be transferred at pilot scale is taken directly from chapter 4. Thorough specifications of the equipment are already present there.

7.3.1.2 Sartorius Biostat B 5 L. Inoculum cultures

The first step of inoculation consisted on a 24 h growth in shake flasks containing complex media, YPD, which has, per liter, 10 g of yeast extract, 20 g of peptone, and 20 g of glucose. Zeocin was also introduced, at a concentration of 500 μg L^{-1}. The initial pH was 7.4 and stirring speed, 150 rpm (HT Multitron Incubator, Infors AG, Bottmingen, Switzerland). The already grown culture was centrifuged at 4500 x g and the cells were re-suspended in bioreactor culture medium and used to inoculate a 5 L Sartorius Biostat B bioreactor (Sartorius, Göttingen, Germany). Inoculums for the Biostat UD were grown in a 5 L Biostat B (Sartorius) fermenter. Initial volume was set at 2 L. Cells were inoculated in basal salts medium (BSM), with only 20 g of glycerol per liter, to meet the desirable final biomass concentration to inoculate in the larger fermenter. This process, then, consisted on a GBP, keeping DO at higher values than 25 % air saturation. pH was kept at 5.5 and temperature at 30ºC.

7.3.2 Total protein

Extracellular protein concentration was determined with the PierceTM Coomassie (Bradford) Protein Assay Kit (Prod. No. 23200, Rockford, IL, USA), according to the manufacturer's instructions. Bovine serum albumin (BSA) was used as the protein standard for the calibration curve. Assays were taken in triplicate and the RSD was about 5%.

7.3.3 Biomass concentration

Biomass concentration was determined by the dry cell weight (DCW) analysis, as described elsewhere in this dissertation. Assays were taken in triplicate and the RSD was about 5%.

7.3.4 Substrate concentration determination and control

For MNLFB strategy, methanol concentration was monitored by the Methanol Sensor System (Raven Biotech Inc., Vancouver, Canada) and controlled by performing a predictive-adaptive PI control strategy, as described previously.

Apart from that, it was also quantified offline by HPLC as previously reported [23]. RSD was estimated about 2 %.

7.3.5 ROL activity assay

Lipase activity was determined by performing an assay with the Roche Lipase Assay kit, as described previously. RSD was estimated to be about 5 %.

7.3.6 SDS-PAGE

Samples were run in sodium dodecyl sulfate polyacrylamide gel electrophoresis (SDS–PAGE) to analyze the secreted proteins, detect the product of interest and other proteins that could interfere. Gels were 12% polyacrylamide-composed, and were run in a Mini-PROTEAN II apparatus using Mini-PROTEAN® TGX Stain-Free™ Protein Gels (Bio-Rad Laboratories Inc., Hercules, CA) following this procedure. At a 3:1 proportion, samples were mixed with sample buffer (90% v/v of 4x Laemmli Sample Buffer (Bio-Rad), 10% v/v of ß-Mercaptoethanol). The mix was incubated at 95 ºC during 5 min. Precision Plus Protein™ All Blue Prestained Protein Standards (Bio-Rad) was used as molecular weight (MW) marker. 5 µL of MW marker and 25 µL of sample mix were loaded to their corresponding well. Gel revelation was performed in Gel Doc EZ System (Bio-Rad) with a visible spectrum protocol and further analyzed using the software Image Lab 6.0 (Bio-Rad).

All samples analyzed were subjected, first, centrifugated 15 min at 7000 x g, at 4 ºC. This was followed by a 0.45 µm to end with an ultrafiltration and diafiltration at 10 kDa, to remove the great amount of salts in the medium that would difficult the analysis, and concentrate the proteins.

7.3.7 Zymography

Zymogram was carried out to determine which bands separated by SDS-PAGE actually showed lipolytic activity.

Firstly, proteins were separated by SDS-PAGE as it is described in section 7.3.6. Right after that, SDS was removed from the gel by incubation in a 2.5% Triton X-100 solution for

1 h at room temperature, to renaturalize the enzymes. The gel was washed then twice with a Tris-HCl 20 mM buffer solution at pH 7 for 15 min, and was finally incubated in a solution of MUF-butyrate (Sigma-Aldrich, St. Louis, MO) 100 mM, using the same buffer as solvent. The gel was activated 30 s in UV and bands were detected by its fluorescence in Gel Doc EZ System (Bio-Rad), and further analyzed by the software Image Lab 6.0 (Bio-Rad).

7.3.8 Western Blot

Samples were first run in SDS–PAGE as it is explained in section 7.3.6. In this case, Precision Plus Protein™ Unstained and All Blue Protein Standards were used as molecular weight markers and 10 ng and 50 ng of a ROL standard solution (obtained from Bioingenium, SL, Barcelona, Spain) were loaded in two wells. Gel visualization was performed after UV activation using the Gel Doc EZ System. To carry out Western blots after SDS-PAGE, proteins were transferred to a nitrocellulose membrane (10 min, 2.5A, 25V) using the Trans-Blot® Turbo™ Transfer System. The membrane was blocked during 1 h incubation in 5% skim milk in washing buffer (1% v/v of Tween 20) and then incubated with a 1:10000 mouse anti-ROL antiserum (obtained from the Servei de Cultius Cel·lulars, Producció d'Anticossos i Citometria, Universitat Autònoma de Barcelona, Bellaterra, Spain) for 1h. After washing, the membrane was incubated with 1:1000 HRP-conjugated polyclonal anti-mouse IgG (Sigma Aldrich, St Louis, MO, US) as a secondary antibody during 1h. Detection was carried out by incubating the membrane for 5 minutes with Clarity™ Western ECL Substrate. Further image analysis and quantification was performed with Molecular Imager® ChemiDoc™ XRS System and the software Image Lab 6.0 (Bio-Rad).

7.3.9 Free RNA concentration

The concentration of RNA was determined by using a NanoDrop 1000 Spectrophotometer (ThermoFisher Scientific, Waltham, MA). 2µL of water were loaded to blank it. 2µL of sample were loaded and the software calculated the absorbance corresponding to the concentration of RNA present in the sample.

7.3.10 Theory and calculations

Procedures to calculate yields ($Y'_{X/S}$, $Y'_{P/X}$), discrete and mean specific rates (μ, q_S, q_P, q_{O2}, q_{CO2}) elemental balances and performance indexes (volumetric productivity, Q_P; specific productivity, Q_{Ps}) are specified elsewhere (chapters 4 and 5).

7.4 Results and discussion

7.4.1 Change of scale of a MNLFB strategy

The transference of *Pichia pastoris* cultures up to larger scales has already been brought off during the last decades, as scarce examples from the literature illustrate. However, there is no source of work carried out in terms of producing ROL. Recently and focusing on the production of this lipase, some non-published data obtained by Surribas (2007) [11] and Arnau (2011) [12].

As stated in chapter 4 and published in [13], the best methanol concentration set point (S_{SP}) to be followed during the MIP is 3 g L^{-1} in a MNLFB strategy using the present *Pichia pastoris* strain, in terms of achieving the optimum specific production rate (q_P). Due to this fact, it has been the most widely applied operational strategy among the research surrounding ROL production in *P. pastoris* under P_{AOX1} control, also present in this dissertation and in published articles [8]. Therefore, this alternative was selected for the scale upgrading to a 50 L bioreactor.

The performance of the main state variables, i.e, *X*, *S* and *P* is collected and graphically represented in Figure 7.3 along the analog data from the 25% DO experiment taken from chapter 3 of this thesis.

As it is appreciated in Figure 7.3, the induction time was selected as independent variable for better understanding of the differences between the two scales, in terms of durability and divergences between the evolution of *X, S* and *P*. An overview of the results it offers a clear evidence that profiles of *X* and *P* at a pilot scale did not follow the performance of their analogues at lab scale. Despite the *S* values being close to each other (reminding *S* was a condition imposed to the system and, therefore, controlled all along MIP), *X* and *P* resulted unexpectedly downgraded, concretely, with final values (for the same induction

time) of *X* 1.3-fold lower at pilot scale, while the factor is enwidened up to 6.5 when final activity is referred.

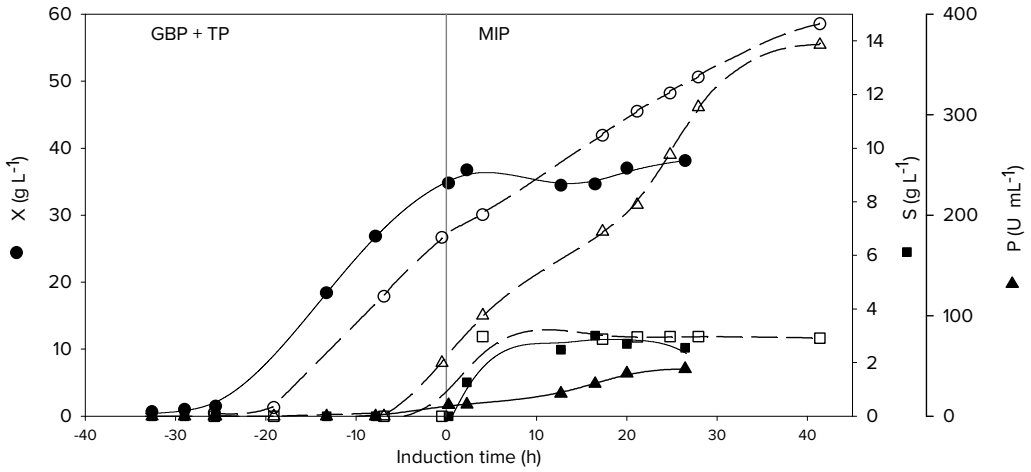

Figure 7.3. Induction time profiles of the performance of pilot plant (50 L) fermentation alongside lab scale (5 L) process. Pilot scale biomass concentration (*X*, ●), methanol concentration (*S*,■) and ROL activity (*P*, ▲). Lab scale *X* (○), *S* (□) and *P* (Δ). Lines (pilot scale, ——; lab scale, — —) are spline interpolations of the offline data shown.

This behavior, in consequence, foresees a descent of specific rates. Their mean values for both scales were calculated and further included in

Table 7.1 Comparison of physiologic parameters and main performance indexes of both scale MNLFB strategies, alongside with volumetric productivity, the key performance index that was meant to be achieved in this change of scale.

Firstly, even though yield of biomass-substrate ($Y^{'}_{X/S}$) is approximately a 15 % lower in pilot scale process, it is not considered as a significant divergence, since estimation of the volume in Biostat UD is not as straightforward as in the lab scale, which can lead to some error (5 %). Moreover, $Y^{'}_{X/S}$ is reported to fit in a range of 0.11 – 0.30 for recombinant *P. pastoris* cultures growing on methanol as a sole carbon source [14–16,8,17,18]. This similar yield indicates that both μ and q_S were downgraded at approximately the same factor, which corresponded to a value around 2.2-2.6, as it is shown in

Table **7.1**.

Table 7.1 Comparison of physiologic parameters and main performance indexes of both scale MNLFB strategies

Operational strategy	Units	Pilot scale	Lab scale
μ_{mean}	h^{-1}	0.013 ± 0.002	0.034 ± 0.001
$q_{S,mean}$	g g^{-1} h^{-1}	0.083 ± 0.005	0.181 ± 0.016
$q_{P,mean}$	U g^{-1} h^{-1}	48 ± 6	256 ± 22
$Y_{X/S}$	g g^{-1}	0.16	0.19
$Y_{P/X}$	U g^{-1}	3275	7529
Estimated $q_{O2,mean}$	mmol g^{-1} h^{-1}	4.13	7.35
OTR_{max}	mmol L^{-1} h^{-1}	157	430
ROL titer	U mL^{-1}	59.8	368
Volumetric productivity	U L^{-1} h^{-1}	585	5490

Additionally, taking into consideration that no byproducts were detected by HPLC analysis and this non-dramatic divergence that existed between $Y_{X/S}$ from both experiments, $q_{O2,mean}$ was estimated by assuming the accomplishment of the degree of reduction balance (or electron balance, EB) and the elemental carbon balance (CB). The need to perform this estimation is due to the lack of O_2 and CO_2 off-gas analyzers in the pilot plant set-up. So, this value was expected to be lower in large scale. Indeed, it is reflected in

Table **7.1** that pilot scale $q_{O2,mean}$ was the 56% of the lab scale one, both obtained by performing the same operational strategy. The difference in the maximal OTR is even wider, due to fact that in bench-top scale, higher biomass concentration was achieved (59 g L^{-1} in respect to 38 g L^{-1}).

Apart from that, and as Figure 7.3 showed ahead, q_P was severely reduced (more than 5 times), having a direct impact on $Y_{P/X}$, producing about the half of activity units (U) per gram of cells in pilot scale using the same feeding strategy in respect to the lab scale.

Everything that has been just stated contributed to diminish significantly the productivity of ROL, stablishing itself in an inferior order of magnitude in pilot scale (see

Table **7.1**). Therefore, and especially because of this last statement, the change of scale carried out by this experimental was proven unsuccessful.

Nevertheless, this unfortunate situation does not lack of precedents, since Surribas (2008) [11] and Arnau (2011) [12] already experimented a decrease on the productivity of ROL. In the first case, concretely, the pilot scale process had been 5 times less productive, and mean specific rates turned out to be at similar levels as the present case. The information on this matter will be extended in section 7.4.3. However, it was expected to finally improve the performance of the change of scale by a strict control of S at 3 g L^{-1} and the reproduction of oxygen transfer conditions, as stated before, by working at a constant dissolved oxygen (25% air saturation). A comparison with results from Arnau (2011) [12] is not as straightforward, though, because the feeding strategies applied consisted on mixed substrates along methanol (glycerol, sorbitol), due to the use of a Mut^s (repression of P_{AOX1}) strain to express ROL. Despite this fact, this trend of the productivity and mean specific rates of the main state variables of the process was also observed in that work. Apart from that, and regardless of the improvements that were achieved there concerning the methanol feeding physical particularities, the requirements of the main performance indexes (P_F, Q_P and $Y^*_{P/X}$) were not accomplished, for two experiments with different μ_{SP} during the induction phase.

7.4.2 Hypothesis I. Operational and process variable limitations

Once reaching this point, one should ask themselves, with the advances in the control of S, N-source and DO (chapter 2) in respect to previous attempts, what is actually holding back the scalability of the process to a mere 10-fold factor of volume? Moreover, this task has already been accomplished downwards (chapter 5).

So, it has been hypothesized that the bottleneck needed to be located in some operational limitation from the Biostat UD itself. While pH was discarded, since Arnau (2011) [12] already performed a study of the mixing inside the Biostat UD and demonstrated there were not concentration gradients of methanol alongside the height of the vessel, fact that can be extrapolated to other solutes present in the medium. However, oxygen transfer is another matter of concern. First of all, excluding $Y^*_{P/X}$, $Y^*_{X/S}$ was approximately maintained after the change of scale, while μ and q_S were parallelly reduced. This

downgrading was analogously observed in chapter 4 [8], at those cultures subdued to low oxygen tension. Second, despite k_La had been appointed to be superior at Biostat UD (section 7.3.1), the previous statement provides the possibility that gradients of dissolved oxygen may exist alongside the height of the bioreactor. Due to the physical impossibility to measure DO at different points of the system, an alternative experiment was proposed, consisting on a batch with methanol pulses strategy.

7.4.3 Outcoming oxygen tension limitations. A physiologic characterization in pilot plant by a methanol pulsed feeding strategy (MPF)

As stated previously, an alternative study in pilot scale was needed to be performed to try to outcome the obstacles found during the change of scale described in the section 7.4.1.

Concretely, to avoid multiple experiments and due to the limited availability of the pilot plant, a single experiment was designed, and it has been thoroughly detailed at section 7.3.1. However, it enabled to obtain plenty of information, regarding physiologic data out of specific rates of growth, methanol consumption and ROL activity production for DO set points of 25, 50 and 70 % air saturation during the MIP. Due to the non-availability of the Methanol Sensor System (Raven Biotech), the pulsed methanol strategy (MPF) was designed and applied. So, the mean values of these rates needed to be determined, now more than before, since methanol concentration is not constant along the different pulses, and they are detailed in Figure 7.4.

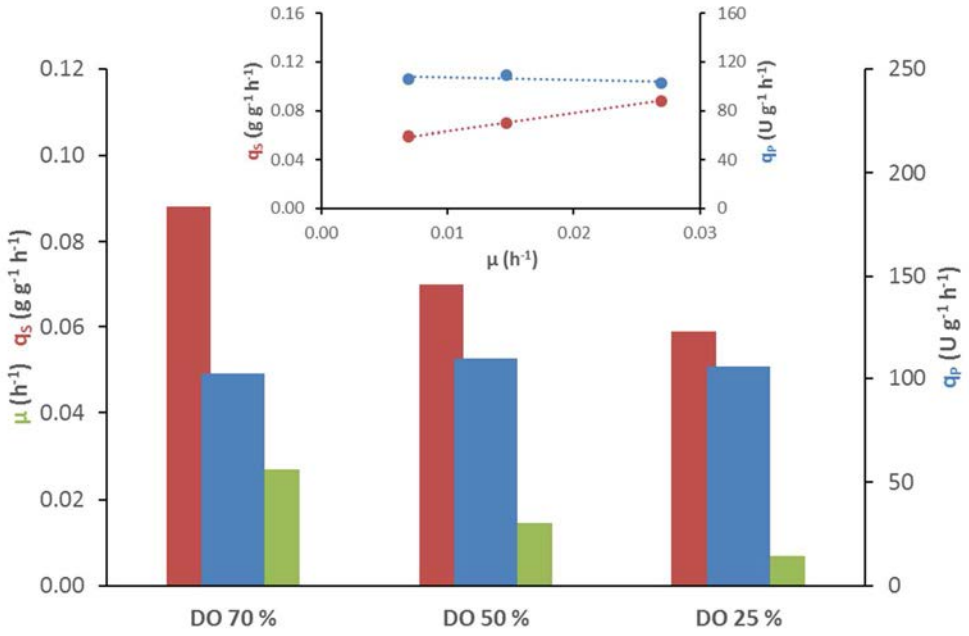

Figure 7.4 Mean specific rates of growth (μ), methanol uptake (q_S) and ROL activity production (q_P) for each condition of oxygen tension for MPF strategy. On top, dependencies of q_S and q_P on μ.

To begin with, regarding the effect of the DO, there is a dependence on it pointed to the same direction of both μ and q_S. Even though this fact matches with the work exposed in chapter 3 [8] in terms of the limitation of the bioprocess efficiency by the levels of DO, it clearly disagree with it in, first, the absolute values of both μ and q_S, significantly lower in the present case, and second, in the position of the maximum of both specific rates, corresponding with the maximum DO_{SP} (70%) in MPF, while in the case of lab scale MNLFB culture, those maximums were present at DO_{SP} of 25%, and also all specific rates were inhibited at the top range of DO (50%). Whereas these affirmations may seem to constitute gross divergences from the previous work discussed, it is necessary to point out that MPF and MNLFB diverge significantly between their *S* profiles, a situation that surely contributes on those differences. In fact, as stated in chapter 4, Lee and his coworkers (2003) [19] improved the specific growth of *P. pastoris* under methanol growth rate at higher DO (30-50% air saturation), while only a slight decrease in productivity was observed by Jazini *et al.* (2014) [15] when subduing the culture at a condition of 70% of DO. Apart from that, the next matter of concern is the low absolute values of μ, q_S and q_P that are still being obtained in contrast with the same expression system in the lab scale. In that sense,

Figure **7.5** has been built to illustrate this situation, where these physiologic parameters from MPF strategy, along with a previous approach of change of scale [11] are confronted to two kinetic models from previous published work [8,20,21] about ROL production by the same *P. pastoris* strain.

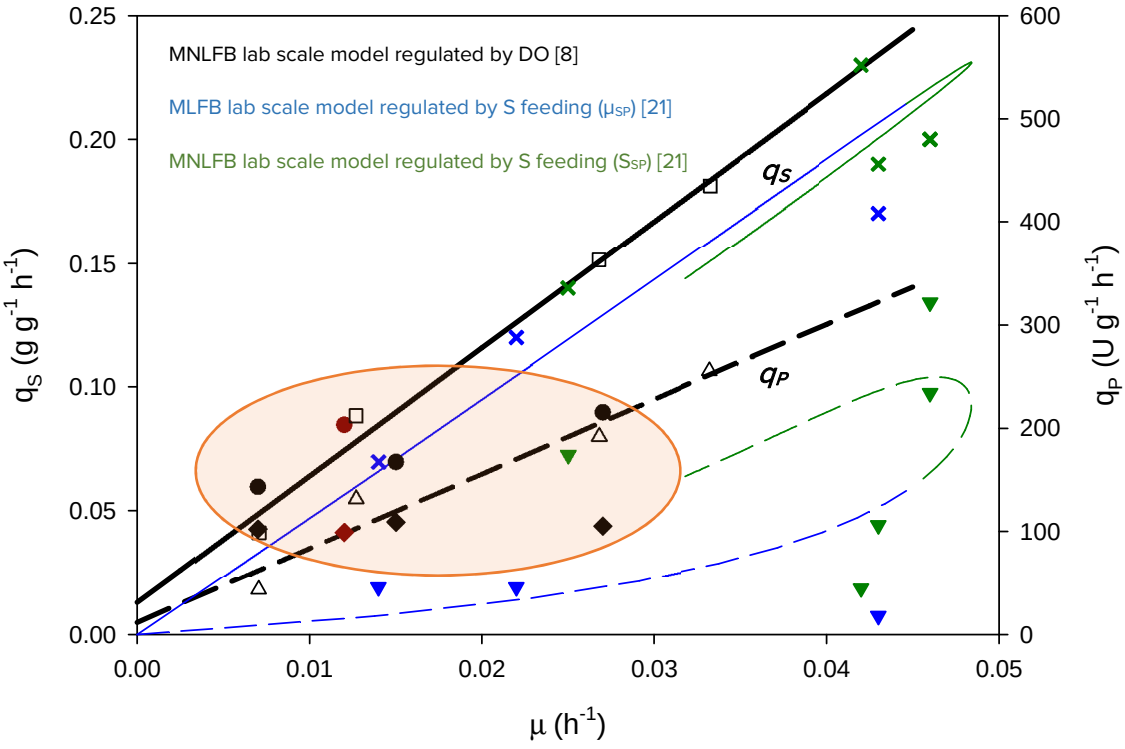

Figure 7.5. Experimental data of mean specific rates from pilot plant and lab scale fermentations confronted to modelling data. Points obtained in this work: $q_{S,mean}$ (●), $q_{P,mean}$ (♦). Non-published data from pilot plant cultivations by Surribas (2008) [11]: $q_{S,mean}$ (●), $q_{P,mean}$ (♦). Published data from chapter 4 [8]: $q_{S,mean}$ (□) , $q_{P,mean}$ (Δ). Experimental data from [13]: $q_{S,mean}$ MLFB (x), $q_{P,mean}$ MLFB (▼), $q_{S,mean}$ MNLFB (x), $q_{P,mean}$ MNLFB (▼). Modelling profiles in respect to μ: q_S from [8] (——), q_P from [8] (— —), q_S from [21] (——), q_P from [21] (MLFB — —, MNLFB — —).

In

Figure **7.5**, the points obtained at pilot scale are circled for their easier location. From this information , those conditions are stated to be closer to those values that correspond to either MLFB strategies [20] or rather MNLFB ones with scarce dissolved oxygen [8]. Moreover, previous non-published results of a change of scale by Surribas (2008) [11] agree quite well with the present study, by fitting in the behavior. The results obtained in the present work, also, agree with the previous non-published data from Surribas (2008),

by fitting in the trend indicated by the three points of q_S and q_P. The fact that those red points are located between the first and second black points of each rate is completely plausible, since Surribas worked at DO levels between 25 and 50 %, precisely coinciding with values that correspond to the operational conditions of these two commented black points. The reason of a higher q_S value may be due to the fact that methanol consumption may be overestimated, since this substrate was, at that time, introduced from the top plate of the reactor, and part of it was stripped to the off-gas. In Table 7.2, this information is broadened, by including, as well, the values of the main performance indexes of industrial interest.

It is simply appreciated in Table 7.2 that bioprocess efficiency of all attempts of bringing this process up to a higher scale did not reach the desired levels. Concretely, the highest Q_P, which is not even achieved by a MNLFB strategy, is not even the half of the one from strategy that was intended to be reproduced. Instead, Q_P pilot scale values are much closer to less productive strategies, as MLFB or MNLFB ones which are more distant to the optimal S levels, as exemplified in the table. It is necessary to be included in this discussion, though, that the fact of working at higher DO_{SP} has helped to improve this performance indexes in respect to the strategy discussed in section 7.4.1. However, they can be hardly compared, since MPF gets the aim of this work away from the path of bringing up the MNLFB alternative up to a higher scale. On the other hand, $Y^*_{P/X}$ and specific productivity behaved, as well, as anticipated, since q_P resulted lower in all cases than the initial expectations, as it has been already stated.

Apart from that, returning to

Figure **7.5**, it is easy to graphically notice that if this series of data was modelled, significantly higher maintenance coefficients (m_S, m_P) would be obtained if they were compared to the two models represented in the figure, indicating major discordance in physiology between both scales.

Hence, reaching this point, it is clear that a lot of uncertainty stands in the path of achieving the goals proposed, constituting a hurdle in the way of bringing this process up to the industrial scale, task that a priori did not seem so troublesome, despite the precedents.

Table 7.2 Comparison of bioprocess efficiency among different fed-batch operational strategies performed at pilot scale (50 L) and lab scale (5 L). ± indicates standard error (SE). Productivities and yields are calculated over all fermentation time.

Feeding strategy		MPF (present work)	MNLFB S_{SP} = 3 g L^{-1} (present work)	MNLFB S_{SP} = 3 g L^{-1} [11]	MNLFB S_{SP} = 3 g L^{-1} DO_{SP} = 25 % [8]	MNLFB S_{SP} = 2 g L^{-1} [13]	MLFB μ_{SP} = 0.02 h^{-1} [13]
Scale	-	Pilot	Pilot	Pilot	Lab	Lab	Lab
Variable of study	-	DO Change of scale	Change of scale	Change of scale	DO	S-μ modelling	S-μ modelling
ROL titer	U mL^{-1}	158	59.8	86	368	103	112
$Y'_{P/X}$	U g^{-1}	4172	1253	-	7700	2004	2644
Volumetric productivity	U L^{-1} h^{-1}	2323	585	1329	5490	2437	1857
Specific productivity	U g^{-1} h^{-1}	60	15	-	93	48	36
μ_{mean}	h^{-1}	0.018	0.013±0.002	0.015	0.034±0.001	0.043±0.002	0.014±0.001
$q_{S,mean}$	g g^{-1} h^{-1}	0.091	0.083±0.005	0.125	0.181±0.016	0.19±0.01	0.07±0.01
$q_{P,mean}$	U g^{-1} h^{-1}	115	48±6	90	256±22	106±9	46±4

7.4.4 Hypothesis II. Physiologic discordances, the own paths of growth/substrate consumption and product secretion

Settling down and gathering all data obtained so far together, it is manifest the right way to follow from this point and on is split into two differentiated paths.

The first one, consists in figuring out why growth and methanol consumption are parallelly so downgraded when subduing the cells at *S* and oxygen availability that are very favorable, as previous reported results show in lab scale. The hypothesis currently being weighed relies on some avoided operational feature that has been skipped until now. With the methanol stripping problem solved and the demonstration of the inexistence of mixing limitations [12], on one hand, and the hint of possible O_2 gradients within the liquid phase by the displacement of the dependence of specific rates on DO, on the other one; scarce alternative flaws, so, are to be detected. A possibility still had to be considered,

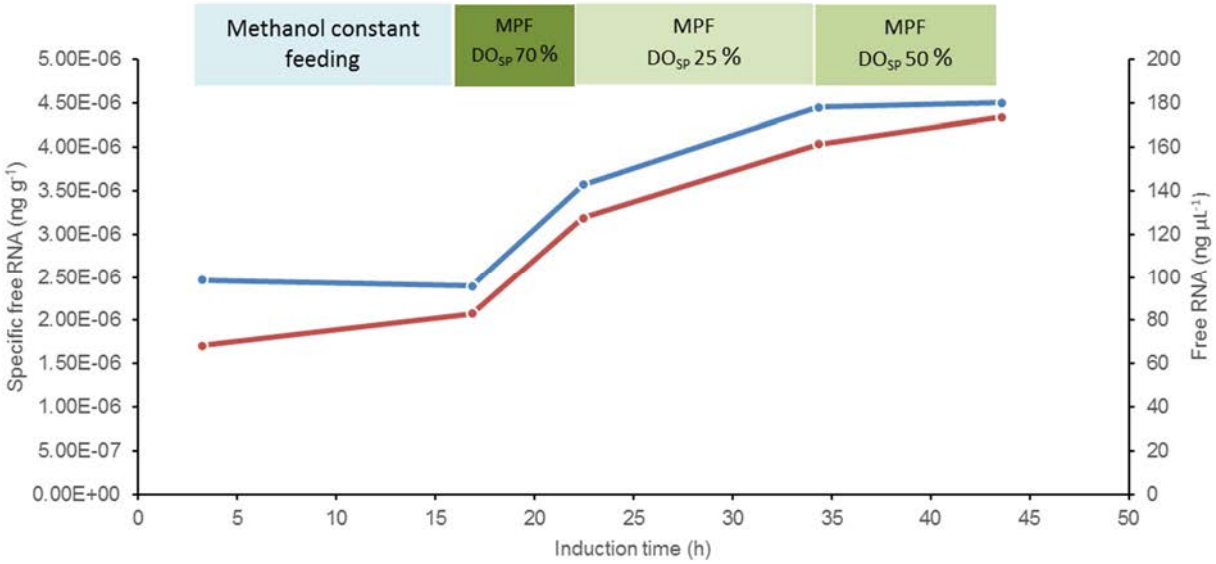

though, which is the higher cutting force that mechanic stirring provides at higher scales could cause harm to the cells, and that would be reflected in lower growth rate, and in consequence, consumption and production rates. To get an approach to this circumstance, posterior free RNA analysis in the supernatant were tested in some of MPF strategy samples. In Figure 7.6 the induction time evolution of this variable is represented.

Higher levels of free RNA in the medium would inquire cell lysis and would reinforce the contemplated hypothesis. However, with the available data from Figure 7.6 either option

Figure 7.6. Induction time evolution of free RNA in the supernatant, both absolut (red) and specific (blue).

cannot be stated categorically. While it is true that the amount of RNA per gram of cell increased along the process, there were two phases where the levels remained practically invariable, and where arbitrarily at the beginning and the end of the MIP, at two different DO_{SP} conditions. To confront the validity of this data, another analogue culture should be carried out at lab scale to compare the levels of specific free RNA. Apart from that, future cultures in pilot scale should also be subjected to further analysis that give more information about the state of the cells, i.e., viability, oxidative stress in terms of reactive oxidative species (ROS) or cell cycle state.

On a different matter, product kinetics have shown no dependence at all on DO levels and, in consequence, on μ itself. As it has been stated, this contradicts what has been obtained in lab scale in previous works. So, to slightly clear part of the uncertainty that surrounds this unexpected low and invariable production rate behavior, a study of the protein quality was proposed, testing the two different strategies applied in pilot scale, while comparing them with alternatives already tested in lab scale.

7.4.5 Easing the path of product formation limitations. Extracellular protein analysis

Following the way proposed in the previous section, a detailed study around the secreted proteins was carried out in order to shed light to the intriguing behavior of the product kinetics in pilot scale. It included a SDS-PAGE to identify whole set of proteins that conforms the secretome and their molecular weight (MW), a zymogram with MUF-butyrate to determine which of those proteins show lipasic activity and, finally, a Western Blot, ROL-specific, to identify the protein of interest and also to roughly calculate ROL concentration in each sample. This last value will be of utterly importance, since it will enable to obtain the specific activity referred to ROL, which permits to compare how active was ROL produced in each strategy. The strategies selected were MFP and MNLFB at pilot scale and the two optimal *S* profile from chapter 4 (OP1 and OP2) for the lab scale cases. These two latter were chosen for publishing needs and because they should not behave differently from MNLFB 3 g L^{-1}, included in the discussion of the present chapter, due to their similar bioprocess efficiency.

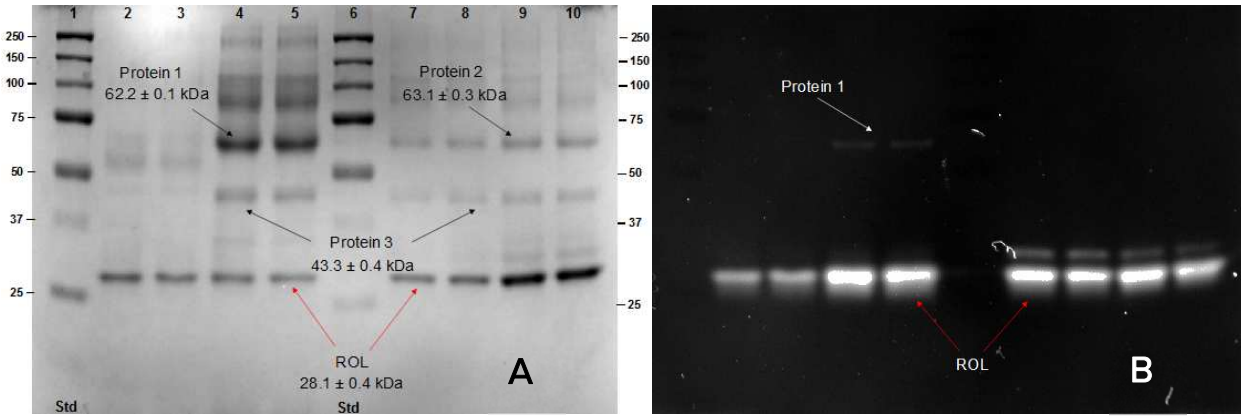

Figure 7.7 (A). SDS-PAGE. Lanes 1 and 6, Precision Plus Protein™ All Blue Prestained Protein Standards (Bio-Rad) molecular weight (MW) markers. Lanes 2-5, pilot plant scale bioreactor samples, 2 and 3 from MPF strategy (replicates), 4 and 5 MNLFB 3 g L^{-1}. Lanes 7-10 Lab scale bioreactor samples, 7 and 8 from OP1, 9 and 10 OP2. (B). Zymogram. Lane distribution is the same as (A).

First of all, ROL was successfully identified, as expected, in all samples, as a thick band of 28.1 kDa, which matches the reported recombinant ROL (rROL) also obtained by *P. pastoris* in a previous characterization of the protein by Guillén *et al.* (2011) [22]. These bands are also detected by zymography, appointing its enzymatic activity, and by Western Blot analysis (

Figure **7.7** and Figure 7.8).

SDS-PAGE, in first terms, provided specially interesting information, regardless of the objectives that were pursued through its fulfillment. Concretely, and most evident, it showed the direct influence of the operational strategy on the secretome of the cell. If lanes 2 and 3 are confronted to the rest of the samples (MPF in respect to MNLFB), one can state that, apart from ROL, the remainder protein profile is significantly different. Concretely, the presence, in MNLFB strategies, of Protein 1 (pilot) and Protein 2 (lab scale), both presenting around the double MW than ROL, is the most significant one. It probably consists on the same protein, but Protein 1, specifically, was also detected by zymogram, indicating that probably part of the activity that was detected in the supernatant derived from that specific molecule. That also brought up the possibility that, under MNLFB conditions in pilot scale, part of the ROL produced was being derived to form a dimer,

since Protein 1, as stated, doubles ROL in MW. That could explain, at least partially, the diminution of the activity on that particular culture, since despite detecting a thick band of Protein 1 in SDS-PAGE, its detection in the zymogram was rather weaker than ROL, indicating that this protein would be less specifically active. The Western Blot performed afterwards was also intended to clarify this aspect of the results.

Nevertheless, to sum up, what can be clearly drawn from these previous results is the direct influence of the strategy on, not only the levels of recombinant protein, but other proteins to be secreted, obtaining different profiles of them if MPF and MNLFB are compared to each other. The set of secreted proteins from MNLFB pilot fermentation indicates also that, for some reason that cannot be currently appointed, proteins of high MW are more present than in lab scale, and concretely, an MUF-butyrate-sensible protein apart from ROL.

Figure 7.8 includes the two Western Blot, one for each scale, that the samples from Figure **7.7** were subjected to.

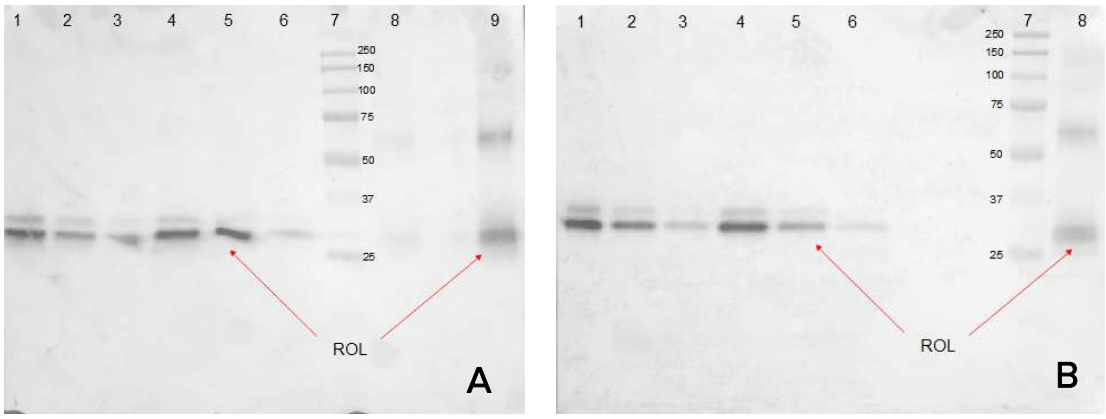

Figure 7.8 Western Blot analysis. (A) Pilot plant fermentations. Lanes 1-3, dilution bank of a sample of MPF strategy. Lanes 4-6, dilution bank of MNLFB 3 g L^{-1} strategy. Lane 7, superposed visible MW marker. Lane 8, purified ROL standard (10 ng). Lane 9, purified ROL standard (50 ng). (B) Lab scale bioreactor fermentations. Lanes 1-3, sample MNLFB strategy (OP1) dilution bank. Lanes 4-6, sample of MNLFB strategy (OP2) dilution bank. Lane 7, superposed visible MW marker. Lane 8, purified ROL standard (50 ng). Each dilution bank contains, in order, samples 1x, 0.5x and 0.2x.

At this point, and from what it is explicitly observed in Figure 7.8, ROL was successfully identified in all samples. However, Protein 1 was not detected, suggesting it may not consist on a ROL dimer. Last years, studies on the secretome of *P. pastoris* have been

published, within which Mattanovich *et al.* (2009) [23] and Huang *et al.* (2011) [24] can be highlighted. While the first one identified the secreted proteins from *P. pastoris* growing under glucose, Huang *et al.* carried out a similar study but using methanol as sole carbon source and cultivating a X-33 strain producing a vaccine, in fed-batch mode, controlling methanol concentration at 1 g L^{-1}, which is more interesting for matching the case of study. The results they showed included a number of proteins around MW of Protein 1 (and 2), some of them hypothetical or unidentified, that could correspond to it, but none explicitly provided lipase catalytic activity. Regarding Protein 3, there were some examples of proteins that were secreted significantly with similar MW, like one that is homologue with *EXG1*, involved in cell wall beta-glucan formation (47.8 kDa, pI 4.53).

Finally, in Table 7.3, concentrations of protein in the samples used, and more importantly, specific activity referred to ROL in each strategy, are specified.

Table 7.3 Conditions of protein load for all protein analysis. Results of specific activity in respect to ROL by quantification from Western Blot (WB) and ROL fraction in the protein extract. ± indicates SD of triplicates of total protein analysis. In specific activity and ROL fraction, it corresponds to the propagated error from both activity assay and the quantification of ROL concentration.

		MNLFB (This work)	**MPF (This work)**	**OP1 (Chap. 4)**	**OP2 (Chap. 4)**
Scale	-	Pilot	Pilot	Lab	Lab
Total protein (SDS-PAGE/Zymogram)	mg_{prot} L^{-1}	285 ± 7	245 ± 4	212 ± 34	268 ± 14
Total protein (Western Blot)	mg_{prot} L^{-1}	43.1 ± 6.3	19.8 ± 3.3	23.8 ± 7.4	13.9 ± 5.1
Specific activity	U ng^{-1}_{ROL}	6.99 ± 0.47	7.79 ± 0.34	5.18 ± 0.07	7.41 ± 0.23
ROL fraction	mg_{ROL} mg_{prot}^{-1}	0.06 ± 0.01	0.13 ± 0.02	0.23 ± 0.07	0.24 ± 0.09

Table 7.3 evidences an order of magnitude between the load of proteins between SDS-PAGE and WB due to the difference of sensitivities of the two analyses. WB samples were prepared to show the same initial activity to fit in the detection limits, which corresponds to an initial sample of around 20 U mL^{-1} and their dilutions according Figure 7.8.

Results on specific activity do not evidence major enough differences between strategies that could justify or demonstrate a similar production of ROL in absolute quantity or concentration but less active in pilot scale processes. Therefore, this hypothesis is discarded. Besides, even though similar strategies like OP1 and OP2 evidence a divergence around the 30% of specific activity, Western Blot cannot be considered as an absolutely accurate method to quantify the amount of ROL in a sample, but indeed can be for detecting major differences, which was the aim suggested for this section. Differences on the ROL purity within scales are evident. OP1 and OP2 more than doubled ROL fraction in the secretome, in respect to pilot plant fermentations. This was hinted qualitatively in SDS-PAGE (

Figure 7.7). This observation leads to state that the protein production may be directed to other endogenous ones, for some reason that cannot currently be attributed to.

7.4.6 Hypothesis III. Future beyond

With this situation straight ahead, the next step in this matter should be deepening into the cause of the huge divergences existing between both scales. Having exposed the main hypothesis and now discarded, the remaining alternatives are summed up:

- Looking up to cell viability and oxidative stress, as a way to detect some unexpected physiological behavior or damage. Monitoring free RNA is also an easy, fast way to detect unexpected genetic material release to the supernatant. However, it must be compared to a standard lab scale fermentation, to value which are the normal concentration levels. Despite having these consequences hypothetically confirmed, the causes would not be appointed.
- Working at lower stirring rates, which would reduce the shear stress, in order to study its influence on the bioprocess efficiency of the process. It must be noticed, though, that this change will also diminish k_La, so that larger pure O_2 flow rates will be needed to maintain the desired levels of OTR. A monitoring of the oxidative stress will also be mandatory to evaluate the possible negative effects of this consequence.

- Deepening into oxygen tension limitations. The mismatch of the culture physiology dependence on that condition between both scales still leads to consider the existence of gradients within the height of the reactor. A way to measure DO from the top of the vessel and height-regulable would be the most desired alternative to outcome the obstacles on this matter.
- Even though Protein 1 was not detected in WB, techniques on trying to dissociate a hypothetic dimer of ROL (e.g. Triton-X-100 treatment [25]) could be put into practice to fully discard this possibility.

7.5 Conclusions

There is no mistake on asserting that, unfortunately, with these new results now extensively discussed, there is still a long path straight ahead to accomplish the change of scale of ROL production by *P. pastoris*. Still, a thorough work has been carried out to uncover and outcome the main physiological limitations and operational, in a bioprocess engineering point of view, and plausible causes of the downgrading of the kinetics have been discarded.

However, a new spectrum of alternatives is now opened to carry on with this path. Bioprocess scaling up is particularly essential to be accomplished regarding the present case of study, as ROL is a potential product of industrial interest and its production has been studied and improved all along the last years, by previous works and specially during the PhD period where this dissertation finds its sense. That has been materialized in the optimization of simple operational strategies that enabled to reach the top levels of bioprocess efficiency (volumetric productivity, ROL final titers) that are potentially transferable to the industry scale, and settled a platform to be applied to straightforwardly design and develop new bioprocesses of production of heterologous protein production.

7.6 References

[1] C. Solà, F. Gòdia, Scale Up, in: J.A. Asenjo, J.C. Merchuk (Eds.), Bioreact. Syst. Des., Marcel Dekker, Inc., New York, 1994: pp. 511–522.

[2] North East Biomanufacturing Center & Collaborative, (n.d.). http://www.biomanufacturing.org/ (accessed July 12, 2017).

[3] J.-D. Yang, C. Lu, B. Stasny, J. Henley, W. Guinto, C. Gonzalez, J. Gleason, M. Fung, B. Collopy, M. Benjamino, J. Gangi, M. Hanson, E. Ille, Fed-Batch Bioreactor Process Scale-Up From 3-L to 2,500-L Scale For Monoclonal Antibody Production From Cell Culture, Biotechnol. Bioeng. 98 (2007) 141–154.

[4] D. Martínez, C. Menéndez, L. Hernández, A. Sobrino, L.E. Trujillo, I. Rodríguez, E.R. Pérez, Scaling-up batch conditions for efficient sucrose hydrolysis catalyzed by an immobilized recombinant Pichia pastoris cells in a stirrer tank reactor, Electron. J. Biotechnol. 25 (2017) 39–42.

[5] P. Vaz de Arruda, J. César dos Santos, R. De Cássia Lacerda Brambilla Rodrigues, D.D. Virgínio da Silva, C.K. Yamakawa, G. Jackson de Moraes Rocha, J.N. Júnior, J.G. da Cruz Pradella, C.E. Vaz Rossell, M. das G. de Almeida Felipe, Scale up of xylitol production from sugarcane bagasse hemicellulosic hydrolysate by Candida guilliermondii FTI 20037, J. Ind. Eng. Chem. 47 (2016) 297–302.

[6] H.B. Reisman, Problems in scale-up of biotechnology production processes, Crit. Rev. Biotechnol. 13 (1993) 195–253.

[7] F. Garcia-Ochoa, E. Gomez, Bioreactor scale-up and oxygen transfer rate in microbial processes: An overview, Biotechnol. Adv. 27 (2009) 153–176.

[8] X. Ponte, J.L. Montesinos-Seguí, F. Valero, Bioprocess efficiency in *Rhizopus oryzae* lipase production by *Pichia pastoris* under the control of P_{AOX1} is oxygen tension dependent, Process Biochem. 51 (2016) 1954–1963.

[9] J.M. Barrigón de San Marcos, Model-based design and implementation of operational strategies for *Rhizopus oryzae* lipase production in *Pichia pastoris* under the *AOX1* promoter, Universitat Autònoma de Barcelona, 2015.

[10] C. Dietzsch, O. Spadiut, C. Herwig, A dynamic method based on the specific substrate uptake rate to set up a feeding strategy for *Pichia pastoris*, Microb. Cell Fact. 10 (2011) 14.

[11] A. Surribas Casalprim, Millora en el procés de producció d'una lipasa de *Rhizopus oryzae* en *Pichia pastoris* mitjançant tècniques de monitoratge i estratègies de cultiu alternatives, Universitat Autònoma de Barcelona, 2008.

[12] C. Arnau Jimenez, Estratègies d'operació per a la producció de lipases de Rhizopus oryzae amb el fenotip Mut^s de *Pichia pastoris* mitjançant substrats mixtes, Universitat Autònoma de Barcelona, 2011.

[13] J.M. Barrigón, J.L. Montesinos, F. Valero, Searching the best operational strategies for Rhizopus oryzae lipase production in Pichia pastoris Mut+ phenotype: Methanol limited or methanol non-limited fed-batch cultures?, Biochem. Eng. J. 75 (2013) 47–54.

[14] J.M. Barrigon, R. Ramon, I. Rocha, F. Valero, E.C. Ferreira, J.L. Montesinos, State and Specific Growth Estimation in Heterologous Protein Production by *Pichia pastoris*, AIChe J. 58 (2012) 2966–2979.

[15] M. Jazini, G. Cekici, C. Herwig, Quantifying the Effects of Frequency and Amplitude of Periodic Oxygen-Related Stress on Recombinant Protein Production in *Pichia pastoris*, Bioengineering. 1 (2014) 47–61.

[16] J. Xie, R. Yang, Q. Zhou, P. Du, R. Gan, Q. Ye, Efficiencies of Growth and Angiostatin Expression in Cultures of *Pichia pastoris* Fed with Mixed Carbon Sources, Chem. Biochem. Eng. Q. 27 (2013) 235–244.

[17] N.K. Khatri, F. Hoffmann, Impact of methanol concentration on secreted protein production in oxygen-limited cultures of recombinant *Pichia pastoris*, Biotechnol. Bioeng. 93 (2006) 871–9. http://www.ncbi.nlm.nih.gov/pubmed/16320364 (accessed November 17, 2015).

[18] S. Curvers, P. Brixius, T. Klauser, J. Th??mmes, D. Weuster-Botz, R. Takors, C. Wandrey, Human chymotrypsinogen B production with *Pichia pastoris* by integrated development of fermentation and downstream processing. Part 1.

Fermentation, Biotechnol. Prog. 17 (2001) 495–502.

[19] C.Y. Lee, S.J. Lee, K.H. Jung, S. Katoh, E.K. Lee, High dissolved oxygen tension enhances heterologous protein expression by recombinant *Pichia pastoris*, Process Biochem. 38 (2003) 1147–1154.

[20] J.M. Barrigón, J.L. Montesinos, F. Valero, Searching the best operational strategies for *Rhizopus oryzae* lipase production in *Pichia pastoris* Mut^+ phenotype: Methanol limited or methanol non-limited fed-batch cultures?, Biochem. Eng. J. 75 (2013) 47–54.

[21] J.M. Barrigon, F. Valero, J.L. Montesinos, A macrokinetic model-based comparative meta-analysis of recombinant protein production by *Pichia pastoris* under *AOX1* promoter, Biotechnol. Bioeng. 112 (2015) 1132–1145.

[22] M. Guillén, M.D. Benaiges, F. Valero, Comparison of the biochemical properties of a recombinant lipase extract from *Rhizopus oryzae* expressed in *Pichia pastoris* with a native extract, Biochem. Eng. J. 54 (2011) 117–123.

[23] D. Mattanovich, A. Graf, J. Stadlmann, M. Dragosits, A. Redl, M. Maurer, M. Kleinheinz, M. Sauer, F. Altmann, B. Gasser, Genome, secretome and glucose transport highlight unique features of the protein production host *Pichia pastoris*., Microb. Cell Fact. 8 (2009) 29.

[24] C.J. Huang, L.M. Damasceno, K.A. Anderson, S. Zhang, L.J. Old, C.A. Batt, A proteomic analysis of the *Pichia pastoris* secretome in methanol-induced cultures, Appl. Microbiol. Biotechnol. 90 (2011) 235–247.

[25] N.C. Robinson, L. Talbert, Triton X-100 induced dissociation of beef heart cytochrome c oxidase into monomers, Biochemistry. 25 (1986) 2328–2335.

8 GENERAL CONCLUSIONS

In a global view, this PhD dissertation has explored and studied the bioprocess of production of *Rhizopus oryzae* lipase by *Pichia pastoris* in a bioprocess engineering point view, looking forward to a feasible industrial process.

In the first place, the focus was placed on the implementation of a new environment of peripherals and the improvement of monitoring and supervision of the system. An automatic feeding strategy for the nitrogen source was developed to favor process reproducibility and avoid limitations that fluctuations of it cause to the ROL production.

On the other hand, a systematic study of the influence of dissolved oxygen on this process was also carried out. A significant effect on the physiology of the cells of the level of oxygen availability was stablished, under normoxic conditions, where an optimal DO of 25 % air saturation during the methanol induction was found.
In the same way, it was also demonstrated that downgrading or rising the value of DO had no significant effect on the yields in respect to substrate or biomass, leading to conclude that DO has not visible influence on the metabolism of methanol uptake in normoxia.
Finally, these results also pointed out the need to characterize the DO effect not only in the present bioprocess, but for the production of other recombinant proteins or even different expression systems, and so, the need of a fine control of this variable, to avoid compromising the bioprocess efficiency by either a lack or an excess of oxygen tension.

Moreover, a successful step forward to optimization of the bioprocess exploited in this thesis was achieved. From modelling data, and mathematical tools of optimization, a simple platform was developed and employed to design new feeding strategies of methanol based on the optimal profiles of this substrate concentration.
Two new alternatives, maximizing product titer and volumetric productivity, respectively, were simulated and successfully validated experimentally, achieving better efficiency when compared to previous MLFB and MNLFB alternatives.
Apart, and not less important, the work carried out in this section constituted a simple, versatile and user-friendly platform that can be extrapolated to other kind of processes, even to other microorganisms, requiring only simple modelling data from the system to work with.

On a second part of this dissertation, scaling studies were performed by taking the production of ROL by *P. pastoris* under P_{AOX1} control as reference, both down to a microbioreactor scale and up to 50 L.

On one hand, the microbioreactor system RoboLector was stablished as a feasible tool for the development of simple fed-batch operational strategies of *P. pastoris* growing on methanol and for screening assays for clone selection.

On the other hand, the production of ROL was brought up to a 50 L scale and it was not possible to achieve the desired levels of any of the performance indexes that were found in lab scale.
After performing several analyses, the most plausible hypothesis that was driven out of the results is the possible problems of homogeneity of the dissolved oxygen alongside the reactor height. Alongside with this, future work has to focus as well to clarify if dimers of ROL are being produced when certain operational conditions are given.

To conclude, the main objective of this PhD dissertation is very important to be remarked at this point: to achieve a reliable, robust bioprocess to obtain, as a product of interest, the lipase of *Rhizopus oryzae*, heterologously produced

by *P. pastoris* using methanol as the only carbon source. From this point, reaching top levels of bioprocess efficiency was paramount, since it enables to reinforce *Pichia* as a cell factory. The work described throughout this dissertation has been successful on this matter by fulfilling the points that have been reviewed here.